

1
2
3
4
5
6
7
8
9

Igneous Activity at Yucca Mountain: Technical Basis for Decision Making

A Draft Report
Prepared by the
Advisory Committee on Nuclear Waste, US NRC



10
11
12
13
14
15
16
17
18

Looking south along the crest of Yucca Mountain, Nevada towards Amargosa Valley and Lathrop Wells volcano to the right of the crest in the mid-background

December 2006

19
20
21
22
23
24
25
26
27
28
29
30
31
32
33
34
35
36
37
38
39
40
41
42
43
44
45
46
47
48
49
50
51
52
53
54
55
56
57
58
59
60
61

“The Committee should provide the Commission with an analysis of the current state of knowledge regarding igneous activity which the Commission can use as a technical basis for its decision making.” [SRM M060111B, February 9, 2006]

Igneous Activity at Yucca Mountain: Technical Basis for Decision Making

**A Report Prepared by the
Advisory Committee on Nuclear Waste, US NRC**

***Executive Summary*¹ [Exclusive of Conclusions Chapter]²**

Eighty thousand years ago a small-volume basaltic volcano (Lathrop Wells) erupted about 15 miles south of the Department of Energy’s (DOE) proposed high-level waste (HLW) repository in Yucca Mountain, Nevada. This was the first volcanism in the immediate vicinity of Yucca Mountain for a million years, but one of a series of infrequent basaltic volcanoes that have occurred in the vicinity of the proposed repository site during the past 10 million years. This report presents the Advisory Committee on Nuclear Waste’s (ACNW) summary and evaluation of the range of views of the Committee, Nuclear Regulatory Staff (NRC) staff, and other stakeholders on the nature, likelihood and potential consequences of future igneous activity at the proposed Yucca Mountain repository.

The effect of igneous activity on the performance of the proposed repository has been investigated by DOE as well as by the NRC and other stakeholders for many years. These investigations have identified a number of uncertainties and a spectrum of legitimate professional views regarding the nature and potential impact of igneous activity on the repository. At the Commission’s request [SRM M060111B, February 9, 2006], the Committee has reviewed and analyzed the current state of knowledge regarding igneous activity, including the range of technical views by experts and stakeholders. This report summarizes current knowledge of potential igneous activity at the proposed repository site, including igneous activity scenarios and their potential impacts on the repository performance. It also provides an assessment of differing professional views, including the views of experts representing DOE, NRC, the State of Nevada, and other experts. The State of Nevada has not established specific views on the impact of future igneous activity at Yucca Mountain, however, experts supported by the State of Nevada have published several journal articles related to the probability of an igneous event intersecting the proposed repository that are reviewed in this report.

¹ References to sources of information presented are excluded in the Executive Summary. Detailed references to all specific sources of information and views on future igneous activity at Yucca Mountain are provided in the body of this report.

² Conclusions will be added upon completion of Conclusions Chapter (7) after review of the results of the ACNW Working Group Meeting on Igneous Activity that will be held on February 13 and 14, 2007.

62 The State of Nevada and the Yucca Mountain region are located in the Central Basin and
63 Range geological province (the Western Great Basin) which is noted for a complex geologic
64 history with tectonic activity that was initiated some 25 million years (Ma) ago and continues
65 today. This tectonic activity has manifested itself in at least four pulses of basaltic volcanism
66 during the last 10 million years. These include the ~80 ka Lathrop Wells cone, flows, and
67 remnants of its ejecta blanket, ~1 Ma events (Pleistocene or Quaternary) and multiple events
68 dated ~3–6 Ma (Pliocene-U. Miocene) and ~8–13 Ma (Miocene) in Crater Flat adjacent to
69 Yucca Mountain. Other young basalts in the Yucca Mountain region include Little Black Peak
70 (~0.3 Ma) and Hidden Cone (~0.4 Ma), 35 km NW of Yucca Mountain. Miocene-age basalts
71 also occur in western Crater Flat, and as a dike complex in Solitario Canyon on the
72 northwestern flank of Yucca Mountain. Aeromagnetic surveys and drilling indicate that additional
73 basalts are buried beneath alluvium in Crater Flat and the Amargosa Desert to the south. Rates
74 and volumes of basaltic volcanism have declined significantly since Miocene time.

75
76 Assessment of repository performance includes evaluation of the impact of igneous
77 activity as well as other features, events and processes. A risk-informed performance
78 assessment uses the risk triplet for this evaluation. The risk triplet for igneous activity are: the
79 nature/scenarios of a potential igneous event, the probability of an igneous event intersecting
80 the proposed repository, and the consequences to the repository and to persons assumed to be
81 residing nearby the repository, the “RMEI (RMEI)”. The impact is measured as the expected
82 dose estimate from igneous activity at the repository site to the RMEI.

83 84 **Nature/Scenarios of Potential Igneous Activity**

85
86 If igneous activity intersects the proposed repository, there are two possible scenarios for
87 this potential interaction; the intrusive and extrusive scenarios.. The processes and
88 consequences for future radiological exposures vary significantly between these. The intrusion
89 scenario, involves intersection of the repository drifts by a dike extending upward and outward
90 from the source of the magma. An ascending dike could theoretically be deflected around a
91 repository by topographic and/or thermal-mechanical stress. In the latter case, for example, the
92 stress barrier that develops around a hot repository during the first 2000 years after closure
93 could deflect the dike. However, in the absence of definitive evidence to the contrary it is
94 generally assumed that the dike would propagate vertically under all circumstances and would
95 intersect the repository.

96
97 If a dike reaches the level of the repository, magma would be available to flow into drifts at
98 a rate that dependent on the magma viscosity and the rate of magma solidification as it contacts
99 the relatively cold drip shields, waste packages, and tunnel walls. The flow rate would also be
100 influenced by frictional losses at the dike/drift interface and partial obstruction of the tunnel by
101 waste packages and drip shields. DOE reports estimate that magma could fill a drift in about 5
102 minutes, given a dike ascent rate of 1 m/s and low viscosities between 10 Pa·s and 100 Pa·s.
103 Magma rising at 10 m/s could fill a drift in less than 1 minute. Recent work considering the loss
104 of water from the magma on approaching the surface suggests that magma viscosities could be
105 orders of magnitude higher than previously assumed, which would reduce the rate of magma
106 entry to drifts The potentially critical effects of higher viscosity magma, quenching and
107 solidification of magma on waste packages and drift walls have yet to be thoroughly evaluated
108 by DOE and NRC.

109
110 The Electrical Power Research Institute (EPRI) has analyzed plausible consequences of
111 magma entry into a repository. Given the possibility of higher viscosities than previously used in

112 analyses, EPRI concluded that partial intrusion of magma into a drift could create three zones.
113 The first zone, adjacent to the dike intersection, would result in magma fully engulfing the drip
114 shields and waste packages. This 'Red Zone' would be characterized by disrupted drip shields,
115 thermally weakened Alloy-22, and failure of spent fuel cladding. The waste packages in this
116 zone would have increased susceptibility over time to the effects of groundwater moving
117 through the unsaturated zone. Beyond the 'Red Zone' would be a 'Blue Zone,' where drip
118 shields and waste packages would not be inundated by magma, but would experience high
119 temperatures and potentially corrosive gases. Drip shields would remain intact, but failure of
120 the waste package outer barrier and spent fuel cladding could occur within a relatively short
121 time after the intrusive event. Beyond the Blue Zone would be the 'Green Zone' where waste
122 packages experience modest (<350° C) temperatures and the possible deposition of reactive
123 magmatic volatiles onto waste package surfaces. Waste packages and their drip shields would
124 be unaltered with respect to their resistance to corrosion in this zone.
125

126 An alternative intrusion scenario for magma-repository interaction has been proposed in
127 which magma would fill a drift and create enough pressure to generate a secondary dike to the
128 surface at a distance from the entry point. This so-called "dogleg" scenario with a resultant flank
129 eruption could potentially affect a large number of waste packages than a simple eruption
130 through the repository. The key factor here is whether the magma has the ability to fill the drift
131 quickly and re-pressurize it to the extent of nucleating a new dike elsewhere along the drift, in
132 spite of the dike continuing to the surface. This scenario arose from observations that
133 secondary (flanking) breakouts of magma sometimes occur elsewhere in association with
134 basaltic eruptions. Analysis of this "dog-leg" model by a DOE- organized peer review panel that
135 considered the propagation of pressure and stress through the dike system and the effect of
136 magma cooling has led to the view that the scenario is improbable.
137

138 The extrusive scenario involves the intersection of a cone-forming volcanic conduit to the
139 surface through the repository drift. The transition from flow in dikes to vent flow occurs early in
140 an eruptive sequence, and vents form under various conditions. In low-viscosity basalts, the
141 transition may occur when narrow parts of the dike freeze followed by mechanical and thermal
142 erosion of wider sections as the flow is repartitioned. A key difference between a volcanic vent
143 and a dike is that the vent is much smaller in diameter (generally <75 m) than a dike is long (1-5
144 km or more). Given a repository drift spacing of >50 m, a vent could directly intersect only one
145 drift and a relatively small number of waste packages within the cross-section of the vent. Due
146 to the perceived complexity of the processes involved, both NRC and DOE assume that the
147 small number of waste containers (approximately 1-10) entrained within a conduit during its
148 lifetime would be completely destroyed and the contents carried to the surface and ejected with
149 volcanic debris (tephra) of varying sizes. The degree to which ceramic or glass waste forms
150 and spent nuclear fuel could be reduced to fine particulate materials in a volcanic conduit is
151 uncertain, particularly during the first 1000 years when the waste packages and waste forms
152 should still be relatively intact. The manner and degree to which the fragments would be
153 incorporated in volcanic tephra is uncertain, but would involve magma quenching around the
154 ejected debris.
155

156 A detailed understanding of these scenarios is needed for estimating potential radiation
157 doses associated with igneous activity. The largest hypothetical radiation dose from extrusive
158 igneous activity during the first 1000 years after repository closure would result in the largest
159 contribution of igneous activity to radiation dose. After that time potential doses diminish
160 significantly because substantial fractions of shorter-lived radionuclides will have decayed.
161 Waste packages should be minimally degraded during the first 1000 years and therefore would
162 be more resistant to igneous thermal/physical effects during that time. However, packages

163 damaged during an intrusion or “dog-leg” scenario would be more susceptible to release of the
164 radioactive waste to ground water and eventually contamination of the water supplies of the
165 RMEI.
166

167 In considering the nature of the anticipated future igneous activity in the Yucca Mountain
168 region and its impact on the proposed repository, the DOE and NRC agree on several aspects.
169 This agreement is based on a study of on geologic analogs, especially those in the immediate
170 vicinity of the repository, and knowledge of the geological and tectonic history of the Yucca
171 Mountain region. Areas of agreement include the following:
172

173 Igneous events will be of similar nature to the Pleistocene volcanoes (~1 Ma) of the Yucca
174 Mountain region and particularly the most recent volcano, Lathrop Wells. That is igneous
175 events will occur as small-volume basaltic volcanoes that have effusion rates, power, and
176 duration similar to the Lathrop Wells volcano. The future occurrence of high power and
177 volume and long duration volcanic events involving felsic ash flows typical of those of
178 Miocene age in the Yucca Mountain region are not supported by evidence.
179

180 A portion of the duration of any volcanism will involve violent Strombolian activity with
181 plumes of ash distributed over the Yucca Mountain region. Analogous with the Lathrop
182 Wells eruption, fallout from a sustained eruption plume are likely to result in ash falls
183 extending to a few 10s of kilometers.
184

185 Multiple dikes are possible associated with an igneous event. The dike orientation will likely
186 be parallel to the maximum horizontal compressive stress in the region, roughly spanning an
187 azimuth from N to N30°E, and thus will favor extension of the dikes into Yucca Mountain
188 from volcanic activity within the northern portion of Crater Flat.
189

190 The diameter of the volcanic conduit assumed by both the NRC and DOE has a mean value
191 of about 50 m. NRC anticipates a range in diameter of 25 to 75 m.
192

193 Any dike intersecting the repository will continue to the surface above the repository.
194

195 Areas of disagreement between the DOE and NRC with regard to the nature of potential
196 igneous activity include:
197

198 The DOE assumes a single eruption (monogenetic) volcanic event associated with each
199 dike approaching the surface. In contrast NRC supports the possibility of multiple vents
200 including the potential for flank eruptions from a volcanic cone leading to satellite
201 (secondary) eruptions of lesser intensity.
202

203 The length of potential intruding dikes remains a matter of differing views. The DOE, on
204 the basis of interpretation of dikes associated with Pleistocene volcanoes in the Yucca
205 Mountain region, indicates that dike lengths will be of the order of magnitude of 1 km.
206 However, NRC considers a mean dike length of roughly 6 km with a range from 2 to 11
207 km to be more realistic based on dike lengths interpreted from both Pliocene and
208 Pleistocene igneous activity in the region.
209

210 In the event of formation of multiple dikes, DOE has considered the dikes to be of the
211 order of 1 to 2 m in width, while the NRC assumes a wider range from 1 to 10 m with a
212 mean of roughly 5 m.
213

214 **Probability of Future Igneous Activity**
215

216 The volume of basaltic volcanism near Yucca Mountain has dramatically declined during the
217 last 10 million years such that the Crater Flat volcanic field represents a zone of low activity
218 compared to other volcanic fields in the Central Base and Range region. This decline suggests
219 that magmatic systems near Yucca Mountain are waning. Further evidence of this lies in the
220 declining maximum lava effusion rate and fissure length of Plio-Pleistocene basaltic activity in
221 the Yucca Mountain region. There are no precursory indicators that volcanic activity is likely in
222 the immediate future (the next few years) in the region.
223

224 Results of recent drilling on magnetic anomalies following completion of the 2004
225 aeromagnetic survey have not yet been incorporated into published estimates of the probability
226 of igneous activity intersection of the proposed repository. However, information from the drilling
227 should reduce some of the uncertainty about buried basalts in the region and may influence the
228 statistical-mathematical models used in determining probability. Preliminary indications are that
229 these results will lead to a lowering the likelihood of future repository intersection by igneous
230 activity.
231

232 Both DOE and EPRI rely on probability estimates from the 1996 Probabilistic Volcanic
233 Hazard Assessment (PVHA) expert elicitation (i.e., $\sim 2 \times 10^{-8}/\text{yr}$). This analysis is being updated
234 with new scientific information, but published results will not be available until 2008. In
235 response to NRC staff concerns, DOE has agreed to provide (along with their licensing case)
236 the results of a single point sensitivity analysis for extrusive and intrusive igneous processes at
237 an annual probability of $10^{-7}/\text{yr}$. The NRC considers that the $10^{-7}/\text{yr}$ analyses will provide a
238 reasonably conservative approach for evaluating risks from igneous activity, but use of a single
239 point value fails to capture the impact of the uncertainty in probability estimates inherent to a
240 risk-informed analysis. The State of Nevada contractors suggest that the probability of future
241 volcanism may be at least an order of magnitude higher based on temporal clustering of
242 volcanic activity, hypothetical linkages between volcanism at Crater Flat and the Lunar Crater-
243 Reville Range area to the north of Yucca Mountain, and incorporation of new data that they
244 recommend be acquired in regions beyond the latest aeromagnetic survey.
245

246 A probability range for repository disruption of $10^{-9}/\text{yr}$ to $10^{-7}/\text{yr}$ is consistent with most
247 previous studies, the observed rate of Pleistocene volcanic activity (6 events in Crater Flat and
248 the northern Amargosa Desert in the last 1.75 million years), and the latest drilling results which
249 reduce the number of suspected buried basalts of post-Miocene age. It is significant that no
250 post-Miocene basalt was found in drilling magnetic anomalies in Jackass Flats. If buried
251 Pliocene basalts had been found there, that would suggest that the Plio-Pleistocene volcanic
252 zone of Crater Flat extends through Yucca Mountain significantly affecting the spatial models of
253 volcanism and increasing the modeled probability of future repository intersection. The recent
254 drilling indicates the opposite.
255

256 The rocks that comprise Yucca Mountain record an integrated tectonic-volcanic history since
257 the ~ 13 million year old surface rocks were deposited. No basaltic dikes have been found in the
258 potential repository footprint at Yucca Mountain despite more than 20 years of intensive site
259 characterization studies. It appears that the fault-bounded block that forms Yucca Mountain has
260 been a zone of relative volcanic quiescence during the last 10 million years. Since that time
261 volcanism has instead mainly focused within the alluvial basins to the east, west, and south,
262 with no evidence of post-Miocene activity (younger than ~ 5 million years) east of Yucca
263 Mountain in Jackass Flats. It is possible that dikes associated with volcanoes in these regions,
264 particularly Crater Flat could reach into Yucca Mountain.

265
266
267
268
269
270
271
272
273
274
275
276
277
278
279
280
281
282
283
284
285
286
287
288
289
290
291
292
293
294
295
296
297
298
299
300
301
302
303
304
305
306
307
308
309
310
311
312
313
314

Consequences of Igneous Activity

The consequences for future radiological exposures vary significantly among the postulated scenarios for volcanic interaction with the repository.

The extrusive event - DOE has estimated that the median number of waste packages that would be disrupted in a volcanic eruption scenario (i.e., intercepted by a conduit) is fewer than 10. The NRC staff currently assumes that volcanic vents would have an average diameter of ~50 m. The NRC staff further assumes that if the center of a vent were to coincide with the axis of a drift, then ~5 waste packages could be entrained within the cross-section of the conduit and potentially transported to the surface. Neither the NRC nor DOE evaluate magma-drift-waste package interactions in any detail. They instead assume that a small number of waste containers are completely destroyed and the entire contents are carried to the surface through a volcanic conduit in a cone-forming event. However, it is unclear how or whether the Alloy-22 waste packages, spent fuel elements, or the ceramic or glass waste forms themselves would be reduced to particles of respirable size, as currently assumed by the DOE and NRC staff. EPRI has concluded, based on multiple lines of evidence, that it is unlikely that waste packages would be breached by magma during an active eruption period. EPRI found that the expected consequence of an igneous extrusive event would be zero releases of radioactive matter from the repository to the atmosphere.

The intrusive event - DOE has estimated the number of waste packages that could be damaged in a potential future intrusive event. The igneous intrusion scenario shows a range of consequences, extending from virtually damage to no waste packages to damage to nearly all waste packages in the repository. The 50th percentile value indicates approximately 1600 waste packages could be impacted, out of over 11,000 waste packages in the repository. In performance assessment (TPA 4.1) the NRC staff estimated a mean value of 37 magma-induced mechanical failures from an intrusion event, based on a log uniform distribution from 1 to 1402 waste package failures. Igneous activity causes the largest increase in dose conditionally from both groundwater and airborne pathways, but the risk is still small when the probability of the volcanic event is factored into the calculations. EPRI concluded that magma viscosity would be larger than previously assumed. They estimate that only 0-6 waste packages could become engulfed by magma intrusion in a waste emplacement drift. They further estimate that 14-24 waste packages could be significantly affected by heat and corrosive gases, but not engulfed by magma.

Viscosity is the most important magma property to understand because it controls the flow behavior and the distance that magma could penetrate a repository. The Committee observes that previous researchers have not been consistent in their approach to estimating the viscosity of the Yucca Mountain basalt as it ascends and degasses with approach to the surface. There has been a tendency to assume rheological properties pertaining to both wet, cool magmas and dry, hot magmas, leading incorrectly to the postulate of a highly explosive system with highly mobile lavas. Therefore, previous claims of severe consequences of igneous intersection appear to be poorly founded. The potential Yucca Mountain magma is probably a wet, cool explosive magma with relatively immobile lavas. The Pleistocene lava flows in Crater Flat and at Lathrop Wells demonstrate that the lavas had high viscosities and were relatively immobile. Characteristics of these lava flows indicate viscosities orders of magnitude larger than had been assumed in analyses of igneous interaction with a repository. These high viscosities, along with magma solidification effects, would significantly reduce the distance that

315 magma could penetrate into tunnels and thereby reduce the number of impacted waste
316 packages.

317
318 The so-called “dogleg” scenario refers to a hypothetical scenario proposed by the NRC staff
319 in which magma might rapidly fill a drift and create enough pressure to generate (at a distance
320 from the entry point) a secondary dike to the surface. This “dog-leg” model was analyzed by the
321 Igneous Consequences Peer Review (ICPR) Panel (Detournay et al., 2003), by EPRI, and by
322 DOE. In TPA 4.1 analyses the NRC staff assumed that a mean value of 51 waste packages
323 could be entrained by an extrusive event and contained in volcanic ejecta. ICPR considered the
324 propagation of either a magmatic or pyroclastic “dog-leg” scenario to be quite improbable, found
325 that the initial and boundary conditions in the model are unrealistic, but recommended further
326 analyses to assess the impacts of a partially coupled pyroclastic flow scenario on repository
327 performance. EPRI concluded that their independent modeling results show that pressure
328 conditions in a repository intersected by magma would be significantly less forceful than
329 postulated by the NRC staff. DOE concluded that the “dogleg” model overestimates the
330 violence of magma-repository interaction. Use of realistic boundary conditions (including
331 compressible walls and backfill, permeable country rock and backfill, phase separation in the
332 magma-volatile mixture, partial blockage of the drift by waste canisters and other engineering
333 features, and the axial spacing of the canisters) would greatly reduce the amplitude of any
334 shock wave that might form. Use of realistic initial conditions such as those at the dike tip would
335 preclude shock waves for all but the most rapid magma ascent rates.

336
337 **Remobilization** – DOE has performed studies of ash distribution near Lathrop Wells to
338 evaluate the fraction of basaltic ash components as a function of distance from the tephra sheet.
339 These data indicate that the concentration of basaltic ash in surface sediments would decrease
340 to about 50 percent within 1 km of the head of the tephra sheet drainage on the eastern side of
341 Lathrop Wells. DOE’s TSPA model calculates doses using the initial ash-layer thicknesses and
342 radionuclide concentrations from ASHPLUME, modified by a time dependent soil removal
343 factor, estimated to range from 0.02 to 0.04 cm/yr. Given these erosion rates, ash layers would
344 be removed within a few centuries, depending on the initial thickness.

345
346 DOE has developed an alternative ash redistribution model that assumes areas of the
347 RMEI location that have not been subject to fluvial erosion or deposition over the last 10 kyr will
348 not be subject to fluvial activity within the next 10 kyr. The alternative model does not
349 incorporate eolian erosion or deposition or the long-term geologic dynamics of fan interchannel
350 divide and channel interactions. This model includes several key assumptions: (1) the climate
351 through much of the regulatory period will be similar to today’s climate and will have relatively
352 little impact on the Fortymile Wash alluvial fan; (2) distributary channels in the RMEI location will
353 not migrate during the time period of interest; and (3) eolian transport to the RMEI location can
354 be neglected because it is not significant when compared to fluvial transport processes.

355
356 The NRC staff has developed a sediment-budget approach to model the long-term fluvial
357 redistribution of basaltic tephra in Fortymile Wash that flows into the vicinity of the RMEI. Using
358 parameters specific to Fortymile Wash and a hypothetical eruption at Yucca Mountain, they
359 concluded that substantial tephra deposits can persist for more than 1,000 years in arid terrains,
360 even with a period of accelerated erosion after the eruption. It is estimated that ~98 percent of
361 the tephra deposit remains in the Fortymile Wash catchment basin after 100 years and 50
362 percent remains after 1,800 years. NRC suggests that the amount of remobilized tephra may
363 be large—even when mixed with ambient sediment—and could significantly affect airborne
364 radioactive particle concentrations for the RMEI. The NRC staff assumes that all contaminated

365 ash that is fluviually remobilized would be deposited in an “active” fan located west of the RMEI,
366 but once there, no ash is permitted to leave this fan area except by wind erosion.
367

368 The Committee has observed that large floods would dominate the process of fluvial
369 erosion and transport and would carry contaminated ash beyond the active fan and all the way
370 to the Amargosa River and beyond. In the short period of historical record, two large floods in
371 the Fortymile Wash/Amargosa River system have reached Death Valley. The sediments most
372 likely to be suspended and transported long distances are the smallest particles – the same
373 particles of concern for respiration or ingestion.
374

375 EPRI has commented on various conservatisms used in the NRC and DOE analyses.
376 EPRI’s model of ash transport modeling showed that particles smaller than 130 microns in
377 diameter would not be deposited at the compliance point. Both DOE and NRC use a
378 conservative assumption that all deposited material is in the respirable size range, although
379 neither NRC nor DOE discuss realistic mechanisms that would break down tephra in this way.
380

381 Wind (eolian) transport could result in an inhalation dose to the RMEI in the extrusive
382 scenario. Wind transport can move radioactively contaminated ash from fluvial deposits as well
383 as from material deposited on the surface of the ground as a result of the eruption itself. The
384 mechanism of wind transport is the same in both cases: ash is remobilized by wind, and the
385 remobilized ash is carried and dispersed predominantly downwind. The shape of the
386 remobilized plume depends on particle mass and density, their aerodynamic properties, and on
387 meteorological conditions. Both DOE and NRC have estimated triangular particle size
388 distribution of ash particles, with the mean and mode at 1 micron aerodynamic diameter. Both
389 agencies have estimated the dimensions and density of spent fuel particles that could be
390 incorporated into and dispersed with the ash. The code ASHPLUME has been used to model
391 this dispersion. The NRC has designed a new module, REMOB, for estimating resuspension
392 and remobilization, but the Committee has not seen the foundations for results from this model.
393 Performance assessment shows that igneous activity will increase the dose to the RMEI if a
394 volcanic event occurs within the first few thousand years after closure of the repository. The
395 effect of an igneous event relative to other contributors to the RMEI dose will decrease with
396 time.
397

398 The uptake models of Federal Guidance Report (FGR) 13 as a source of dose conversion
399 factors are widely accepted as a refinement compared to earlier clearance models. Both NRC
400 and DOE use FGR 13 dose conversion factors in their analyses although some of these dose
401 conversion factors are conservative.
402

403 **[Note: Conclusions to be added throughout the text of the Executive Summary upon**
404 **completion of the Igneous Activity Working Group meeting.]**
405

406
407
408
409
410
411 **Abbreviations and Acronyms**

412		
413	AMAD	Activity mean aerodynamic diameter [for particles]
414	BSC	Bechtel SAIC Company LLC
415	CFR	Code of Federal Regulations

416	CNWRA	Center for Nuclear Waste Regulatory Analyses (San Antonio, TX)
417	CRWMS M&O Contractor	Civilian Radioactive Waste Management System Management and Operating Contractor
418		
419	DOE	US Department of Energy
420	EPA	US Environmental Protection Agency
421	EPRI	Electric Power Research Institute
422	FEP	Features, Events, and Processes
423	ICPR	Igneous Consequences Peer Review [Panel] [Detournay et al., 2003]
424	NMSS	[NRC's] Office of Nuclear Material Safety and Safeguards
425	NRC	US Nuclear Regulatory Commission
426	NWTRB	US Nuclear Waste Technical Review Board
427	OCRWM	[DOE's] Office of Civilian Radioactive Waste Management
428	PVHA	Probabilistic Volcanic Hazard Assessment
429	PVHA-U	Probabilistic Volcanic Hazard Assessment - Update
430	RMEI	Reasonably maximally exposed individual
431	TPA	NRC's Total-System Performance Assessment
432	TSPA	DOE's Total System Performance Assessment
433	USGS	US Geological Survey
434	YMP	[DOE's] Yucca Mountain Project
435		
436		

437 Glossary of Terms [Incomplete]

438		
439	aa flow	a Hawaiian term for lava flows typified by a rough, jagged, spinose, clinkery surface [Neuendorf et al., 2005]
440		
441		
442	adiabatic expansion	increase in the volume of a substance during which no gain or loss of heat is allowed to occur [Lewis, 1993]
443		
444		
445	aeromagnetic anomalies	spatial disturbance in the magnetic field of the Earth caused by horizontal variations in the magnetic polarization of the Earth
446		
447		
448	agglomerate	chaotic assemblage of coarse angular pyroclastic materials [Neuendorf et al., 2005]
449		
450		
451	aggrade	build up vertically
452		
453	alluvium	clay, silt, sand, and gravel deposited during comparatively recent geologic time by a stream or other body of running water [Neuendorf et al., 2005]
454		
455		
456		
457	AMAD	activity median aerodynamic diameter; the diameter of a sphere, of density 1 gm/cm ³ , that has the same terminal settling velocity in air as that of an aerosol particle whose activity is the median for the entire aerosol [Shleien et al, 1998].
458		
459		
460		
461		
462	ash (volcanic)	fine pyroclastic material (under 2 mm diameter); the term usually refers to unconsolidated material [Neuendorf et al., 2005]
463		
464		

465	basalt	a general term for dark-colored mafic igneous rocks, commonly
466		extrusive but locally intrusive (e.g., as dikes), composed chiefly of
467		calcic plagioclase and clinopyroxene [Neuendorf et al., 2005]
468		
469	caldera	a large, basin-shaped volcanic depression, more or less circular or
470		cirquelike in form, the diameter of which is many times greater than
471		that of the included vent or vents, no matter what the steepness of
472		the walls or form of the floor. It is formed by collapse during an
473		eruption [Neuendorf et al., 2005]
474		
475	cation	an atom or molecule that has lost an electron and thus acquired a
476		positive electric charge [Lewis, 1993]
477		
478	compliance period	
479		
480	corrosion	the electrochemical degradation of metals or alloys due to reaction
481		with their environment, which is accelerated by the presence of
482		acids or bases [Lewis, 1993]
483		
484	crustal plate	a torsionally rigid thin segment of the Earth's lithosphere, which
485		may be assumed to move horizontally and adjoins other plates
486		along zones of seismic activity [Neuendorf et al., 2005]
487		
488	density	mass per unit volume [Lewis, 1993]
489		
490	desert pavement	a natural residual concentration of wi-polished, closely packed
491		pebbles, boulders, and other rock fragments, mantling a desert
492		surface where wind action and sheetwash have removed all smaller
493		paricles, and usually protecting the underlying finer-grained material
494		from further deflation [Neuendorf et al., 2005]
495		
496	desert varnish (rock varnish)	a thin dark shiny film or coating composed of iron oxide
497		accompanied by traces of organic matter, manganese oxide, and
498		silica [Neuendorf et al., 2005]
499		
500	dike	a tabular igneous intrusion that cuts across the bedding or foliation
501		of the country rock [Neuendorf et al., 2005]
502		
503	drift	a nearly horizontal passageway (tunnel) in the repository [Merriam-
504		Webster,1988]
505		
506	elicitation	a formal, highly structured, and well-documented process for
507		obtaining the judgments of multiple experts. [Kotra et al, 1996]
508		
509	en echelon	said of geologic features (e.g., faults or dikes) that are in an
510		overlapping or staggered arrangement [Neuendorf et al., 2005]
511		
512	eolian	borne, deposited, produced, or eroded by the wind (from Eolus, god
513		of the winds) [Merriam-Webster,1988]
514		

515	equilibrium constant	a number that relates the concentrations of starting materials and products of a reversible chemical reaction to one another [Lewis, 1993]
516		
517		
518		
519		
520	exsolve	
521	extrusive scenario	
522		
523	fan (alluvial)	a low, outspread, relatively flat to gently sloping mass of loose rock material, shaped like an open fan or a segment of a cone, deposited by a stream at the place where it issues from a narrow mountain valley upon a plain or broad valley [Neuendorf et al., 2005]
524		
525		
526		
527		
528		
529	felsic	an adjective describing an igneous rock with abundant light colored minerals, e.g., quartz, feldspars, and muscovite
530		
531		
532	Fickian diffusion	the spontaneous mixing of one substance with another when in contact or separated by a permeable membrane. The rate of diffusion is proportional to the concentration of the substances. The theoretical principles are stated in Fick's laws. [Lewis, 1993]
533		
534		
535		
536		
537	fluvial	of or pertaining to rivers
538		
539	geodetic data	
540		
541	high-level radioactive waste	(1)the highly radioactive material resulting from the reprocessing of spent nuclear fuel, including liquid waste produced directly in reprocessing and any solid material derived from such liquid waste that contains fission products in sufficient concentrations; (2) Irradiated reactor fuel [10CFR63.2]
542		
543		
544		
545		
546		
547	igneous activity	
548	ignimbrite	the deposits of a pyroclastic flow [Neuendorf et al., 2005]
549		
550	intrusive scenario	
551		
552	isothermal	at constant temperature [Lewis, 1993]
553		
554	kernel function	
555	liquidus	
556	lithosphere	the outer, relatively rigid layer of the Earth that responds to the emplacement of a load by flexural bending [Neuendorf et al., 2005]
557		
558		
559		
560	lithostatic stress	a state of stress in which the normal stresses acting on any plane are equal (a term used for overburden stress in the Earth's crust) [Neuendorf et al., 2005]
561		
562		
563		
564	lognormal distribution	the exponential of a normal distribution
565		

566	mafic	said of an igneous rock composed chiefly of one or more ferromagnesian, dark-colored minerals [Neuendorf et al., 2005]
567		
568		
569	magma	naturally occurring molten or partially molten rock, generated within the Earth and capable of intrusion and extrusion from which igneous rocks are derived [Neuendorf et al., 2005]
570		
571		
572	mantle rock	
573	order of magnitude	a range of values which begins at any value and extends to ten times that value [Lewis, 1993]
574		
575		
576	orogeny	the process of forming mountains [Neuendorf et al., 2005]
577		
578	oxidation	originally, a reaction in which oxygen combines chemically with another substance; usage has broadened to include any reaction in which electrons are transferred. The substance that loses electrons is oxidized; the substance that gains electrons is reduced [Lewis, 1993]
579		
580		
581		
582		
583	paleosurface	
584	petrologic	
585	phenocryst	
586	plate tectonic paradigm	
587	pyroclastic	
588	radiation dose	a generic term that includes absorbed dose (the amount of ionizing radiation absorbed in matter), effective dose, equivalent dose, committed effective/equivalent dose. See the definition for total effective dose equivalent . [Shleien et al, 1998]
589		
590		
591		
592		
593	radioactive material	any material exhibiting radioactivity. See radionuclide
594		
595	radionuclide	an isotopic form of an element (either natural or artificial) that exhibits radioactivity. Radioactivity is atomic emission resulting from natural or artificial nuclear transformation. [Lewis, 1993]
596		
597		
598		
599	remobilization	
600	Reynolds number	the function used in fluid flow calculation to determine whether flow is streamline or turbulent; proportional to flow velocity and density; inversely proportional to viscosity [Lewis, 1993]
601		
602		
603		
604	rheology	
605	rhyolitic	
606	RMEI	the reasonably maximally exposed individual is a hypothetical person who (a) lives in the accessible environment above the highest concentration of radionuclides in the plume of contamination; (b) has a diet and living style representative of the people who now reside in Amargosa Valley, Nevada. (c) uses well water with average concentrations of radionuclides based on an annual water demand of 3000 acre feet; (d) drinks 2 liters of water per day from wells drilled into the ground water at the location specified in (a); and (e) is an adult [10 CFR 63.312]
607		
608		
609		
610		
611		
612		
613		
614		
615		
616	scoria	

617	sedimentary	
618	seismicity	
619	spent fuel cladding	the outer jacket of nuclear fuel elements which contains and
620		supports the fuel material, protects the fuel, and prevents the release
621		of fission products into the reactor coolant [OTA 1985]
622	stratocone volcanoes	
623	Strombolian	
624	subduction	
625	tectonic event	
626	tephra	
627	tomographic methods	a method for finding the velocity and reflectivity (or other physical
628		properties depending on the type of geophysical observations)
629		distribution from a multitude of observations using combinations of
630		(seismic) source and receiver locations (Sheriff, 1991)
631		
632	total effective dose equivalent	the sum of the dose equivalent for external exposure and the
633		committed effective dose equivalent for internal exposure. The dose
634		equivalent is the product of the absorbed dose, quality factor, and all
635		other necessary modifying factors at the location of interest. The
636		committed dose equivalent is the dose received from an intake of
637		radioactive material during the 50-year period following the intake.
638		[Shleien et al, 1998]
639		
640	TPA	NRC's total performance assessment of the proposed repository.
641		Performance assessment is a process which (1) Identifies the
642		features, events, processes and sequences of events that might
643		affect the Yucca Mountain disposal system and their probabilities of
644		occurring during 10,000 years after disposal; (2) Examines the
645		effects of these on the performance of the disposal system; and (3)
646		Estimates the dose incurred as a result of releases [10 CFR 63.2]
647		
648	TSPA	DOE's total system performance assessment of the proposed
649		repository
650		
651	viscosity	the internal resistance to flow exhibited by a fluid [Lewis, 1993]
652		
653	volatile	an element or compound that has a vapor pressure equal to or
654		greater than 0.1 mm Hg that is not a gas at ambient temperatures
655		[Lewis, 1993]
656		
657		
658		
659		
660		

661
662
663
664
665
666
667
668
669
670
671
672
673
674
675
676
677
678
679
680
681
682
683
684
685
686
687
688
689
690
691
692
693
694
695
696
697
698
699
700
701
702
703
704
705
706
707
708
709

CONTENTS

1. Introduction

- 1.1 Igneous Activity and the Proposed Yucca Mountain Repository**
- 1.2 Objective and Rationale of Report**
- 1.3 Scope of Report**
- 1.4 Content and Organization of Report**
- 1.5 Report Preparation Process**
- 1.6 Constraints on the Report**
- 1.7 Previous Reviews of Igneous Activity Technical Bases**

2. Brief Geologic History of the Yucca Mountain Region

3. Overview of Igneous Activity Processes

- 3.1 Introduction**
- 3.2 Origin and Nature of Igneous Activity**
 - 3.2.1 Magma Generation**
 - 3.2.2 Magma Composition**
 - 3.2.3 Volcanoes and Their Products**
- 3.3 Magma/Repository Interaction**
 - 3.3.1 Nature of Magma Ascent**
 - 3.3.2 Key Features of Magmatic Dikes**
 - 3.3.3 Basic Nature of Eruptive Event**
 - 3.3.4 Interaction with Repository and Canisters**
- 3.4 Dispersal of Contaminated Ash**
 - 3.4.1 How is Ash Dispersed?**
 - 3.4.2 How does Ash become Contaminated?**
- 3.5 Remobilization and Resuspension of Contaminated Ash**
- 3.6 Doses from Contaminated Ash**
 - 3.6.1 Inhalation Dose**
 - 3.6.2 Ingestion Dose**

4. Nature of Potential Igneous Events in the Yucca Mountain Region

- 4.1 Introduction**
- 4.2 Volcanic Analogs**
- 4.3 NRC and DOE positions**
 - 4.3.1. NRC/DOE KTI Agreement on the Likely Range of Tephra Volumes**
 - 4.3.2. DOE Approach to Event Definition**
 - 4.3.3. NRC/CNWRA Approach to Event Definition**
- 4.4 Summary**

5. Probability of Potential Igneous Activity

- 5.1 Introduction**
- 5.2 Spatial and Temporal Distribution of Igneous Activity**
 - 5.2.1 Introduction**
 - 5.2.2 Surface Exposures**
 - 5.2.3 Known Occurrences of Buried Basalts**
 - 5.2.4 Undetected Igneous Activity**
 - 5.2.5 Change in Basaltic Volcanism With Time**

710	5.3 Time Period Used in Extrapolation of Igneous Activity
711	5.4 Controls on Occurrence of Igneous Activity
712	5.5 Prediction Methods
713	5.5.1 Physical Precursors
714	5.5.2 Linkages to Other Volcanic Zones
715	5.5.3 Mathematical and Statistical Techniques
716	5.5.3.1 General Methodology
717	5.5.3.2 Locally Homogeneous Spatial and Temporal Models
718	5.5.3.3 Nonhomogeneous Spatial Models
719	5.5.3.3.1 Parametric Spatial Density Function
720	5.5.3.3.2 Nonparametric Spatial Density Function
721	5.5.3.4 Nonhomogeneous Temporal Models
722	5.6 Treatment of Probability in Performance Assessments
723	5.6.1 DOE Analysis
724	5.6.2 EPRI Analysis
725	5.6.3 NRC Analysis
726	5.7 Views on Igneous Activity Probability
727	5.7.1 NRC Staff
728	5.7.2 Department of Energy
729	5.7.3 Probabilistic Volcanic Hazard Analysis (PVHA)
730	5.7.4 DOE Igneous Consequence Peer Review Panel (ICPR)
731	5.7.5 Electric Power Research Institute (EPRI)
732	5.7.6 State of Nevada and Consultants
733	5.7.7 Nuclear Energy Institute (NEI)
734	5.7.8 Other Estimates of Probability
735	5.7.9 ACNW Observations of PVHA-U
736	5.8 Summary
737	
738	6. Consequences of Igneous Activity Intersecting Repository
739	6.1 Introduction
740	6.2 Effects from an Intrusive Event (Magma/Drift Interaction)
741	6.2.1 Critical Magmatic Aspects
742	6.2.1.1 Magma Composition
743	6.2.1.2 Magma Viscosity
744	6.2.1.3 Perspectives on Magma Viscosity
745	6.2.1.3.1 DOE Perspective
746	6.2.1.3.2 EPRI Perspective
747	6.2.1.3.3 Additional Comments on Magma Viscosity
748	6.2.2 DOE, EPRI, and NRC Perspectives on the Magma-Waste Package
749	Interactions
750	6.2.2.1 DOE Perspective
751	6.2.2.2 EPRI Perspective
752	6.2.2.3 NRC Perspective
753	6.2.2.4 Summary of Views
754	6.3 Effects from an Extrusive (Volcanic) Event
755	6.3.1 Number of Waste Packages Potentially Affected by an Eruption
756	6.3.2 NRC Approach in Performance Assessment
757	6.3.3 EPRI Approach and Conclusions
758	6.3.4 Comments on Potential Fate of High-Level Waste in a Volcanic Vent
759	6.4 Remobilization of Contaminated Volcanic Ash

760 **6.4.1 Introduction**
761 **6.4.2 Characteristics of Fortymile Wash Drainage System**
762 **6.4.3 Approaches to Fluvial Sediment Transport and Erosion**
763 **6.4.3.1 NRC Approach to Fluvial Volcanic Ash Redistribution**
764 **6.4.3.2 EPRI Analysis of Fluvial Transport from Extrusive Volcanic**
765 **Activity**
766 **6.4.3.3 DOE Volcanic Ash Fluvial Redistribution Model**
767 **6.4.3.4 NWTRB Comments on Potential Consequences of Igneous**
768 **Activity**
769 **6.4.4 NRC and DOE Analysis of Effects of Eolian Transport and Erosion**
770 **6.4.4.1 NRC Analysis**
771 **6.4.4.2 DOE Analysis**
772 **6.4.5 Summary**
773 **6.5 Summary (Igneous Consequences)**
774

775 **7. Conclusions**

776 [Conclusions will be added to this report upon completion of the ACNW Igneous Activity
777 Working Group Meeting in Rockville, MD on February 13 and 14, 2007. The primary
778 questions to be addressed at this meeting by the Committee, stakeholders, and external
779 experts are:

- 781 • Does the ACNW report on the technical basis of igneous activity probability and
782 consequences address the risk-significant topics related to igneous activity at Yucca
783 Mountain?
- 784 • Does the report capture the range of views of the interested parties with respect to
785 the technical basis for decision making on these topics including definitions of
786 volcanic events, geologic periods of interest in predicting probability, igneous activity
787 probability, magma/drift interaction leading to both extrusive, intrusive scenarios,
788 potential consequences for the risk from a high-level waste repository, etc. If not, the
789 positions detailed in the report will be clarified from published position papers in the
790 final ACNW report.]
791

792
793
794
795 **List of Figures**

- 797 Figure 1.1 a False color Landsat image shows local geographic features and Plio-Pleistocene
798 (last 5 million years) volcanic centers near Yucca Mountain and the proposed high-level waste
799 repository. The location of this image is shown in Figure 1.1b. [After O’Leary et al., 2002]
- 800 Figure 1.1 b Location map of Figure 1.1a shown in green in south-central Nevada and adjacent
801 California. [After O’Leary et al., 2002]
- 802 Figure 1.2 a Logic chart of components involved in determining the definition of the nature of
803 possible future igneous events at Yucca Mountain.
- 804 Figure 1.2 b Logic chart of components involved in determining the probability of future igneous
805 activity intersecting the proposed Yucca Mountain HLW repository.

806 Figure 1.2 c Logic chart of components involved in determining the consequences of an
807 intrusive event intersecting the Yucca Mountain HLW repository.

808 Figure 1.2 d Logic chart of components involved in determining the consequences a volcanic
809 event intersecting the Yucca Mountain HLW repository.

810 Figure 1.3 The prediction of the basaltic volcanism in the Yucca Mountain region during the time interval 4 to 2
811 Ma based on the occurrence of volcanism in the region during the prior 2 Myr (6 to 4 Ma). Basaltic volcanism
812 during the period of 6 to 4 Ma is shown in green. [After Crowe, 2005]

813 Figure 1.4 The observed basaltic volcanism in the Yucca Mountain region during the time interval 4 to 2 Ma
814 based on the occurrence of volcanism in the region during the prior 2 Myr (6 to 4 Ma). Basaltic volcanism
815 during the period of 4 to 2 Ma is shown in green and magnetic anomalies in Amargosa Valley that are
816 interpreted to have a source in basaltic volcanism during this time interval are shown by green stars. [After
817 Crowe, 2005]

818 Figure 2.1 Timeline of events in the Yucca Mountain region related to igneous activity and
819 geological periods of time.

820 Figure 2.2 Elevation map of the southwestern United States showing the position of Yucca
821 Mountain and major geologic, structural, and topographic features. [After McKague et al., 2006]

822 Figure 2.3 Geological Map of the Yucca Mountain Region. [After Valentine et al., 2006a]

823 Figure 2.4 (Top) Interpretation of seismic reflection profile across Crater Flat and Yucca
824 Mountain. (Bottom) Gravity model along seismic profile with density of rock units in gm/cm^3 .
825 [After Brocher et al., 1998]

826 Figure 2.5 The limit of the Southwestern Nevada Volcanic Field (from Byers et al., 1989)
827 indicated by the dashed line. Several volcanic calderas have been identified as the sources of
828 the intense felsic volcanic activity in the field. The caldera is no longer generally recognized
829 (Crowe et al., 1995). [After Crowe et al., 1995]

830 Figure 3.1 Conceptual model of igneous activity. Magma rises via dikes (left) leading to effusion
831 of magma fountains along the length of dikes that reach the surface (center) and finally to
832 focusing magma eruption in a conduit resulting in a volcanic cone (right). [After Valentine, 2006]

833 Figure 3.2 Inferred eruption events at the Lathrop Wells volcano. a) and b) are respectively
834 simplified cross-sections and plan views of the early stage of eruption and c) and d) illustrate the
835 later stage of eruption with cone building dominated by fallout (c) and effusion of the eastern
836 lava field (d). [After Valentine et al., 2005]

837 Figure 3.3. Schematic depiction of the anticipated repository tunnel (drift) containing waste
838 packages within Yucca Mountain.

839 Figure 3.4 Identification and linkages of abstractions in the igneous intrusion scenario of DOE's
840 TSPA. [After Valentine, 2006]

841 Figure 3.5 Schematic of the steady flow geometry that may enable a steady basaltic eruption to
842 develop (dog-leg scenario: a) with flow along the original dike; b) with magma being diverted
843 along the drift before surfacing along a new fissure; and c) with magma being diverted along the
844 drift and into the main access drift from where it vents to the surface. [After Woods et al., 2002]

845 Figure 3.6 Identification and linkages of abstractions in the eruption scenario of DOE's TSPA.
846 [After Valentine, 2006]

847
848 Figure 3.7. A contour plot illustrating the expected tephra dispersion for eruption and
849 meteorological parameters listed in Table 3.1. The plot coordinates indicate location of the
850 deposited material with respect to the eruption site. The vertical axis is in a northerly direction;
851 the horizontal axis, easterly. The numbers refer to universal transverse Mercator UTM grid
852 locations; units are meters. From
853 <http://www.cas.usf.edu/~cconnor/parallel/tephra/tephra.html#input>.

854 Figure 3.8 Schematic diagram of processes involved in ash remobilization.

855 Figure 3.9 Resuspended fraction of deposited material from the Anspaugh et al. (2002)
856 equation for long-term resuspension. Graph shows the fraction of resuspended material that is
857 carried 20 miles by wind.

858 Figure 4.1 Photo of Pleistocene volcanoes in Crater Flat as viewed over the crest of Yucca
859 Mountain. From right to left the volcanoes are Black Cone, Red Cone, and Little Cone. Bare
860 Mountain is in the mid-background.

861 Figure 5.1 Locations of basaltic volcanoes in the Yucca Mountain region. Letters and numbers
862 are magnetic anomalies of high to moderate confidence that represent possible buried basalts.
863 Drilling at "A", "B", "D", "G", 23P, and JF-3 (not shown-just north of 23P) has detected basalts.
864 Map coordinates in UTM Zone 11 Meters, North American Datum 1927. [After Connor et al.,
865 2002 and Coleman et al., 2004]

866 Figure 5.2. (A) Lathrop Wells cone (Age is 80 ka and height is ~130 m). (B). View of the ~1 Ma
867 old cinder cones in Crater Flat, as seen looking northeast from Steve's Pass at the southern
868 margin of Crater Flat. Yucca Mountain is on the far horizon at right side of image. (C). Little
869 Black Peak, ~0.3 Ma (in foreground).

870 Figure 5.3. Person at left is standing on a dike of Pliocene age in southeastern Crater Flat.
871 The distant cone at center is the Pliocene-aged Black Cone. Between Black Cone and the
872 figures at right are the eroded remnants of two Pliocene vents (conduits).

873 Figure 5.4 High-resolution aeromagnetic anomaly map and locations of holes (solid white
874 circles) drilled to determine if the magnetic anomalies are derived from basalts. Solid red circles
875 indicate selected pre-existing drill holes that provide key constraints on the location of buried
876 basalt near Yucca Mountain. Qb=Quaternary basalt, Pb=Pliocene basalt, Mb=Miocene basalt.
877 [After Perry et al., 2005 and Perry et al., 2006]

878 Figure 5.5. Estimated extension rates in Crater Flat basin as a function of time and magma
879 volume erupted as a function of time. [After Fridrich et al., 1999]

880 Figure 5.6 Age vs. volume of Plio-Pleistocene volcanic episodes in the Yucca Mountain region.
881 Figure includes buried Pliocene basalts in the northern Amargosa Desert. The diameter of the
882 circles is proportional to volume. The dot at far lower right represents Lathrop Wells. The dot to
883 its left represents Sleeping Butte. The small circle at 1.1 Ma represents the five Pleistocene
884 cones of Crater Flat. [After Perry, 2006]

885 Figure 5.7 Plot of fissure length (lines) and lava effusion rate (dots) for Plio-Pleistocene
886 volcanoes of the Southwestern Nevada Volcanic Field. Note that age determinations do not
887 allow discrimination of relative ages amongst the five Pleistocene volcanoes in Crater Flat,
888 therefore they are plotted in random order around 1 Ma. The eruptive products of SW and NE
889 Little Cones are largely buried by alluvium and mapped by aeromagnetic anomalies [Valentine
890 et al., 2006]; their volumes are lumped together in this plot. [After Valentine and Perry, 2006]

891 Figure 5.8 Age and distribution of Pliocene-Pleistocene basaltic volcanoes in Crater Flat-Lunar
892 Crater zone (CFLC). [After Smith et al., 2002]

893 Figure 5.9 Time-event plot showing episodic nature of volcanism in the Crater Flat-Lunar Crater
894 zone. [After Smith et al., 2002]

895 Figure 5.10 (top) Mean dose arising from extrusive igneous activity shown with various times for
896 the volcanic even in 350 realizations. (below) Contribution of extrusive igneous activity to the
897 total dose, weighted by an annual probability for the volcanic event of 10^{-7} /year. [After Mohanty
898 et al., 2004, p. 3-84].

900 Figure 5.11. Comparison of selected estimates of the probability of future volcanic intersection
901 of a repository at Yucca Mountain (from Perry et al., 2000).

902 Figure 6.1 Schematic depiction of two stages of Cinder Cone volcanism and the underlying
903 magmatic eruptive column. Magma rich in dissolved volatiles saturates and vesiculates with
904 approach to Earth's surface and reduction in confining pressure. In essence the magma gets
905 the 'Bends.' Increased bubble formation eventually leads to fragmentation of the magma and
906 the explosive production of tephra and ash. Also shown for each stage are the governing
907 magma viscosities (left column) as estimated for each stage of the eruptive process. Notice the
908 large contrast in viscosity between the gas rich tephra and the late stage lava flows. (A) The
909 early stage of Cinder Cone formation and eruption, schematically depicting explosive tephra and
910 ash production leading to formation of the volcanic cone and an ash plume. (B) The later stage
911 of Cinder Cone eruption when the ascending magma has progressively degassed with
912 approach to the surface and the eruption is dominated by the extrusion of highly viscous,
913 sluggishly moving lava flows emanating from the basal area of the cone.

914 Figure 6.2 Relative viscosity as a function of capillary number (source: B. Marsh).

915 Figure 6.3 Viscosity (μ) as a function of crystallinity (Φ). [After Mooney, 1951; Roscoe, 1952;
916 Gay et al., 1969]

917 Figure 6.4 Magma phase diagram showing change in viscosity (μ) as a function of temperature.

918 Figure 6.5 Phases in a volcanic eruption column showing the three regimes (wet magma, water
919 saturated bubbly magma, and particulate-laden gas) and associated phase equilibria diagram
920 for Lathrop Wells basalt.

921 Figure 6.6 Phase diagram for Lathrop Wells basalt under dry and wet conditions. [After Marsh
922 and Coleman, 2006]

923 Figure 6.7. Magma viscosity calculated at 1150° C during near-surface ascent and degassing
924 [After Detournay et al., 2003].

925 Figure 6.8. The solubility of volatiles in magmas is a function of temperature, pressure, and the
926 compositions of the liquids and gases. This diagram shows the solubility of water in basaltic
927 magma as a function of water pressure at 1100 deg. C. The pressure of another gas, such as
928 carbon dioxide, would decrease the solubility of water. At earth surface conditions (pressure =
929 1 bar) the solubility of water is virtually zero (vertical axis of diagram is marked in kilobars) [After
930 McBirney, 2007].

931 Figure 6.9 Radial extent of the Lathrop Wells, Nevada lava field as a function of the duration of
932 the flow event. The observed flow extent is about 1 km.

933 Figure 6.10. Schematic of zones of intruding magma effects in a repository drift on the
934 engineered barrier system (EBS). Magma is assumed to completely the spaces in the “Red
935 Zone,” with significant thermal/chemical effects on Alloy 22 in the adjacent “Blue Zones.” No
936 effects on the EBS are assumed for the “Green Zones.” [After EPRI, 2005 (Figure ES-1)]

937 Figure 6.11 Schematic cross-section through Shirtcollar Butte, Crater Flat, Nevada, a Pliocene
938 (3.7 Ma) basalt volcano. The degree of fusing and welding of scoria increases up-section and
939 grades into dense basalt on the top of the butte. [Source: PVHA-U Field Trip Guidebook, May
940 1-4, 2006].

941 Figure 6.12. LANDSAT Thematic Mapper image showing the Fortymile Wash drainage system.
942 The Pleistocene depositional basin has an Area of 136 km². Map Projection: Universal
943 Transverse Mercator, Zone 11 North, in Meters. [After Hooper, 2005 (Figure 3-1)].

944 Figure 6.13 Landsat Thematic Mapper image showing the active part of the Fortymile Wash
945 depositional (or alluvial) basin in red. Area of the active fan is 24 ± 2 km² [9.3 ± 0.8 mi²]. Map
946 projection: Universal Transverse Mercator Zone 11 North, in meters.

947

948 **List of Tables**

949 Table 3.1 Input parameters for the Suzuki model example shown in Figure 3.7. Values for all
950 input parameters are supplied by the analyst using the code.

951 Table 3.2 Summary of computed values of mass interception fractions of fallout from nuclear
952 tests at the Nevada test site [After Anspaugh et al., 2002].

953 Table 5.1. Summary information for completed PVHA-U drill holes (footnotes are interpretations
954 presented by Perry et al., 2006).

955 Table 5.2. Previous Confidence Rankings for Anomalies Now Re-interpreted with Data from
956 PVHA-U Drilling and Dating. [After Hill and Stamatakos, 2002]

957 Table 5.3 Summary of Published Positions on Probability of Igneous Activity.

958 Table 6.1 Summary of the impacts on waste packages and specifically containment and
959 controlled-release functions of barriers, for each of the three zones for the expected intrusive-
960 release variant case. [After EPRI, 2005].

961 Table 6.2. Peak discharges at stream gauges along Fortymile Wash [from Table 1-2 of Hooper,
962 2005, which was based on data from CRWMS M&O (2000a) and Tanko and Glancy, 2001].

963 Table 6.3. Estimated peak discharges along stream channels of Fortymile Wash at Yucca
964 Mountain.

965
966

967

968 **References**

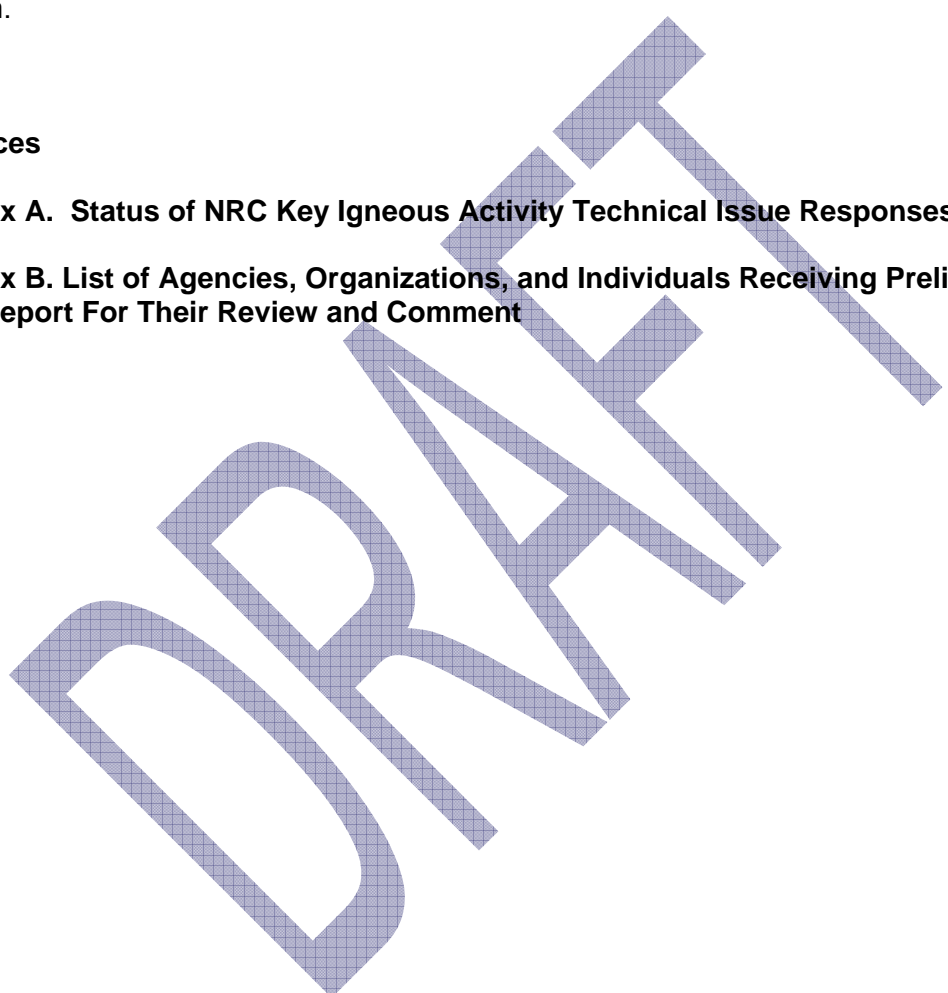
969

970 **Appendix A. Status of NRC Key Igneous Activity Technical Issue Responses (2006)**

971

972 **Appendix B. List of Agencies, Organizations, and Individuals Receiving Preliminary Draft**
973 **of this Report For Their Review and Comment**

974



975
976
977
978
979
980
981
982
983
984
985
986
987
988
989
990
991
992
993
994
995
996
997
998
999
1000
1001
1002
1003
1004
1005
1006
1007
1008
1009
1010
1011
1012
1013
1014
1015
1016
1017

Igneous Activity at Yucca Mountain: Technical Basis for Decision Making

A Report Prepared by the Advisory Committee on Nuclear Waste, US NRC

“Given for one instant an intelligence which could comprehend all the forces by which nature is animated and the respective situation of the beings who composed it – an intelligence sufficiently vast to submit these data to analysis – it would embrace in the same formula the movements of the greatest bodies of the universe and of the lightest atom; for it, nothing would be uncertain and the future, as the past, would be present to its eyes.”

P-S. Laplace, 1776

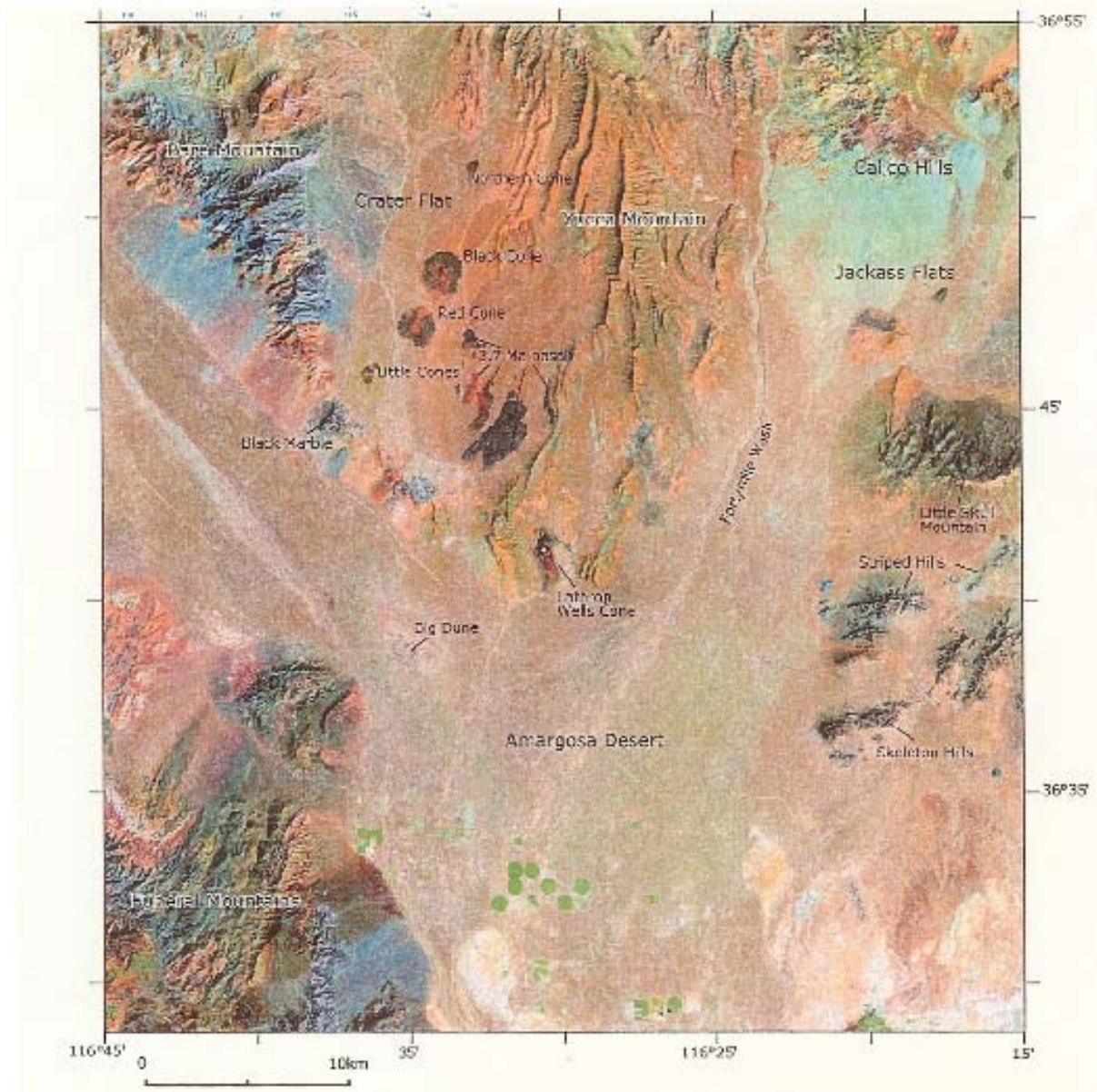
1. Introduction

1.1. Igneous Activity and the Proposed Yucca Mountain Repository

Eighty thousand years ago a small-volume *basaltic*³ volcano, the Lathrop Wells volcano (Figure 1.1 a), erupted about 15 miles south of the Department of Energy’s (DOE) proposed high-level waste (HLW) repository in Yucca Mountain, Nevada. This was the first volcanism in the immediate vicinity of Yucca Mountain for a million years, but one of a series of infrequent basaltic volcanoes that have occurred in the vicinity of the proposed repository site during the past 10 million years. This report presents the Advisory Committee on Nuclear Waste’s (ACNW) summary and evaluation of the range of views of the Committee, Nuclear Regulatory Staff (NRC) staff, and other stakeholders on the nature, likelihood and potential consequences of future igneous activity at the proposed Yucca Mountain repository.

Considering the documented ongoing volcanism, the proposed Yucca Mountain repository could be compromised by igneous activity during its lifetime. Accordingly, potential doses from hypothetical *igneous activity* interacting with the proposed repository have been investigated as part of the assessment of the Yucca Mountain site. Uncertainty in the results of these studies has resulted in a spectrum of legitimate professional views regarding the potential impact of igneous activity.

³ Italicized words are included in the glossary.



1018
 1019
 1020
 1021
 1022

Figure 1.1 a False color Landsat image shows local geographic features and Plio-Pleistocene (last 5 million years) volcanic centers near Yucca Mountain and the proposed high-level waste repository. The location of this image is shown in Figure 1.1 b. [After O'Leary et al., 2002]



1023
1024

1025 Figure 1.1 b Location map of Figure 1.1a shown in green in south-central Nevada and adjacent
1026 California. [After O'Leary et al., 2002]

1027

1028

1029

1030

1031

1032

1033

1034

1035

1036

1037

1038

Assessment of repository performance includes evaluation of the impact of igneous activity as well as other features, events and processes. A risk-informed performance assessment uses the risk triplet for this evaluation. Components of the risk triplet for igneous activity are: What is the nature of a potential igneous event? What is the probability of an igneous event intersecting the proposed repository? And if the repository is intersected, what are the consequences of the igneous activity to the repository, the stored high-level radioactive waste (HLW), and the impact of its potential release on dose to the reasonably maximally exposed individual (RMEI) assumed to be residing in the near vicinity to Yucca Mountain. A review and analysis of the range of views on the answers to these questions is the subject of this report.

1039

1.2. Objective and Rationale of Report

1040

1041

1042

1043

1044

This report responds to the following charge from the U.S. Nuclear Regulatory Commission as described in the Staff Requirements Memo (M060111B) dated February 9, 2006:

1045

1046

1047

1048

“The [ACNW] Committee should provide the Commission with an analysis of the current state of knowledge regarding igneous activity which the Commission can use as a technical basis for its decision making.”

1049

1050

1051

1052

1053

1054

1055

Igneous activity describes processes associated with the origin, nature, transport, and solidification of molten rock, or magma. Magma comes from rock melted in the Earth that may rise to the surface because of the net effects of gravitational forces and gas pressure. Rising magma may solidify at depth to form intrusions or may breach the surface to form volcanoes. Volcanic and intrusive activity is restricted to regions that are actively undergoing sub-crustal dynamic or tectonic processes, and the location of the proposed DOE HLW repository at Yucca Mountain occurs within such a region. Risks to health may arise if people are exposed to

1056 radioactive materials from the repository during volcanic activity, by resuspension of deposited
1057 material, or by premature release to groundwater of radionuclides from waste packages
1058 damaged by magma entering into the proposed repository. As a result, the DOE has conducted
1059 extensive studies over the past few decades to evaluate the potential risk from igneous activity
1060 at the Yucca Mountain site and surrounding region. Other interested parties including the
1061 Nuclear Regulatory Commission (NRC) also are evaluating the risk from igneous activity.
1062

1063 Evaluation of hazards and risk from igneous activity over periods of thousands of years or
1064 more is a major challenge to the scientific community. Such an evaluation has been the subject
1065 of only limited investigation prior to the need to assess the long-term performance of the
1066 proposed HLW repository. Understanding the processes and precursor events leading to
1067 igneous activity at any specific location is rudimentary except for near-term events at existing
1068 volcanoes. Longer-term quantitative predictions, as required in the case of the HLW repository,
1069 have been made only in recent decades using primarily probabilistic techniques based on past
1070 igneous events of the region. However, procedures for implementing predictions and the nature
1071 of the data used in making predictions are not standardized and there are limitations in data and
1072 experimental evidence. This leads to varying professional judgments with attendant
1073 uncertainties and variations in hazard estimates, particularly in the case of infrequent, low-
1074 volume basaltic volcanism, as in the Yucca Mountain region.
1075

1076 There is a base of knowledge regarding the fundamental magmatic processes leading to
1077 volcanic activity and near-surface intrusions in the Yucca Mountain region, but many
1078 uncertainties remain. In addition, it is virtually impossible to determine the existence of low-
1079 volume magma source zones at their sub-crustal depths as well as the controls on the
1080 movement of magma through the Earth's crust which could be useful in long-term predictions of
1081 the occurrence of volcanic events.
1082

1083 Appraisal of risk from igneous activity is further complicated by differences in views
1084 regarding the nature and behavior of magma and its potential impact on entering underground
1085 openings that contain waste packages. Appropriate geologic analogs of consequences from the
1086 intersection of magma and underground openings do not exist. As a result, both evaluating the
1087 probability of igneous activity at the proposed repository and the impact of this activity on the
1088 repository throughout the long time of compliance period have been the subject of extensive
1089 investigations and considerable variation in professional views.
1090

1091 During the past few decades significant progress has been made in determining the
1092 technical bases for predicting risk from an igneous event at the HLW repository. Accordingly,
1093 the purpose of this report is to present the range of the technical bases for making decisions
1094 regarding the potential doses from igneous activity, including the nature and probability of
1095 igneous activity intersecting the repository during the mandatory time of compliance, the
1096 potential consequences of this interaction, and hypothetical radiation doses based on the
1097 currently available information.
1098

1099 EPA and NRC regulations pertaining to the proposed Yucca Mountain HLW repository
1100 specify that assessment of the performance of the repository provide reasonable assurance that
1101 the EPA dose standard will be met throughout the time of compliance. Performance assessment
1102 is used for the quantitative evaluation of the repository. It is a probabilistic methodology that
1103 incorporates the uncertainty in the scenarios, models, and parameters and involves repeated
1104 calculation of the performance of the repository ("realizations") using samples of the input
1105 parameter distributions. Cumulative distributions of the results are compared to the standards
1106 established by EPA for the repository.

1107
1108 Assessment of the potential risk from a geologic repository for high-level waste is based
1109 on the quantitative evaluation of the answers to the risk triplet (Kaplan and Garrick, 1981;
1110 Garrick and Kaplan, 1995): What can go wrong? How likely is it? What are the consequences?
1111 In practice, the product of probability and consequence that is calculated for each scenario
1112 constitutes a realization in performance assessment. In this report the technical basis for
1113 decision making regarding the impact of igneous activity on the proposed Yucca Mountain
1114 repository is centered on the risk triplet.

1115
1116 **1.3. Scope of Report**

1117 This report reviews the technical bases for making decisions regarding the risk from
1118 igneous activity that could occur at the proposed Yucca Mountain high-level waste repository
1119 over its prescribed time of compliance. Accordingly, the scope of this report is limited to the
1120 post-closure period of the repository after the underground repository has been sealed off from
1121 the surface. The post-closure period is restricted, unless otherwise indicated, by the risk from
1122 igneous activity during the 10,000 years following closure based on the period of time that has
1123 been considered in the majority of existing igneous activity investigations of Yucca Mountain.
1124 The Environmental Protection Agency's (EPA) current draft revised standards for the Yucca
1125 Mountain repository (EPA, 2005) prescribe that consideration of features, events, and
1126 processes (FEPs), which includes igneous events, shall be based on the 10,000 years following
1127 repository closure as had been detailed in the current standards 40 CFR 197 (EPA, 2001). This
1128 is incorporated into the proposed changes to 10 CFR 63 (NRC, 2005b) based on the EPA's
1129 assertion that data and models used to prepare performance assessment for the first 10,000
1130 years provide adequate support for projections through the period of geologic stability and limits
1131 uncertainties associated with speculation of performance over very long time periods (i.e.,
1132 hundreds of thousands of years).

1133
1134 The report provides a review of the current public positions taken by DOE, NRC, and other
1135 interested parties on issues dealing with the nature, probability, and impact of igneous activity
1136 on the proposed Yucca Mountain repository. Where appropriate, observations are provided on
1137 positions unsupported by measurement or extrapolated from existing data or on positions that
1138 differ from Environmental Protection Agency (EPA) standards or NRC regulations. Every
1139 attempt is made to identify uncertainties in positions and issues. The State of Nevada has not
1140 established specific views on the impact of future igneous activity at Yucca Mountain, however,
1141 experts supported by the State of Nevada have published several journal articles related to the
1142 probability of an igneous event intersecting the proposed repository that are reviewed in this
1143 report.

1144
1145 **1.4. Content and Organization of Report**

1146
1147 Chapter 2 is a brief review of the geologic history of the Yucca Mountain region which
1148 serves as the basis for presentations in subsequent chapters on the nature of future igneous
1149 activity and the likelihood of its occurrence. Figures in this chapter show the geographic location
1150 of various geologic features treated in subsequent chapters.

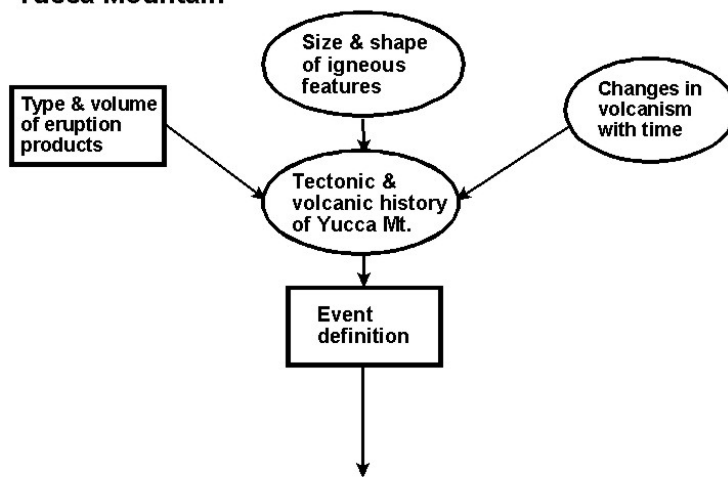
1151
1152 Chapter 3 presents an overview of the principal processes involved in igneous activity.
1153 Knowledge of these processes is fundamental to understanding the potential igneous activity at
1154 Yucca Mountain and its impact on the repository and the potential radiation doses to the RMEI

1155 as defined in the EPA standards for Yucca Mountain (EPA, 2001). Additional background is
1156 available from cited references.

1157
1158 Individual chapters (Chapters 4, 5, and 6) of this report present a review of the state of
1159 knowledge available in documents and published materials of interested parties regarding the
1160 nature, likelihood, consequences, and doses from potential igneous activity in the context of the
1161 risk triplet questions.

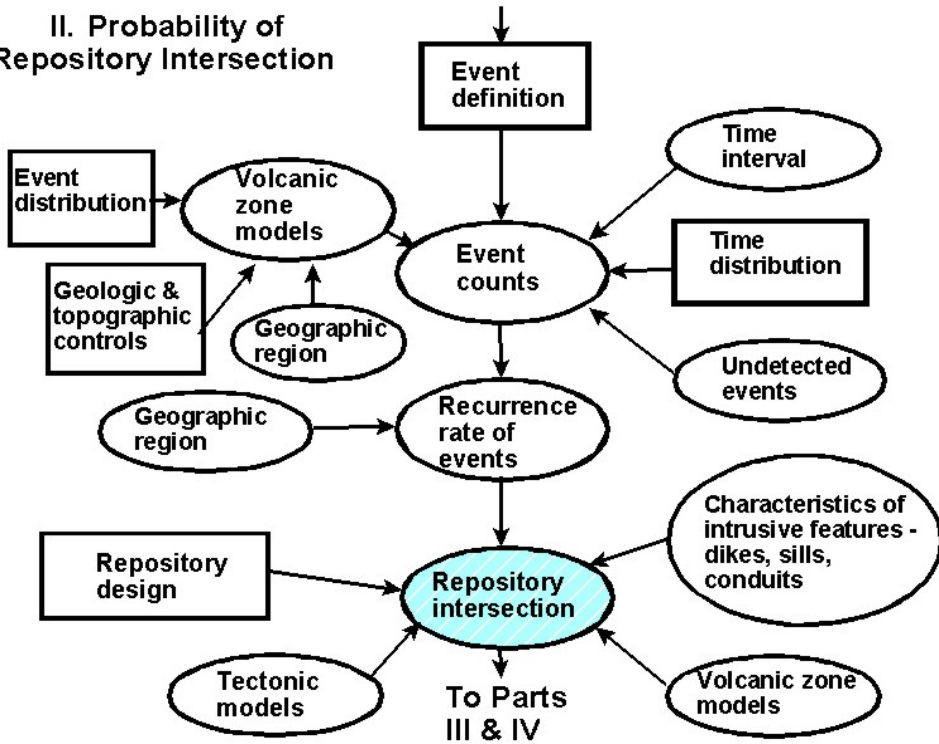
1162
1163 The essential components involved in answering each question are shown in the logic
1164 diagram of Figure 1.2 a, b, c, and d, a modification and expansion to include consequence
1165 effects of a figure originally published in Crowe et al. (2006). The oval shapes in the figure are
1166 uncertain elements of the logic flow and are treated probabilistically, while the rectangular
1167 shapes are decision parameters that have been determined either subjectively or by general
1168 agreement of the engineering and scientific community. The bold ovals are conditional
1169 parameters that are convolved (multiplied) to determine the performance assessment dose
1170 probability as a function of time which is compared to the standards of the repository and the
1171 irregular hexagon is the performance assessment probability.

I. Nature of Possible Future Volcanism at Yucca Mountain



1172
1173 Figure 1.2 a Logic chart of components involved in determining the definition of the nature of
1174 possible future igneous events at Yucca Mountain.

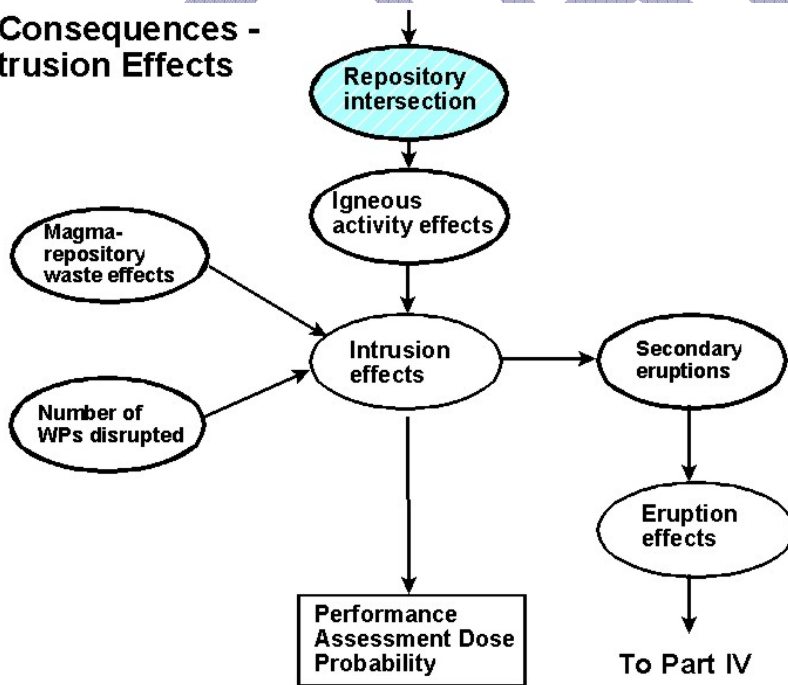
II. Probability of Repository Intersection



1176

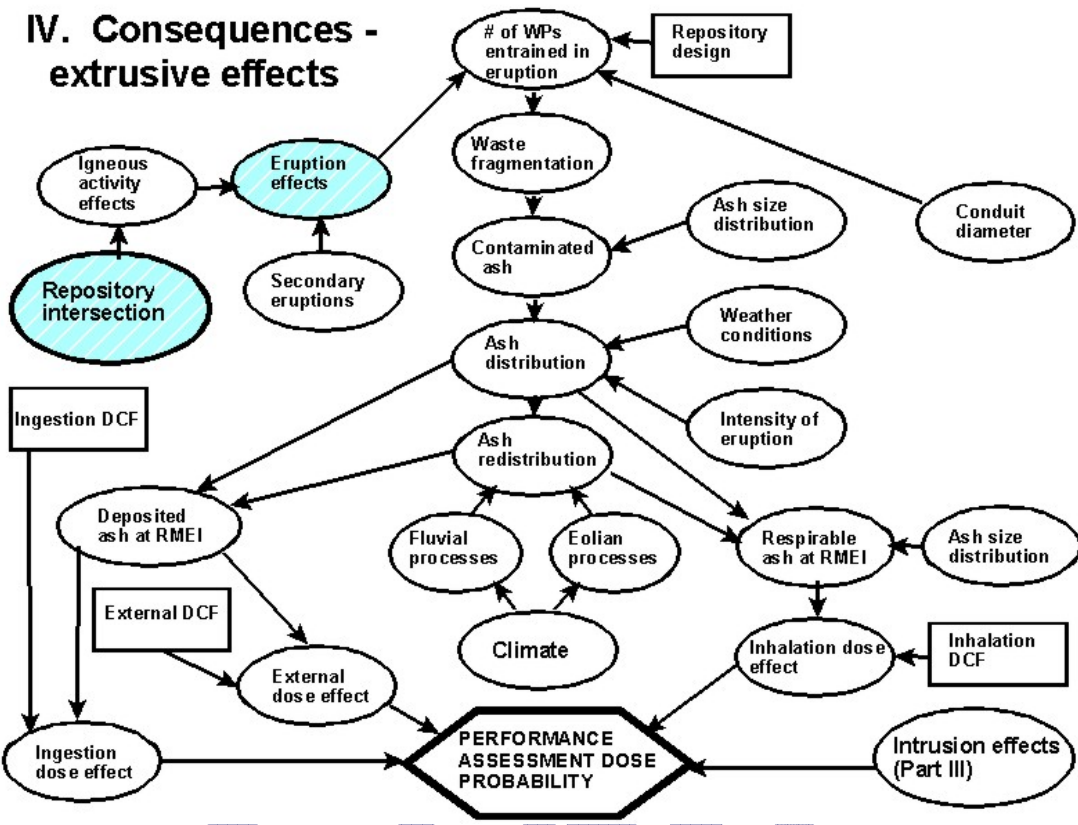
1177 Figure 1.2 b Logic chart of components involved in determining the probability of future igneous
1178 activity intersecting the proposed Yucca Mountain HLW repository.

III. Consequences - Intrusion Effects



1179

1180 Figure 1.2 c Logic chart of components involved in determining the consequences of an
1181 intrusive event intersecting the Yucca Mountain HLW repository.



1183

1184 Figure 1.2 d Logic chart of components involved in determining the consequences a volcanic event intersecting the Yucca Mountain HLW repository.
 1185

1186

1187 The conclusions reached in this report on the analysis of the range of views regarding the
 1188 technical bases for decision making are presented in Chapter 7. A listing of the status of NRC
 1189 key technical issue responses and the agencies, organizations, and individuals receiving an
 1190 initial draft of this report for their review and comment are provided in appendices.

1191

1192 **1.5. Report Preparation Process**

1193

1194 This report has been prepared by members and staff of the ACNW assisted by a
 1195 consultant who is an expert on igneous activity. An initial draft of the report was sent to the
 1196 NRC, DOE, the State of Nevada and other germane stakeholders as well as a group of external
 1197 experts in related disciplines for their review and comment. A list of recipients invited to
 1198 comment on the draft report is given in Appendix B. Subsequently, the stakeholders were
 1199 invited to a working group meeting convened by the ACNW to permit them to discuss their
 1200 views on igneous activity at Yucca Mountain and provide them with an opportunity to
 1201 recommend appropriate revisions to the report. Specifically, stakeholders were requested to
 1202 address the following questions:
 1203

- 1204
- 1205
- 1206
- 1207
- 1208
- 1209
- 1210
- 1211
- 1212
- 1213
- 1214
- Does the ACNW report address the risk-significant topics related to igneous activity at Yucca Mountain?
 - Does the report capture the range of views of the interested parties with respect to the technical bases for decision making on these topics including definitions of volcanic events, geologic periods of interest in predicting probability, igneous activity probability, magma/drift interaction leading to both extrusive, intrusive scenarios, potential consequences for the risk from a high-level waste repository, etc? If not, the positions detailed in the report will be clarified from published position papers in the final ACNW report.

1215

1216

1217

1218

1219

1220

1221

1222

1223

1224

1225

1226

1227

1228

1229

1230

1231

1232

1233

1234

1235

1236

1237

1238

1239

1240

1241

1242

1243

1244

1245

1246

1247

1248

1249

1250

1251

1252

1253

Additionally, at the working group meeting a group of distinguished experts on the various aspects of igneous activity provided an overview of the challenges facing technical decision making on igneous activity at Yucca Mountain and a description of the status of knowledge of relevant volcanic features, events, and processes. The experts also participated in a panel discussion on the completeness and quality of the content of the ACNW report where they commented on the following questions:

- Has an effective and accurate understanding of the various views on volcanism been identified and documented in the report?
- Have the risk significant topics regarding igneous activity been identified?
- Are the technical bases for positions taken for determining risk from igneous activity at Yucca Mountain scientifically correct?
- Are there risk-significant topics regarding igneous activity that have not been adequately addressed considering the current state of the science? If so, how can they be addressed?

The public also was invited to present their comments on the draft. All of the comments and results of the discussion of the working group were reviewed and considered by the ACNW as part of finalizing the report.

1.6. Constraints on the Report

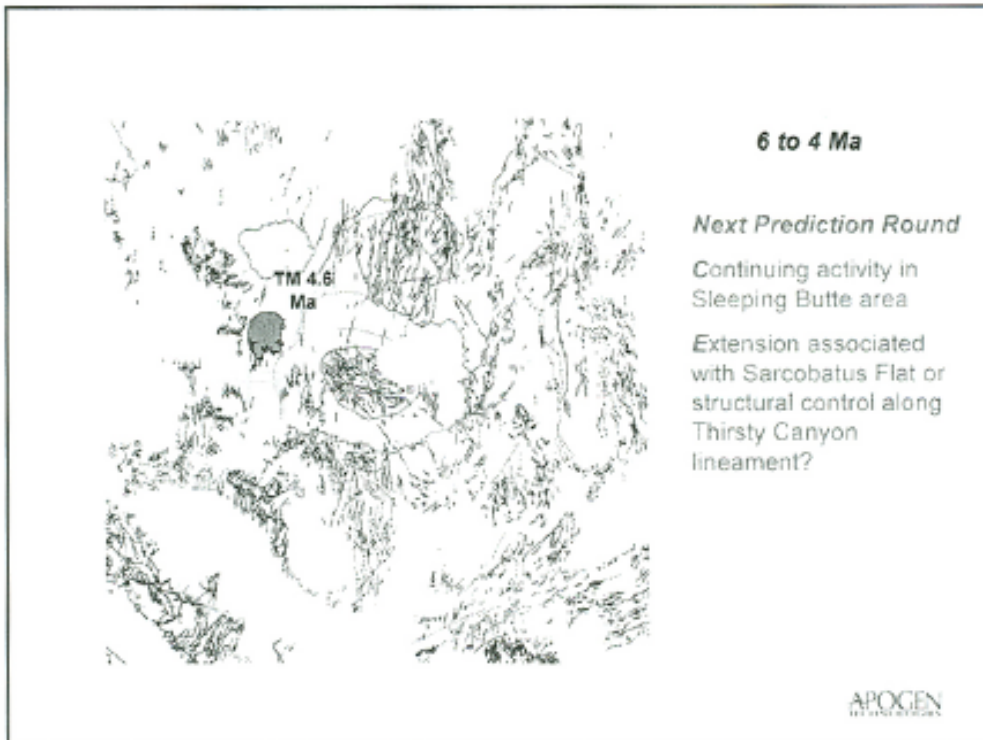
There are several constraints on the report and its conclusions that limit the technical bases for decision making regarding igneous activity. These include:

- Critical decisions about the design of the repository and *waste canisters* that may affect the probability and consequences of igneous activity are not final. For example, there is as yet no decision on the maximum temperature that the repository will be allowed to attain. This decision will affect the distribution of waste packages and the areal size of the repository, both important parameters in establishing the probability and consequences of igneous activity. Pending decisions about backfill of the drifts, the alloy to be used in construction of the waste canisters, and the use of an inner canister also are important to the effects of igneous activity.
- The DOE and the NRC continue to conduct studies that relate to the probability and effects of igneous activity. DOE, for example, is currently in the process of updating the 1996 Probabilistic Volcanic Hazard Analysis (PVHA – U) expert elicitation using data from new geosciences investigations. Several reports are

1254
1255
1256
1257
1258
1259
1260
1261
1262
1263
1264
1265
1266
1267
1268
1269
1270
1271
1272
1273
1274
1275
1276
1277

anticipated from the DOE during the first half of 2007 that specify the technical bases for their positions on various aspects of igneous activity. NRC is in the process of conducting investigations and developing views on a variety of igneous activity issues and thus they have not been reported on. Examples are the studies of eolian (wind) redistribution of contaminated ash to the vicinity of the RMEI and the interaction of magma and the repository and waste packages.

- Many process models are incorporated into the performance assessment of igneous activity at Yucca Mountain, but few of these models have been validated with realistic data or simulations. Accordingly there are limitations in the confidence that can be placed in the results of the analyses. For example, the volcanic models used to determine the hazard from basaltic volcanism are largely determined from past volcanic events of the region, but prediction of basaltic volcanism over several time slices within the past 10 million years in the Yucca Mountain region (Crowe, 2005) using previous volcanism and the geologic structure of the region as a predictive tool were not notably successful in specifying the location of actual new clusters of volcanoes or volcanic fields that occurred within the region over the period of the time slice. Figure 1.3 shows the results of Crowe's prediction of volcanism between 4 and 2 Ma based on the record of basaltic volcanism in the Yucca Mountain region between 6 and 4 Ma. The actual volcanism observed from this time period is shown in Figure 1.4. As noted by Crowe (2005) in this figure the actual volcanism (results) are mostly unexpected based on the basaltic volcanism of the previous 2 million years.



1278
1279
1280
1281
1282

Figure 1.3 The prediction of the basaltic volcanism in the Yucca Mountain region during the time interval 4 to 2 Ma based on the occurrence of volcanism in the region during the prior 2 Myr (6 to 4 Ma). Basaltic volcanism during the period of 6 to 4 Ma is shown in green. [After Crowe, 2005]

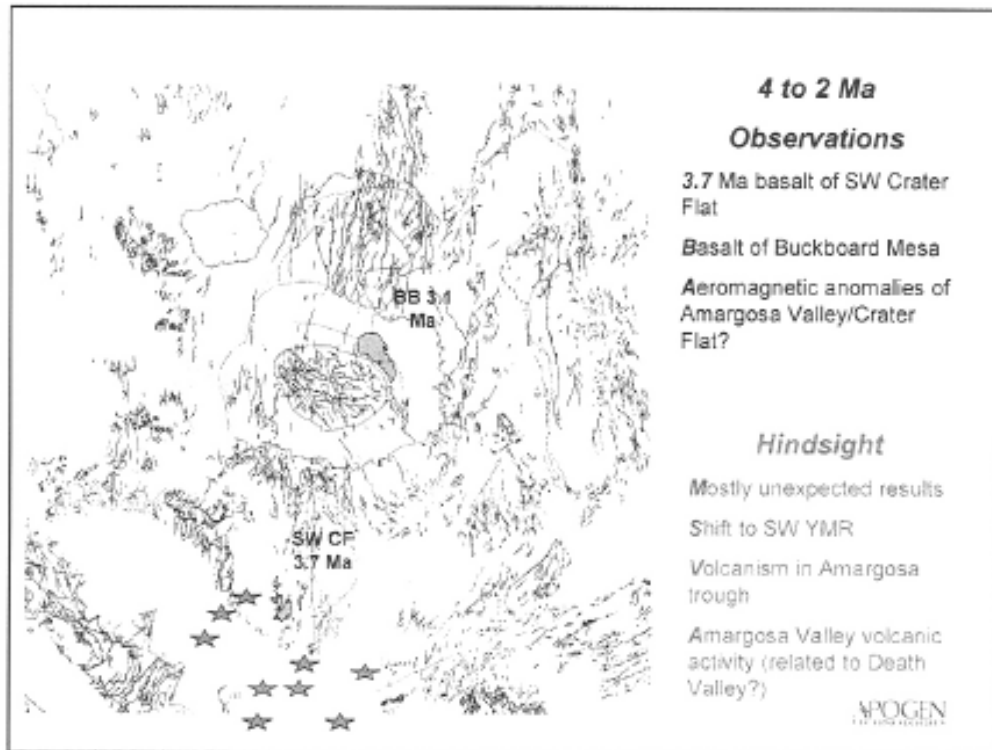


Figure 1.4 The observed basaltic volcanism in the Yucca Mountain region during the time interval 4 to 2 Ma based on the occurrence of volcanism in the region during the prior 2 Myr (6 to 4 Ma). Basaltic volcanism during the period of 4 to 2 Ma is shown in green and magnetic anomalies in Amargosa Valley that are interpreted to have a source in basaltic volcanism during this time interval are shown by green stars. [After Crowe, 2005]

- Studies related to igneous activity at Yucca Mountain published in professional journals generally are subjected to intense peer review. As a result, the data and conclusions of journal articles are credible. However, subsequent studies may show different results and interpretations of the data. Thus, conclusions presented in journal articles, such as those referenced in this report, must be carefully evaluated in the light of subsequent publications. A case in point is geodetic data that describe the ambient strain of the Yucca Mountain region which has considerable importance to understanding and predicting potential seismicity and volcanic activity in the region. Geodetic observations prior to the mid-1999 that were obtained from point global positioning satellite (GPS) observations replicated at intervals showed a strain of an order of magnitude greater than indicated by geologic observations which reflect mean long-term strain rates (Wernicke et al., 1998). This led Wernicke et al. (1998) to conclude that hazard analysis may be underestimated by an order of magnitude. However, follow-on investigations suggest that these results may be in error (Savage et al., 1999) or represent a geologically recent spike of increased crustal strain (Connor et al., 1998; Wernicke et al., 2004). Subsequent GPS studies in the Yucca Mountain region are based on continuous observations which enhance the data quality. They suggest that the earlier strain rates may be too high by a factor of roughly two (Wernicke et al., 2004).

1311 • Preclosure igneous activity is not considered in the report. Although the unlikely
1312 probability exists that igneous activity could occur during the preclosure period of
1313 the repository with its resulting impact upon waste stored on the surface for aging
1314 purposes and emplaced in drifts of the repository as well as on workers and
1315 surface structures, systems, and components at the repository, there is no
1316 evidence from precursor indicators that imminent igneous activity is likely over the
1317 short span of the preclosure period (100 years). DOE (1999) in its preclosure event
1318 prevention strategy is designing preclosure structures, systems, and components
1319 to withstand bounding igneous events, but the NRC (2005a) has pointed out the
1320 lack of consideration of tephra and ash falls which could impact the roof loads and
1321 effects on ventilation and filter systems. Consideration of igneous activity has been
1322 the subject of investigation only in a limited manner by the NRC (2005a).
1323 Accordingly, the scope of this report is limited to the post-closure period of the
1324 repository after the underground repository has been sealed off from the surface.
1325

1326 **1.7. Previous Reviews of Igneous Activity Technical Bases**

1327

1328 Understanding and predicting the role of igneous activity throughout the lifetime of the
1329 proposed Yucca Mountain repository has been one of the more challenging topics of the
1330 characterization of the repository site. Accordingly, progress on the technical bases for making
1331 decisions on igneous activity has been under review for nearly two decades. The U.S. Nuclear
1332 Waste Technical Review Board (NWTRB) has monitored progress in the DOE program at
1333 regular intervals and the U.S. NRC's program in igneous activity has held the interest of the
1334 Advisory Committee on Nuclear Waste (ACNW) since the inception of the Committee. The
1335 igneous activity program of the NRC and the differing opinions regarding the results of the
1336 program among the State of Nevada, the DOE, and the NRC has encouraged reviews by
1337 standing advisory (review) committees and ad hoc panels of specialized experts.
1338

1339 The ACNW has sent eight letters to the Chairman of the Commission with its observations
1340 and recommendations on the NRC's igneous activity since 1989. These letters have dealt with
1341 the importance of a multidisciplinary approach to igneous activity studies, the significance of
1342 accurate isotopic dating of basalts of the Yucca Mountain region to the estimation of the
1343 probability of future igneous events, the importance of minimizing uncertainties in the results of
1344 the studies, and the need for a risk-informed approach to igneous activity studies. In addition,
1345 the Center for Nuclear Regulatory Waste Analyses (CNWRA), the laboratory supporting the
1346 NRC staff's repository analysis program, has conducted external previews of the Center's
1347 igneous activity studies. These reviews have made specific recommendations regarding topics
1348 that should receive special attention.
1349

1350 The DOE's igneous activity study program, supported by personnel from the U.S.
1351 Geological Survey and Las Alamos National Laboratory, has been complemented with external
1352 peer review panels. In 1996 the DOE completed a two-year expert elicitation, the Probabilistic
1353 Volcanic Hazards Assessment, which established the probability distribution of the annual
1354 frequency of intersection of the proposed repository by volcanic activity on the basis of ten
1355 experts following the guidelines for expert elicitations set forth in NUREG 1563. This elicitation
1356 is being updated (Probabilistic Volcanic Hazards Assessment – Update) taking into the account
1357 the considerable amount of new geosciences information about igneous activity at the proposed
1358 repository. Support for this new elicitation came from the DOE's external Igneous
1359 Consequences Peer Review (ICPR) Panel (Detournay et al., 2003) which was constituted to
1360 review the potential consequences and effect upon risk due to an igneous intrusion intersecting
1361 the proposed repository. A major emphasis of this panel, which released its final report in 2003,

1362 was to review the interaction between the intruding magma and the repository drifts and to
1363 recommend studies by the DOE that would reduce uncertainties in the overall igneous activity
1364 program. The results of these reviews have brought knowledgeable, fresh insight into the
1365 program.
1366

1367 The Nuclear Waste Technical Review Board (NWTRB) reviews the DOE studies on
1368 igneous activity on a regular basis. The NWTRB has reported the results of these reviews and
1369 suggestions for further studies in regular reports to Congress and letters to the DOE Office of
1370 Civilian Radioactive Waste Management since 2000 (NWTRB 2001, 2002, 2003, 2004).
1371
1372

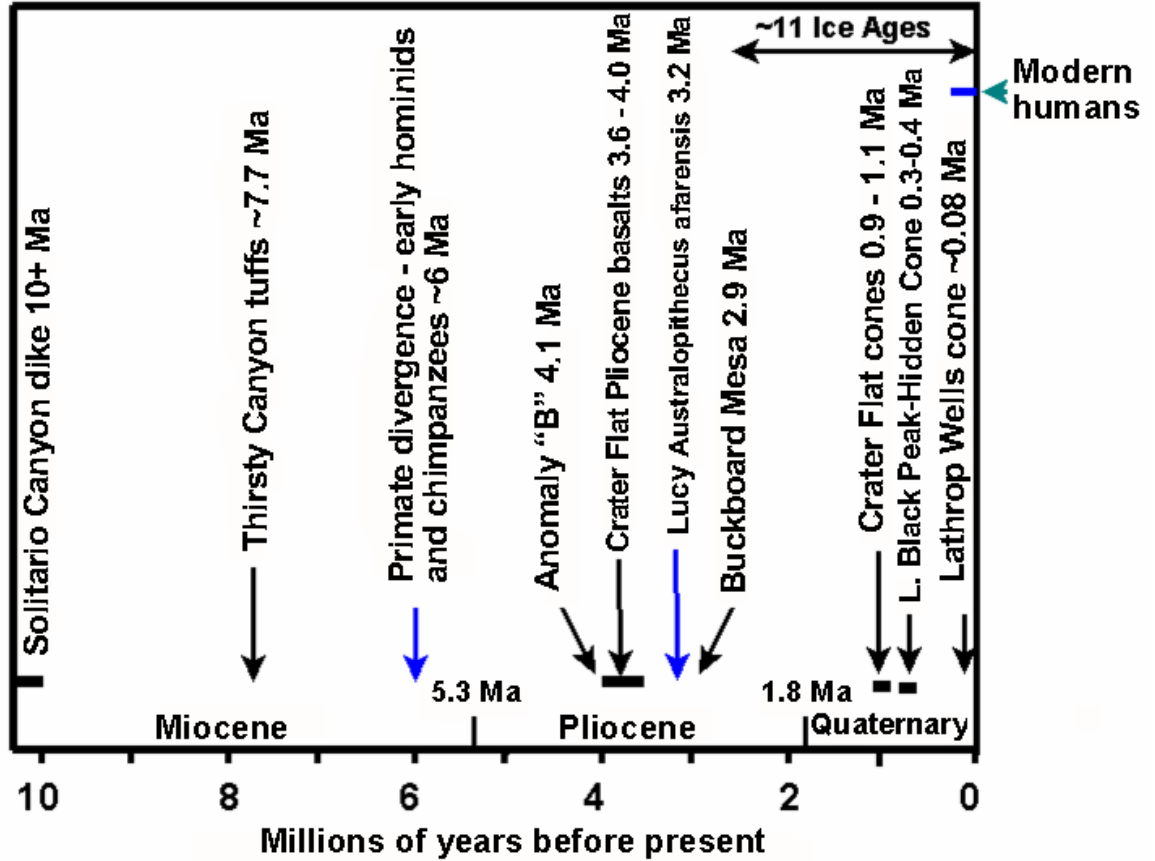
1373 **2. Brief Geologic History of the Yucca Mountain Region**

1374

1375 The geologic history of the Yucca Mountain region including both its structural
1376 development (*tectonics*) and history of volcanic activity form the foundation for understanding
1377 the past and predicting the future igneous history of the region. The geological structure of the
1378 region has a direct impact on the magma source zones and the specific location of volcanic
1379 activity. As a result the nature of tectonism is critical to predicting the probability and nature of
1380 volcanism. As stated by McKague et al. (2006) in referring to the implications of tectonic models
1381 on the probability of occurrence of a volcanic eruption or igneous intrusion at Yucca Mountain
1382

1383 “For volcanism to occur, the physical and chemical conditions for magma formation must
1384 exist at some depth, and a path must be established between this magma source and the
1385 earth’s surface. Both these sets of conditions together with the style and frequency of
1386 igneous activity are determined by tectonic setting. More locally, the in situ stress state
1387 and presence or absence of faulting and fracturing are factors controlling magma ascent
1388 through the crust.”
1389

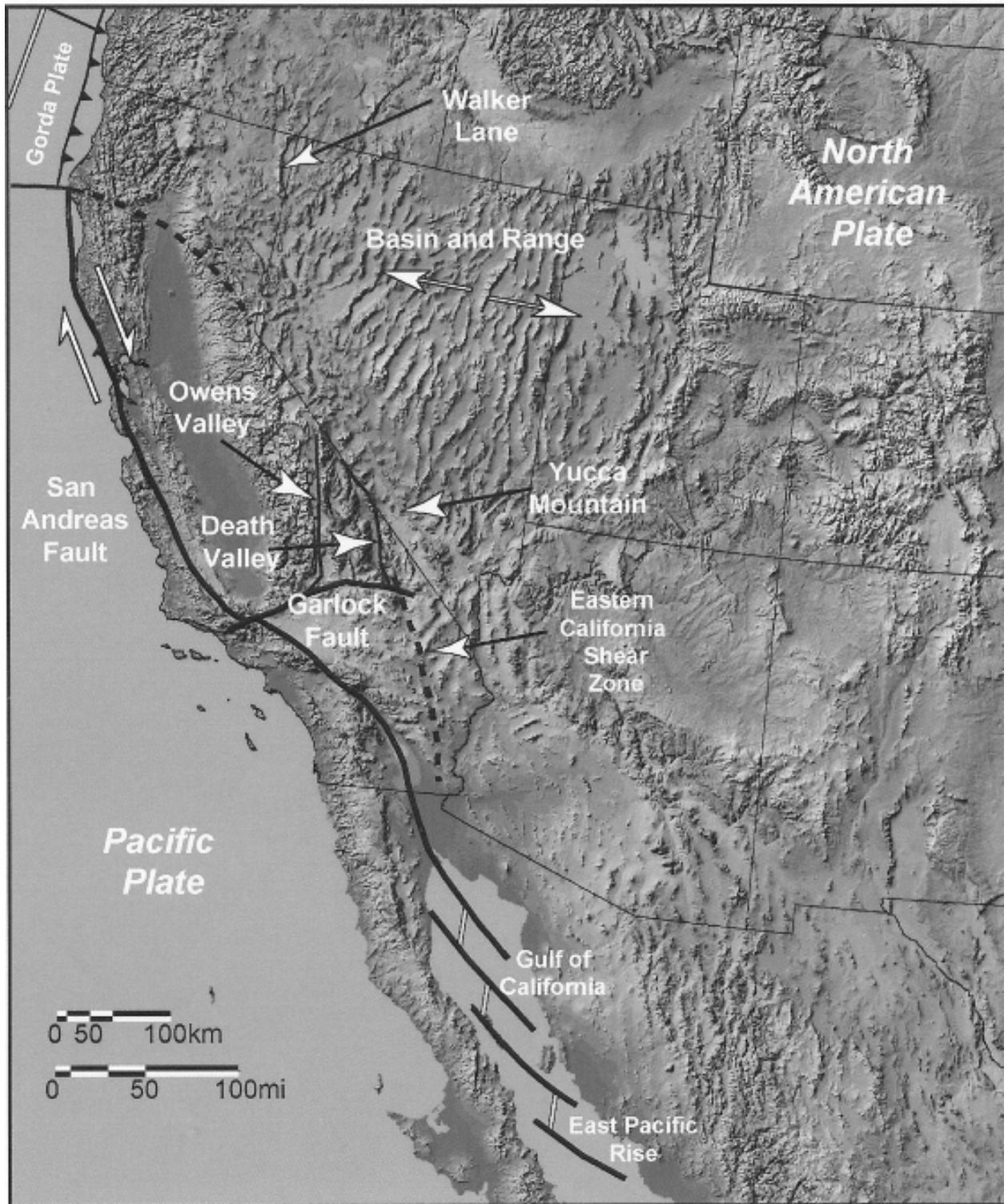
1390 In addition, the primary method of predicting future volcanism in the Yucca Mountain
1391 region is on the basis of past igneous activity, an important part of the geologic history of the
1392 region. Accordingly, this section provides an overview of the tectonic and igneous activity history
1393 of the region. The literature on this topic is too extensive to cover comprehensively in this report,
1394 but useful recent reviews of the subject that contain critical references have been prepared by
1395 Crow et al. (1995; 2006), Parsons (1995), O’Leary (1996), Grauch et al. (1999), and McKague
1396 et al. (2006). A simplified history of the Yucca Mountain region is illustrated in Figure 2.1.
1397



1398
1399 Figure 2.1 Timeline of events in the Yucca Mountain region related to igneous activity and
1400 geological periods of time.
1401

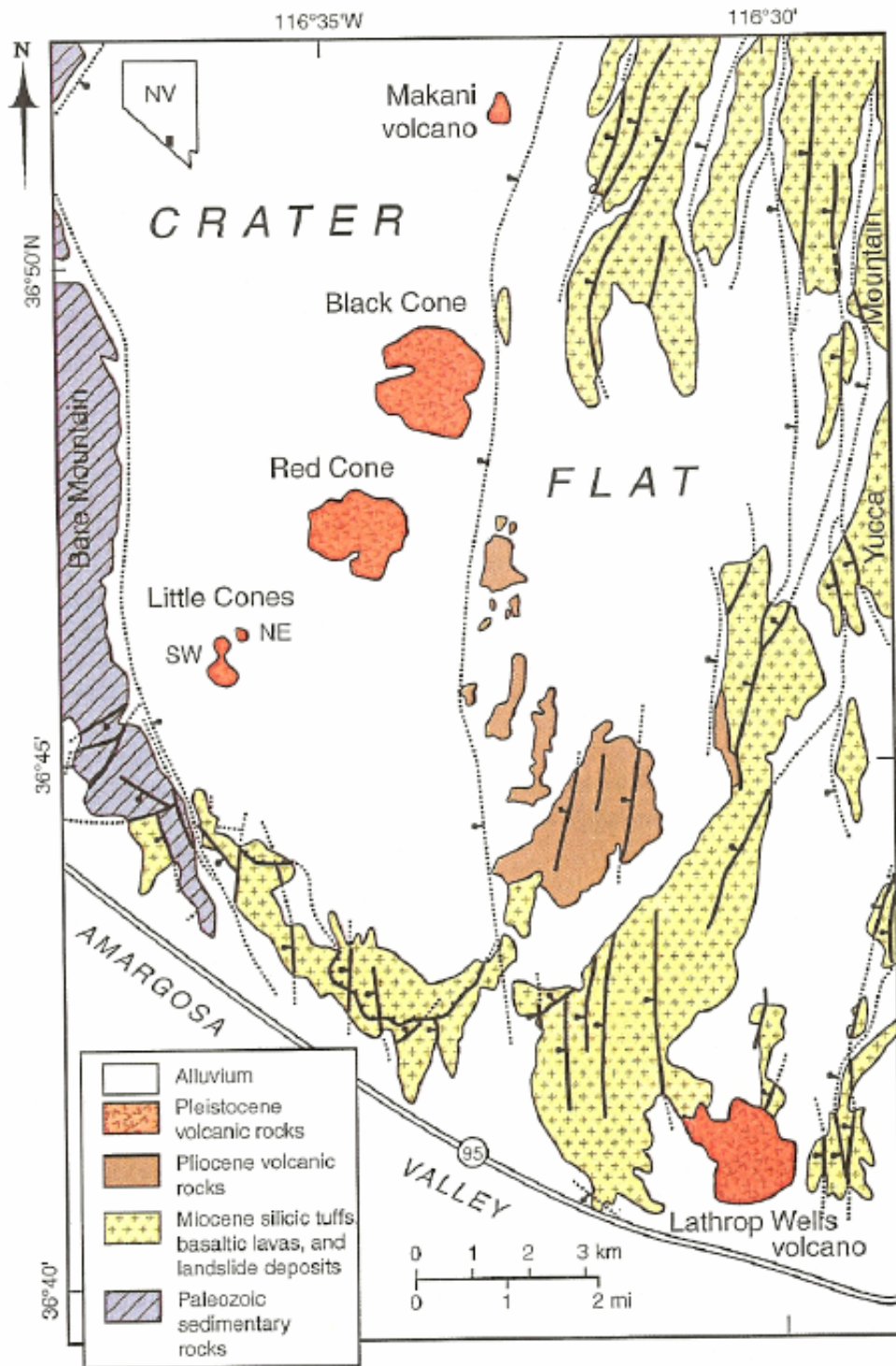
1402 The State of Nevada and the Yucca Mountain region are located in the Central Basin
1403 and Range geological province (the Western Great Basin) which is noted for topography
1404 consisting of generally north-south trending, alternate elongate valleys (basins) and mountain
1405 ranges that extend into adjacent states and continue south into northwestern Mexico (Figure
1406 2.2). The geological history of this region is long and complex with periods of tectonic activity, as
1407 illustrated in the general geologic map of the region (Figure 2.3). The area was last subject to
1408 mountain building during the Laramide *orogeny* that occurred as a series of tectonic pulses
1409 separated by quiescent periods, from about 70 to 40 Ma⁴. The Rocky Mountains, with generally
1410 easterly-directed thrust faults and folds that extend from Alaska to northern Mexico, originated
1411 during this orogenic event. The mountain building episode was caused by collision of a *crustal*
1412 *plate* off the west coast with the North American plate. The western plate was *subducted*
1413 beneath the North American plate at a low angle resulting in the broad zone of mountain
1414 building observed in the western United States. The *sedimentary* and *igneous rocks* that form
1415 the base of the volcanic rocks in the Yucca Mountain region were complexly faulted and folded
1416 during the Laramide and earlier orogenies.
1417

⁴ Ma is the abbreviation for age in millions of years, Myr is the abbreviation for a duration of time in millions of years.



1418
 1419
 1420
 1421
 1422
 1423
 1424

Figure 2.2 Elevation map of the southwestern United States showing the position of Yucca Mountain and major geologic, structural, and topographic features. [After McKague et al., 2006]

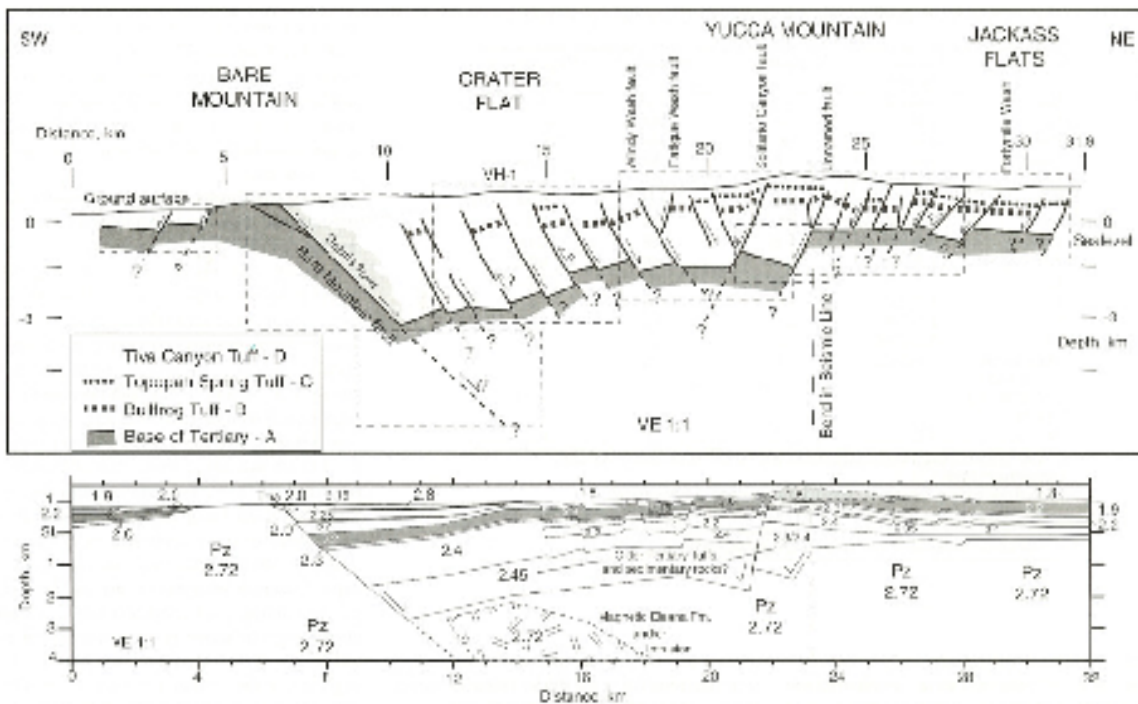


1425
 1426
 1427
 1428
 1429
 1430
 1431

Figure 2.3 Geological Map of the Yucca Mountain Region. [After Valentine et al., 2006a]

The Basin and Range province is an active extensional region within the North American western Cordillera. It is named for the topographic manifestation of the most recent mode of extension which consists largely of block faulting with normal faults typically dipping at a steep

1432 angle to the west. The current tectonic activity within the region is indicated by its high heat flow,
 1433 seismic activity, recent basaltic volcanism, thin crust, and observed strain rates. Unlike most rifts
 1434 that have undergone *normal faulting* and *lithospheric* extension, the Basin and Range province
 1435 is very broad, reaching a width of more than 900 km. Extension commencing about 25 Ma ago
 1436 resulting in a variable amount of stretching across the region with an average total extension of
 1437 approximately 100%. Relatively small magnitude extension in the Yucca Mountain region of the
 1438 Central Basin and Range from approximately 13 to 10 Ma produced the steep (~ 60°) normal
 1439 faulting that results in the characteristic Basin and Range topography with the ranges such as
 1440 Yucca Mountain and basins such as the adjacent Crater Flat and Jackass Flats (Figure 2.4).
 1441 The Crater Flat structure as shown by the geophysical interpretation in Figure 2.4 extends from
 1442 Bare Mountain to the east of Yucca Mountain into Jackass Flats. The cause of the extension is
 1443 uncertain, but it is thought to originate from the Pacific Plate moving northwest relative to the
 1444 North American Plate. This same force created the San Andreas fault. Other forces may be
 1445 involved, including those related to the movement of the North American Plate over the
 1446 spreading center associated with a plate to the west. There is evidence that an early stage of
 1447 extension may have occurred at the end of the Laramide orogeny as a result of gravitational
 1448 collapse of an overthickened crust followed by extension related to spreading of the continental
 1449 crust associated with disintegration or steepening of the plunge of the subducting oceanic plate.
 1450



1451
 1452
 1453 Figure 2.4 (Top) Interpretation of seismic reflection profile across Crater Flat and Yucca
 1454 Mountain. (Bottom) Gravity model along seismic profile with density of rock units in gm/cm³.
 1455 [After Brocher et al., 1998]
 1456

1457 In addition to the late-stage normal faults, several other types of faulting have occurred
 1458 in the region. Low-angle normal faults that occur in isolated locations represent an earlier stage
 1459 of extension, but their origin remains controversial. The Yucca Mountain region is a complex
 1460 structural belt resulting from its location in the transition between the Walker Lane, which lies on
 1461 the eastern margin of a distributed shear zone, the Eastern California Shear Zone (Figure 2.2),

1462 that extends north-northwest from the southeastern corner of Nevada, across Nevada, and into
1463 California, and the Basin and Range province to the north and east. The Walker Lane structural
1464 feature, dating back a few tens of millions of years, is characterized by north-northwest striking
1465 right-lateral displacement and north-northeasterly directed left-lateral displacement faults and
1466 consists of an assemblage of independent structural units. Its origin lies in distributed shear
1467 forces arising from movements in the continental crust to the west. Both normal faults of the
1468 Basin and Range province and the shear faults of the Walker Lane are prominent in the Yucca
1469 Mountain region.

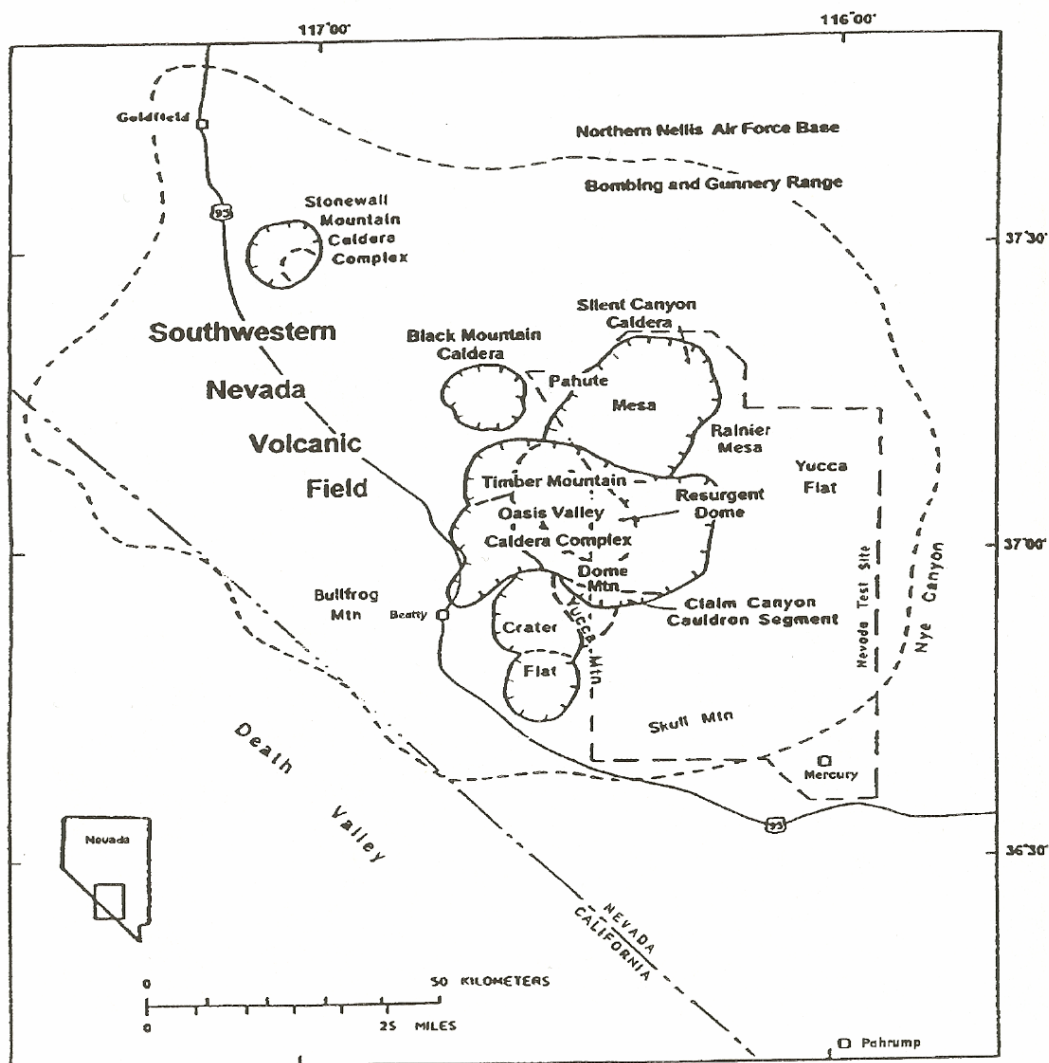
1470
1471 Several tectonic models have been proposed to explain the origin of the structures of the
1472 Yucca Mountain region and to assist in extrapolating those features into the subsurface. It is
1473 their subsurface extent and orientation that have a significant role in relating them to volcanic
1474 and seismic activity. The models can be classified into three groups based on the principal
1475 mode of deformation that is incorporated into their explanation: extension, shear, and volcanic.
1476 This is not surprising because of the overlap in the region of shear deformation associated with
1477 the Walker Lane, the extensional forces prominent in the Basin and Range province, and the
1478 massive intense volcanism 11 to 15 Ma ago. McKague et al. (2006) recognize eleven viable
1479 models and present a description of and the bases for each of these models employing the
1480 most recent geologic, geodetic, and geophysical data. They conclude that no single tectonic
1481 model explains the structural deformation of the region. However, they point out (McKague et
1482 al., 2006 [Table 6.1]) that the active faults, high strain rates, and deep faults identified with the
1483 shear models are of concern for the occurrence of igneous activity in the Yucca Mountain region
1484 over the lifetime of the repository.

1485
1486 Igneous activity appears coeval with the Basin and Range province extension, but the
1487 relationship is variable across the province. Magmatism is particularly well correlated with the
1488 early stage of extension involving low-angle faulting, but not necessarily with late stage normal
1489 faulting. The widespread igneous activity over the Basin and Range province is well
1490 summarized by, for example, Parsons (1995).

1491
1492 Voluminous *felsic* volcanism occurred in the Yucca Mountain region 15 to 9 Ma ago. This
1493 is the final portion of the extensive "ignimbrite flare up" of felsic, relatively high silica, volcanism
1494 which advanced across the Basin and Range province from the north to the Yucca Mountain
1495 region. The source of the felsic volcanic rocks is largely from the melting of crustal rocks as a
1496 result of heat from the mantle and intrusions into the lower crust. The felsic rocks are the result
1497 of collapse of *calderas* over felsic magma chambers causing immense flows of hot ash
1498 (ignimbrites) and ash falls which make up Yucca Mountain. These rocks which have been
1499 subsequently faulted by late stage normal faulting and shear faulting of the Walker Lane make
1500 up the repository rocks. They consist of both welded and unwelded tuffs. The welded tuffs are
1501 ash flows deposited in a sufficiently hot state that the ash particles welded together.

1502
1503 During the period from about 9 to 11 Ma the felsic volcanism in the Yucca Mountain region
1504 transitioned to mafic (basaltic) magmatism. At least four known pulses of basaltic volcanism
1505 have occurred [DOE, 2003] in the Yucca Mountain vicinity. These include the ~80 ka Lathrop
1506 wells cone and flows, ~1 Ma events (Pleistocene or

1507
1508



1509 Figure 2.5 The limit of the Southwestern Nevada Volcanic Field (from Byers et al., 1989)
 1510 indicated by the dashed line. Several volcanic calderas have been identified as the sources of
 1511 the intense felsic volcanic activity in the field. The caldera is no longer generally recognized
 1512 (Crowe et al., 1995). [After Crowe et al., 1995]
 1513
 1514

1515 Quaternary⁵) in Crater Flat, and multiple events dated ~3–6 Ma (Pliocene-U. Miocene) and ~8–
 1516 13 Ma (Miocene). Other young basalts in the Yucca Mountain region (YMR) include Little Black
 1517 Peak (~0.3 Ma) and Hidden Cone (~0.4 Ma), 35 km NW of Yucca Mountain Large exposures of
 1518 Miocene basalts occur in Jackass Flats, at Dome Mountain in the Timber Mountain caldera, and
 1519 in proximity to the Black Mountain caldera. Miocene-age basalts also occur in western Crater
 1520 Flat, and as a dike complex in Solitario Canyon on the northwestern flank of Yucca Mountain.
 1521 All of these occur within the Southwestern Nevada Volcanic Field (Christiansen et al., 1977;
 1522 Grauch et al., 1999) which is the site of intense episodic, voluminous magmatism and variable
 1523 intense extension over the period from 17 to 9 Ma and subsequent waning basaltic volcanism

⁵ The Pleistocene Epoch and the Quaternary Period are used synonymously in this document and much of the literature on igneous activity of the Yucca Mountain region for the time period between 11.5 ka and 1.75 Ma.

(Figure 2.5). It covers an irregular area with a radius of roughly 50 km generally centered on the Timber Mountain Caldera Complex immediately north of the proposed repository.

Rates and volumes of basaltic volcanism have declined significantly since Miocene time [DOE, 2003]. Magnetic surveys indicate that additional basalts may be buried beneath alluvium in Crater Flat and the Amargosa Desert [Stamatakos et al., 1997; Connor et al., 2000; O’Leary et al., 2002; Hill and Stamatakos, 2002; Perry et al., 2005]. Basaltic rocks have an intense magnetization in contrast to the alluvial sediments of the basins and, thus, are readily mapped by anomalies in the normal earth’s magnetic field. The *magnetic* variations (*anomalies*) resulting from buried basalts may be either positive or negative depending on the polarity of the Earth’s magnetic field at the time the basalts solidified. Additional details regarding the temporal and spatial occurrence of basalts dating back to 10 Ma are presented in Chapter 5.

3. Overview of Igneous Activity Processes

3.1. Introduction

The logic charts of Figure 1.2 a, b, c, d, and e show the components involved in evaluating the nature and likelihood of future igneous activity at Yucca Mountain and the potential consequences of this activity. The consequences are based on both the *intrusive* and *extrusive* scenarios and their interaction with the repository and the waste canisters. The processes involved in these scenarios are integral to the technical bases for decisions about igneous activity at the proposed Yucca Mountain HLW repository. Accordingly, this chapter briefly explains processes related to the origin and nature of igneous activity (Figure 1.2 a), magma/repository interaction (Figure 1.2 b, c, and d), dispersal of contaminated ash and its remobilization (Figure 1.2 e), and the doses to the RMEI from the contaminated ash (Figure 1.2 e).

3.2. Origin and Nature of Igneous Activity

3.2.1 Magma Generation

The origin and nature of igneous activity is important to understanding the processes that may impact the risk from the proposed Yucca Mountain repository. Knowledge of the scientific basis of igneous activity has progressed steadily during the past century, but growth has been particularly dramatic in the past 40 years, with the development of the *plate tectonic* paradigm and rapid advances in the geochemistry of igneous rocks and modeling of magmatic processes (e.g., Fisher, Heiken, and Hulen, 1997; Decker and Decker, 1997; Schmincke, 2004).

Magma is primarily generated at depths of several tens of kilometers in the lower *crust* and upper *mantle* along crustal boundaries where plates making up the outer *lithosphere* of the Earth are colliding (convergent boundaries) or being pulled apart (divergent boundaries) by sub-lithospheric movements within the mantle. Plates at convergent boundaries may be drawn into the Earth (subducted) to depths where components of the subducting slabs have melting points that are less than the ambient temperature of the Earth causing partial melting. Alternatively, water within subducted surface rocks may cause the melting point of rocks to decrease to a point where they melt or locally melting may occur by frictional heating of the down-moving subducting slab against adjacent rocks. At divergent boundaries the extensional regime acting upon the lithosphere may decrease pressure causing a lowering of the melting temperature of the rocks causing melting along mid-ocean ridges and continental rifts. This melting may be

1574 enhanced by the upward (buoyant) movement of hotter rocks from deep within the mantle.
1575 These rising plumes of hotter rocks may occur independent of plate margins producing localized
1576 igneous activity and voluminous volcanism on both the continents (e.g., Yellowstone) and
1577 oceans (e.g., Hawaiian Islands).
1578

1579 Partial melting of chemically primitive mantle rock produces basaltic magma which
1580 ascends due to buoyancy as magma-filled cracks and magmatic plumes. Most basaltic magma
1581 does not reach the Earth's surface, but becomes encumbered at depth due to solidification or
1582 loss of buoyancy. In continental terrains, stalled basaltic magma contains sufficient heat to melt
1583 the already hot lower continental crust and generate fresh magma that moves upward toward
1584 the surface as in the case of the volcanism that pervaded the Yucca Mountain region 10 to 12
1585 Ma. This rising magma reflects the composition of the local continental crust, which is much
1586 closer to *granite* (i.e., *rhyolitic*) in composition, and is distinctly non-basaltic as are the volcanic
1587 rocks making up Yucca Mountain. Volcanism in continental terrains, like the western U.S.
1588 including Yucca Mountain, is thus commonly bimodal, rhyolitic from the melting of the lower
1589 crust and basaltic from the venting of small mantle reservoirs of partial melts. Small-volume
1590 basaltic volcanism, as has occurred over the past several million years in the Yucca Mountain
1591 region, commonly are related to residual pockets of magma that are triggered into movement
1592 toward the surface by tectonic movements.
1593

1594 **3.2.2 Magma Composition**

1595

1596 The physical nature and behavior of magma intimately reflects its chemical composition.
1597 All Earth magmas are *polymeric* solutions of silica (SiO₂) diluted by varying amounts of cations
1598 (mainly, Al, Fe, Mg, Ti, Ca, Na, K, P). The silica content of magma, the basis of all rock
1599 classification schemes, varies from ~50 to 75 % by mass reflecting the chemistry of the source
1600 rock from which the magma was generated. There is a complete compositional gradation from
1601 basalts with ~50 % silica to rhyolites (essentially molten granite) with 70-75% silica. The
1602 temperature range of crystallization, the viscosity (or rheology), and most other transport
1603 properties are strongly dependent on magma silica content. Basalts crystallize at much higher
1604 temperatures and are much less viscous than rhyolites. This reflects the less polymerized
1605 nature of the melt forming the magma. The viscosity of a melt increases and becomes more
1606 difficult to deform as it becomes more silica-rich and thus more polymerized. At the same
1607 temperature and free of crystals, basalt is a factor of ~10⁴ times less viscous than rhyolite.
1608

1609 The single most important influence on the rheology, a critical parameter in determining
1610 the consequences of igneous activity at Yucca Mountain, of any given magma is the buildup of
1611 crystals as magma crystallizes. Most magmas crystallize over a span of about 200° C in
1612 temperature. Crystals build up from none at the liquidus to 100% by volume at the solidus.
1613 Liquidus temperatures vary from the order of 1200° C in basaltic rocks to as low as 700° C in
1614 granitic rocks depending on their composition, depth, and volatile content. Higher concentration
1615 of crystals strongly increases magma viscosity and as the maximum packing of crystals at ~50%
1616 approaches, the magma becomes a rigid, dilatant solid that expands upon shear and resists all
1617 motion. At maximum packing, as in a cup full of ice cubes, all solids (crystals) are touching and
1618 cannot undergo shear unless the assemblage expands as neighboring crystals move outward
1619 and past one another. With magma held within solid rock, there is no room for expansion.
1620 Consequently, no magma is ever erupted containing more than ~50 % crystals of a given size.
1621

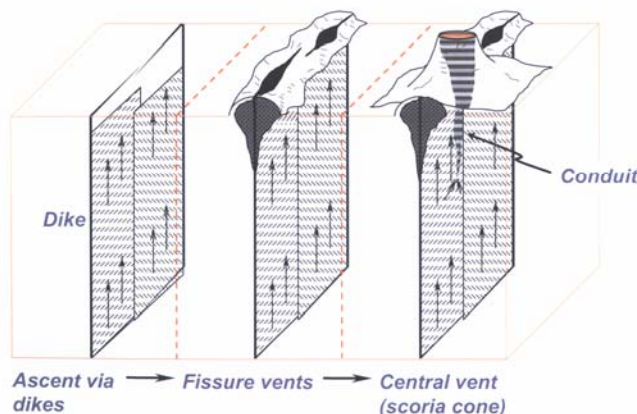
1622 Volatiles dissolved in magma are of central importance in determining the nature of
1623 volcanism and the risk from igneous activity at the proposed repository. Magma composition
1624 and confining pressure, aside from the availability of volatiles, are the major factors in controlling

1625 the concentration of volatiles in magma; temperature is of minor importance. The principal
1626 magmatic volatiles are H₂O, CO₂, and SO₂, with water the most common primary constituent.
1627 Water solubility is directly proportional to pressure and also to magma silica content. A silica-
1628 rich magma (e.g., rhyolite), for example, can contain far more water than basalt at the same
1629 pressure and temperature. Because the solubility of water in magma is zero under surface
1630 conditions of one atmosphere total pressure, as magma approaches Earth's surface it inevitably
1631 becomes saturated with water and generates bubbles, much as when a diver gets the bends
1632 from bubbles forming in the blood. Volatiles also have a major effect on the *viscosity* of magma.
1633 Water in solution, for example, de-polymerizes the melt structure, greatly reducing viscosity.
1634 Adding 5 % (mass) water to a rhyolite at 1000°C and sufficiently high pressure will reduce the
1635 viscosity by a factor of 10⁷. The effect is much smaller with basalt, but still important. Water also
1636 significantly reduces the temperatures of crystallization.

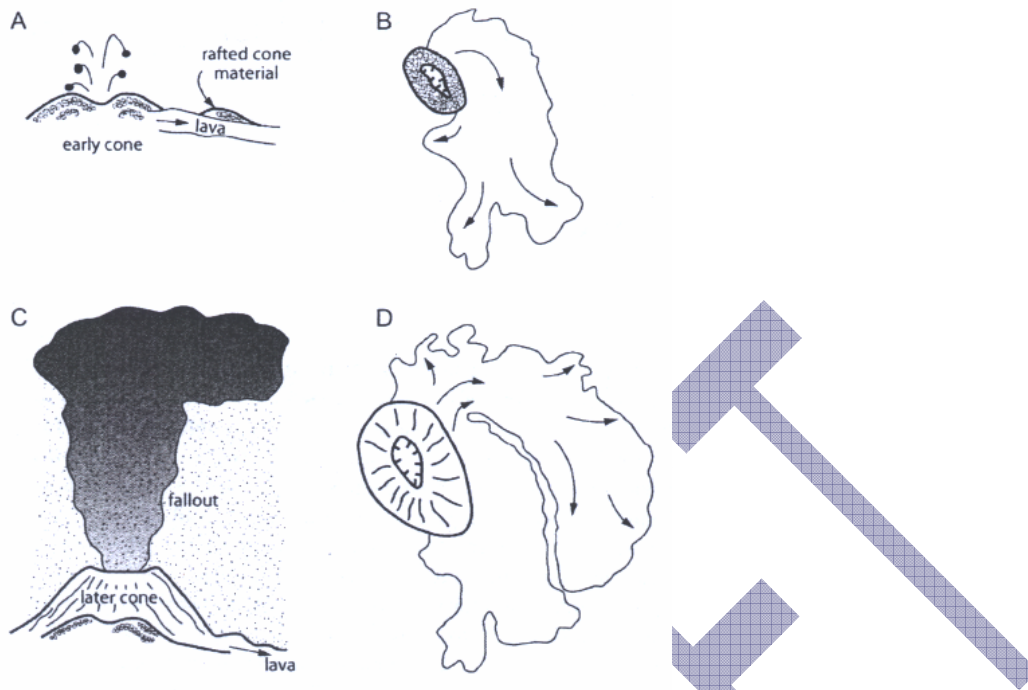
1637 3.2.3 Volcanoes and Their Products

1640 Magmas rise from source regions of molten rocks by buoyancy because of the lower
1641 density of the melt and included gas bubbles of vapor and when the overpressure exceeds the
1642 tensile strength of the overlying rocks. The melts rise largely as near-vertical disk-like slabs,
1643 typically a meter or two in width, in fractures that propagate in the direction perpendicular to the
1644 maximum compressive stress into the overlying rocks. The magma may be captured within the
1645 Earth, but if the magma reaches the surface a volcanic eruption occurs with the ejection of
1646 molten lava, gases, and fragmental materials through a vent into the atmosphere (Figure 3.1).
1647 The nature of the eruption controls the characteristics of the volcanic deposits and the relative
1648 proportion of eruptive products. For example, at the 80 ka Lathrop Wells volcano (Figure 3.2)
1649 eruption began with cone building and fan like lava flows (Figure 3.2 a and b) that led to violent
1650 Strombolian activity with episodes of sustained eruption columns that deposited tephra over the
1651 adjacent region depending on the wind direction that produced the major portion of the scoria
1652 cone (Figure 3 c). The latter was accompanied by additional lava flows as indicated in Figure 3
1653 d. The estimated volumes of the products of the Lathrop Wells volcano (Krier et al., 2006) are:
1654 1) eruptive products – 0.07 km³, 2) scoria cone – 0.02 km³, and 3) lava flows – 0.03 km³.
1655

Conceptual Model for Igneous Activity



1656 Figure 3.1 Conceptual model of igneous activity. Magma rises via dikes (left) leading to effusion
1657 of magma fountains along the length of dikes that reach the surface (center) and finally to
1658 focusing magma eruption in a conduit resulting in a volcanic cone (right). [After Valentine, 2006]
1659
1660



1662
 1663 Figure 3.2 Inferred eruption events at the Lathrop Wells volcano. a) and b) are respectively
 1664 simplified cross-sections and plan views of the early stage of eruption and c) and d) illustrate the
 1665 later stage of eruption with cone building dominated by fallout (c) and effusion of the eastern
 1666 lava field (d). [After Valentine et al., 2005]
 1667

1668 Volcanic cones are Nature's attempt to cap an erupting, runaway magma fountain, much
 1669 in the fashion of man capping a flaming oil well with a smothering mass. The pile of material
 1670 forming the volcano, in volume, textural detail, and composition, reflects the nature and
 1671 sequence of arrival of the ascending magma. Two convenient measures of the material type
 1672 and of volcanic activity itself are the explosivity and mobility of erupted materials. The volatile
 1673 content of the magma is central to this process as is the silica content or general composition of
 1674 the magma. The most explosive and devastating eruptions, by far, involve large volumes (10s to
 1675 1000s of km³) of silica-rich and volatile-rich magma (ash flows) that erupt as dense clouds of
 1676 ash and gas (ash flows) which flow along the surface moving under the force of gravity to lower
 1677 elevations.
 1678

1679 Ash flow eruptions have not occurred in the Yucca Mountain region for roughly 10 million
 1680 years. Instead, the eruptions have been of small volume silica-poor, basaltic magma. Basaltic
 1681 magmatic systems characteristically low in volatiles, like Hawaii, emit mainly high temperature
 1682 (i.e., low crystallinity), low viscosity, low explosivity lavas of high mobility that can flow
 1683 considerable distances (10s of km). Flow distance depends greatly on erupted volume and
 1684 terrain slope. On the other hand, basaltic magmas of high volatile contents (>~1% by mass)
 1685 become saturated in volatiles in approaching the surface and generate a bubble phase that can
 1686 expand rapidly, fragmenting the magma into material ranging from fine ash (mm) to coarse
 1687 tephra (cm) or cinders. The overall process is somewhat akin to the uncapping of a vigorously
 1688 shaken bottle of soda. The early phase of the eruption is marked by high explosivity with the
 1689 transport of ash into the atmosphere which is distributed to the surrounding region depending on

1690 intensity of the explosivity and the local meteorological conditions and the ejection of tephra that
1691 is deposited in a local cone around the vent, generally called a cinder cone. This phase of the
1692 eruptive sequence is called the *violent Strombolian phase* in reference to Stromboli volcano in
1693 the Mediterranean Sea, which has delivered gas-charged eruptions of this type since before the
1694 days of Aristotle. The extrusion of sluggish, high viscosity, low mobility lava flows follows the
1695 violent Strombolian phase. Small volume ($< \sim 5 \text{ km}^3$) cinder (scoria) cone systems of this nature
1696 are typical of those in the Yucca Mountain region. The outpourings are generally short-lived
1697 ($< \sim 10$ yrs) and occur in a single (i.e., monogenetic) episode, although polygenetic cinder cones
1698 are also not uncommon. Because cinder cone events often commence with eruption from a long
1699 fissure (~ 1 km or more) (Figure 3.1), there is the potential that a dike associated with a cinder
1700 cone event adjacent to Yucca Mountain could reach and compromise the integrity of the
1701 repository and its contents as could an eruption directly through the proposed repository.

1702 **3.3. Magma/Repository Interaction**

1703 **3.3.1 Nature of Magma Ascent**

1704
1705
1706
1707 Low viscosity magmas flow like thick syrup, can travel rapidly in small meter-size cracks
1708 and spread rapidly as lava flows. The transfer of basaltic magma in the upper crust, especially
1709 during establishment of a new volcanic center, is mainly by magma-filled elastic crack
1710 propagation, as evidenced by the common occurrences of dikes of basalt in eroded volcanic
1711 terrains. The rate of propagation is limited by the ability of the magma to flow into the opening
1712 crack. If magma viscosity becomes too large, dike propagation and ascent stall and magma
1713 may pool or solidify in place.

1714 **3.3.2 Key Features of Magmatic Dikes**

1715
1716
1717 The features of magmatic dikes that are critical to a Yucca Mountain igneous event are
1718 rapid rate of propagation, the azimuthal orientation, and the large aspect ratio (length/width).
1719 Dikes can travel as fast as a seismic shear wave, on the order of kms/sec, and typical aspect
1720 ratios can be on the order of 100 to 1000. The dike is envisioned as a thin circular disk
1721 expanding upward in all directions from the point of initiation and driven by an internal
1722 overpressure or buoyancy. A single dike one meter thick can lengthen to one kilometer or more
1723 as it approaches Earth's surface. The volume of available magma limits the size of any dike as
1724 well as the number of dikes that can be generated in any single event. Once the dike intersects
1725 the surface, the internal driving pressure is dissipated through venting of the magma
1726 compromising further expansion. Propagation is normally in the plane of the least principal
1727 stress, which in Earth is generally vertical, and the strike or azimuthal orientation of the dike is
1728 strongly influenced by the principal horizontal stresses, whose magnitude and orientation reflect
1729 the structural makeup of the crust and the prevailing tectonic conditions. These are generally
1730 referred to as 'regional stress patterns.' Local topographic conditions, which alter the local
1731 stress field, can literally steer the dike to a limited degree as it reaches the surface.

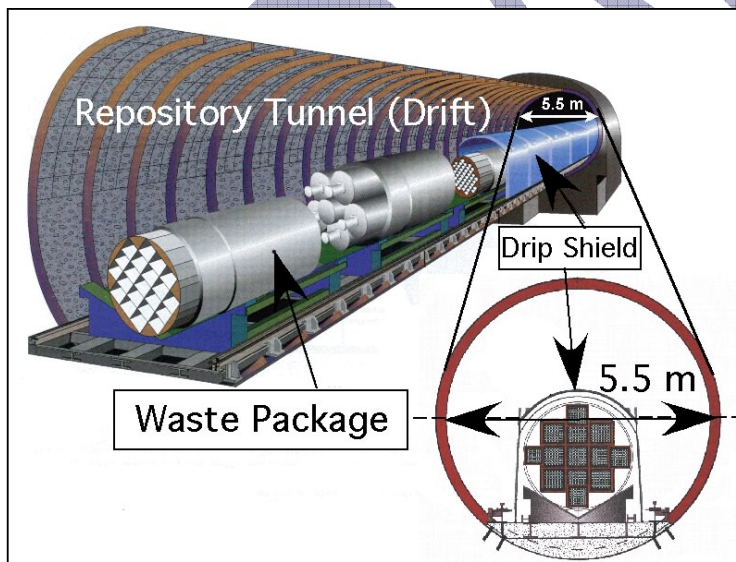
1732 **3.3.3 Basic Nature of Eruptive Event**

1733
1734
1735 The nature of the eruptive event as the dike intersects the surface depends critically on the
1736 type of magma, its viscosity and, especially, the volatile content of the magma. The solubility of
1737 water and other volatiles is strongly dependent on the prevailing pressure and magma
1738 composition and much less so on temperature. With the amount of volatiles expected for typical
1739 basaltic magmas in the Yucca Mountain region, the magma will be undersaturated with volatiles
1740 until it comes within about 5 km of the surface. At the point of saturation a separate vapor phase

1741 will form as an assemblage of bubbles to further accelerate ascent. The increasing strength of
1742 this vapor phase event will eventually fragment the magma and form an explosive eruptive
1743 column into the atmosphere of hot gas laden with quenched particles of magma. The sizes of
1744 these particles will vary from fine ash to popcorn-like tephra. The strength and duration of an
1745 event depends on the volume of magma involved, the volatile inventory, the number of eruptive
1746 vents, and the geometry of the eruptive system. The explosive phase of the eruption is followed
1747 by a cone-building phase consisting of deposition of tephra, spatter, and similar products about
1748 the vent. This is followed by the extrusion of lava pushing out through the base of the cone and
1749 flowing under gravity in directions dictated by topography.

1751 3.3.4 Interaction with Repository and Canisters

1752
1753 In the unlikely event that volcanic activity would intersect a repository (Figure 3.3), there
1754 are three scenarios for potential interaction with the repository. The consequences for future
1755 radiological exposures vary significantly among these. The first scenario, the intrusion scenario,
1756 involves hypothetical intersection of the repository drifts by a volcanic dike (see Figure 1.2 c and
1757 3.4). An ascending dike could theoretically be deflected around a repository by topographic
1758 and/or thermal-mechanical stress (Hardy and Bauer, 1991). Nonetheless, NRC, DOE, and
1759 EPRI have considered the possible consequences by assuming that a dike could intersect and
1760 propagate through the repository and interact with the waste canisters within the tunnels (drifts).
1761 As a dike approaches the level of the drifts, the crack tip would advance ahead of the magma
1762 front. This advancing vapor-filled cavity would be the first part of the propagating dike to reach
1763 the drift. DOE now models the pressure in this cavity to be negligible because of the very high
1764 gas permeability of the fractured tuff country rock (Detournay et al., 2003 [p. 50]).
1765



1766
1767
1768 Figure 3.3. Schematic depiction of the anticipated repository tunnel (drift) containing waste
1769 packages within Yucca Mountain.

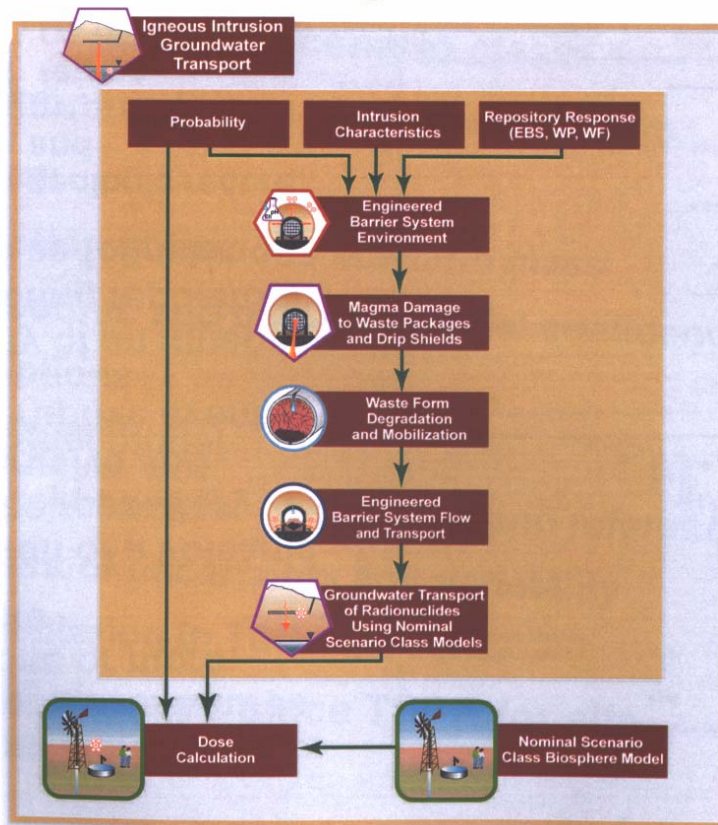
1770
1771 Detournay et al. (2003, p. 49) also commented on the possible effects of a repository on
1772 dike propagation, as follows:

1773
1774 The stress barrier that develops around a hot repository during the intermediate period
1775 spanning the first 2000 years [since closing of the repository] could cause the dike to be

1776
1777
1778
1779
1780
1781
1782
1783

deflected so as to avoid crossing of the repository, promote the creation of a sill, or halt propagation of the tip approaching the repository if the dike is centered a few kilometers north or south. Such protection is time-limited, however; it is therefore conservative to assume that the dike would propagate vertically under all circumstances and would intersect the repository. The major impact of the thermal perturbation would be to reduce significantly the size of the tip cavity ahead of the magma front and perhaps to increase the magma pressure gradient behind the magma front.

Identification and Linkages of Abstractions—Igneous Intrusion



1784
1785
1786
1787
1788
1789
1790
1791
1792
1793
1794
1795
1796

Figure 3.4 Identification and linkages of abstractions in the igneous intrusion scenario of DOE's TSPA. [After Valentine, 2006]

It is of interest that the stress barrier described by Detournay et al. (2003) would apply during the time when potential risk from volcanism is at its greatest. After the first 1000 years the hypothetical doses would diminish significantly (see Figure 5.10 below) because substantial amounts of shorter-lived radionuclides would have decayed away.

As the basaltic magma moves upward it may degas steadily or catastrophically. Steady release of gas would diminish the volatile content such that the magma front would not likely produce violent explosive behavior when it encounters the repository, and it would instead flow effusively into the drifts. In the hypothetical case where gas explosively exsolves, magma could

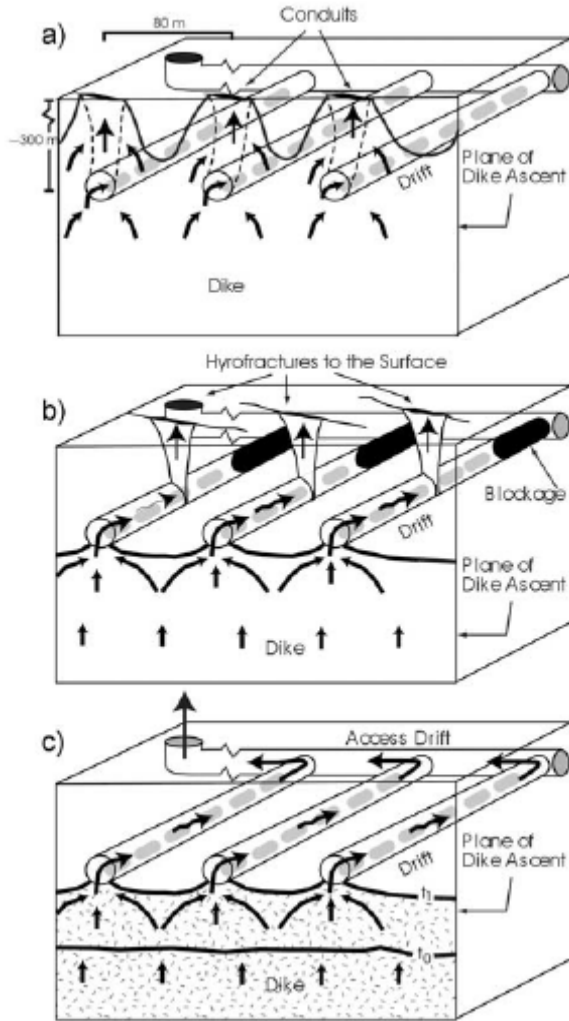
1797 flow into drifts as a two-phase gas-magma flow, generating tephra instead of a magma flow.
1798 The flow of magma into drifts may slow the progress of the magma front to the surface, but it
1799 should have little effect on the tip of the dike cavity, which would already have begun
1800 accelerating given the diminishing overburden pressure as it approached the surface. The dike
1801 tip would probably reach the surface in seconds after passing the repository horizon (BSC,
1802 2003a). Flow of magma into a tunnel would lower the pressure in the dike directly above the
1803 drift, but this would last only as long as it takes for the tunnel to become filled with magma or to
1804 become obstructed by a plug of tacky, incandescent tephra.
1805

1806 If a dike reaches the level of the repository, magma would be available to flow into drifts at
1807 a rate that would strongly depend on the magma viscosity and the rate of magma solidification
1808 as it contacts the relatively cold drip shields, waste packages, and tunnel walls. The flow rate
1809 would also be influenced by frictional losses at the dike/drift interface and partial obstruction of
1810 the tunnel by waste packages and drip shields. DOE (2003) estimates that magma could fill a
1811 drift in about 5 minutes, given a dike ascent rate of 1 m/s and very low viscosities between 10
1812 Pa·s and 100 Pa·s. Magma rising at 10 m/s could fill a drift in less than 1 minute. Recent work
1813 suggests that magma viscosities could be orders of magnitude higher than previously assumed,
1814 which would reduce the rate of magma entry to drifts (Marsh and Coleman, 2006). The
1815 potentially critical effects of quenching and solidification on waste packages and drift walls have
1816 yet to be fully evaluated by DOE and NRC.
1817

1818 EPRI (2004) has analyzed plausible consequences of magma entry into a repository.
1819 Given the possibility of higher viscosities than previously used in analyses, EPRI concluded that
1820 partial intrusion of magma into a drift could create three zones within a tunnel. The first zone
1821 would be close to the dike intersection, where drip shields and waste packages would be
1822 assumed to be fully engulfed by magma. This 'Red Zone' would be characterized by disrupted
1823 drip shields, thermally weakened Alloy-22, and failure of spent fuel cladding. The waste
1824 packages in this zone would have increased susceptibility over time to the effects of ground
1825 water moving through the unsaturated zone. Beyond the 'Red Zone' would be a 'Blue Zone,'
1826 where drip shields and waste packages would not be inundated by magma but would
1827 experience high temperatures and potentially corrosive gases (EPRI, 2004). Drip shields would
1828 remain intact, but failure of the waste package outer barrier and spent fuel cladding could occur
1829 within a relatively short time after the intrusive event. Beyond the Blue Zone would be the
1830 'Green Zone' where waste packages experience modest (<350°C) temperatures and the
1831 possible deposition of reactive magmatic volatiles onto waste package surfaces. Waste
1832 packages and their drip shields would be unaltered with respect to their resistance to corrosion
1833 (EPRI, 2004).
1834

1835 A second scenario for magma-repository interaction has been proposed whereby magma
1836 might fill a drift and create enough pressure to generate (at a distance from the entry point) a
1837 secondary dike to the surface as illustrated in Figure 3.5 [Woods et al., 2002]. This so-called
1838 "dogleg" scenario could potentially affect a large number of waste packages. The key factor
1839 here is whether the magma has the ability to fill the drift quickly and re-pressurize it to the extent
1840 of nucleating a new dike elsewhere along the drift, in spite of the initial flow continuing to the
1841 surface. This scenario arose from observations that secondary breakouts of magma sometimes
1842 occur in association with basaltic eruptions. This "dog-leg" model was analyzed in BSC (2003a)
1843 which considered the propagation of pressure and stress through the dike system and the effect
1844 of magma cooling. Detournay et al. (2003) considered the propagation of either a magmatic or
1845 pyroclastic "dog-leg" scenario to be improbable, but recommended further analyses to assess
1846 the impacts of a partially coupled pyroclastic flow scenario on repository performance.
1847

1848
1849



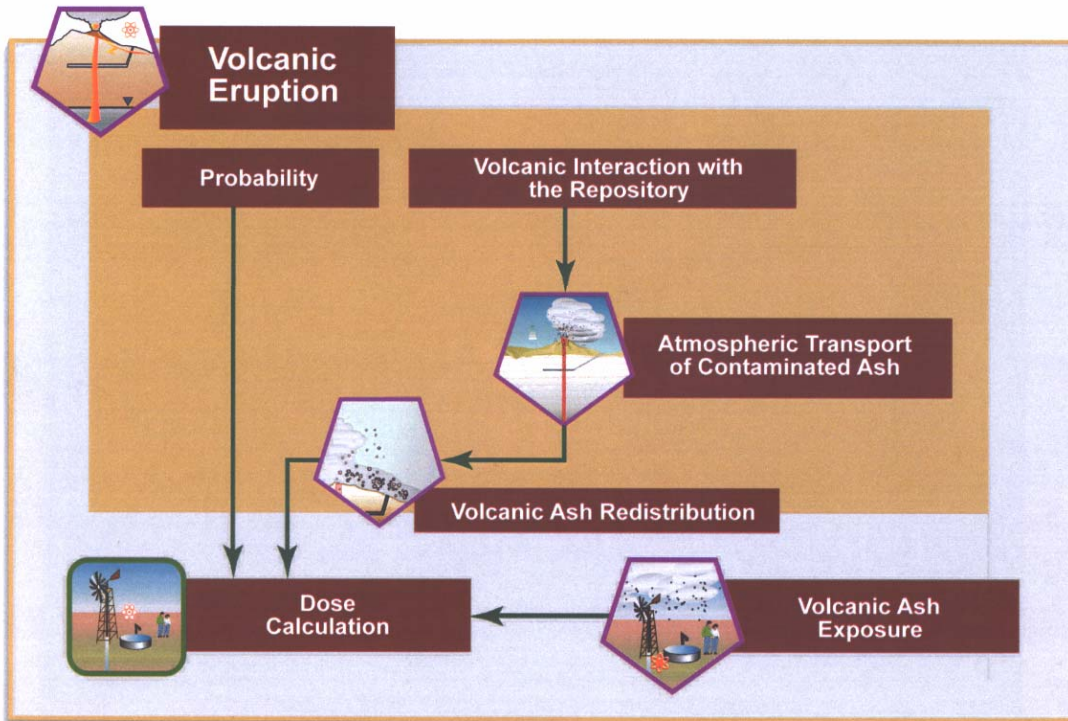
1850
1851
1852
1853
1854
1855
1856
1857
1858
1859
1860
1861
1862
1863
1864
1865
1866
1867
1868

Figure 3.5 Schematic of the steady flow geometry that may enable a steady basaltic eruption to develop (dog-leg scenario: a) with flow along the original dike; b) with magma being diverted along the drift before surfacing along a new fissure; and c) with magma being diverted along the drift and into the main access drift from where it vents to the surface. [After Woods et al., 2002]

The third igneous scenario involves the intersection of a tephra-cone-forming volcanic vent (i.e., conduit) within the repository drift (see Figures 1.2 e and 3.6). The transition from flow in dikes to vent flow occurs early in an eruptive sequence, and vents form under various conditions. In low-viscosity basalts, the transition may occur when narrow parts of the dike freeze followed by mechanical and thermal erosion of wider sections as the flow is repartitioned (e.g., Bruce and Huppert, 1990). A key difference between a volcanic vent and a dike is that the vent is much smaller in diameter (generally <75 m) than a dike is long (1-5 km or more). Given a repository drift spacing of >50 m, a vent could directly intersect only one drift along with a relatively small number of waste packages within the cross-section of the vent. Due to the perceived complexity of the processes involved, both NRC (Mohanty et al., 2004) and DOE (2003) assume that the small number of waste packages (approximately 1-10) entrained within a conduit would be completely destroyed and the contents carried to the surface and ejected as

1869 tephra of varying sizes. The degree to which ceramic or glass waste forms could be reduced to
 1870 fine particulate materials in a volcanic conduit is highly uncertain, particularly during the first
 1871 1000 years when the waste packages and waste forms should still be relatively intact. The
 1872 manner and degree to which the fragments would be incorporated in volcanic tephra is
 1873 uncertain, but would involve the well-known phenomenon of magma quenching.
 1874
 1875

Identification and Linkages of Abstractions—Volcanic Eruption



00731DC_0047.ai

1876
 1877 Figure 3.6 Identification and linkages of abstractions in the eruption scenario of DOE's TSPA.
 1878 [After Valentine, 2006]
 1879

1880 The importance of gaining a detailed understanding of these scenarios can be appreciated
 1881 from the point of view of estimating potential radiation doses associated with magmatic activity.
 1882 The largest hypothetical radiation dose would arise if extrusive igneous activity were to occur
 1883 during the first 1000 yrs after repository closure (Mohanty et al., 2004 [see their Figs. 3-45 & 3-
 1884 46]). After that time potential doses to future generations diminish significantly because
 1885 substantial fractions of shorter-lived radionuclides will have decayed. Waste packages should
 1886 be minimally degraded during the first 1000 years and therefore would be more resistant to
 1887 igneous thermal/physical effects during that time.
 1888

3.4 Dispersal of Contaminated Ash

1889
 1890

1891 Ash⁶ emitted during an extrusive event that erupts through the proposed repository may
1892 contain fragmented radioactive waste. The contaminated ash will contribute to the dose to the
1893 RMEI primarily through inhalation (Figure 3.6). If the ash is not contaminated by radioactive
1894 materials, and is present in sufficient concentration, it can cause respiratory problems, but these
1895 will be minor and transient in healthy individuals (Calabrese and Kenyon, 1991). Accordingly,
1896 studies of the impact of ash on humans have been directed at radioactively contaminated ash.
1897

1898 **3.4.1 How is Ash Dispersed?**

1899

1900 Contaminated ash will be dispersed in the same way as uncontaminated ash from a
1901 violent Strombolian eruption. The ash plume consists of a vertical high-speed jet, a mixture of
1902 gases and particles that rises adiabatically to an altitude where its buoyancy is neutral; i.e.,
1903 where the plume temperature is the same as the ambient temperature (DOE, 2000). At that
1904 altitude, further dispersion of the ash depends on meteorological conditions. Wind has a first-
1905 order effect, and meteorological conditions that impact the crosswind movement of gases and
1906 particles have a second-order effect (Wark et al., 1998).
1907

1908 Dispersion of ash particles by meteorological conditions can be modeled and predicted in
1909 several different ways. The Suzuki model (Suzuki, 1983) is generally accepted as representing
1910 the dispersion of ash from a violent Strombolian eruption correlates well with reported data on
1911 ash fallout (Suzuki, 1983, Figures 2 and 3). The basic premises of this model are::
1912

- 1913 • Movement of dispersing particles in the air is random
- 1914 • Small particles diffuse both vertically and horizontally
- 1915 • The scale of horizontal turbulence is much greater than the scale of vertical turbulence.
1916

1917 The Suzuki models involve turbulent diffusion by combining several theoretical diffusion
1918 formulations with empirical observation instead of using the *Fickian diffusion* equation that most
1919 Gaussian models employ (see, e.g., Wark et al., 1998, Chapter 4),
1920

1921 **3.4.2 How does Ash become Contaminated?**

1922

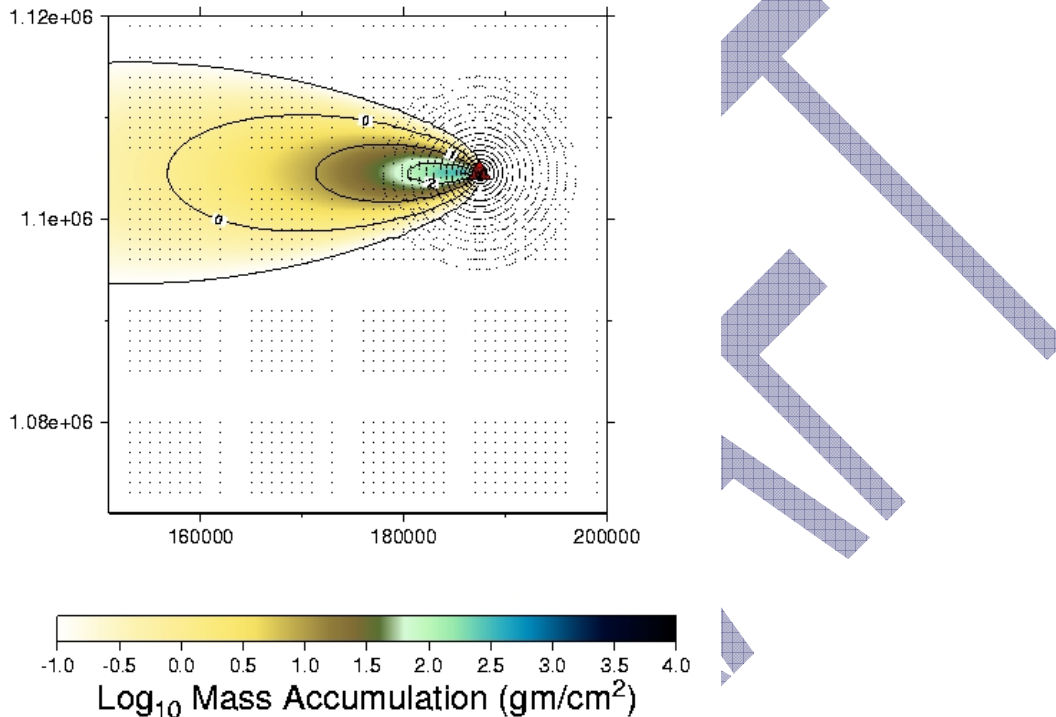
1923 The ash from the postulated extrusive event would be radioactively contaminated by the
1924 incorporation of spent nuclear fuel particles and gases. Two types of contaminated ash can
1925 result from the interaction of magma and spent fuel: (1) direct incorporation of spent fuel and (2)
1926 incorporation of the more volatile fission products. Uncontaminated ash will also be emitted and
1927 dispersed. Incorporation depends on the relative densities of ash particles and spent fuel
1928 particles. The major constituent of spent fuel is uranium dioxide, which has a density of about
1929 10 gm/cm³ – about five times the density of volcanic ash – so that incorporation of this material
1930 would result in relatively dense ash. Jarzempa and LaPlante (Jarzempa, 1997; Jarzempa and
1931 La Plante, 1996) estimate that the net maximum density of ash contaminated with spent fuel will
1932 be about 5 gm/cm³, resulting in relatively dense ash particles. On the other hand, less dense
1933 radionuclides like radiocobalt and volatile radionuclides like radiocesium, as CsCl, although
1934 likely to adhere to or condense on ash particles, would not increase the ash particle density
1935 significantly.
1936

1937 Suzuki postulates ash particles with a mean actual diameter of about 1000 microns and
1938 standard deviations of 1000, 4000, and 2 x 10⁴ microns. He also postulates ash particle

⁶ The material ejected during a violent volcanic eruption regardless of size is tephra, but very small particles (< 2 mm) of tephra often are referred to simply as “ash,” and are so designated in this document.

1939 densities between 0.1 and 2.4 gm/cm³, but includes in his model particle densities up to 10
 1940 gm/cm³. Assumptions about ash particle diameter and density are important to modeling both
 1941 the direct air dispersion and the remobilization of ash particles by wind. As expected, larger,
 1942 denser ash particles fall out of the eruption plume close to the vent, while smaller, less dense
 1943 particles are carried farther from the eruption site at the time of the eruption. Suzuki models the
 1944 footprint of the plume of smaller (1000 to 4000 microns) ash particles as extending as far as 60
 1945 km downwind. The range postulated by Suzuki encompasses the Jarzemba and La Plante
 1946 (1996) assumption that the density of contaminated ash could vary up to 5 gm/cm³.

1947
 1948 Figure 3.7, provided here as an example, shows a sample of Suzuki model output produced by
 1949 modeling an eruption (at Irazu volcano, Costa Rica)
 1950



1951
 1952 Figure 3.7. A contour plot illustrating the expected tephra dispersion for eruption and
 1953 meteorological parameters listed in Table 3.1. The plot coordinates indicate location of the
 1954 deposited material with respect to the eruption site. The vertical axis is in a northerly direction;
 1955 the horizontal axis, easterly. The numbers refer to universal transverse Mercator UTM grid
 1956 locations; units are meters. From
 1957 <http://www.cas.usf.edu/~cconnor/parallel/tephra/tephra.html#input>.
 1958

1959 Table 3.1. Input parameters for the Suzuki model example shown in Figure 3.7. Values for all
 1960 input parameters are supplied by the analyst using the code.

Parameter	Value
total_ash_mass (kg)	6x10 ¹⁰
maximum_particle_diameter_considered (microns)	10 ⁶
minimum_particle_diameter_considered (microns)	10,000

particle_mean_diameter_erupted (microns)	30,000
part_sigma_size (diameter standard deviation)	10,000
part_mean_density (gm/cm ³)	1.1
part_shape_factor (dimensionless)	0.5
vent_height	0.0
max_column_height (m)	8000
column_beta (parameter governing the shape of the beta distribution) ⁷	0.01
initial_eruption_velocity (at the vent) (m/s)	100
avg_windspeed (m/s)	10

1961
1962
1963
1964
1965
1966
1967
1968
1969
1970
1971
1972
1973
1974
1975
1976
1977
1978
1979
1980
1981
1982
1983
1984
1985
1986
1987
1988
1989
1990
1991
1992
1993

The downwind distance that ash particles are transported depends on the height of the emitted column of ash, the wind speed, and the density and diameter of the particles. Particles with activity mean aerodynamic diameter (AMAD)⁸ larger than about 100 microns, as well as particles with density greater than about 5 gm/cm³, would generally fall to the ground before reaching terminal velocity (Wark et al., 1998). Settling of these particles would most likely be within tens of meters of the eruption vent. Smaller and less dense particles would be transported by water, by way of overland runoff to stream channels, and by wind. The particles would be carried predominantly downwind if the original jet is vertical.

3.5. Remobilization and Resuspension of Contaminated Ash

After deposition, the loose ash in a tephra sheet can be exposed to surface processes. Wind, rain, and ephemeral surface water flow begin to erode, rework, transport, sort, and redistribute the finer-grained ash (Figure 3.8). These fine-grained materials have potential health significance because only they can be picked up from the surface by winds and transported toward the RMEI. Current models assume that the radioactive materials in or on such particles are resuspended and inhaled or incorporated into soils and foods grown from those soils. There are a significant number of assumptions used to make these calculations. Many of them rely on assumptions on the availability for removal and mobilization and solubility of radioactive materials incorporated in or on ash particles. There are additional assumptions on the incorporation of mobilized radioactive materials into these exposure pathways.

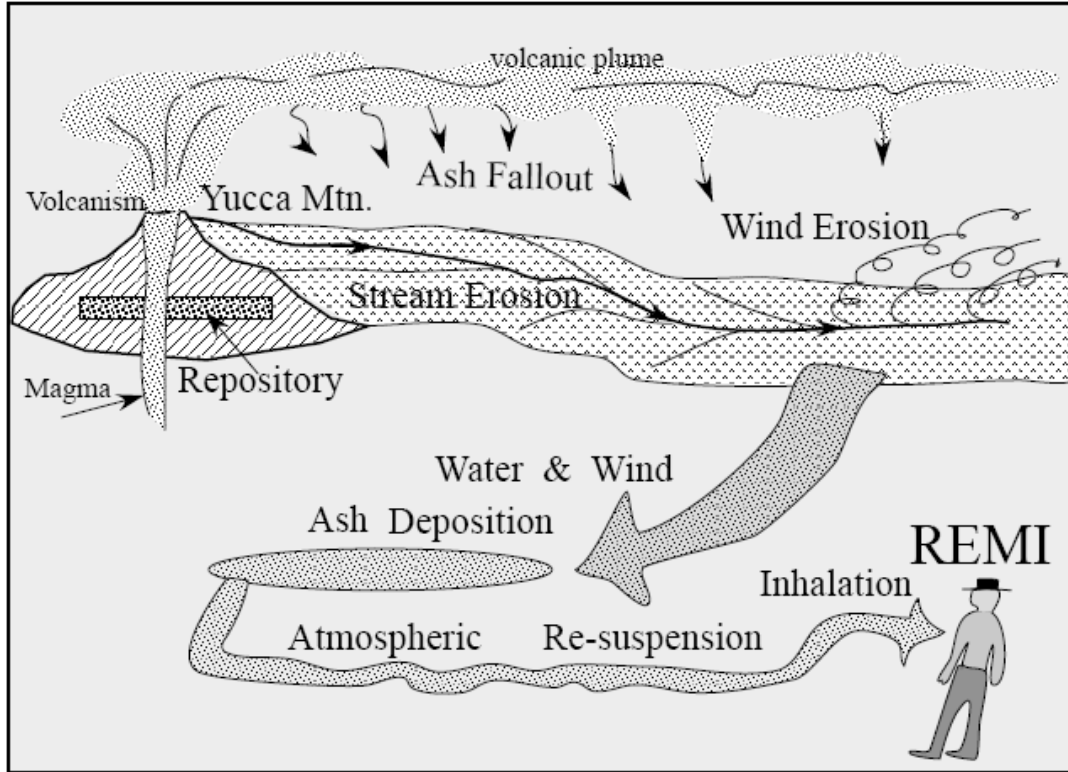
Wind is an almost continuous process, but it will not always blow from an area with contaminated ash toward the compliance area with the RMEI. Most of the volcanic ash would not be contaminated, and only particles with AMADs less than about 50 microns would be lofted by the wind. Radioactively contaminated particles of AMAD 20 microns contribute more than larger sized particles to calculated doses because of the patterns of deposition in the respiratory tract of humans. Larger particles would contribute only minimally to a RMEI dose, if at all.

Intense, ephemeral floods associated with major storms have the potential to extensively erode tephra deposits, but the large flood discharges also can transport radioactive materials to the

⁷ The shape of a beta distribution is determined by two parameters, so that by adjusting these arbitrary parameters the distribution can take any of a number of shapes, from Gaussian, to log-normal, to uniform. The analyst can thus adjust the form of the input distribution to best of the data.

⁸ . Movement of particles is often modeled by giving particles the radial dimension they would have if they were spherical particles of density 1 gm/cm³. This is the activity mean aerodynamic diameter, or AMAD.

1994 vicinity of the RMEI or far beyond. Floods are especially capable of transporting fine-grained
 1995 materials important to the inhalation dose for long distances.
 1996
 1997 Realistic analyses of potential doses must consider all of these processes as well as particle
 1998 size and density.
 1999
 2000
 2001

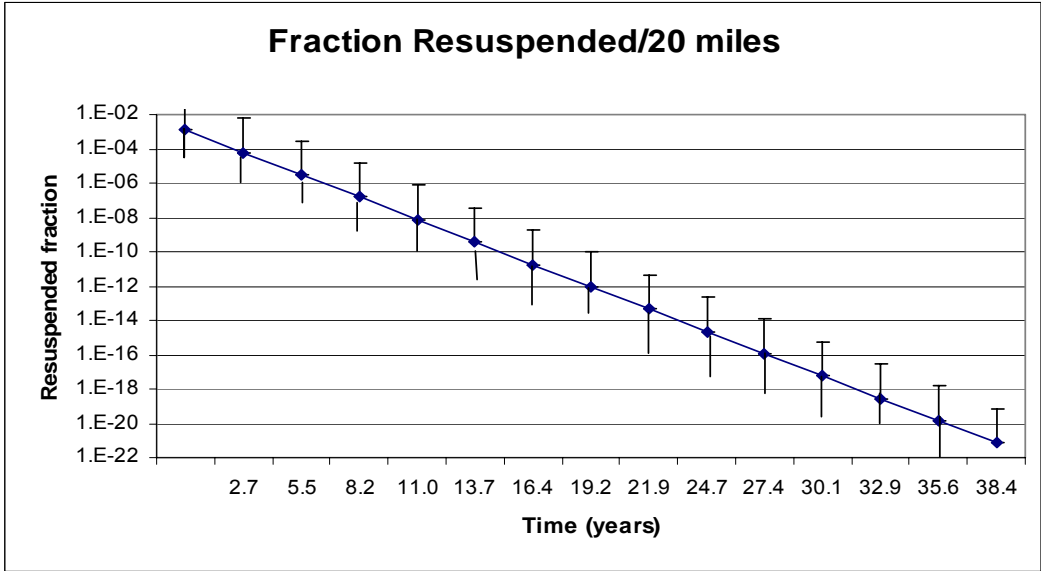


2002
 2003
 2004 Figure 3.8 Schematic diagram of processes involved in ash remobilization.
 2005
 2006

2007 Airborne particles that are resuspended after having been deposited on the ground can be
 2008 major contributors to inhaled particulate matter, and thus to an inhalation dose. The fraction of
 2009 deposited material that can be resuspended, and the distance it can travel, are controversial
 2010 because relatively few measurements of these parameters have been made. Anspaugh et al.
 2011 (2002) have developed both a short-term and a long-term model for resuspension and the
 2012 dispersion of resuspended material. Anspaugh et al. (2002) points out that there is at least an
 2013 order of magnitude uncertainty in any long-term model of resuspension. Long-term models are
 2014 empirically derived from a large data base that includes measurements from the Nevada Test
 2015 Site as well as Chernobyl.
 2016

2017 Anspaugh (2004) points out that a substantial amount of material will be available for
 2018 resuspension 15 or more years after the particles are deposited (Figure 3.9), suggesting that
 2019 even after decades some resuspended ash will be available for inhalation by the RMEI. This
 2020 resuspended and ultimately redeposited contaminated ash may also contribute to an ingestion
 2021 dose if taken up by agriculturally important vegetation. Ingested radionuclides generally

2022 contribute less to the total committed dose because the food ingestion pathway dilutes the
2023 radioactive material more than the direct inhalation pathway.
2024



2025
2026 Figure 3.9 Resuspended fraction of deposited material from the Anspaugh et al. (2002)
2027 equation for long-term resuspension. Graph shows the fraction of resuspended material that is
2028 carried 20 miles by wind.
2029

2030 3.6. Doses from Contaminated Ash

2031 Dispersed contaminated ash can deliver radiation doses externally, from inhaled particles,
2032 and from ingested radionuclides. External doses from particles deposited on the ground
2033 (groundshine) and from particles suspended in the air (cloudshine) would occur at the time of
2034 the eruption or shortly thereafter. Potential cloudshine doses are several orders of magnitude
2035 less than groundshine and can usually be neglected. Groundshine is not considered for this
2036 analysis because direct hazards to occupants during an eruption would involve more serious
2037 risks. Internal doses to the RMEI subsequent to the volcanic eruption by Inhalation and
2038 ingestion of radioactively contaminated materials are identified in the logic diagram (Figure 1.2
2039 d).
2040
2041

2042 A conservative estimate of dose to the RMEI would involve consideration of contaminated
2043 ash derived from waste packages sufficiently damaged that the spent fuel matrix itself would be
2044 damaged and particles of both the spent fuel itself and activated metal from the clad and waste
2045 package could be entrained in the ejected material. The exposure pathways for the
2046 contaminated ash to reach the RMEI would then be by: (1) external exposure to deposited
2047 radionuclides, (2) inhalation of contaminated ash, and (3) ingestion of radionuclides in
2048 contaminated ash taken up by plants or dissolved in drinking water.
2049

2050 If the igneous event were to occur after roughly the first thousand years after closure of the
2051 repository, the very radioactively strong gamma emitters (e.g., Cs¹³⁷) would have radioactively
2052 decayed to negligible levels, so that the external dose rate from deposited radionuclides would
2053 be relatively small and might not be readily detectable. In addition, the external dose from the
2054 much longer-lived actinides would be small, because the specific activity of these radionuclides
2055

2056 is relatively small and because the gammas they emit are relatively less energetic. Doses to the
 2057 RMEI from direct exposure to contaminated volcanic ash would be primarily inhalation doses,
 2058 which are committed doses, usually considered committed for 50 years. Direct exposure can
 2059 come about from direct inhalation of airborne contaminated ash and from remobilized
 2060 resuspended contaminated ash.

2061
 2062 The dose delivered by an inhaled and absorbed radionuclide depends on metabolism and
 2063 particle size; the most penetrating particles are about 0.3 microns (AMAD). The energy
 2064 absorbed by various organs and the type of radiation are reflected in the dose conversion
 2065 factors (DCFs) for each radionuclide (Eckerman and Ryman, 1993; Eckerman, et al, 1999;
 2066 Leggett and Eckerman, 2003).

2067
 2068 **3.6.1 Inhalation Dose**

2069
 2070 The inhalation dose is considerably larger than any ingestion dose. The inhalation dose to
 2071 a receptor is a function of the concentration of radioactively contaminated particles in breathable
 2072 air, the fraction of those particles that can be inhaled, and the dose from what is inhaled into the
 2073 respiratory system and distributed throughout the body. The particles are made available for
 2074 inhalation by the resuspension of particles by atmospheric processes. Radioactively
 2075 contaminated particles of AMAD 20 microns or less, because of the patterns of deposition in the
 2076 respiratory tract of humans, contribute more than larger sized particles to doses. Larger
 2077 particles would contribute only minimally to a RMEI dose, if at all.

2078
 2079 The dose delivered by an inhaled or ingested radionuclide also depends on its rate of
 2080 absorption by the target organs. The dependence of dose on particle size is expressed in an
 2081 approximately lognormal distribution with a maximum at one micron AMAD, including significant
 2082 contributions from less than one to 10 microns.

2083
 2084 The type of radiation and the energy absorbed by various organs of the human body are both
 2085 reflected in the dose conversion factors (DCFs) for each radionuclide (Eckerman and Ryman,
 2086 1993; Eckerman et al., 1999; Leggett and Eckerman, 2003).

2087
 2088 **3.6.2 Ingestion Dose**

2089
 2090 Anspaugh et al. (2002) reviews measurements of vegetation uptake of deposited
 2091 radionuclides at the Nevada Test Site following atmospheric tests of nuclear devices. Table 3.2
 2092 shows the computed fractions of fallout particles that were intercepted by vegetation.

2093
 2094
 2095 Table 3.2 Summary of computed values of mass interception fractions of fallout from nuclear
 2096 tests at the Nevada test site. [After Anspaugh et al. 2002]

Parameter	Computed values of mass interception fractions m ² of contaminated surface/kg vegetation dry weight			
	Native desert vegetation		Pasture-type vegetation	
	Total fallout	≤44 μm	Total fallout	≤44 μm
Arithmetic mean	0.18	0.81	0.20	1.9
Standard deviation	0.25	1.3	0.29	4.29
Geometric mean	0.062	0.37	0.081	0.82
Standard deviation	6.3	3.7	4.8	3.2

2098
2099
2100
2101
2102
2103
2104
2105
2106
2107
2108
2109
2110
2111
2112
2113
2114
2115
2116
2117
2118
2119
2120
2121
2122
2123
2124
2125
2126
2127
2128
2129
2130
2131
2132
2133
2134
2135
2136
2137
2138
2139
2140
2141
2142
2143
2144
2145

Smaller particles are more likely to be taken up by vegetation than larger particles, and dissolved material is the most likely to be absorbed. Some of the immediate fallout could be absorbed by pasture-type vegetation, since alfalfa is grown in the Amargosa Desert, and a small but non-negligible ingestion dose could result. Fluvial mobilization could also result in vegetation uptake of deposited contaminated ash.

Uptake of radionuclides by vegetation and the transfer of those radionuclides by herbivores to meat products or milk is expressed in radionuclide-specific food transfer factors. Virtually no agricultural products intended for human consumption are produced in the area occupied by the RMEI. Lee et al. (2005) have observed that rainfall would have to increase about ten fold to provide enough water for locally grown crops or enough water for families to grow a significant fraction of their own food. Thus, ingestion dose would probably be limited to meat and milk for this scenario. Alfalfa is grown in the Amargosa Desert today, but there is not enough locally grown alfalfa to maintain either beef or dairy cattle. As was observed in the 2004 ACNW tour of the Amargosa Desert, the one commercial farm, a dairy farm, imports most of its alfalfa from outside the Valley.

4. Nature of Potential Igneous Events in the Yucca Mountain Region

4.1 Introduction

The initial question in the risk triplet (Figure 1.2 a) – what can happen is the subject of Chapter 4. What can happen in this case is an igneous activity event that impacts the proposed Yucca Mountain repository. Events may be initiated directly beneath the proposed repository or may reach the tunnels of the repository by dikes associated with the event extending into the footprint of the repository.

The volcanic history of Yucca Mountain, and the changes in volcanism that have occurred with time in the Yucca Mountain region, suggest that a future igneous activity event would involve a particular type and volume of volcanic eruption and produce volcanic conduits of a particular size and shape. This assumption is supported by the geologic and tectonic history of the region and the comprehensive site characterization of the Yucca Mountain region that has provided information on basaltic volcanism during the past 10 Myr. Additionally, geologic investigations of other volcanic regions of similar age of the Basin and Range province and volcanological studies of modern volcanoes and their processes contribute useful information about the range of anticipated igneous events. There is general agreement among investigators on many, but not all, of the characteristics of possible future igneous activity. These views and their current status are identified in this chapter.

4.2 Volcanic Analogs

To evaluate the likelihood and consequences of an igneous event intersecting the proposed repository it is necessary to estimate the type, size, and shape of future igneous events, and their location and orientation. The importance of these attributes is illustrated in comparing a volcanic vent (conduit) of limited diameter (e.g., 50-75 m) to a dike whose length is measured in kilometers. The latter is more likely to intersect the repository. Volcanic vents typically form along dikes at sites where eruptive activity becomes locally enhanced, resulting in erosion and expansion of a local segment of dike to form a conduit or vent. Accordingly, if a repository were to be intersected by a future volcanic vent, it would also be intersected by at

2146 least one dike. The orientation and length of the dikes is important because of the possibility of
2147 a dike extending into the repository from outside Yucca Mountain and the control these
2148 characteristics have over the number of drifts of the repository that would be intersected by the
2149 dike.

2150
2151 Examination of volcanic analogs, in particular those originating during the past several
2152 million years (see Table 4.1), provides a practical method for estimating the characteristics of
2153 volcanic features. The time period used to evaluate future volcanism should be reasonably
2154 representative of present-day conditions in the Yucca Mountain region. DOE has adopted the
2155 Pliocene-Pleistocene (*Plio-Pleistocene*) time period⁹ for extrapolation of events, consistent with
2156 the approach by members of the 1996 DOE-PVHA expert panel (Geomatrix Consultants, 1996).
2157 However, several members of that panel considered the Pleistocene (previous 1.75 Ma) Epoch
2158 to be the most representative and the preferred time period from which to extrapolate. For
2159 young (Pleistocene) volcanoes, the presence of tephra cones conceals the actual dimensions of
2160 the underlying vent or conduit, but provides useful information on the nature and volume of the
2161 events. Pliocene vents, such as those cropping out in Crater Flat, can be evaluated in some
2162 detail because they have been heavily eroded, exposing interior cores filled with *agglomerate*
2163 (pyroclastic debris). The dimensions of the agglomerate mass provide an estimate of former
2164 conduit size.

2165
2166 The volcanic cones and lava flows of Pleistocene age near Yucca Mountain provide direct
2167 analogs of the igneous activity events that could occur in the region in the future. The
2168 Pleistocene volcanic cones of Crater Flat, along with the Lathrop Wells cone, all occur in basin
2169 areas although two of the eight Pleistocene volcanoes in the Yucca Mountain region occur on
2170 topographic highs. The dimensions of the Crater Flat volcanoes indicate that the volume of
2171 volcanic material ranges from 0.002 km³ (Makani volcano) to 0.06 km³ (Red and Black Cones),
2172 while Pliocene volcanoes in Crater Flat and elsewhere within the Yucca Mountain have
2173 significantly greater volumes (see Table 4.1). The products of these events also provide
2174 information on the eruptive power of future volcanic events anticipated in the Yucca Mountain
2175 region. The presence of tephra suggests that violent Strombolian activity was present, with
2176 plumes of volcanic material injected into the atmosphere, during portions of the volcanic events.
2177 The maximum lava effusion rate is generally about 1 to 4 m³/s for the Pleistocene Crater Flat
2178 volcanoes while the effusion rate of the Pliocene volcanoes is an order of magnitude larger
2179 (Table 4.1). Valentine and Perry (2006) have concluded that the total length of the fissures
2180 associated with the Pleistocene volcanoes, which is the length of the intersection of the
2181 originating dike with the surface, is less than 2 km, while Pliocene volcanoes are associated
2182 with fissures (dikes) roughly twice this length. Valentine et al. (2005) have investigated the
2183 make up of the Lathrop Wells cone and find that the bulk of the cone is composed of fine
2184 grained eruptive materials consistent with sustained columns of well-fragmented eruptive
2185 materials and laterally extensive fallout deposits as much as 20 km from the vent.

2186

⁹ The Plio-Pleistocene time period includes both the Pliocene (5 - 1.75 Ma) and the Pleistocene (1.75 Ma - 11.5 ka) Epochs.

Volcano	Age, Ma	Rock Type ^a	Volume, km ³	Fissure Length, km	Lava Flow Length, km	Maximum Lava Effusion Rate, ^b m ³ /s	Brief description
Thirsty Mountain	4.63 ± 0.02 ^c	Basaltic trachyandesite	2.28	5 ^d	6	80	Broad shield volcano consisting of stacked lava flows and a central remnant of pyroclastic (near vent) deposits. ^c
Pliocene Crater Flat (aka Southeast Crater Flat)	3.73 ± 0.02 ^c	Basalt	0.56	3.6	4	40	Low shield volcano, now broken by normal faults and partially buried by alluvium, with multiple lavas and pyroclastic vent facies exposed.
Buckboard Mesa	2.87 ± 0.06 ^c	Basaltic trachyandesite	0.84	2.5	7.3	100	Large lava field with remnant of a main pyroclastic cone in northern part, fissure inferred from ridge of lava and pyroclastics that extends SE from main cone.
Black Cone	0.986 ± 0.047 ^c	Trachybasalt	0.06 ^e	0.6 (1.8) ^f	1	0.9	Pyroclastic cone remnant preserving Strombolian and violent Strombolian facies, and two lava fields that vented from the base of the cone. ^e
Red Cone	0.977 ± 0.027 ^c	Trachybasalt	0.06 ^e	0.5 (1.6) ^f	1.4	3	Pyroclastic cone remnant preserving Strombolian and violent Strombolian facies, and two lava fields that vented from the base of the cone. ^e
SW Little Cone	1.042 ± 0.045 ^c	Trachybasalt	0.03	0.3 (0.8) ^f	0.7	0.4	Pyroclastic cone remnant, open to the south, with single lava field mainly buried by alluvium. ^e
NE Little Cone	1.042 ± 0.045 ^c	Trachybasalt	Included with SW Little Cone	0.2 (1.8) ^f	1.8	4	Pyroclastic cone remnant, open to the south, with single lava field mainly buried by alluvium. ^e
Makani volcano (aka Northernmost)	1.076 ± 0.026 ^c	Trachybasalt	0.002 ^e	0.4	0.4	0.1–0.2	Small lava mesa with pyroclastic deposits marking location of short fissure. ^g
Little Black Peak	0.323 ± 0.027 ^c	Basalt to trachybasalt	0.014	0.4 (1) ^f	1.3	2	Pyroclastic cone with lavas that extend from its base.
Hidden Cone	0.373 ± 0.042 ^b	Basalt to trachybasalt	.03	0.3 (0.8) ^f	1.6	4	Pyroclastic cone on side of butte with two lava field extending from its base.
Lathrop Wells	0.076 ± 0.005 ^b	Trachybasalt	0.09 ^h	0.8 (1.8) ^f	1.6	4	Single pyroclastic cone with two lava flow fields that vented from the base of the cone. ^h

^aClassification of *Lo Bos et al.* [1986] as determined by *Fleck et al.* [1996].

^bMaximum lava effusion rate estimated from Figure 4 of *Walker* [1973].

^cWeighted mean values of *Fleck et al.* [1996].

^dInferred from geophysical data [*Grauch et al.*, 1997] and geologic map [*Minor et al.*, 1998].

^e*Valentine et al.* [2006].

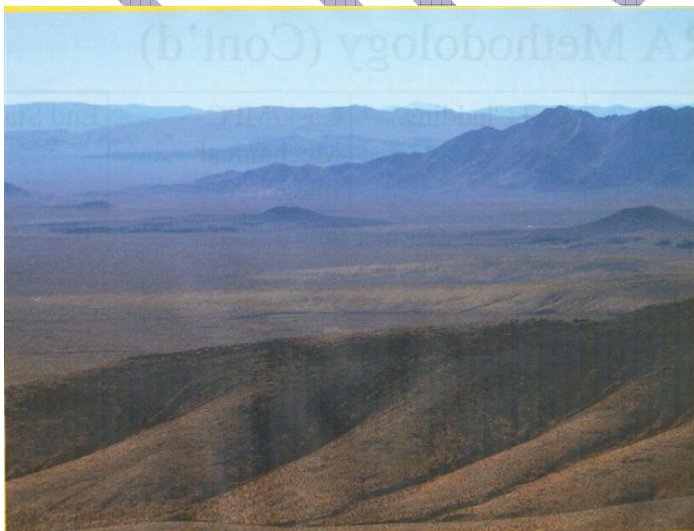
^fValue provided represents diameter of main cone, which is the source for all preserved eruptive material [*Valentine et al.*, 2006], representing the expected value. Value in parentheses is the total length that could be buried by all eruptive deposits, representing the maximum possible value.

^gAge of Q₁ flow [*Holzner et al.*, 1999].

^h*Valentine et al.* [2005]. Note that loose pyroclastic deposits, including a fallout tephra deposit that extends up to 20 km from the cone, is preserved at Lathrop Wells volcano due to its young age. This results in a larger estimate of volume than at older volcanoes such as Red Cone and Black Cone, which are otherwise similar in size.

2187
2188
2189
2190
2191
2192
2193

Table 4.1. Ages, volumes, and eruptive characteristics of Pliocene-Pleistocene volcanoes in the Southwestern Nevada Volcanic Field. [After Valentine and Perry, 2006]



2194
2195
2196
2197

Figure 4.1 Photo of Pleistocene volcanoes in Crater Flat as viewed over the crest of Yucca Mountain. From right to left the volcanoes are Black Cone, Red Cone, and Little Cones. Bare Mountain is in the mid-background.

2198
2199
2200
2201
2202
2203
2204
2205
2206
2207
2208
2209
2210
2211
2212
2213
2214
2215
2216
2217
2218
2219
2220
2221
2222
2223
2224
2225
2226
2227
2228
2229
2230
2231
2232
2233
2234
2235
2236
2237
2238
2239
2240
2241
2242
2243
2244
2245
2246
2247

The change in rate and volume of the volcanoes and of fissure length is indicative of waning heat energy and related volcanism, such as evidenced in the Reville Range, which is approximately 100 km north of Yucca Mountain (Yogodzinski et al., 1996). Valentine et al. (2006) have concluded that the Pleistocene Crater Flat volcanoes are derived from a single vent (monogenetic) formed in a single eruptive episode lasting only a few years. Valentine and Perry (2006) have inferred that the dikes rise vertically with little lateral propagation and have a curved, convex upward, leading edge in a shape similar to a tongue depressor. The occurrence of volcanoes on local topographic highs (Little Black Peak and Hidden Cone), without vents that intersect the surface at lower elevations, provide evidence for the lack of lateral propagation. Most basaltic dikes of Miocene age, as mapped by Valentine and Krogh (2006) in the Paiute Ridge volcanic center of the Nevada Test Site, occupy normal faults. Similarly, Valentine and Perry (2006) based on geophysical data and field evidence suggests that Plio-Pleistocene volcanoes erupted along existing faults.

4.3 NRC and DOE Positions

4.3.1 NRC/DOE KTI Agreement on the Likely Range of Tephra Volumes

A Key Technical Issue (KTI) agreement related to the likely range of tephra volumes from volcanoes in the Yucca Mountain region was reached by DOE (2003) and NRC. This agreement is reflected in a letter from NRC (Kokajko, 2005). However, in this letter the NRC expressed concern that the range of tephra volumes used by DOE in performance assessment did not correspond to the volumes interpreted for volcanoes that have occurred in Crater Flat during the time interval used in DOE's probability calculations. For example the eroded remnants of scoria cones of Pliocene volcanoes in Crater Flat, which are included in the DOE probability results, indicate larger tephra volumes than those accounted for in the current DOE parameter range (BSC, 2003b). However, the magnitude of differences between DOE and NRC estimates of tephra volumes for past Yucca Mountain region volcanic events (NRC, 1999) does not appear to affect performance calculations significantly (NRC, 2004).

4.3.2 DOE Approach to Event Definition

The DOE (2003) evaluated characteristics of volcanic features in their Technical Basis Document (#13) on volcanic events. In the PVHA expert elicitation (Geomatrix Consultants, 1996), the expert panel defined a volcanic event as a point in space representing a volcano, and an associated dike having length, orientation, and location relative to the point. Associated eruptive products may include ash, tephra, and lava flows. The Paiute Ridge intrusive/extrusive center, dated at 8.6 Ma and located on the northeastern margin of the Nevada Test Site (DOE, 2003; Valentine and Krogh, 2006), is a possible analog. A study of this center can elucidate the relationship between intrusive and extrusive components of a volcanic event. Paiute Ridge is a small-volume Miocene volcanic center comparable in volume and composition to Pleistocene volcanoes near Yucca Mountain. Like the Pleistocene cones, Paiute ridge igneous activity is believed to have occurred during a brief magmatic pulse represented by a single volcanic event. The vents and associated dike system formed in a NNW-trending extensional graben, and exposures of the system include remnants of surface lava flows, volcanic conduits, and dikes and sills intruded into tuff country rock at depths of ~250 m from the paleosurface. Dike lengths at Paiute Ridge range from less than 1 km to 5 km and widths from 1.2 to 9 m. At Paiute Ridge parts of some dikes terminated within ~100 m of the surface without erupting, while other parts of the same dike did erupt, as evidenced by associated lava flows and volcanic conduits. This

2248 contrasts with the current assumption by both the DOE and NRC that any dike which intrudes
2249 the repository will vent out to the surface.

2250
2251 Volcanic events occurring outside of the repository footprint must have sufficient length to
2252 intersect and breach the repository. Longer event lengths will result in higher intersection
2253 probabilities. The mean dike length associated with a volcanic event in the Yucca Mountain
2254 region is 4 km, and 95 percent of dikes are shorter than 10.1 km (DOE, 2003), consistent with
2255 observed volcanic features in the Yucca Mountain region. The maximum aligned-vent spacing
2256 in the Yucca Mountain region is 5.4 km between Black and Makani (Northern) Cones, and
2257 volcanic-vent alignment lengths are typically in the range of 2 to 5 km (e.g., Hidden Cone-Little
2258 Black Peak, Amargosa aeromagnetic Anomaly A, and Red Cone-Black Cone) (DOE, 2003).
2259 The longest proposed vent alignment in the Yucca Mountain region is the Pleistocene Crater
2260 Flat alignment with a length of about 11 km, if one assumes it represents only one volcanic
2261 event. If in fact that alignment represents a single event, the effect would be to reduce the Plio-
2262 Pleistocene recurrence rate significantly.

2263
2264 Dikes such as those at Paiute Ridge range in length from less than 1 to 5 km. Dike and
2265 vent alignments of the 3.7 Ma basalts in Crater Flat are no more than 4 km long. More recent
2266 studies have indicated much smaller dike (fissure) lengths as shown in Table 4.1 and discussed
2267 Section 4.2 of this chapter.

2268
2269 DOE (2003) cites Delaney and Gartner (1997) in noting that 97 percent of the 174 dike
2270 lengths measured in the San Rafael volcanic field are less than 5 km. The median of the length
2271 distribution at San Rafael is approximately 1.1 km, and the longest dikes are 8 to 9 km. DOE
2272 (2003) estimated a measure comparable to dike half-length, the distance from the end of the
2273 dike nearest the repository to the point of origin (the midpoint) of the volcanic event, using
2274 information elicited in the PVHA (Geomatrix Consultants, 1996). The mean of this distribution is
2275 2 km, the 5th-percentile is 0.2 km, and the 95th-percentile is 5.6 km, agreeing well with
2276 observed volcanic-event features in the Yucca Mountain region.

2277
2278 It was noted in Section 4.2 above that there is little or no evidence that dikes in the
2279 Yucca Mountain region propagate laterally. Crowe et al. (1983) measured basaltic dikes
2280 intruded into tuff at eroded volcanic centers of the Yucca Mountain region, and observed dike
2281 widths ranging from 0.3 m to 4 m. Most dikes were between 1 and 2 m wide. The typical dike-
2282 width dimension assigned by the PVHA experts was 1 m (Geomatrix Consultants, 1996). DOE
2283 (2003) reports that most basaltic volcanoes in the Yucca Mountain region are small in volume
2284 and fed by one main dike. Sets of dikes (dike swarm) may be present with spacing between
2285 individual dikes of up to a few hundred meters. There may also be small dikes that radiate
2286 outward from the conduit of the main cone, analogous to the crudely radiating dikes that are
2287 enclosed in near-vent scoria at the eroded Pliocene basalt centers of Crater Flat. The Paiute
2288 Ridge volcanic complex may have as many as 10 dikes, in addition to sill-like bodies.

2289
2290 Data from a variety of basaltic fields indicates that the spacing between multiple dikes
2291 (dike swarm) can vary from about 100 m to approximately 1 km (DOE, 2003). For the Paiute
2292 Ridge complex, measurements suggest that the mean dike spacing for dikes greater than 1 km
2293 long is approximately 995 m (maximum 1,440 m; minimum 250 m) (Perry et al., 1998). For the
2294 3.7-Ma-old Crater Flat basalts, dike spacing is approximately 385 m (Perry et al., 1998). Dike
2295 spacing in the Yucca Mountain region ranges from about 100 m to 690 m (DOE, 2003).

2296
2297 The DOE has determined that an average of 77 percent of the basaltic, repository-
2298 intersecting intrusive events would result in at least one volcano occurring within the repository

2299 footprint. This is based on observed vent spacing in the Yucca Mountain region and an
2300 assumption that the volcanoes could occur randomly along the length of the dike or to
2301 preferentially localize near a repository drift.
2302

2303 Basaltic eruptions begin from fissures that focus into roughly conical (base upward)
2304 conduit eruptions. The best data on conduit diameters and depths to which conduits extend
2305 come from observations of basaltic volcanic necks that have been exposed by erosion.
2306 However, few volcanic necks have been mapped in detail, at least those with the basaltic
2307 compositions of interest in the Yucca Mountain region. Without such mapping, estimates of
2308 potential conduit diameters are based on measurements at analog volcanoes (DOE, 2003).
2309 The transition from magma flow in a subplanar dike to flow in a conduit has been inferred at
2310 many field locations (e.g., Delaney and Pollard, 1981; Hallett, 1992). A planar dike is the
2311 preferred form for movement of magma through brittle and elastic host rock, whereas a conical
2312 conduit is the preferred form for magma flow and delivery to the surface (Delaney and Pollard,
2313 1981). Once a zone of widening and flow focusing has initiated, the evolving conduit may
2314 continue to widen via erosive and hydromagmatic processes. Solidifying magma may choke
2315 portions of a conduit so that only a fraction of the vent may be active at any given time during an
2316 eruption. Basaltic conduits vary greatly in diameter, depth and geometry. Valentine and Groves
2317 (1996) used the well-established sedimentary stratigraphy beneath tephra deposits at the
2318 Lucero Volcanic field (New Mexico) to evaluate variations in conduit size beneath a basalt
2319 center. They calculated that the conduit ranged in diameter from 3.5 to 10 m. Conduit-size
2320 calculations based on the proportion of rock fragments in these hydromagmatic deposits
2321 indicate that a cylindrical conduit up to 40 m wide may have formed in the uppermost strata. A
2322 flared conduit could also have developed, varying in size from 6 m at depth to 300 m at the
2323 surface.
2324

2325 The diameter of the Grants Ridge conduit in New Mexico (Keating and Valentine, 1998;
2326 WoldeGabriel et al., 1999) suggests that an upper bound for basaltic conduit diameter in the
2327 Yucca Mountain region is 150 m. This is a conservative upper bound for Yucca Mountain
2328 because the Grants Ridge plug formed during an eruption of several cubic kilometers of alkali
2329 basalt (compared, for example, to the much smaller Lathrop Wells volcano with its approximate
2330 total volume of 0.09 km³) (DOE, 2003). Doubik and Hill (1999) used a process that may
2331 overestimate the volume fraction of tuff xenoliths to estimate a 50-m conduit diameter for the
2332 Lathrop Wells scoria cone. Thick Miocene volcanic units beneath the Lathrop Wells volcano are
2333 lithologically similar, making it difficult to assign relative proportions of those units represented
2334 by rock fragments of the walls of the feeder. Given the limitations on specific data to test the
2335 assumptions made by Doubik and Hill (1999), their estimate of a 50-m conduit diameter for the
2336 Lathrop Wells Cone was used as a most likely value for conduit diameter at depth for potential
2337 eruptions at Yucca Mountain (DOE, 2003).
2338

2339 Based on data from the Yucca Mountain region and selected analogs, the conduit
2340 diameter for a future basalt volcano was constrained at its lower bound by 1- to 2-m wide dikes,
2341 and at its upper bound by the 150-m Grants Ridge plug (DOE, 2003). The ongoing PVHA-U
2342 has been tasked with reevaluating the volcanic event definition used in the 1996 expert
2343 elicitation. The panelists have been asked to assess the following aspects of future volcanic
2344 events that could hypothetically affect Yucca Mountain during the next 1 million years:
2345

- 2346 • Magnitude of event
- 2347
- 2348 • Intrusive event geometry
- 2349 – Dike system length, azimuth, and location relative to point event and dike

- 2350 width (similar to 1996 assessment)
- 2351 – Description of dike swarm (e.g. number and spacing of parallel dikes along
- 2352 length of dike system)
- 2353 – Influence of repository opening on dike intersection
- 2354
- 2355 • Extrusive event geometry
- 2356 – Number and location of eruptive centers (conduits) associated with
- 2357 volcanic event
- 2358 – Conduit diameter at repository level
- 2359 – Influence of repository opening on eruptive conduit location.
- 2360

2361 The final report of the PVHA-U is not expected to be published until 2008, therefore this
2362 report cannot incorporate the revised assessments. Based on ACNW observations of PVHA-U
2363 proceedings, some significant changes are being considered to the 1996 study (Geomatrix
2364 Consultants, 1996). Most panelists appear to emphasize the nature of Pleistocene activity
2365 (instead of earlier activity), consider dikes that are shorter in length, discuss the possibility of
2366 sills, and consider increased flexibility in possible dike orientations. Event (eruption) cycles are
2367 being discussed, and fewer hidden events are now being considered, based on the results of
2368 drilling of aeromagnetic anomalies that have been interpreted as possibly derived from hidden
2369 basaltic igneous events. There remains considerable challenge in applying spatial and temporal
2370 models in a region where volcanism is so infrequent and has greatly declined. Future *phreatic*
2371 eruptions (*maar volcanoes*) involving heating and expansion of ground water are unlikely
2372 because the water table is expected to change by 20 to 30 m at most, as a result of climate
2373 change in the Yucca Mountain region.

2374

2375 **4.3.3 NRC Approach to Event Definition**

2376

2377 The NRC/CNWRA, in Connor et al. (2000), noted that the most prominent vent alignment
2378 in the YMR is the arcuate northeast trending Pleistocene Crater Flat alignment consisting of five
2379 cinder cones. Three magnetic anomalies are mapped along the alignment that reveal the
2380 presence of older, buried basaltic lavas. They propose that geology and geophysical mapping
2381 indicate that the Crater Flat alignment is up to 16 km long and may have been reactivated
2382 through time. However, recent high-resolution aeromagnetic surveying provides no support for
2383 connecting the outcropping and sub-cropping vents. The aeromagnetic data show no indication
2384 of anomalies related to magnetic intrusive dikes connecting the vents.

2385

2386 The alignment of magnetic Anomalies G, F, and H provides further evidence of NE
2387 trending alignments. At aeromagnetic Anomaly G (Figure 5.1), drill hole USW VA-2 confirmed
2388 that 3.8 Ma basalt lies at a depth of 119 m. Based on alignment and similar magnetic
2389 signatures of Anomalies H and F, these anomalies are also interpreted to be related to Pliocene
2390 basalts. Other vent alignments in the region include the 0.3 Ma Sleeping Buttes alignment,
2391 consisting of two cinder cones aligned on a NE trend, ~40 km northwest of Yucca Mountain,
2392 and the Pliocene Crater Flat vents, which form a north-trending alignment of 6–8 vents, erupted
2393 3.8 Ma ago. In all, five vent alignments with a total of 18 vents have formed or reactivated
2394 during Plio-Pleistocene time. Six remaining Plio-Pleistocene vents are not included in
2395 recognized alignments. Four of these are known only from magnetic mapping and one from
2396 drilling (Anomaly B, basalt of Pliocene age). There may be multiple vents associated with some
2397 of these anomalies. It is possible that future volcanic activity may produce similar alignments.

2398

2399 Connor et al. (2000) estimated the probability of future volcanic intersection at Yucca
2400 Mountain, assuming that half of any future volcanic events would not create alignments and

2401 would only disrupt the repository if they fell within the site boundary, and that the remaining half
2402 would form alignments that could affect areas 5.5 to 8 km beyond the midpoint of a dike.
2403 Connor et al. (2000) point out that the three youngest alignments in the Yucca Mountain region
2404 trend along azimuths 20–30°, parallel to the maximum principal horizontal compressional stress
2405 in the region (Morris et al., 1996). Connor et al. (2000) also pointed out that faults may locally
2406 control the locations of vents regardless of whether vent alignments develop. For example, a
2407 normal fault crossed by a strike-slip fault will tend to dilate more at the fault intersection, creating
2408 additional space for the intrusion of ascending magma. They reported evidence of such
2409 localization of cinder cones along faults in the Yucca Mountain region. The Pliocene aged
2410 basalt of Anomaly B occurs at the intersection of the north-trending Gravity and Rock Valley
2411 faults in the Amargosa Desert. The Carrara fault basalt is located at the intersection of north-
2412 trending normal and NW trending strike-slip faults. The Lathrop Wells volcano is located along
2413 the trend of the Stage Coach fault, south of Yucca Mountain at the intersection with several
2414 north-trending faults (Connor et al., 2000).
2415

2416 The igneous activity parameters used in the most recently published version of total
2417 performance assessment by the CNWRA are shown in Table 4.2 (Mohanty et al., 2004). This
2418 table shows that the geographic orientation of a dike intersecting the repository is assumed to
2419 be N7.5°E with a range from N0°E to N15°E. The width of the dike is assumed to have a mean
2420 width of 5.5 m with a range from 1.0 to 10.0 m and the mean length of the dike is 6.5 km with a
2421 range of 2 to 11 km. Multiple conduits are assumed to form along a dike during a single igneous
2422 event, but the base case is only one conduit. The range of diameters of the conduit is uniform
2423 from 24.6 to 77.9 km with a mean of 51.3 m. The volume of ash associated with an eruption
2424 event is estimated using better preserved volcanoes which serve as analogs to the basaltic
2425 volcanism of the Yucca Mountain region. NRC (1999) observes that the range of ash-to-cone
2426 volume ratios at historical analog volcanoes range from approximately 1:1 to 6:1. Based on
2427 these ratios and estimation of the power and duration ranges of potential igneous events, the
2428 ash-volume ranges from 6×10^5 to 3×10^8 m³ with an average volume of 3×10^7 m³. The DOE
2429 has determined an average volume of 1×10^8 m³ with a range of 2×10^6 to 4.4×10^8 m³.
2430

2431 **4.4 Summary**

2432
2433 A concise summary of the positions regarding the nature of future Yucca Mountain region
2434 igneous activity is constrained by the lack of published materials that discuss current
2435 investigations. The DOE (2006) anticipates that changes to the input parameters to
2436 performance assessment, based on analog geologic data, will involve:

- 2437 • Dike length, width, orientation, and number of dikes
- 2438 • Conduit size, and number and locations of conduits
- 2439 • Fraction of eruptive material in tephra, cone, and lavas.

2440
2441 There are several areas of agreement between DOE and NRC regarding the nature of
2442 igneous events impacting the proposed repository. These are based on geologic analogs and
2443 the geological and tectonic history of the Yucca Mountain region. They include the following:

- 2444 • Igneous events will be of similar nature to the Pleistocene volcanoes of the
2445 Yucca Mountain region and particularly the most recent volcano, Lathrop
2446 Wells. That is igneous events will occur as small-volume basaltic volcanoes
2447 that have effusion rates, power, and duration similar to the Lathrop Wells
2448 volcano. The occurrence of high power and volume and long duration
2449 volcanic events involving felsic ash flows typical of those of Miocene age in
2450 the Yucca Mountain region are not supported by evidence.

2451
 2452
 2453
 2454
 2455
 2456
 2457
 2458
 2459
 2460
 2461
 2462
 2463

- A portion of the duration of any volcanism will involve violent Strombolian activity with plumes of ash distributed over the Yucca Mountain region. Analogous with the Lathrop Wells eruption, fallout from a sustained eruption plume are likely to result in ash falls extending to a few 10s of kilometers.
- Multiple dikes including en echelon dikes are possible associated with an igneous event. The dike orientation will be parallel to the maximum horizontal compressive stress in the region, roughly spanning an azimuth from N to N30°E.
- The diameter of the volcanic conduit assumed by both the NRC and DOE has a mean value of about 50 m. NRC anticipates a range in diameter of 25 to 75 m, while the DOE cites diameters from 15 to 150m.
- Any dike intersecting the repository will continue to the surface above the repository.

Parameter	Mean Value	Distribution
Volcano model (1 = geometric, 2 = distribution)	1	—
Time of next volcanic event in region of interest	5.05×10^3 years	Finite exponential; 100.0, 10,000.0, 1.0×10^{-7}
X location in region of interest	5.48×10^5 m	—
Y location in region of interest	4.08×10^6 m	—
Random number to determine if extrusive or intrusive volcanic event	5.00×10^{-1}	Uniform; 0.0, 1.0
Fraction of time volcanic event is extrusive	9.99×10^{-1}	—
Angle of volcanic dike measured from north—clockwise	7.50°	Uniform; 0.0, 15.0
Length of volcanic dike	6.50×10^3 m	Uniform; 2,000.0, 11,000.0
Width of volcanic dike	5.50 m	Uniform; 1.0, 10.0
Diameter of volcanic conduit	5.13×10^1 m	Uniform; 24.6, 77.9
Density of air at standard pressure	1.29×10^{-3} g/cm ³	—
Viscosity of air at standard pressure	1.80×10^{-4} g/cm-s	—
Constant relating fall time to eddy diffusivity	4.00×10^2 cm ² /sec ^{0.2}	—
Maximum particle diameter for particle transport	1.00×10^1 cm	—
Minimum fuel particulate size	1.00×10^{-4} cm	—
Mode fuel particulate size	1.00×10^{-3} cm	—
Maximum fuel particulate size	1.00×10^{-2} cm	—
Minimum ash density for variation with size	0.8 g/cm ³	—
Maximum ash density for variation with size	1.60 g/cm ³	—
Minimum ash log diameter for density variation	-2.00	—
Maximum ash log diameter for density variation	-1.00	—
Particle shape parameter	5.00×10^{-1}	—
Incorporation ratio	3.00×10^{-1}	—
Wind direction	-90°	—
Wind speed	1.20×10^3 cm/sec	Exponential; 8.3×10^{-4}

2470
 2471
 2472
 2473
 2474
 2475
 2476
 2477
 2478

Table 4.2 Igneous activity input parameters to total performance assessment. [After CNWRA, 2004]

2479 Areas of disagreement between the DOE and NRC include:

2480

2481 • The DOE assumes a single eruption (monogenetic) volcanic event
2482 associated with each dike approaching the surface. In contrast NRC supports
2483 the possibility of multiple vents including the potential for flank eruptions from
2484 a volcanic cone leading to satellite (secondary) eruptions of lesser intensity.

2485 • The length of potential intruding dikes remains an issue of disagreement. The
2486 DOE, on the basis of interpretation of dikes associated with Pleistocene
2487 volcanoes in the Yucca Mountain region, indicates that dike lengths will be of
2488 the order of magnitude of 1km. However, NRC considers a mean dike length
2489 of roughly 6 km with a range from 2 to 11 km to be more realistic based on
2490 dike lengths interpreted from both Pliocene and Pleistocene igneous activity.

2491 • In the event of formation of multiple dikes, DOE has considered the dikes to
2492 be of the order of 1 to 2 m in width, while the NRC assumes a wider range
2493 from 1 to 10 m with a mean of roughly 5 m.
2494

2495 **5. Probability of Potential Igneous Activity**

2496

2497

5.1 Introduction

2498 The second question of the risk triplet, What is the probability of an igneous event
2499 intersecting the proposed repository? is the subject of Chapter 5. This question is one of the
2500 most comprehensively studied of all those asked about Yucca Mountain and remains vexing
2501 and controversial today among government agencies and authors of scientific journal articles.
2502 Considering the limitations in knowledge of the past basaltic volcanism in the Yucca Mountain
2503 region and the imperfections in the understanding of volcanic processes, it is impossible to
2504 specify the time and location of future igneous activity precisely. The probability of an event is
2505 further complicated by the range of characteristics of the dikes from the igneous event that may
2506 intersect the repository (i.e., length, orientation, as well as location). However, it is possible to
2507 predict, in a stochastic framework, the recurrence rate of such an event within an area
2508 encompassing Yucca Mountain. The predicted recurrence rate can be translated into the
2509 probability of repository intersection given the footprint of the proposed repository and
2510 assumptions regarding the volcanic zone and tectonic models and the nature of the igneous
2511 activity. A useful review of the history of probability estimates is given by Crowe et al. (2006).

2512 The Environmental Protection Agency set the generic standard for geologic high-level
2513 waste repositories (EPA, 1993) and confirmed, in the standard for the proposed Yucca
2514 Mountain repository (EPA, 2001), that an event, such as an volcanic event, does not require
2515 evaluation if the probability of occurrence is less than 0.01% in ten thousand years, i.e., less
2516 than one chance in one hundred million (10^{-8}) per year. This is roughly equivalent to the
2517 probability estimated for mass global extinction of life caused by the impact of an extra-
2518 terrestrial body on the Earth (Crowe et al., 2006). Probability estimates for repository
2519 intersection by an igneous event range from one part in a million to one part in a hundred million
2520 (10^{-6} to 10^{-9}), thus necessitating consideration of the consequences from such an event.

2521 In evaluating the probability of an igneous event intersecting the proposed repository it is
2522 important to understand the impact on the standards and the regulations for licensing the
2523 repository of the change in the time of compliance from 10,000 years to a million years. The
2524 Environmental Protection Agency's (EPA) current draft revised standards for the Yucca
2525 Mountain repository (EPA, 2005) and the NRC's draft revised regulations (NRC, 2005b)

2526 prescribe that consideration of features, events, and processes (FEPs), which includes igneous
2527 events, shall use the results obtained for the 10,000 years following repository closure. This is
2528 based on the assertion that the data and models of the first 10,000 years provide sufficient
2529 support to analyze performance during long time periods up to a million years without invoking
2530 undue uncertainty associated with long term projections. As a result, the probability estimates
2531 based on a 10,000 year repository lifetime that were made prior to the increase in repository
2532 time of compliance remain valid and are discussed herein.

2533 The logic diagram showing the major components that enter into the evaluation of the
2534 probability of an igneous event intersecting the repository is shown in Figure 1.2 b. These
2535 include results presented in the previous chapter regarding event definition and the number of
2536 events that have occurred in the germane region over a specified duration of geologic time. This
2537 evaluation also requires decisions regarding the number of undetected events and change in
2538 number of events with time. Assumptions regarding volcanic zone models and to a lesser extent
2539 tectonic models also enter into the evaluation as indicated in the logic chart (Figure1.2b).

2540
2541 It is useful to understand that the issue of probability of volcanism at Yucca Mountain
2542 poses an interesting paradox. Crowe et al. (2006) describe this contradiction. The small
2543 number of past eruptions is the best evidence that the probability of future volcanism near
2544 Yucca Mountain will be low had there been more volcanic events to study there would be more
2545 data on spatial and temporal patterns to project future volcanism. But in that hypothetical case
2546 the risk from future volcanism would be substantially higher than is the case for the Yucca
2547 Mountain site. As discussed below, the volume of basaltic volcanism near the site has
2548 dramatically declined over time such that the Crater Flat volcanic field represents a zone of very
2549 low activity compared to other volcanic fields in the region (e.g., Cima, CA and Springerville,
2550 AZ).

2551 **5.2 Spatial and Temporal Distribution of Igneous Events**

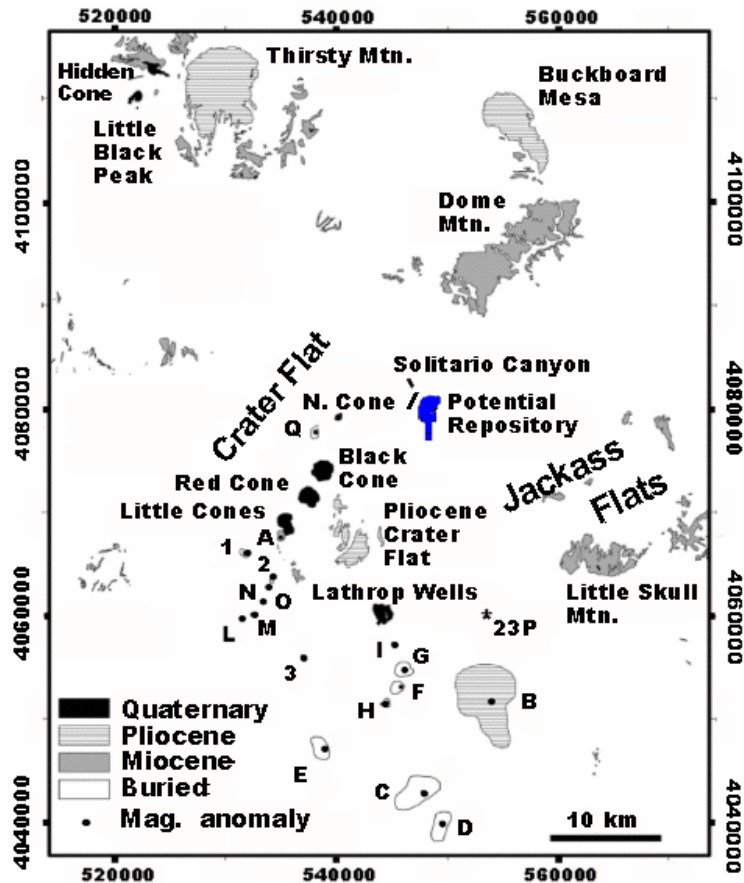
2552 **5.2.1 Introduction**

2553
2554 The spatial distribution of basaltic igneous events in the Yucca Mountain region and their
2555 absolute age is fundamental to formulating volcanic zone and temporal models of igneous
2556 activity used in predicting the probability of future activity at the proposed repository site.
2557 Geologic mapping has identified numerous surface features, both volcanic cones or their
2558 remnants and dikes, and isotopic dating of samples obtained from them, has been used to
2559 determine their age to a high degree of accuracy. Detritus eroded from the topographic
2560 highlands (ranges) has been deposited in the adjoining basins and may have buried igneous
2561 event features. Fortunately, the basaltic rocks have a significantly stronger magnetization than
2562 the alluvium in the basins. Thus, hidden basaltic features in the basins can be isolated by
2563 magnetic (geophysical) mapping of *anomalies*. However, alternative sources of the magnetic
2564 anomalies are possible. Thus, drilling on the magnetic anomalies or a representative of a group
2565 of anomalies to test for the presence of basalt is required to complete the analysis. Basalt
2566 samples obtained from the drill core are dated to determine the age of the feature. The
2567 resolution of the magnetic method is limited, so that deeply buried, small, and thin basaltic
2568 features may not be mapped by the magnetic method. Thus, undetected basaltic features may
2569 be present in the region. Accordingly, the geographic location of surface and buried basaltic
2570 volcanic rocks and their absolute age, and the possible presence of undetected features, are all
2571 considered in estimating the probability of intersection of the proposed repository by an igneous
2572 event.
2573
2574
2575

2576 **5.2.2 Surface Exposures**

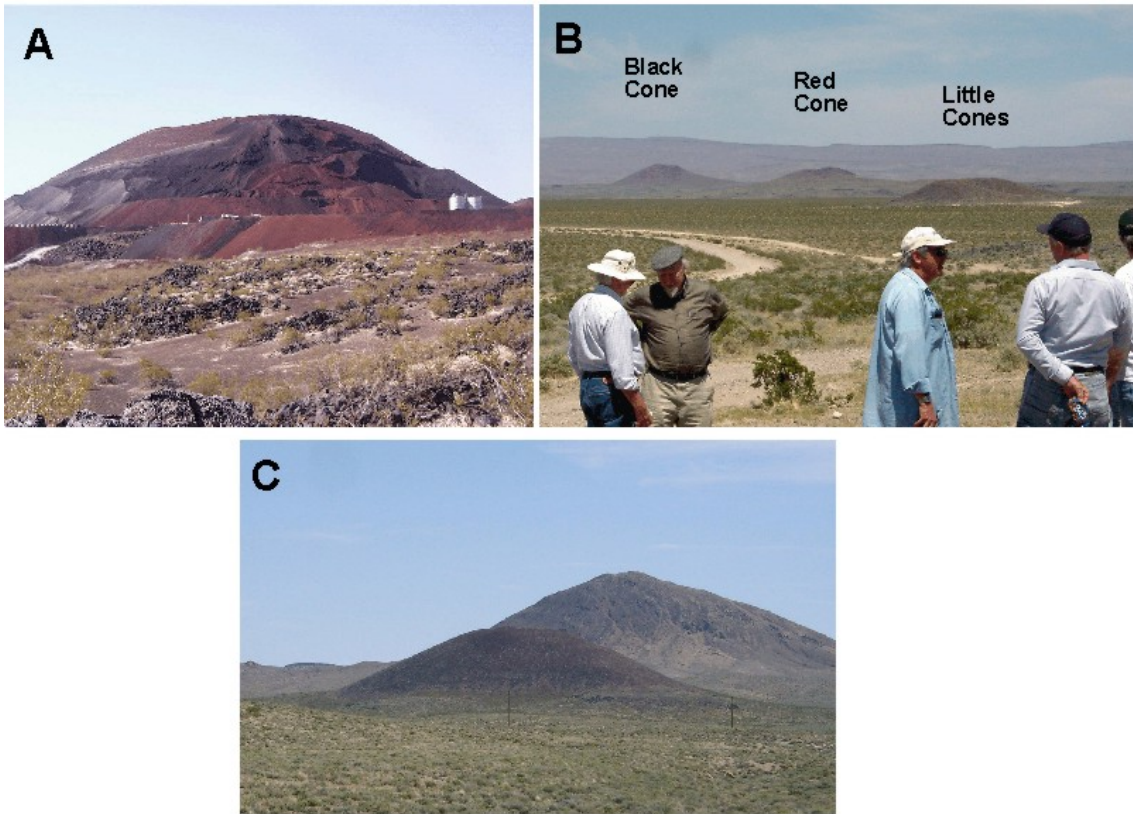
2577
 2578 Figure 5.1 shows the locations of surface exposures of basalts in the vicinity of Yucca
 2579 Mountain. At least four known pulses of basaltic volcanism have occurred (DOE, 2003) in the
 2580 Yucca Mountain vicinity. These include the ~80 ka Lathrop wells cone and flows (Figure 5.2 A),
 2581 ~1 Ma events in Crater Flat (Red Cone, Black Cone, Northern [Makani] Cone, and Little Cones)
 2582 (Figure 5.2 B), and multiple events dated ~3–6 Ma (Pliocene-U. Miocene) and ~8–13 Ma
 2583 (Miocene). Other young basalts in the Yucca Mountain region include Little Black Peak (~0.3
 2584 Ma) (Figure 5.2 C) and Hidden Cone (~0.4 Ma), 35 km northwest of Yucca Mountain.
 2585

2586 The Lathrop Wells cone has undergone extensive research because of its relative youth
 2587 and its proximity to Yucca Mountain. It is the only known igneous activity that occurred near
 2588 Yucca Mountain since the formation of the ~1-Ma-old-cones in Crater Flat. Two large basalt
 2589 flows occur east and south of the Lathrop Wells cone which were formed after an earlier
 2590 Strombolian phase when ash and tephra were ejected, forming a cinder cone.
 2591



2592
 2593
 2594 Figure 5.1 Locations of basaltic volcanoes in the Yucca Mountain region. Letters and numbers
 2595 are magnetic anomalies of high to moderate confidence that represent possible buried basalts.
 2596 Drilling at “A”, “B”, “D”, “G”, 23P, and JF-3 (not shown-just north of 23P) has detected basalts.
 2597 Map coordinates in UTM Zone 11 Meters, North American Datum 1927. [After Connor et al.,
 2598 2002 and Coleman et al., 2004]
 2599

2600 Pliocene-age basalt flows and several remnants of volcanic conduits occur in eastern
2601 Crater Flat (Figure 5.3). Other Pliocene basalts occur east of Little Black Peak near Thirsty
2602 Mountain, and at Buckboard Mesa on the margin of the Timber Mountain caldera. Large
2603 exposures of Miocene basalts occur in Jackass Flats, at Dome Mountain in the Timber
2604 Mountain caldera, and in proximity to the Black Mountain caldera. Miocene-age basalts also
2605 occur in western Crater Flat, and as a dike complex in Solitario Canyon on the northwestern
2606 flank of Yucca Mountain.
2607



2608
2609
2610 Figure 5.2. (A) Lathrop Wells cone (Age is 80 ka and height is ~130 m). (B). View of the ~1 Ma
2611 old cinder cones in Crater Flat, as seen looking northeast from Steve's Pass at the southern
2612 margin of Crater Flat. Yucca Mountain is on the far horizon at right side of image. (C). Little
2613 Black Peak, ~0.3 Ma (in foreground).
2614
2615



2616
2617
2618
2619
2620
2621
2622
2623
2624
2625
2626
2627
2628
2629
2630
2631
2632
2633
2634
2635
2636
2637
2638
2639
2640
2641
2642
2643
2644
2645
2646
2647
2648
2649

Figure 5.3. Person at left is standing on a dike of Pliocene age in southeastern Crater Flat. The distant cone at center is the Pliocene-aged Black Cone. Between Black Cone and the figures at right are the eroded remnants of two Pliocene vents (conduits).

5.2.3 Known Occurrences of Buried Basalts

Samples obtained from drilling in the alluvial basins show that buried basalts exist at several locations around Yucca Mountain, and previous magnetic surveys also indicate that additional basalts may be buried beneath the alluvium in Crater Flat and the Amargosa Desert (Connor et al., 2000; O’Leary et al., 2002; Hill and Stamatakos, 2002, Perry et al., 2005). Anomaly “B” in Figure 5.1 was confirmed by drilling to be a Pliocene basalt (~3.8 Ma) buried under 73 m of alluvium (O’Leary et al., 2002; DOE, 2003; Ziegler, 2003). A basalt in borehole NC-EWDP-23P located S-SE of Yucca Mountain has a Miocene age (9.48 ± 0.05 Ma) (Ziegler, 2003). This basalt lies buried beneath 400 m of alluvium. Another buried basalt was penetrated by drill hole VH-2, with a Miocene K/Ar age of 11.3 ± 0.4 Ma (Carr and Parrish, 1985). Basalt was also found in drill hole J-11 in northeastern Jackass Flats and at Anomaly “D” in Figure 5.1.

In support of the updated PVHA expert elicitation, a 30 × 30 km, high-resolution aeromagnetic survey was conducted of Yucca Mountain, Crater Flat, Jackass Flats, and northern Amargosa Desert by the DOE to optimize detection of buried basalts. The helicopter-borne survey was made along east-west flight lines at 60 m spacing. Over flat terrain the magnetometer was maintained at an altitude of ~45 m and roughly twice that over mountainous terrain to insure the safety of the aircraft. In a presentation to ACNW in July, 2006, Frank Perry (LANL) described the new survey as providing high resolution and broad coverage that allows better interpretation of buried basalt vs. alluvium and tuff, faults beneath shallow alluvium, and relationships between faulting and volcanic features (Perry et al., 2006). Based on the new magnetic map, anomaly targets were chosen for further study with drilling using the following criteria:

- Location with respect to impact on probability estimates (distance from repository, impact on event lengths),
- Sampling of each major cluster or alignment of anomalies,

2650
2651
2652
2653
2654
2655
2656
2657
2658
2659
2660
2661
2662
2663
2664
2665
2666

- Consideration of a range of potential ages based on differences in burial depth and magnetic polarity, and a
- Balance of “high confidence” vs. “low confidence” anomalies (basalt vs. tuff).

Seven new drill holes were completed at locations of geomagnetic anomalies in Crater Flat, Jackass Flats, and the northern Amargosa Desert. Their locations are shown on the high-resolution magnetic anomaly map (Figure 5.4) together with selected existing drill holes and selected geologic features and the repository area. Table 5.1 summarizes the results of the drilling. Four of the seven drill holes penetrated basalt. Only in one case, Anomaly “Q,” was unexpected basalt encountered (faulted tuff was the predicted source). Preliminary age determinations have been obtained revealing that three of the anomalies are due to buried Miocene basalt, one is due to Pliocene basalt, two are caused by Miocene tuffs, and one anomaly (JF-6) is probably due to faulted tuff (but it is possibly due to Miocene basalt).

Table 5.1. Summary information for completed PVHA-U drill holes
(footnotes are interpretations presented by Perry et al., 2006)

Magnetic Anomaly	Drillhole	Location	Magnetic Source	Predicted Source	Depth and Thickness of Basalt (m)	Age (Ma)
A ^a	USW VA-1	Crater Flat	Basalt (basanite)	Basalt	148 / 62	~10.1 Ma (Miocene)
Q ^b	USW VA-4a	Crater Flat	Basalt	Tuff	141 / >22	~11.1 Ma (Miocene)
JF-5 ^c	UE-25 VA-10	Jackass Flats	Basalt	Basalt	77 / >17	~9.4 Ma (Miocene)
JF-6 ^d	UE-25 VA-11	Jackass Flats	Likely tuff	Unknown	n/a	n/a
I ^e	USW VA-5	Amargosa Desert	Tuff	Tuff	n/a	n/a
O ^f	USW VA-3	Amargosa Desert	Tuff	Tuff	n/a	n/a
G ^g	USW VA-2	Amargosa Desert	Basalt	Basalt	119 / 31	~3.8 Ma (Pliocene)

2667
2668
2669
2670
2671
2672
2673
2674

^aBasanite represents a *mafic* magma composition not previously seen in the Yucca Mountain region; the drilled body may be an intrusive sill

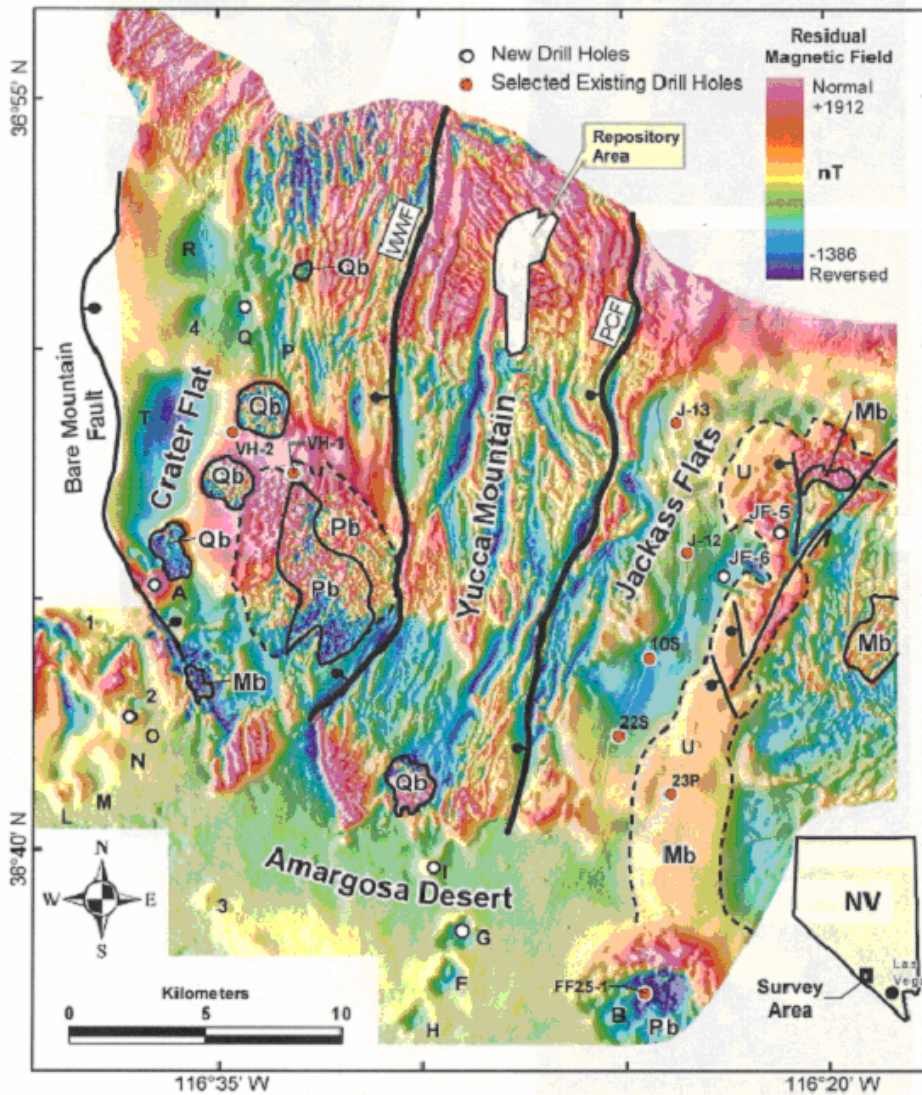
^bAnomalies “R” and “4” are considered an expression of the same basalt; possible stratigraphic correlation with basalts of VH-2 and southern Crater Flat

^cBasalt correlates with basalts in drill holes J-11 and Nye 23P

^dLikely due to faulted tuffs. Any basalt that may exist below borehole depth of 196 m is likely to be Miocene

- 2675 ^eDrillhole terminated in tuff at 200 m
- 2676 ^fSimilarity of magnetic signatures suggests that anomalies “L,” “M,” and “N” also
- 2677 represent faulted tuffs, not a volcanic alignment
- 2678 ^gAlignment and similar magnetic signatures of anomalies “H” and “F” suggest that these
- 2679 likewise represent Pliocene basalts
- 2680

2681 Hill and Stamatakos (2002) presented a relative ranking of low-medium-high confidence in
 2682 the interpretation of buried basalts associated with magnetic anomalies. Their table of
 2683 confidence rankings (Figure 2-1), which is shown herein as Table 5.2, provides previous
 2684 rankings by the USGS (O’Leary et al., 2002) and by the expert panelists of PVHA (Geomatrix
 2685 Consultants, 1996).
 2686



2687
 2688
 2689 Figure 5.4 High-resolution aeromagnetic anomaly map and locations of holes (solid white
 2690 circles) drilled to determine if the magnetic anomalies are derived from basalts. Solid red circles
 2691 indicate selected pre-existing drill holes that provide key constraints on the location of buried
 2692 basalt near Yucca Mountain. Qb=Quaternary basalt, Pb=Pliocene basalt, Mb=Miocene basalt.
 2693 [After Perry et al., 2005; Perry et al., 2006]

Table 5.2. Previous Confidence Rankings for Anomalies Now Re-interpreted with Data from PVHA-U Drilling and Dating [After Hill and Stamatakos, 2002]						
Magnetic Anomaly	O'Leary et al. (2002)	Geomatrix Consultants (1996)	Hill and Stamatakos (2002)	Source	Age (Ma)	Notes
A	1 ^a	0.20 ^b	H ^c	Basalt (basanite)	~10.1 Ma (Miocene)	
Q	4	n/r ^d	M	Basalt	~11.1 Ma (Miocene)	
R	4	n/r	L	Basalt -interpreted similar to Q by Perry et al. (2006)	Miocene	
4	4	n/r	L	Basalt - interpreted similar to Q by Perry et al. (2006)	Miocene	
JF-5	n/r	n/r	n/r	Basalt	~9.4 Ma (Miocene)	
JF-6	n/r	n/r	n/r	Likely tuff (Perry et al. (2006)	n/a	
I	2	n/r	M	Tuff	n/a	
O	3	n/r	M	Tuff	n/a	
L	3	n/r	M	Tuff - interpreted similar to O by Perry et al. (2006)	n/a	
M	3	n/r	M	Tuff - interpreted similar to O by Perry et al. (2006)	n/a	
N	3	n/r	M	Tuff - interpreted similar to O by Perry et al. (2006)	n/a	
G	1	0.36	H	Basalt	~3.8 Ma (Pliocene)	
F	1	0.37	H	Basalt -interpreted similar to G by Perry et al. (2006)	Pliocene	
H	1	n/r	H	Basalt -interpreted similar to G by Perry et al. (2006)	Pliocene	

^aRelative confidence ranking (1 = highest, 4 = lowest)

2696 ^bAverage confidence that the anomalies represent basalt
2697 ^cH = high, M = medium, L = low
2698 ^dn/r = not recognized
2699

2700 The results of drilling on anomalies following completion of the 2004 aeromagnetic survey
2701 reduce some of the uncertainty about buried basalts in the region and can be used to update
2702 previous probability models. Consider, for example, dataset CFB_plio-quat-Mag (Connor et al.,
2703 2002), which represents 29 Plio-Pleistocene events (dated basalts + 10 anomalies that were
2704 assumed to be post-Miocene basalts) in the Crater Flat basin. The number of basaltic events in
2705 this dataset is now reduced to 22 events by eliminating seven anomalies (A, I, L, M, N, O, and
2706 Q). This would lower the apparent Plio-Pleistocene volcanism recurrence rate from $5.5 \times 10^{-6}/\text{yr}$
2707 (Coleman et al., 2004) to $4.2 \times 10^{-6}/\text{yr}$., which is also consistent with the Pleistocene recurrence
2708 rate of $4.4 \times 10^{-6}/\text{yr}$ that is based solely on the eight known Quaternary basalts that exist in the
2709 Yucca Mountain region (Coleman et al., 2004). These results show that the new data will
2710 influence some statistical-mathematical models by lowering the probability of future repository
2711 intersection by volcanism. It is significant that no post-Miocene basalt was found in Jackass
2712 Flats at drill holes JF-5 and JF-6. If buried Pliocene basalts had been found there, that would
2713 suggest that the Plio-Pleistocene volcanic zone of Crater Flat extends through Yucca Mountain
2714 significantly increasing the modeled probability of future repository intersection.
2715

2716 The occurrences of buried basalt features help to interpret the pattern of surface basalts.
2717 For example, the Lathrop Wells cone, which previously appeared to be an isolated volcanic
2718 event in an area of no prior activity, is now seen as occurring midway along a band of Pliocene
2719 basalts that extend from Crater Flat southeastward to the buried basalts of Pliocene age found
2720 at Anomalies G and B.
2721

2722 **5.3.4 Undetected Igneous Activity**

2723
2724 Some analyses of the probability of igneous activity at Yucca Mountain (e.g., Geomatrix
2725 Consultants, 1996) provide for estimates of the number of basaltic events in the Yucca
2726 Mountain region that remain undetected. One objective of the 2004 high-resolution magnetic
2727 survey was to minimize the number of these events that need consideration in the analysis.
2728 However, constraints on the resolution of the survey and the inherent ambiguity of potential field
2729 methods such as the magnetic method limit the usefulness of the magnetic mapping. For
2730 example, there is no distinctive anomaly associated with the Miocene-aged basalt penetrated by
2731 drill hole NC-EWDP-23P. This basalt lies buried beneath 400 m of alluvium. The depth is too
2732 great and the magnetic contrast too small to magnetically differentiate this deep basalt from its
2733 geologic surroundings. Likewise, the Solitario Canyon dike, also of Miocene age, was not
2734 detected by the high-resolution survey, probably because it is a narrow and discontinuous
2735 tabular feature (<1 m wide), and the Tiva Canyon tuffs that were invaded by the dike locally can
2736 have enhanced magnetization that can mask the magnetic signature of the dike. Failure to
2737 detect these and other Miocene basalts that are deeply buried by alluvium or occur as narrow
2738 dikes have no adverse effect on probability models that are based on the rates of Pleistocene or
2739 Plio-Pleistocene volcanic activity. DOE in its evaluation of probability does consider Miocene
2740 basaltic volcanism, but the NRC has in some of its analyses.
2741

2742 Coleman et al. (2004) argue that despite the report of partial burial of Pleistocene
2743 volcanic features (DOE, 2003) in alluvial basins that under the arid to semi-arid climates of the
2744 Quaternary Epoch erosion and deposition should be sufficiently limited to preserve the evidence
2745 of any Pleistocene volcanic activity. Accordingly is unlikely that Pleistocene events are
2746 undercounted. Their conclusion is supported by the results of the recent drilling that supports

2747 PVHA-U, which has not found any buried Pleistocene basalts. Most of the newly drilled basalts
2748 are Miocene in age. Anomaly G, and by association Anomalies F and H, are now interpreted as
2749 Pliocene basalts, which is consistent with the previous discovery of extensive buried basalts of
2750 similar age (~3.8 Ma) at Anomaly B (see Figures 5.1 and 5.4). The depth of these buried
2751 basalts is a function of their age, the elevation of the paleosurface on which they were
2752 deposited, proximity to paleodrainage systems, and local sedimentation rates since the time of
2753 volcanic activity. The buried Pliocene basalts occur at depths between 73 m (Anomaly B) and
2754 119 m (Anomaly G). The buried Miocene basalts range in depth from 77 m (JF-5) to 400 m
2755 (Nye 23P).

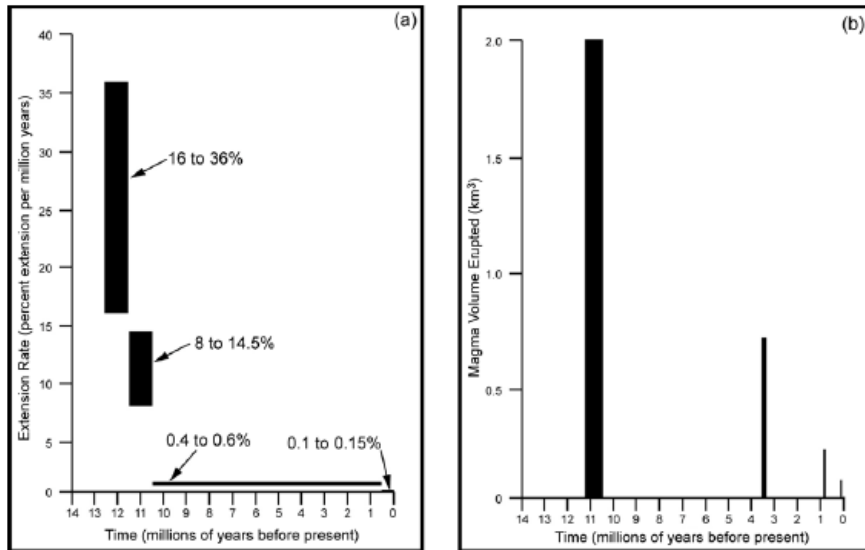
2756
2757 The rocks that comprise Yucca Mountain record an integrated tectonic-volcanic history
2758 since the ~13 Ma tuffs were deposited by large-scale pyroclastic flows and volcanic ash falls.
2759 More than 20 years of intensive site characterization studies have included detailed geologic
2760 surface mapping, geophysical surveys, and construction and mapping of ~6 km of tunnels in or
2761 near the repository footprint. Hundreds of surface drill holes of varying depths have been drilled
2762 in the Yucca Mountain site vicinity. Coleman et al. (2004) conclude that it is unlikely that multiple
2763 dikes could exist in the repository footprint and escape detection in the site characterization.
2764 Drilling is an ineffective way to discover near-vertical dikes, but if drill holes are deep enough
2765 they can locate basaltic sills. Aeromagnetic methods also can have difficulty locating basalts if
2766 dikes are small, because of interference with high amplitude, short-wavelength anomalies
2767 produced by faulted tuffs [Hill and Stamatakos, 2002]. The best techniques for finding basaltic
2768 dikes include detailed mapping of drift walls and surface geology.

2769
2770 No dikes have been found in the potential repository footprint at Yucca Mountain; this is a
2771 key observation. The horst block that forms Yucca Mountain appears to represent a zone of
2772 relative volcanic quiescence during the last 10 Myr. Since that time volcanism has instead
2773 mainly focused within the alluvial basins to the east, west, and south, with no evidence of post-
2774 Miocene activity east of Yucca Mountain in Jackass Flats. If in future the repository footprint
2775 would be expanded westward, then one known dike would exist within that footprint, the
2776 Solitario Canyon dike, which intruded segments of the Solitario Canyon fault during Miocene
2777 time.

2778 2779 **5.2.5 Change in Basaltic Volcanism With Time**

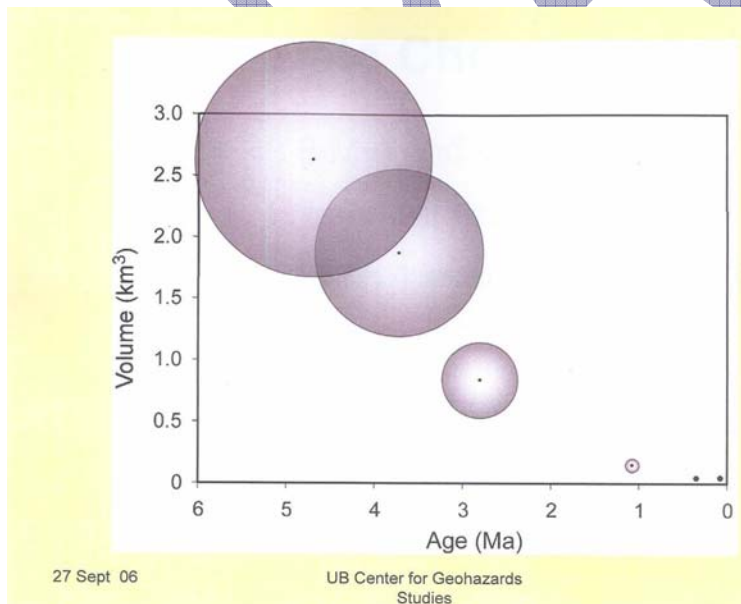
2780
2781 Rates of extension and volumes of basaltic volcanism have significantly declined in the
2782 four recognized episodes during the last 11 Myr (since late Miocene time) (Figure 5.5). There is
2783 compelling evidence that volcanism has waned in concert with this great reduction in crustal
2784 strain. Fridrich et al. (1999) suggested that the ascent of basalt through the crust is structurally
2785 controlled in the Crater Flat basin because volcanic vents form a northwest-trending belt that
2786 coincides with the strongest transtensional (lateral and extensional) deformation in the basin.
2787 The approximate temporal correlation of volcanism and rates of extension suggest that they
2788 represent a single phenomenon—a tectonic system that may once have been among the most
2789 active zones in the Great Basin, comparable to tectonism in Death Valley today. Fridrich et al.
2790 (1999) interpret that the Crater Flat basin remains tectonically active, but is now in an advanced
2791 stage of decline. Although the overall pattern is declining, extensional faulting has been cyclical
2792 and has varied partly in parallel with episodic volcanism.

2793



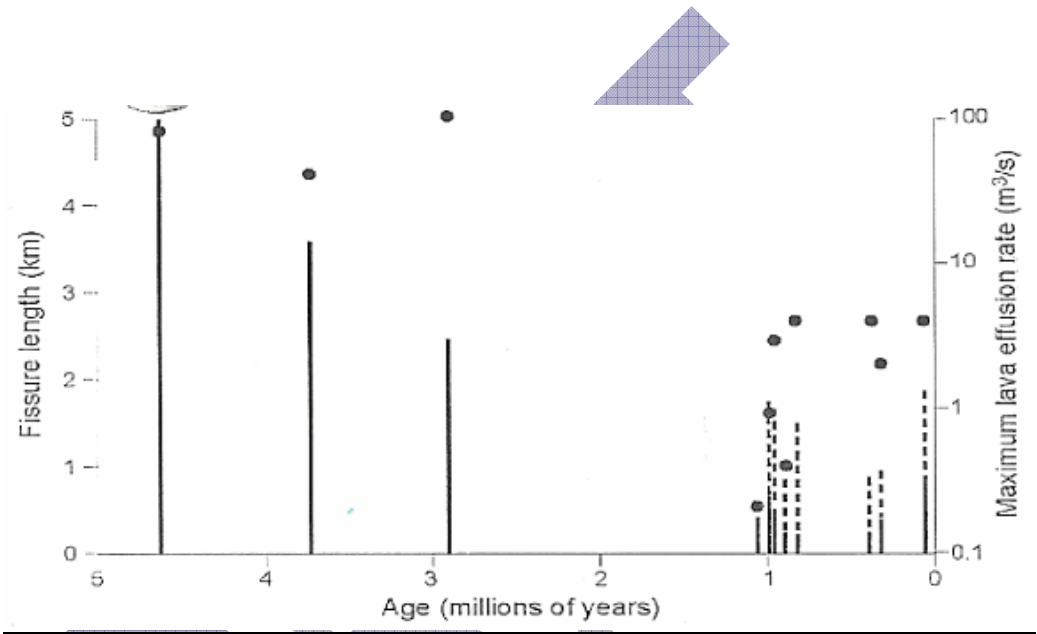
2794 Figure 5.5. Estimated extension rates in Crater Flat basin as a function of time and magma
 2795 volume erupted as a function of time. [After Fridrich et al., 1999]
 2796
 2797

2798 The cumulative extension map of Fridrich et al. (1999) integrates the extension over the
 2799 last 12 Myr in Crater Flat. It was previously known that the volumes of volcanic events
 2800 significantly declined after Miocene time. Figure 5.6, developed by Frank Perry (LANL), shows
 2801 that volumes of Pliocene to Pleistocene volcanism have also declined, suggesting that
 2802 magmatic systems near Yucca Mountain are dying. Further evidence lies in the declining
 2803 maximum lava effusion rate and fissure length of Plio-Pleistocene basaltic activity in the Yucca
 2804 Mountain region (Figure 5.7).
 2805



2806 Figure 5.6 Age vs. volume of Plio-Pleistocene volcanic episodes in the Yucca Mountain region.
 2807 Figure includes buried Pliocene basalts in the northern Amargosa Desert. The diameter of the
 2808 circles is proportional to volume. The dot at far lower right represents Lathrop Wells. The dot to
 2809 its left represents Sleeping Butte. The small circle at 1.1 Ma represents the five Pleistocene
 2810 cones of Crater Flat. [After Perry, 2006]
 2811

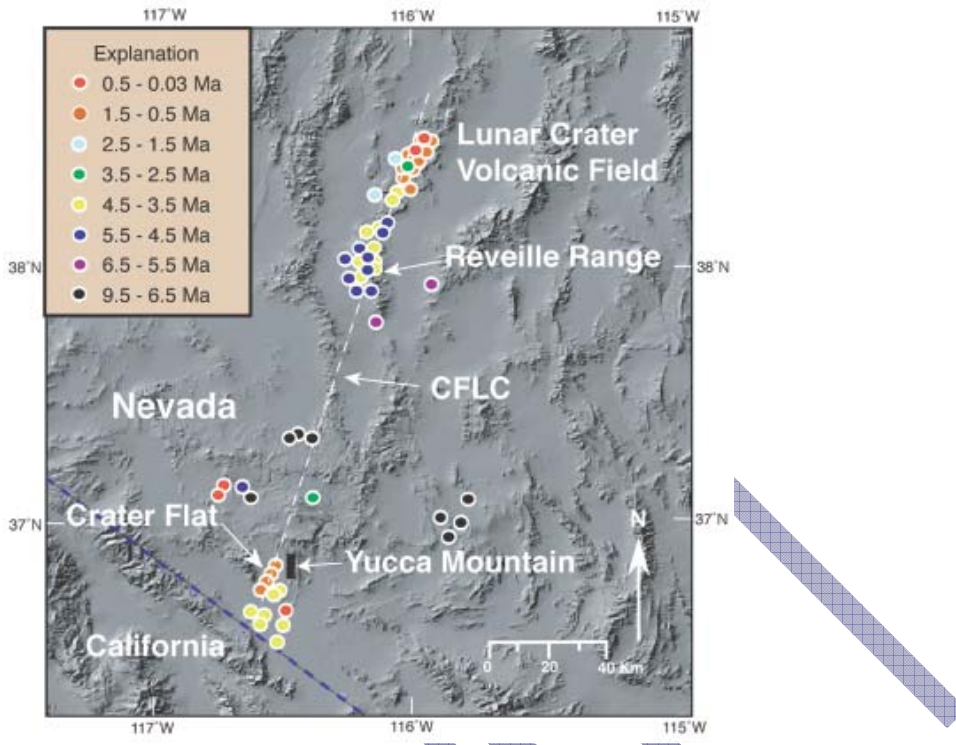
2812 The 80-ka Lathrop Wells volcano represents the youngest event in the vicinity of the
 2813 Crater Flat basin. Fridrich et al. (1999) report that it lies between the southern ends of the
 2814 Windy Wash and Stagecoach Road faults, the most active site of late Pleistocene faulting in the
 2815 Crater Flat basin. They also report a close spatial and temporal relationship between sites of
 2816 extension and volcanism throughout this basin. The occurrence of the three episodes of post-
 2817 Miocene volcanism in the southwestern part of Crater Flat suggests that volcanism is less likely
 2818 to occur at Yucca Mountain, which lies outside the transtensional zone in an area where no
 2819 post-Miocene volcanism has occurred. Fridrich et al. (1999) reported that other geologic and
 2820 geophysical studies provide corroborative evidence that areas of maximum extension in the
 2821 southwestern Crater Flat basin correspond closely to volcanic source zones.
 2822
 2823
 2824
 2825



2826
 2827
 2828 Figure 5.7 Plot of fissure length (lines) and lava effusion rate (dots) for Plio-Pleistocene
 2829 volcanoes of the Southwestern Nevada Volcanic Field. Note that age determinations do not
 2830 allow discrimination of relative ages amongst the five Pleistocene volcanoes in Crater Flat,
 2831 therefore they are plotted in random order around 1 Ma. The eruptive products of SW and NE
 2832 Little Cones are largely buried by alluvium and mapped by aeromagnetic anomalies [Valentine
 2833 et al., 2006]; their volumes are lumped together in this plot. [After Valentine and Perry, 2006]
 2834

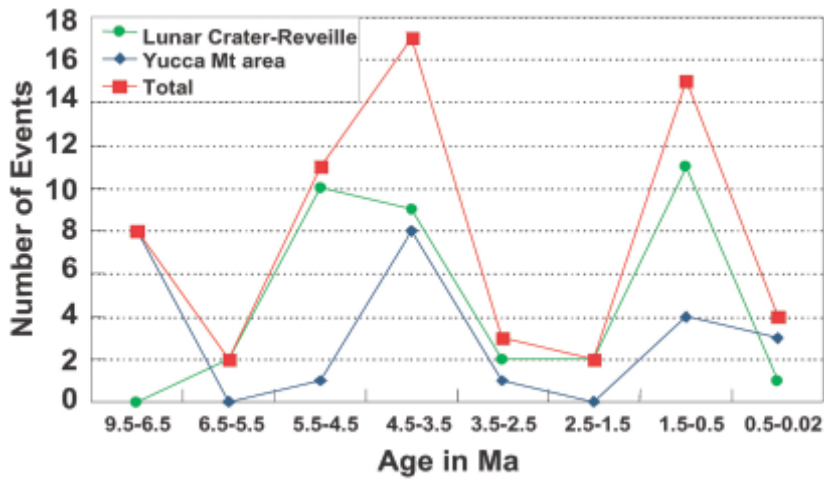
2835 Alternatively, Smith et al. (2002) and Ho et al. (2006) suggest that the volcanism in the
 2836 Yucca Mountain region is related to a mantle zone of melt that extends from Death Valley
 2837 through Crater Flat to Lunar Crater volcanic field roughly 100 km north of Yucca Mountain
 2838 (Figure 5.8). They hypothesize that the episodic volcanism of the Crater Flat-Lunar Crater trend
 2839 shown in Figure 5.9 is related to varying strain accumulation in the lithosphere and "...
 2840 volcanism is not dead and another eruption peak is possible". (Smith et al., 2002, p.9). However,
 2841 the interpretation of the connection between the Crater Flat and Lunar Crater volcanic fields is
 2842 questionable as a result of the geochemical studies of Yogodzinski and Smith (1995) and
 2843 Yogodzinski et al. (1996) that show that the Yucca Mountain region and Lunar Crater volcanic
 2844 rocks have fundamentally different mantle sources, with the source of the former being relatively
 2845 "cold". Accordingly, the Yucca Mountain region source may be unlikely to produce frequent or
 2846 large volumes of basalt.
 2847

2848



2849
2850
2851
2852
2853
2854

Figure 5.8 Age and distribution of Pliocene-Pleistocene basaltic volcanoes in Crater Flat-Lunar Crater zone (CFLC). [After Smith et al., 2002]



2855
2856
2857
2858
2859
2860
2861
2862
2863

Figure 5.9 Time-event plot showing episodic nature of volcanism in the Crater Flat-Lunar Crater zone. [After Smith et al., 2002]

5.3 Time Period Used in Extrapolation of Igneous Activity

The time period used to evaluate future volcanism in the Yucca Mountain region should be reasonably representative of present-day geologic and tectonic conditions. For example,

2864 there is no evidence that the extensive felsic *pyroclastic* eruptions that formed the surface rocks
2865 at Yucca Mountain ~13 Myr ago will reoccur. The dramatic decline in both tectonism and
2866 basaltic volcanism over the last 11 Myr indicates that crustal conditions during post-Miocene
2867 time (<5.3 Myr) are more representative of present-day conditions than of those that prevailed
2868 during the Miocene Epoch. The last tuff-forming eruptions occurred in the region ~7.7 Myr ago,
2869 depositing the Thirsty Canyon Tuff. There is also greater uncertainty about the actual numbers
2870 of Miocene events because of concealment by younger volcanics and the longer time available
2871 for physical erosion and burial by alluvium. In developing estimates of volcanism recurrence
2872 rates, more reliable counts can therefore be made of Pliocene, and especially of Pleistocene,
2873 events for extrapolation purposes (Coleman et al., 2004).
2874

2875 **5.4 Controls on Occurrence of Igneous Activity**

2876
2877 In developing a sound basis for estimating the probability of igneous event at the proposed
2878 Yucca Mountain repository, it is necessary to identify the most likely areas of the Yucca
2879 Mountain area for the occurrence of igneous activity. An active magma chamber and crustal
2880 conditions favorable for the magma to rise to the surface are both needed for basaltic igneous
2881 activity to occur.
2882

2883 Efforts have been made to isolate active magma chambers in the upper mantle of the
2884 Yucca Mountain region using tomographic methods to identify seismic velocity variations
2885 associated with the partial melts of the magma chambers (e.g., Evans and Smith, 1992 and
2886 1995). Unfortunately, these studies have not led to definitive results. Evans and Smith (1995)
2887 find a weak low seismic velocity feature beneath Crater Flat that may represent crustal heating
2888 beneath the basin. However, Biasi (2005) reported to the PVHA-U panel that he has mapped
2889 variations in seismic velocity in the upper mantle in the Yucca Mountain region that he relates to
2890 surface features. He interprets the velocity variations within the mantle as a dehydrated root
2891 extending to depths of 300 km beneath the Timber Mountain/Silent Canyon caldera complex
2892 north of Yucca Mountain that is related to the caldera volcanism. Post-Miocene basaltic events
2893 occur on the margin of the dehydrated root. He further suggests that the waning volcanism is
2894 more indicative of the effect of the dehydrated root than cooling of the system. His investigations
2895 indicate that the Plio-Pleistocene volcanism has dehydrated the mantle underlying Crater Flat,
2896 thus somewhat cooling it and increasing its melting temperature, suggesting that the area may
2897 be less prone to volcanism in the future. Other remote sensing techniques of isolating the
2898 magma chambers are insufficiently sensitive to the minor effects of the magma reservoirs
2899 associated with the basaltic volcanism.
2900

2901 O'Leary (2001) described possible tectonic controls on basaltic volcanism near Yucca
2902 Mountain. He noted that the Plio-Pleistocene basalts near Yucca Mountain are transitional
2903 alkaline-olivine basalts or trachybasalts, which are typical of other basalts of that age in the
2904 western Great Basin. Such basalts are generally thought to originate as partial melts of
2905 lithospheric mantle, uncontaminated by crustal components. Each volcano probably represents
2906 a batch of magma collected from a resident equilibrium melt, with upward pathways being
2907 provided by local tectonic conditions. Given the low rate of post-Miocene extension, O'Leary
2908 (2001) proposed that present-day melt generation near Yucca Mountain would not likely be
2909 influenced by decompression, and further stated that the small extrusive volumes are not likely
2910 influenced by buoyancy.
2911

2912 Most of the volcanic centers originating over the past 5 Myr are located in Crater Flat basin
2913 or in the Amargosa Desert. Some of the cones show a NNE-oriented alignment. This alignment
2914 of small-volume eruptions, the relatively high volatile content of the erupted materials, and lack

2915 of crustal contamination or evidence of fractionation suggest that the magmas ascend directly
2916 from an upper mantle source along fractures influenced by right-lateral (dextral) transtension
2917 (O'Leary, 2001). A tectonic model that treats Crater Flat basin and the Amargosa trough as a
2918 *graben*/rift feature modified by dextral shear, and accounts for extension effects and fracturing in
2919 the upper mantle melt zone, provides a mechanism for basalt rise through the crust as well as a
2920 structural association with observed tectonic features. Consistent with the apparent waning
2921 volcanism, activity should decrease over time as local magma reservoirs are depleted and the
2922 magma solidification temperature is pushed to greater mantle depths with a cooling lithosphere
2923 (O'Leary, 2001).

2924
2925 DOE (2003) summarizes stress conditions near Yucca Mountain. Along with faulting,
2926 magma intrusion is an important component of worldwide crustal extension (Parsons and
2927 Thompson, 1991). Yucca Mountain lies in the southern Great Basin in the Basin and Range
2928 province, which is undergoing active ESE–WNW extension (Zoback and Zoback, 1989). The
2929 crustal stress in the Yucca Mountain region has been investigated using hydraulic-fracturing
2930 stress measurements, borehole breakouts, drilling-induced fractures, earthquake focal
2931 mechanisms and fault-slip orientations (Stock and Healy, 1988). Dikes tend to strike orthogonal
2932 to the direction of the least compressive horizontal stress, and parallel to the direction of the
2933 greatest compressive horizontal stress (Pollard, 1987). The orientation of the greatest
2934 compressive horizontal stress in the Yucca Mountain region is approximately N30E ±15
2935 degrees. Uncertainty in this orientation results from both inaccuracies in measurement and real
2936 variations in stress with depth and location, which vary by up to 40° in Yucca Mountain
2937 boreholes (Stock et al., 1985).

2938
2939 The Crater Flat structural domain is a basin bounded on the west by the Bare Mountain
2940 fault (Figure 2.1) and on the east by structures beneath Jackass Flats. Seismic reflection
2941 surveys show that the Crater Flat basin is deepest on the western side (Brocher et al. 1998). It
2942 includes the Crater Flat topographic basin on the west and Yucca Mountain near the center of
2943 the structural domain. Because the potential repository lies within the Crater Flat structural
2944 basin, the structural and geophysical features of the domain, and the degree to which they
2945 influence the location of volcanism within the domain, have been key factors in conceptual
2946 models of volcanism for assessing hazards to the repository (DOE, 2003).

2947
2948 Connor et al. (2000) report that magmas ascending a steeply dipping fault may be
2949 diverted laterally by as much as 5 km depending on the depth of dike capture by the fault and
2950 the dip of the fault plane. Dikes also have a tendency to break out of the fault system and
2951 propagate vertically at shallow depth because of rapid changes in the magnitude and orientation
2952 of the stress field. Therefore cinder cones are often located beside faults in the hanging wall of
2953 the fault. The arcuate map pattern of the Pleistocene Crater Flat alignment may partly owe its
2954 origin to this mechanism. The dip of the Bare Mountain Fault shallows progressively northward
2955 (Ferrill et al., 1996) and cinder cones along the alignment are displaced progressively eastward.
2956 Basin and Range normal faults commonly grow by formation, propagation, and amalgamation of
2957 smaller normal faults (Ferrill et al., 1999). This progressive fault growth commonly involves
2958 development of en echelon fault systems with individual normal fault segments separated by
2959 relay ramps. Ferrill et al. (1999) identified the Solitario Canyon fault and related west dipping
2960 faults on the western edge of Yucca Mountain as one such set of left-stepping en echelon faults
2961 produced by progressive deformation. The Pliocene vents immediately south and west of these
2962 fault segments reflect this trend, forming a left-stepping array of vent alignments. *En echelon*
2963 fault geometries may therefore provide preferential pathways to the surface for magmas
2964 ascending along fault segments. Linear, north-trending magnetic anomalies intersect Northern
2965 Cone, located in Crater Flat. These anomalies result from vertical offsets across faults that are

2966 arguably part of the same array of left-stepping normal faults. At the western edge of the
2967 proposed repository, a Miocene-aged dike intruded a segment of the Solitario Canyon fault.
2968 Such relationships indicate that the en echelon array of faults has hosted dikes at least three
2969 times in Miocene through Pleistocene time.

2970
2971 Spatially, most of the Plio-Pleistocene basalts near Yucca Mountain erupted in basins
2972 rather than on topographically high ranges. Basalts in basins include the Pleistocene aged
2973 cones of Crater Flat, the Lathrop Wells cone, Pliocene Crater Flat, and buried basalts of
2974 Pliocene age located by drilling (Anomalies B and G, and by inference, Anomalies F and H).
2975 The clear preference for Plio-Pleistocene basalts to erupt in basins, the shortest path to the
2976 surface for dikes, has been informally discussed by panelists of the ongoing PVHA-U. They
2977 have requested that DOE develop a dataset of lithostatic (overburden) pressure variations to
2978 compare with areas where past volcanism has occurred. At Yucca Mountain itself intrusions
2979 may have been inhibited over the last 10-12 Myr by higher rock pressure compared to the
2980 Crater Flat basin area to the west. Lithostatic pressure data provides information on likely
2981 magma flow paths in the upper crust. In waning volcanic systems like the Crater Flat region, the
2982 driving energy of the magma systems is low enough that lithostatic pressure variations may be
2983 sufficient to help guide magma flow paths. Eruptions from such systems would hypothetically be
2984 favored to occur in basins where the pressure from the overlying rocks is lower rather than in
2985 adjacent topographically high areas like Yucca Mountain. This concept was investigated by
2986 Parsons et al. (2006) using three-dimensional finite-element modeling to determine the
2987 sensitivity of basalt intrusions and faulting to the magnitude and orientation of the least principal
2988 stress in extensional terranes such as the Yucca Mountain region. They found that in the
2989 absence of fault slip, lithostatic pressure variations favored intrusions into Crater Flat. However,
2990 when faults were allowed to slip, intrusions were not favored in either Crater Flat or the central
2991 Yucca Mountain block, but rather near fault terminations. They find the latter situation is
2992 consistent with the Lathrop Wells volcano.

2993
2994 There are exceptions, but most of the basaltic eruptions near Yucca Mountain occurred in
2995 the basins. More energetic magma systems of greater volume (e.g., Reville Range-Lunar
2996 Crater) could be less sensitive to lateral lithostatic pressure variations and, therefore, show a
2997 lesser tendency to concentrate eruptions in topographic lows.

2998 2999 **5.5 Prediction Methods**

3000
3001 Many methods have been used to predict future volcanism. Most are directed toward the
3002 near real-time eruption of existing volcanoes. These predictions are increasingly successful with
3003 increasing knowledge of the cause and mechanisms of volcanic activity. However, consideration
3004 of volcanic activity at the proposed Yucca Mountain repository involves the likelihood, location,
3005 and nature of new igneous activity that could intersect the repository over time frames of tens
3006 and hundreds of thousands of years. In this section the methods of prediction are described
3007 including the use of physical precursors, analysis of hypothetical linkages between volcanic
3008 fields, and various mathematical and statistical methods that can be used to analyze past
3009 spatial and temporal patterns of volcanism. The latter is the generally used method for studying
3010 Yucca Mountain region igneous activity and thus is the primary focus.

3011 3012 **5.5.1 Physical Precursors**

3013
3014 The ability to predict future volcanic activity is uncertain, especially for regions where
3015 volcanism has occurred sporadically over long periods of geologic time. Predictive methods are
3016 mostly based on analysis of temporal and spatial patterns of past activity. Many volcanoes

3017 repeatedly erupt in one place over geologic time (polycyclic volcanoes). Examples include
3018 Kilauea in Hawaii, Mount Suribachi, Mount Etna, Vesuvius, and the Cascade volcanoes (Mounts
3019 Rainier, St. Helens, Hood, and many others). The main eruption of Mount St. Helens in 1980
3020 was anticipated by real-time phenomena, such as an increase in seismic activity, changes in
3021 gaseous emissions from the summit crater, and changes in the volcano's topography. A large
3022 area was evacuated around the volcano, but even so the speed and total energy of the eruption
3023 was greater than expected, resulting in a larger area being affected and loss of life. Nine main
3024 pulses of activity have occurred at Mount St. Helens in the last 40,000 years, with multiple
3025 eruptions in each pulse (Tilling et al., 1990). There is no evidence that the basaltic eruptions
3026 during the last 5 million years near Yucca Mountain were polycyclic (Valentine et al., 2006a).
3027 They formed discrete cinder cones and associated lava flows. The most recent volcanic activity
3028 near Yucca Mountain formed the Lathrop Wells cone and basalt flows that have undergone
3029 extensive study (Zreda et al., 1993; Fleck et al., 1996; Heizler et al., 1999; Nicholis and
3030 Rutherford, 2004; Valentine et al., 2005).

3031
3032 As reported by Fridrich et al (1999) there is an observed relationship in the Yucca
3033 Mountain region between strain rate and volcanism. Wernicke et al. (1998) had suggested that
3034 the region is experiencing an epoch of anomalously rapid crustal strain accumulation, and that
3035 hazard analyses based only on the local record of magmatic and tectonic events would
3036 underestimate the probability of future events by an order of magnitude. The claim of
3037 anomalous strain was countered by Savage (1998) who reported a N65°W strain rate of 8 ± 20
3038 nanostrain/yr. He found that Wernicke et al. (1998) did not included monument instability in
3039 their error budget and did not give proper weight to the strain effects of the 1992 Little Skull
3040 Mountain earthquake. Later work by Savage et al. (2001) continues to find that the principal
3041 extension rate averaged over their 50-km geodetic array is substantially less than reported by
3042 Wernicke et al. (1998) and is consistent with the low extension rate inferred from the geologic
3043 record. Likewise, Connor et al. (1998) noted that the lack of a known volcano younger than the
3044 Lathrop Wells event diminished the argument that volcanic recurrence rates have been
3045 underestimated by an order of magnitude. Therefore, present-day strain rates do not support an
3046 order of magnitude increase in hazard from tectonic or magmatic events. Furthermore, as
3047 discussed above, seismic tomographic methods have not provided definitive information on the
3048 presence of magma chambers within the mantle because of their great depth and limited size.
3049 Therefore, in regions with such low rates of volcanic activity, it appears there are no precursors
3050 of activity that can be used to anticipate the location and time of igneous activity. Other
3051 approaches need to be considered.

3052 3053 **5.5.2 Linkages to Other Volcanic Zones**

3054
3055 Smith et al. (2002) and Ho et al. (2006) propose that the volcanoes near Yucca Mountain
3056 are part of a larger zone of basaltic volcanism associated with a common area of hot mantle.that
3057 extends from Death Valley northward to the Reveille Range-Lunar Crater (RLC) volcanic area
3058 (Figure 5.8). Within this zone volcanism is of similar age and episodic, with three peaks of
3059 volcanism: one between 9.5 and 6.5 Ma, the second from 4.5 to 3.5 Ma, and the most recent
3060 between 1.5 and 0.5 Ma (Figure 5.9). Smith et al. (2002) report that volcanism in this zone is
3061 relatively quiet at present, with only three eruptions in the last 80,000 years. Episodic volcanism
3062 in the Crater Flat-Lunar Crater zone may be related to episodes of rapid strain accumulation in
3063 the lithosphere. They concluded that a zone of hot, buoyant mantle exists beneath this zone
3064 and provides a common driving force for magmatism. In other words, Smith et al. (2002)
3065 propose that the magma that erupted in these volcanic zones had a common source.
3066

3067 Volcanism recurrence rates in the RLC are approximately four times higher than in
3068 Crater Flat near Yucca Mountain. Smith and Keenan (2005) suggested that the higher
3069 recurrence rates in the RLC may occur in the future in the Yucca Mountain area. They further
3070 suggested a need for additional geophysical surveys in areas beyond those covered by the
3071 DOE's new high-resolution aeromagnetic survey (Perry et al., 2006). They concluded that the
3072 higher recurrence rates, along with data from future surveys, could result in a probability of
3073 volcanic disruption of a repository that is 1-2 orders of magnitude greater than the EPA
3074 guideline for consideration of disruptive events (i.e., one chance in 10,000 in 10,000 years, or
3075 $10^{-8}/\text{yr}$). Smith and Keenan (2005) suggested that the probability of repository disruption could
3076 be as high as $10^{-7}/\text{yr}$ to $10^{-6}/\text{yr}$.
3077

3078 Linkages between the Crater Flat area and the RLC have been questioned because of
3079 significant isotopic differences in their basalt composition (e.g., Yogodzinski and Smith, 1995),
3080 and also because the RLC is more than 90 km distant and is a much larger volcanic field. Smith
3081 and Keenan (2005) have suggested that the isotopic differences can be explained by
3082 contamination of rising magma by lithosphere of different composition or age.
3083

3084 **5.5.3 Mathematical and Statistical Techniques** 3085

3086 For existing volcanic fields, various methods can be used to analyze spatial and
3087 temporal patterns of past volcanism to gain insights about where future events might occur.
3088 Most volcanic fields are only partially characterized. The Crater Flat volcanic field is relatively
3089 well-studied both in terms of surface exposures and buried basalts that have been identified
3090 with geophysical studies and subsequently drilled and dated. Extensive field geology and
3091 petrographic work have also been performed on basalts near Yucca Mountain.
3092

3093 **5.5.3.1 Data-Based Approach**

3094 Estimates of the probability of an igneous event intersecting the proposed repository have
3095 employed a general methodology used for predicting events in existing volcanic fields. The
3096 critical variables in this methodology are the spatial and temporal models developed from the
3097 intensive studies of the volcanoes in the Yucca Mountain region and their products. However,
3098 interpretation of the results of these studies has led to differing input parameters to the
3099 methodology and a range of probabilities covering roughly two to three orders of magnitude.

3100 The general method used in determining the probability of a future intersecting event is the
3101 product of two quantities; the estimated recurrence rate,

3102 $N(R,T)/T$, the recurrence rate, which is the number of igneous events within a specified
3103 volcanic zone adjacent to or including the site of the repository over a specified time period
3104 $[N(R,T)]$ divided by the specified time period $[T]$

3105 and the conditional probability of disruption within the footprint of the repository $[a_r]$, given the
3106 occurrence of an igneous event,

3107 a_r/A which is the area of the footprint of the repository divided by the area of the
3108 volcanic zone $[A]$ used in establishing the number of igneous events. The conditional probability
3109 of disruption relates the recurrence rate to the footprint of the repository and the area over which
3110 the recurrence rate is calculated. Thus, the probability of a future igneous event intersecting the
3111 repository per year at any time during the next 10,000 year period is

3112 $P = [N(R,t)/T] \times [a_r/A]$

3113 where the time duration (T) is given in years.

3114 A variation on this methodology has been considered by Ho et al. (2006) that
3115 incorporates procedures prescribed by the US Federal Aviation Administration for licensing
3116 commercial space launches and reentry to limit risks to public health and safety.

3117 The recurrence interval is based on the spatial and temporal distribution of events, which
3118 in turn is determined from the volcanic, geologic, and tectonic history of the Yucca Mountain
3119 region. It requires consideration of numerous components as illustrated in the logic chart (Figure
3120 1.1b) including definition of the following

- 3121 • an igneous event,
- 3122 • the volcanic zone model which specifies the area and geographic location of the
3123 region of similar volcanic features adjacent to or including the proposed repository,
- 3124 • the temporal model which specifies the number of igneous events in the volcanic
3125 model zone mapped from surface exposures and geophysical exploration and the
3126 number of events that are assumed to occur without being detected,
- 3127 • the interval of time extending into the past which is representative of future
3128 igneous events at the proposed repository, and
- 3129 • the location and area of the repository.

3130 There is considerable uncertainty in most of these components except for the location and area
3131 of the repository and the number of igneous events mapped by surface exposures and
3132 geophysical studies. As a result the evaluation of probability is treated statistically by including
3133 the potential range of uncertainty assigned to each component of the probability equation. The
3134 result is a range of probability of intersection of the proposed repository which is incorporated
3135 into the performance assessment analysis. The uncertainty in P can be constrained by
3136 incorporating distribution functions specified by assumed controls on the occurrence of events in
3137 the equation for P (e.g., Connor et al., 2000). This is sometimes referred to as a Bayesian
3138 approach.

3139 The recurrence rate term dominates the estimate of the probability of intersection and is
3140 the main source of uncertainty. Most estimates of the recurrence rate (events per year) range
3141 from 10^{-5} to 10^{-6} and conditional distribution probability values vary from 10^{-2} to 10^{-3} . Thus, in the
3142 simplest case the probability of intersection ranges from 10^{-7} to 10^{-9} per year.

3143

3144 **5.5.3.2 Locally Homogeneous Spatial and Temporal Model**

3145 Temporal models that describe the frequency of occurrence of an event include both
3146 homogeneous and non-homogeneous models. Homogeneous models are based on a uniform
3147 rate of volcanism over the specified duration of time over the area of the volcanic zone model. In
3148 contrast nonhomogeneous models assume a non-uniform rate of igneous activity. Spatial
3149 models employ identified spatial source zones which reflect the presence and nature of igneous

3150 events and assumed geologic controls, e.g., faults and topography, on future igneous events in
3151 the zone. These source zones may consider nonhomogeneous, nonparametric models based
3152 on the location of existing events and their limits may be smoothed using various functions to
3153 describe the change in recurrence rate over the source zone.

3154
3155 Homogeneous Poisson models are commonly used to represent hazards from rare
3156 events. A key assumption is that one can identify a region where the rate of occurrence of
3157 volcanic events can be considered uniform in space and time over the period of interest. The
3158 Poisson model provides a reasonable representation for the combined effects of multiple
3159 independent processes, even when the individual processes may be non-Poissonian
3160 (Geomatrix Consultants, 1996). Areas of interest are divided into non-overlapping zones within
3161 which the frequency of intersection of volcanic events is calculated. One zone might be a large
3162 region with diffuse (background rate) volcanic activity, while another zone might display more
3163 concentrated volcanic activity. The rate of occurrence is estimated from data from a zone. The
3164 maximum likelihood estimate is given by the number of observed events in a time interval,
3165 divided by that interval.

3166 **5.5.3.3 Nonhomogeneous Spatial Models**

3167 **5.5.3.3.1 Parametric Spatial Density Function**

3168
3169
3170 Parametric methods are mathematical procedures for hypothesis testing that assume
3171 that the distributions of the variables being assessed belong to known families of probability
3172 distributions. For example, analysis of variance assumes that the underlying distributions are
3173 normally distributed and that the variances of the distributions being compared are similar.
3174 While parametric techniques are robust (statistically powerful), some distributions violate the
3175 underlying assumptions so much that non-parametric methods are more likely to detect
3176 differences or similarities.

3177
3178
3179 Sheridan (1990) developed a model for volcanic fields that represents the spatial density
3180 of events using a bivariate Gaussian distribution. The resulting mathematical representation
3181 has an elliptical shape defined by five parameters: coordinates of the field center, lengths of the
3182 major and minor axes, and the orientation (aximuth) of the major axis. Members of the 1995
3183 PVHA (Geomatrix Consultants, 1996) used this method (and others), estimating the parameters
3184 of Gaussian volcanic fields using data from the Yucca Mountain area.

3185 **5.5.3.3.2 Nonparametric Spatial Density Function**

3186
3187
3188 Non-parametric methods differ from parametric methods because the model structure is
3189 determined entirely from data. No assumptions are made about the frequency (or other)
3190 distributions of the variables being assessed. A histogram is an example of a simple
3191 nonparametric estimate of a probability distribution. The Chi-square test is one of the most
3192 frequently used non-parametric statistical tests.

3193
3194 Stochastic *kernels* are commonly used in density estimation. Connor and Hill (1995)
3195 presented three nonhomogeneous spatial models for evaluating volcanic hazards. These three
3196 models included kernel density estimation, spatial-temporal nearest neighbor density estimation,
3197 and nearest neighbor kernel density estimation. Connor and Hill (1995) and Connor et al.
3198 (2000) presented a geologic and statistical basis for probabilistic hazard assessment at Yucca
3199 Mountain. Connor (2000) and Connor et al. (2002) developed software and accompanying data
3200 sets that use kernel density estimators to calculate probability surfaces using the location and

3201 timing of past, discrete volcanic events. They used both *Gaussian* and *Epanechnikov* kernels.
3202 The software by Connor et al. (2002) added several features, including the ability to represent
3203 the length and orientation of dikes and vent alignments. Also, isostatic gravity anomaly data
3204 could be incorporated into the analysis using a weighting factor determined by the user.
3205

3206 Coleman et al. (2004) used the software and data sets of Connor et al. (2002) to
3207 evaluate numbers of volcanic events in the region that should have been expected if recurrence
3208 rates were as frequent as claimed by some researchers. For example, some have claimed that
3209 the probability of volcanic intersection at Yucca Mountain could be as high as 10^{-6} /yr. The
3210 model and data sets of Connor et al. (2002) suggest that 40 to 192 eruptions should have been
3211 expected in the region in the last million years if the probability is as high as 10^{-6} /yr. However,
3212 only 8 events are known in all of the Pleistocene (1.75 Ma).
3213

3214 **5.5.3.4 Nonhomogeneous Temporal Models**

3215
3216 Several investigators have used non-homogeneous models. Ho (1991, 1992) suggested
3217 that the rate of volcanic activity in the YMR was not stationary in time and that the rate of activity
3218 could be modeled as a nonhomogeneous Poisson process using a *Weibull* function. Crowe
3219 (1995) applied a model in which the event rate of igneous activity intersecting the proposed
3220 repository was estimated by dividing the instantaneous rate of magma production by the time-
3221 varying volume per volcanic event. One PVHA expert used this method in his analysis
3222 (Geomatrix Consultants, 1996).
3223

3224 **5.6 NRC, DOE, and EPRI Treatment of Probability in Performance Assessments**

3225
3226 NRC staff, DOE, and EPRI have performed detailed performance assessments of the
3227 proposed repository at Yucca Mountain using varying ranges and point values of probability of
3228 an igneous event intersecting the proposed repository.
3229

3230 **5.6.1 DOE Analysis**

3231
3232 The DOE used the probability range developed by expert elicitation in the 1990's
3233 (Geomatrix Consultants, 1996). That probability range was recalculated (BSC, 2003a [p. 113])
3234 using PVHA outputs to account for the proposed license application (LA) repository footprint
3235 (the outline of the waste emplacement area) and extended to include the probability of an
3236 eruption within the proposed LA repository footprint, conditional on dike intersection (5th
3237 percentile = 7.4×10^{-10} /yr; Mean = 1.7×10^{-8} /yr; 95th percentile = 5.5×10^{-8} /yr). It is expected
3238 that if the repository layout is changed or expanded, that would be considered in the
3239 documentation for a license application. An update of the PVHA is now being conducted that
3240 includes new information gathered since 1996, including the results of a basalt anomaly
3241 exploratory drilling program.
3242

3243 The DOE had agreed to resolve the probability subissue with NRC by
3244 "... providing in the Site Recommendation and License Application, in addition to DOE's
3245 licensing case, the results of a single point sensitivity analysis for extrusive and intrusive
3246 igneous processes at an annual probability of 10^{-7} . By agreeing to provide these analyses, [the
3247 NRC] staff consider the probability subissue closed-pending, because the 10^{-7} analyses provide
3248 a reasonably conservative approach for evaluating risks from igneous activity." (Hill and
3249 Connor, 2000 [p. 74]).
3250

3251 **5.6.2 EPRI Analysis**

3252
3253 EPRI (2005) has adopted the PVHA (Geomatrix Consultants, 1996) probability value (i.e.,
3254 1.6×10^{-8} /yr, which is the expected frequency of volcanic intersection.
3255

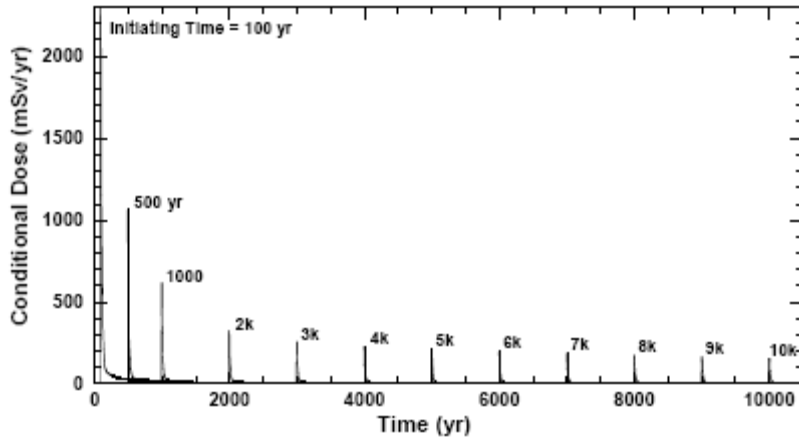
3256 **5.6.3 NRC Analysis**

3257
3258 The NRC performance assessments do not use a range of values for volcanism
3259 probability, but instead use the single-point value of 10^{-7} /yr as the probability that a volcanic
3260 conduit (extrusive scenario) could intersect a repository drift (Mohanty et al., 2004). The ACNW
3261 has commented that instead of using a single value of probability in performance assessments,
3262 the NRC staff should consider a range of estimates on the order of 10^{-7} /yr to 10^{-8} /yr based on
3263 studies published by NRC and previous ACNW views. If the staff decides to use a single-point
3264 value approach, the staff should document how this decision will support a risk-informed review
3265 of the consequences of an igneous event in a potential license application. The NRC staff
3266 responded that:

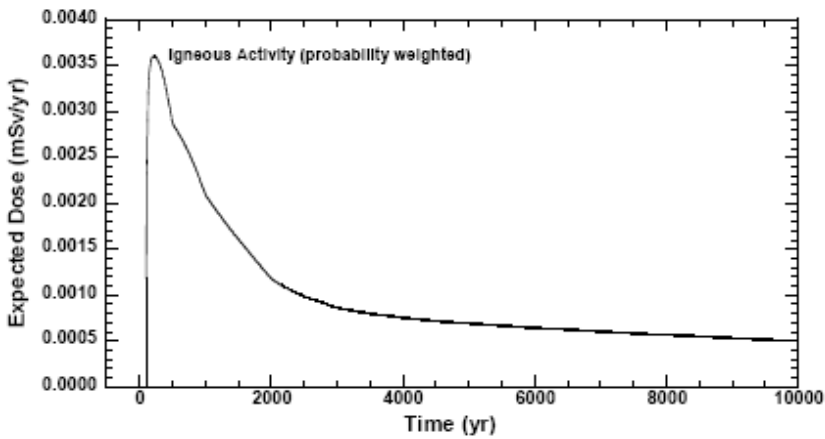
3267
3268 “...the significance of alternative conceptual probability models can be evaluated as
3269 single values in performance calculations. By using a representative probability value as
3270 a baseline in calculations, staff can evaluate the risk significance of any available
3271 probability value by simple comparison to the baseline value. Staff continues to evaluate
3272 new data and conceptual models for igneous event probabilities developed by DOE and
3273 other scientists, as well as DOE’s ongoing expert elicitation on Probabilistic Volcanic
3274 Hazard Assessment and associated field and laboratory investigations. The potential
3275 risk significance of this new information can be determined and communicated by using
3276 a combination of review methods.”
3277

3278 It remains unclear to the ACNW why the NRC staff continues to use a constant value to
3279 represent volcanism probability. The value used, 10^{-7} /yr, appears to be overly conservative – it
3280 does not represent a mean estimate but instead lies near the upper limit of most calculated
3281 probability ranges. This deterministic and bounding approach by the staff is inconsistent with
3282 the risk-informed approach used elsewhere in their Total-System Performance Assessment
3283 (TPA) for Yucca Mountain. The rationale presented to date (see preceding paragraph) does not
3284 provide a coherent or acceptable response to ACNW concerns.
3285

3286 A key conclusion by the NRC staff is that the largest estimated doses to the RMEI arise
3287 if a repository were to be intersected by volcanism in the first 1000 years after closure. This is
3288 illustrated in Figure 5.10 where it can be seen that mean doses decrease substantially after the
3289 first 1000 years. The reason for this is that a large fraction of the inventory of short-lived
3290 radionuclides decays during the first 1000 years, diminishing the remaining activity in the spent
3291 fuel and reducing possible doses from extrusive igneous events.
3292
3293



3294



3295

3296

3297

3298

3299

3300

3301

3302

3303

3304

3305

3306

Figure 5.10 (top) Mean dose arising from extrusive igneous activity shown with various times for the volcanic even in 350 realizations. (below) Contribution of extrusive igneous activity to the total dose, weighted by an annual probability for the volcanic event of 10^{-7} /year. [After Mohanty et al., 2004, p. 3-84].

5.7 Views on Igneous Activity Probability

Table 5.3 presents a summary of published views on the probability of an igneous event intersecting the proposed high-level waste repository at Yucca Mountain.

Table 5.3 Summary of Published Positions on Probability of Igneous Activity

Source	Probability range for volcanic disruption	Notes
Crowe et al. (1982)	10^{-10} /yr to 10^{-8} /yr	Based on two estimation methods: one based on rate of magma production in the Nevada Test Site area and a second using the number of volcanic vents over a specified time period.
Smith et al. (1990)	Assigned the site of the Yucca Mountain repository to risk-category 3	Based on a proposed qualitative index of volcanic risk for areas in the Yucca Mountain region. In this index, risk level 5 is highest and 1 is lowest.

Ho et al. (1991)	Probability not specified – see notes	Estimated the recurrence rate of volcanic eruption (not the probability of intersecting a repository). Values obtained: $5 \times 10^{-6}/\text{yr}$ $5.9 \times 10^{-6}/\text{yr}$ $5 \times 10^{-6}/\text{yr}$
Crowe et al. (1993)	$2.6 \times 10^{-8}/\text{yr}$	Median value of probability distribution
Connor and Hill (1995)	$1-5 \times 10^{-8}/\text{yr}$	Range of 3 alternative models for probability of an eruption (volcanic conduit intersecting the repository)
Crowe et al. (1995)	$1.8 \times 10^{-8}/\text{yr}$	Median value of 22 alternative probability models
Geomatrix Consultants (1996)	$1.5 \times 10^{-8}/\text{yr}$ $5.4 \times 10^{-10}/\text{yr}$ to $4.9 \times 10^{-8}/\text{yr}$	Expected frequency of intersection 90% confidence interval
Ho and Smith (1997)	$1.4 \times 10^{-7}/\text{yr}$ to $3.0 \times 10^{-6}/\text{yr}$	Consideration of Bayesian methods
Ho and Smith (1998)	(1) $1.5 \times 10^{-8}/\text{yr}$ (2) $1.09 \times 10^{-8}/\text{yr}$ to $2.83 \times 10^{-8}/\text{yr}$ (3) $3.14 \times 10^{-7}/\text{yr}$	Authors presented 3 alternative models
Wernicke et al. (1998)	Probability not specified – see notes	Yucca Mountain area experiencing epoch of anomalously rapid strain accumulation. Hazard analyses based on local geologic record may underestimate volcanism probability by an order of magnitude. Lathrop Wells may represent onset of a cluster of volcanism that could continue over the next few tens of thousands of years.
Savage (1998)	Reply to Wernicke (1998)	Savage (1998) countered the claim of anomalous strain reported by Wernicke et al. (1998), and reported a $N65^{\circ}W$ strain rate of 8 ± 20 nanostrain yr^{-1} . He concluded that Wernicke et al. (1998) had not included monument instability in their error budget and did not give proper weight to the effects of the 1992 Little Skull Mountain earthquake. Later work by Savage et al. (2001) continued to find that the principal extension rate is substantially less than reported by Wernicke et al. (1998), consistent with the low extension rate inferred from the geologic record.

BSC (2003a)	$1.7 \times 10^{-8}/\text{yr}$ 5 th percentile = $7.4 \times 10^{-10}/\text{yr}$ 95 th percentile = $5.5 \times 10^{-8}/\text{yr}$	Revision of probability based on change in area of proposed repository footprint for License Application
CRWMS M&O (1998)	$2.5 \times 10^{-8}/\text{yr}$	Sensitivity analysis that conservatively assumes all aeromagnetic anomalies in Amargosa Desert have Pleistocene age (less than 1.75 Ma)
Connor et al. (2000)	$10^{-8}/\text{yr}$ to $10^{-7}/\text{yr}$	Use of diffusion-based model with gravity weighting, and use of data sets that assume most magnetic anomalies represent post-Miocene basalts
Hill and Connor (2000)	$10^{-7}/\text{yr}$	NRC staff considered the volcanism probability issue closed-pending based on DOE agreement to evaluate risk using this value
Hill and Stamatakos (2002)	Up to an order of magnitude increase in the probability of volcanic disruption. Compared to Connor et al. (2000), this infers a probability up to $10^{-6}/\text{yr}$	At least ten additional basaltic volcanoes may be represented by new aeromagnetic anomalies in the Yucca Mountain region. The first-order effect on probability models could range from negligible, to an order of magnitude increase in volcanic recurrence rates
Smith et al. (2002)	No estimate provided, but this report cited Smith et al. (1990) and Ho and Smith (1997; 1998)	Petrologic arguments suggest that recurrence rates of volcanism used by DOE and NRC may be underestimated and that higher rates typical of the Lunar Crater–Reveille part of the Crater Flat–Lunar Crater zone may be applicable to Yucca Mountain. If models of hot mantle are correct, another eruption peak is possible.
ACNW (2002)	The range of estimated probabilities, $\sim 10^{-9}$ to $\sim 10^{-7}$ per year, of an intrusion into the repository used by DOE in its performance assessment is reasonable. New information from recently completed aeromagnetic surveys needs to be evaluated more fully to determine possible changes in the appropriate probability range.	ACNW letter dated August 1, 2002
Detournay (2003)	No estimate provided	Analog evidence from recent (< 5

		Ma) igneous events that were close to Yucca Mountain (Crater Flat and Lathrop Wells) should be given more weight than earlier or more distant events.
ACNW (2004)	$10^{-8}/\text{yr}$ to $10^{-7}/\text{yr}$	Letter to NRC Chairman dated November 3, 2004
Coleman et al. (2004)	Expected value $5 \times 10^{-8}/\text{yr}$ with a 95% upper bound of $1 \times 10^{-7}/\text{yr}$	Claims of high intrusion frequency (i.e., $10^{-6}/\text{yr}$) fail tests of volcanic recurrence in the Yucca Mountain region; analysis conservatively assumes 5-15 magnetic anomalies are post-Miocene buried basalts
Mohanty et al. (2004; 2005)	$1 \times 10^{-7}/\text{yr}$	Use of single value only – no probability range was used
ACNW (2005)	$10^{-8}/\text{yr}$ to $10^{-7}/\text{yr}$	ACNW recommended that the NRC staff reevaluate the use of a single probability value for volcanic intersection and consider a range of estimates on the order of $10^{-7}/\text{yr}$ to $10^{-8}/\text{yr}$ based on published NRC studies and previous ACNW views.
NRC (2005a)	$1 \times 10^{-7}/\text{yr}$	Use of single value only – no probability range was used
EPRI (2005)	$1.6 \times 10^{-8}/\text{yr}$	EPRI (2005) adopts the PVHA 1996 probability value (the expected frequency of intersection)
Smith and Keenan (2005)	Up to $10^{-7}/\text{yr}$ to $10^{-6}/\text{yr}$	Range that may result by adding data from future geophysical surveys and higher recurrence rates
Reyes (2006)	No probability specified in letter – however, the baseline used in a recent NRC performance assessment (Mohanty et al., 2004) was a single value of $1 \times 10^{-7}/\text{yr}$	Response to Dec. 9, 2005 ACNW letter: “As an alternative (to using a probability range), the significance of alternative conceptual probability models can be evaluated as single values in performance calculations. By using a representative probability value as a baseline in calculations, staff can evaluate the risk significance of any available probability value by simple comparison to the baseline value.”
Ho et al. (2006)	No probability specified.	The authors present a strategy to evaluate “hazards areas” based on a debris-fall model developed for the space transportation industry.
PVHA-Update 2007	-----	Work by expert panel is in progress. Final report not expected until 2008.

5.7.1 NRC Analysis

NRC staff has not clearly adopted a preferred time period for extrapolating the future occurrence of volcanic events. Connor et al. (2000) state: “The proposed high-level radioactive waste repository at Yucca Mountain, Nevada, is located within an active volcanic field. Probabilistic volcanic hazard models for future eruptions through the proposed repository depend heavily on our understanding of the spatial controls on volcano distribution at a variety of scales. On regional scales, Pliocene-Quaternary volcano clusters are located east of the Bare Mountain fault. Extension has resulted in large-scale crustal density contrast across the fault, and vents are restricted to low-density areas of the hanging wall. Finite element modeling indicates that this crustal density contrast can result in transient pressure changes of up to 7 MPa at 40 km depth, providing a mechanism to generate partial melts in areas where mantle rocks are already close to their solidus. On subregional scales, vent alignments, including one alignment newly recognized by ground magnetic mapping, parallel the trends of high-dilation tendency faults in the Yucca Mountain region (YMR). Forty percent of vents in the YMR are part of vent alignments that vary in length from 2 to 16 km. Locally, new geological and geophysical data show that individual vents and short vent alignments occur along and adjacent to faults, particularly at fault intersections, and leftstepping *en echelon* fault segments adjacent to Yucca Mountain. Conditions which formed these structures persist in the YMR today, indicating that volcanism will likely continue in the region and that the proposed repository site is within an area where future volcanism may occur. On the basis of these data the probability of volcanic disruptions of the proposed repository is estimated between 10^{-8} /yr and 10^{-7} /yr.”

Hill and Connor (2000 [p. 74]). “Prior to the August 2000 Technical Exchange with the DOE, staff had identified 12 specific technical concerns regarding the probability subissue. ...To address these concerns, the DOE agreed to resolve the probability subissue by providing in the Site Recommendation and License Application, in addition to DOE’s licensing case, the results of a single point sensitivity analysis for extrusive and intrusive igneous processes at an annual probability of 10^{-7} . By agreeing to provide these analyses, staff consider the probability subissue closed-pending, because the 10^{-7} analyses provide a reasonably conservative approach for evaluating risks from igneous activity.”

Hill and Stamatakos (2002, p. xi). “The U.S. Geological Survey recently completed a large-scale aeromagnetic survey of the Yucca Mountain region. Interpretations of this survey and associated Center for Nuclear Waste Regulatory Analyses ground magnetic surveys indicates there may be twice as many basaltic volcanoes in the Yucca Mountain region than previously recognized. Additional volcanoes also may be present but undetected within approximately 20 km [12 mi] of the proposed repository site due to relatively low resolution of the aeromagnetic survey. Without direct information on the age and composition of these buried volcanoes, associated effects on probability models and risk calculations are highly uncertain. The potential risk significance of this uncertainty ranges from negligible to an order of magnitude increase in the probability of volcanic disruption of the proposed repository site. This uncertainty can be reduced through drilling of anomalies likely to be caused by buried basalt, and to a lesser extent by additional ground magnetic surveys. At present, the range of uncertainty in these interpretations and associated new information clearly exceeds uncertainties and information considered by the U.S. Department of Energy (DOE) during probability model development in 1995. An update to the DOE probability elicitation appears necessary for acceptable use in licensing.”

5.7.2 DOE Analysis

3358 The DOE has adopted the Plio-Pleistocene time period for extrapolation of events,
3359 consistent with the approach by the majority of members of the 1996 PVHA expert panel.
3360 Several members of that panel considered the Pleistocene to be the preferred time period for
3361 extrapolation BSC (2003a [p. 113]). “The result of the PVHA [Geomatrix Consultants, 1996] has
3362 been recalculated using PVHA outputs to account for the proposed LA repository footprint (the
3363 outline of the waste emplacement area) and extended to include the probability of an eruption
3364 within the proposed LA repository footprint, conditional on a dike intersection. A conceptual
3365 framework for the probability calculations, based on PVHA outputs and subsequent studies,
3366 accounts for deep (mantle) and shallow (structural control) processes that influence volcanic
3367 event distribution and recurrence rate in the YMR [Yucca Mountain region]. The framework
3368 presented here emphasizes the close correlation between the distribution of volcanic events
3369 and areas of crustal extension and faulting in the YMR, and within this context, the
3370 appropriateness of volcanic source zone boundaries defined in the PVHA. It also emphasizes
3371 the appropriate selection of parameter distributions that affect probability models and provides
3372 support for comparison of alternative scenarios and parameter selection, within the framework
3373 of the volcanic history of the YMR. Alternative models presented by Connor et al. (2000) that
3374 result in higher eruption probabilities (10^{-7} versus 1.3×10^{-8} per year) than those presented here
3375 are found to employ input parameters that either represent extreme values (e.g., event length)
3376 or assume a specific geologic control (i.e., crustal density) on spatial distribution while not
3377 considering more defensible and observable controls (i.e., crustal extension and structure).
3378 Spatial density models weighted by crustal density result in higher event frequencies at the
3379 proposed repository site, while the same models weighted by an alternative geologic control
3380 such as cumulative crustal extension across the Crater Flat structural domain would likely lead
3381 to decreased event frequencies at the site. Connor et al. (2000) state that the highest value (10^{-7}
3382 per year) in their range of calculated probability values (10^{-8} – 10^{-7} per year) cannot be
3383 considered more or less likely than any other value they have calculated using alternative
3384 probability models. The analysis in this report suggests that the choice of input parameters used
3385 by Connor et al. (2000) compared to those used in the PVHA logically places their highest
3386 probability value at the extreme upper tail of a probability distribution”.

3387 DOE (2003 [p. 2-9]) states that: “In summary, the areas of greatest likelihood for future
3388 volcanic activity in the region are those where previous volcanism has occurred, and where
3389 extensional deformation has been and continues to be greatest, (i.e., the southwestern part of
3390 the Crater Flat structural domain) (Figure 2-5) (Geomatrix Consultants, 1996, pp. RC-5, BC-12,
3391 AM-5, MS-2, GT-2, and expert zone maps). Analysis by the U.S. Nuclear Regulatory
3392 Commission (NRC) also indicates that the highest likelihood of future volcanic activity is in
3393 southwestern Crater Flat (Reamer, 1999 [Sections 4.1.5.4 and 4.1.6.3.3; Figure 28]). The
3394 southern and southwestern part of the Crater Flat basin is the most extended (Ferrill et al.,
3395 1996; Stamatakos et al., 1997; Fridrich et al., 1999) and is the locus of post-Miocene volcanism
3396 (Fridrich et al. 1999; Reamer 1999). Therefore, the volcanic source zones defined in the PVHA
3397 (Geomatrix Consultants, 1996 [Figure 2-5]) are consistent with the tectonic history and structural
3398 features of the Crater Flat structural domain.”

3399

3400

3401

5.7.3 Probabilistic Volcanic Hazard Analysis (PVHA)

3402

3403

3404

3405

3406

The Probabilistic Volcanic Hazard Analysis (Geomatrix Consultants, 1996 [p. 4-14]):
“The results of the PVHA analysis are that the aggregate expected annual frequency of
intersection of the repository footprint by a volcanic event is 1.5×10^{-8} , with a 90-percent
confidence interval of 5.4×10^{-10} /yr to 4.9×10^{-8} . The major contributions to the uncertainty in

3407 the frequency of intersection are the statistical uncertainty in estimating the rate of volcanic
3408 events from small data sets and the uncertainty in modeling the spatial distribution of future
3409 events. Although there are significant differences between the interpretations of the 10 experts,
3410 most of the uncertainty in the computed frequency of intersection is due to the average
3411 uncertainty that an individual expert expressed in developing the appropriate PVHA model.”
3412

3413 **5.7.4 DOE Igneous Consequence Peer Review Panel (ICPR)** 3414

3415 The ICPR panel did not evaluate the probability of future volcanism at Yucca Mountain.
3416 They did provide conclusions and recommendations that relate to evaluating probability.
3417

3418 Detournay et al. (2003): [p. 19-20]: “There are ten known unburied eruptive vents in the
3419 Yucca Mountain region younger than 5 Ma, and seven buried volcanoes were identified in
3420 aeromagnetic surveys up to 1995. This gives a sum of 17 volcanic events over the past 5 Ma,
3421 assuming, for illustrative purposes, each anomaly represents an independent volcanic event. If
3422 the magnetic anomalies recently identified (Blakely et al., 2000; O’Leary et al., 2002) represent
3423 buried basalt flows or tephra deposits that are less than 5-M-yr old, then the total number of
3424 post-Miocene vents is ~30, roughly double previous estimates. If all of the most recently
3425 identified aeromagnetic anomalies are relatively young (e.g., ~ 0.5 Ma to 1 Ma) with eruptive
3426 volumes ~ 0.05 km³, then eruption probabilities would increase significantly. Alternatively, if the
3427 buried volcanics are at the opposite end of the age spectrum (e.g., 2 Ma to 4 Ma), the
3428 probability picture changes — although not dramatically, provided volumes associated with
3429 individual anomalies are ~ 0.05 km³ or less. Finally, if all buried volcanics (magnetic anomalies)
3430 are pre-Pliocene, eruption probabilities change little. A preliminary conclusion is that until better
3431 information regarding the number, volume and the age distribution of buried basaltic lavas and
3432 tephra is available, it will be difficult to know how to adjust estimates of volcanism rate and
3433 recurrence interval most relevant to disruptive igneous activity at the proposed YMR. One of the
3434 recommendations of this Panel is that further attempts be made to define the ages and volumes
3435 of the buried magnetic anomalies.”
3436

3437 [p. 20]: “High-precision geochronological information would enable better estimates of
3438 volcanic recurrence rates at Crater Flat relevant to igneous consequences at the proposed YMR
3439 at relatively modest cost. This issue could be clarified, or at least significantly better constrained,
3440 by an intensive high-resolution geochronological program.”
3441

3442 [p. 76]: “As far as the range of quantitative characteristics of the igneous event
3443 considered is concerned, we have reviewed all the literature available and conclude that the
3444 approach adopted so far — namely, that the analog evidence from recent (< 5 Ma) igneous
3445 events that have occurred close to [Yucca Mountain] (Crater Flats, Lathrop Wells) be given
3446 more weight than earlier events or those further afield — is entirely reasonable. We recommend
3447 that further high-resolution geochronological work be performed to better constrain the ages of
3448 exposed Pliocene and Quaternary basalts in Crater Flat as well as possible basaltic volcanic
3449 rocks identified by aeromagnetic studies.”
3450

3451 [p. 77]: “The probability that a violent erupting mixture could follow dog-leg conduits,
3452 thus potentially entraining a larger number of canisters, is, in our opinion, small and is more than
3453 offset by the level of conservatism built into the existing estimates ... The Panel has not been
3454 able to quantify the probability of a dog-leg conduit in any rigorous fashion, nor its effect on
3455 canisters. The opinion expressed ... above was arrived at by combining our separate
3456 independent views of where the upper limits would lie.”

3457
3458 **5.7.5 Electric Power Research Institute**
3459

3460 (EPRI, 2005 [p. vii]): “There is evidence of volcanic centers near the proposed site at
3461 Yucca Mountain, Nevada for a geologic repository for the disposal of spent nuclear fuel (SNF)
3462 and high-level radioactive waste (HLW). This evidence indicates that potential future igneous
3463 activity (i.e., an “igneous event scenario”) may be a factor in the assessment of post-closure risk
3464 for the proposed repository. In 1996, a panel of independent technical experts for the Yucca
3465 Mountain Project’s Management and Operations (M&O) contractor conducted a study, the
3466 Probabilistic Volcanic Hazards Analysis (PVHA) study, that estimated a mean annual probability
3467 of an igneous event occurring at/near the Yucca Mountain site at 1.6×10^{-8} /year [Geomatrix
3468 Consultants, 1996]. This probability, though extremely low, fell just above the 1.0×10^{-8} /year
3469 regulatory threshold that had been established for the dismissal of extremely low probability
3470 events.”

3471
3472 [p. viii to ix]: “The objectives of this report, which is a companion to EPRI (2004a), are to
3473 analyze the intrusive-release case and determine the potential impact on repository
3474 performance and safety, expressed as probability weighted mean annual dose rate, for the latter
3475 scenario. EPRI’s analyses contained in this report adopt the igneous event probability of $1.6 \times$
3476 10^{-8} /year previously derived by the Probabilistic Volcanic Hazards Analysis (PVHA) panel
3477 [Geomatrix Consultants, 1996]. The analyses also reflect recent data on basaltic eruptive
3478 centers in the Yucca Mountain region that support the conclusion that relatively low-temperature
3479 ($\sim 1010^{\circ}\text{C}$), high viscosity basaltic magmas, as opposed to the $\sim 1200^{\circ}\text{C}$ magmas postulated by
3480 the DOE, are the most representative characteristics of future igneous events. Lower
3481 temperature implies lower and less prolonged thermal-perturbation of the host rock and
3482 contacted waste packages, and magma of much higher viscosity. The high viscosity supports
3483 the contention that such magma will only partially penetrate into emplacement drifts intersected
3484 by the magmatic dike, thereby only impacting a limited number of waste packages.”

3485
3486 **5.7.6 State of Nevada and Consultants**
3487

3488 Ho et al. (1991 [p. 56]): “At this preliminary stage of our work, all we can conclude is that
3489 the probabilistic results of Crowe et al. (1982) are based on idealized model assumptions, a
3490 premature data base, and inadequate estimates of the required parameters. For the reasons
3491 discussed, we think that Crowe et al. underestimate the risk of volcanism at the proposed Yucca
3492 Mountain repository site.”

3493
3494 Ho and Smith (1998 [p. 508]): “The instantaneous temporal recurrence rate (at present
3495 time) estimated from a PLP [power-law process] is about 5.9×10^{-6} /year. Thus, the combined
3496 temporal-spatial recurrence rate calculated for the 3-D NHPP [non-homogeneous Poisson
3497 process] is between 1.36×10^{-9} and 3.54×10^{-9} /(year \times km²). The recurrence rate obtained
3498 based on a 3-D HPP [homogeneous Poisson process] ($= 1.88 \times 10^{-9}$) is in this interval. For this
3499 study, the estimated overall probability of at least one disruption of a repository at the Yucca
3500 Mountain site by basaltic volcanism for the next 10,000 years (= hazard) is: 1.5×10^{-4} for a 3-D
3501 HPP; 1.09×10^{-4} to 2.83×10^{-4} for a 3-D NHPP if λ_s [recurrence rate] is estimated as 2.3×10^{-4}
3502 to 6.0×10^{-4} ; and 3.14×10^{-3} for a Bayesian approach. We also note that the hazard based on
3503 an HPP and an NHPP are very comparable as long as the area of the sample region A (was
3504 estimated as 1953 km² for the 3-D HPP) is bounded between 1035 km² and 2701 km².”

3505
3506 Smith et al. (2002 [p. 9]): “A knowledge of recurrence rates is crucial to the calculation
3507 of probability of magmatic disruption. We contend that there is more uncertainty in recurrence

3508 rate estimates than assumed by the DOE, the expert panel, and the NRC. Our petrologic data
3509 suggest that volcanic fields in the Crater Flat–Lunar Crater zone are linked to a common area of
3510 hot mantle. Also, we show that volcanism is episodic with a good possibility of a new peak of
3511 activity occurring in the future. These observations imply that volcanism is not dead in the Yucca
3512 Mountain area and that a future pulse of activity could have recurrence rates equivalent to those
3513 recorded in the Lunar Crater–Reveille area of the Crater Flat–Lunar Crater zone. Specifically,
3514 the DOE and the NRC have used recurrence rates of from 3.7 to 12 events per m.y. to calculate
3515 probability of volcanic disruption (Connor and Hill, 1995; Crowe et al., 1998; Connor et al.,
3516 2000). Based on our arguments, recurrence rates of 11 to >15 events per m.y. are possible.
3517 Because higher recurrence rates raise the likelihood of magmatic disruption of the repository,
3518 we recommend that future probability studies factor these higher rates into probability models.”
3519

3520 Smith and Keenan (2005) [p. 317-321]: “Perry et al. [2004] speculated that the 20
3521 additional volcanic centers discovered by the aeromagnetic surveys would raise the probability
3522 of site disruption by about 40%. This number is a minimum figure because the surveys do not
3523 cover the entire area.

3524 Volcanic recurrence rates for the RLC [Reveille–Lunar Crater] are as high as 12 events
3525 per million years, four times the rate calculated for the Yucca Mountain area. These figures are
3526 minimum estimates because only 70% of the volcanic centers in the RLC are dated.

3527 A linkage between Yucca Mountain and RLC implies that higher recurrence rates may
3528 occur in the Yucca Mountain area. Adding data from future surveys of uncovered areas and
3529 higher recurrence rates may result in a probability of disruption 1–2 orders of magnitude greater
3530 than the EPA standard. A longer health standard, as ordered by the U.S. Court of Appeals,
3531 makes a disruptive event during the period of compliance even more likely.” [In this article by
3532 Smith and Keenan (2005) they imply that using higher recurrence rates and adding data from
3533 future aeromagnetic surveys may result in a probability of disruption up to 10^{-6} /yr.]
3534

3535 **5.7.7 Nuclear Energy Institute (NEI)**

3536 The Nuclear Energy Institute issued a policy statement (NEI, 2006) titled “Common
3537 Objections to the Yucca Mountain Project, and What the Science Really Says.” This policy
3538 statement gave frequently cited objections to the Yucca Mountain project and the NEI response
3539 based on scientific analysis. For volcanoes (igneous activity), the cited concern is that “A
3540 volcano could erupt through the repository.”

3541 The NEI position is:

- 3542 • A volcanic eruption that affects the repository is a highly improbable event.
- 3543 • There has not been a single volcanic eruption through Yucca Mountain in 10 million
3544 years.
- 3545 • Millions of years of history show that the region surrounding Yucca Mountain is
3546 becoming less volcanically active with time.
- 3547 • Nevertheless, NRC is requiring that DOE analyze the consequences of such an event
3548 and include this analysis in the repository performance assessment.
- 3549 • Volcano itself likely to cause more harm than any radiation it might release.

3550 **5.7.8 Other Estimates of Probability**

3551
3552

3553 Crowe et al. (1982 [p. 185]). “The calculated probabilities of volcanic disruption of a high-
3554 level radioactive waste repository buried within the Yucca Mountain site of the NTS area are
3555 exceedingly small (range calculated for a one year time period of 10^{-8} to 10^{-10}). These values
3556 provide a numerical expression of the low past rates of volcanism in the region. However, there
3557 are several precautions that must accompany the calculations: First, they assume that
3558 volcanism is a random process although geologic studies on a global scale have shown that
3559 volcanism is commonly nonrandom in both space and time. We have attempted to compensate
3560 for this shortcoming by restricting the calculation parameters to a defined volcanic province and
3561 by developing a method for determining the area ratio (a/A) based on the distribution of volcanic
3562 centers. Second, calculated rates of volcanic activity (λ) are averaged over a time scale of
3563 millions of years. They are therefore relatively insensitive to short-term variations in rates of
3564 volcanism. Such short-term variations may be less than or on the order of the required
3565 containment period of waste elements. Third, the calculated rates of volcanism are based on
3566 the past record of volcanism and not on a complete understanding of the future controlling
3567 processes of magma generation. They were calculated from a limited number of data points
3568 and are projected into the future assuming future rates will be the same as in the past. Some
3569 degree of confidence can be placed in this projection however due to the relatively uniform rate
3570 of volcanic activity in the NTS region for the last 6 to 8 m.y.”
3571

3572 Wernicke et al. (1998). “Abstract. Global Positioning System (GPS) surveys from
3573 1991 to 1997 near Yucca Mountain, Nevada, indicate west-northwest crustal elongation at a rate
3574 of 1.7 ± 0.3 millimeters per year (1σ) over 34 kilometers, or 50 ± 9 nanostrain per year. Global
3575 Positioning System and trilateration surveys from 1983 to 1997 on a 14-kilometer baseline
3576 across the proposed repository site for high-level radioactive waste indicate that the crust
3577 extended by 0.7 to 0.9 ± 0.2 millimeter per year (50 to 64 ± 14 nanostrain per year), depending
3578 on the coseismic effect of the M_s 5.4 1992 Little Skull Mountain earthquake. These strain rates
3579 are at least an order of magnitude higher than would be predicted from the Quaternary volcanic
3580 and tectonic history of the area.”

3581 “We suggest that the apparent inconsistency between the observed contemporary
3582 [strain] rates and the geologic history is because the Yucca Mountain area is experiencing an
3583 epoch of anomalously rapid strain accumulation. The integrated strain across the Basin and
3584 Range (length scale of ~ 1000 km) may be continuous at the million-year time scale, but local
3585 magmatic and tectonic events within the province (length scale of ~ 100 km) may be strongly
3586 clustered in both space and time, and have recurrence times or repose intervals of a few
3587 thousand to hundreds of thousands of years [for example, Fleck et al., 1996; Wallace, 1987]. If
3588 the contemporary strain rate in the Yucca Mountain area is any indication, elastic strain
3589 accumulation related to these events may also be strongly episodic. An event of duration
3590 100,000 years occurring every million years would accord well with the overall tectonic and
3591 volcanic history. If so, hazard analyses based on the local record of magmatic and tectonic
3592 events alone would underestimate the probability of such events occurring in the near future at
3593 Yucca Mountain by an order of magnitude. For example, the anomalous strain could reflect the
3594 development of a second line of north-northeast aligned, low-volume eruptive centers,
3595 analogous to the cluster of events near 1.0 Ma on Crater flat, with the eruption of the Lathrop
3596 Wells cone representing the onset of a cluster that would continue over the next few tens of
3597 thousands of years (Smith et al., 1990).”
3598

3599 Savage (1998) [p. 1007b]. The claim of anomalous strain reported by Wernicke et al.
3600 (1998) was countered by Savage (1998) who reported a $N65^\circ W$ strain rate of 8 ± 20 nanostrain
3601 yr^{-1} . He concluded that Wernicke et al. (1998) had not included monument instability in their
3602 error budget and did not give proper weight to the effects of the 1992 Little Skull Mountain
3603 earthquake. Later work by Savage et al. (2001) continued to find that the principal extension

3604 rate averaged over their 50-km geodetic array is substantially less than reported by Wernicke et
3605 al. (1998) and is consistent with the low extension rate inferred from the geologic record.
3606 Likewise, Connor et al. (1998) noted that the lack of a known volcano younger than the Lathrop
3607 Wells event diminished the argument that volcanic recurrence rates have been underestimated
3608 by an order of magnitude. Therefore, present-day strain rates do not support an order of
3609 magnitude increase in hazard from tectonic or magmatic events.

3610
3611 Coleman et al. (2004) [p. 3]. The results show that a dike intersection rate of 10^{-6} /yr (one
3612 expected per million years) is unrealistically high. “If this rate prevailed in the last million yrs, an
3613 expected 40 to 96 volcanoes would have erupted in the YMR (or 80–192 without gravity
3614 weighting). This far exceeds the 8 events known to have occurred in all of the Pleistocene (1.8
3615 Myr), yielding a recurrence rate of only 4.4 per million years. Dividing these numbers by 10
3616 reduces the time scale to 100,000 years. This time scale is especially interesting because we
3617 can test whether the youngest-known volcanic event in the region, Lathrop Wells, began a new
3618 pulse of volcanism, as suggested by Wernicke et al. (1998). For a dike penetration rate of 10^{-6}
3619 /yr, the PVHA results indicate 4–10 (8–19 without gravity weighting) volcanic events would
3620 have been expected in the YMR in the last 100,000 yrs. Only one is known. We conclude that
3621 claims of high intrusion frequency fail tests of volcanic recurrence in the YMR at time scales of
3622 10^6 and 10^5 yrs.”

3623 “We consider that spatial and temporal patterns of Pleistocene volcanism provide the
3624 best available representation of trends in recent geologic time... If future volcanism follows this
3625 pattern, the expected frequency of dike intersection is 5.4×10^{-8} /yr using the PVHA_YM code
3626 with zero gravity weighting, file “Quaternary_8events,” and a recurrence rate of 4.4×10^{-6} /yr (8
3627 events in 1.8 Myr). Considering the statistical uncertainty of the frequency based on eight
3628 events, a 95% upper confidence bound for the intersection frequency is 9.8×10^{-8} /yr [Pearson
3629 and Hartley, 1970]. The recurrence rate would be even smaller if some of the Pleistocene
3630 events in Crater Flat represent fewer events.”

3631 “We agree with Connor et al. [2000] that rates of basaltic volcanism at Yucca Mtn. (i.e.,
3632 ~2–12 events/Myr) have not been comparable to recurrence rates in more active zones, such
3633 as the Cima volcanic field, CA (i.e., ~30 events/Myr). Our analysis raises doubts about claims
3634 that a potential repository could be penetrated by a basaltic dike with a frequency as high as 10^{-6}
3635 /yr (on average, one per million years). Such claims fail simple tests at four time scales.
3636 Furthermore, spatial-temporal models that predict future penetration frequencies $>2 \times 10^{-7}$ /yr are
3637 overly pessimistic, based on nondetection of dikes in the potential repository footprint.”

3638
3639 OECD [Organisation for Economic Co-operation and Development] (2002) [p. 15]. Joint
3640 report by the NEA and the IAEA: “3.3 Disruptive events and human intrusion Disruptive events
3641 – Volcanism at Yucca Mountain is a very low probability event. With regard to volcanism, more
3642 explosive rhyolitic eruptions can occur at the same time as basaltic eruptions (so-called
3643 “bimodal volcanism”). That was not discussed in the TSPA-SR. It is recommended that the
3644 probability of bimodal basaltic-rhyolitic volcanism should be estimated and, if relevant, the
3645 consequences should be analyzed. The IRT considers that the TSPA-SR adequately addresses
3646 seismological influences and finds the analysis in line with other international studies.”

3647 3648 **5.7.9 ACNW Observations of PVHA-U**

3649
3650 The panelists participating in PVHA-U are incorporating new information available since
3651 1996 in their estimates, including possible effects of lithostatic pressure variations that may
3652 favor basins as sites for future eruptions. Based on our observations of PVHA-U proceedings,
3653 most panelists appear to be placing greater emphasis on Pleistocene events rather than on
3654 older events. Eruption cycles are being discussed, and fewer hidden events are now being

3655 considered based on the results of drilling of anomalies. There remains considerable challenge
3656 in applying spatial and temporal models to a region where volcanism is so infrequent.

3657 3658 **5.8 Summary** 3659

3660 The volume of basaltic volcanism near Yucca Mountain has dramatically declined during
3661 the last 10 Myr such that the Crater Flat volcanic field represents a zone of low activity
3662 compared to other volcanic fields in the region (e.g., Cima, CA and Springerville, AZ). This
3663 decline suggests that magmatic systems near Yucca Mountain are waning. Further evidence of
3664 this lies in the declining maximum lava effusion rate and fissure length of Plio-Pleistocene
3665 basaltic activity in the Yucca Mountain region. There are no precursory indicators that volcanic
3666 activity is likely in the immediate future in the region.

3667
3668 Results of recent drilling on magnetic anomalies following completion of the 2004
3669 aeromagnetic survey have not yet been incorporated into published estimates of the probability
3670 of igneous activity intersection of the proposed repository. However, the information from the
3671 drilling should reduce some of the uncertainty about buried basalts in the region and may
3672 influence the statistical-mathematical models used in determining probability by lowering the
3673 likelihood of future repository intersection by volcanism.

3674
3675 Both DOE and EPRI rely on probability estimates from the 1996 PVHA expert elicitation
3676 (i.e., $\sim 2 \times 10^{-8}/\text{yr}$). This PVHA is now being updated with new information but published results
3677 will not be available until 2008. In response to NRC staff concerns, DOE has agreed to provide
3678 (along with their licensing case) the results of a single point sensitivity analysis for extrusive and
3679 intrusive igneous processes at an annual probability of $10^{-7}/\text{yr}$. The NRC considers that the $10^{-7}/\text{yr}$
3680 analyses will provide a reasonably conservative approach for evaluating risks from igneous
3681 activity, but use of a single point value fails to capture the impact of the uncertainty in probability
3682 estimates inherent to a risk-informed analysis. The State of Nevada and consultants suggest
3683 that the probability of future volcanism may be at least an order of magnitude higher based on
3684 temporal clustering of volcanic activity, hypothetical linkages between volcanism at Crater Flat
3685 and the Lunar Crater-Reveille Range area, and incorporation of new data that they recommend
3686 be acquired in regions beyond the latest aeromagnetic survey.

3687
3688 A probability range for repository disruption of $10^{-9}/\text{yr}$ to $10^{-7}/\text{yr}$ is consistent with most
3689 previous studies (see Figure 5.11), the observed rate of Pleistocene volcanic activity (6 events
3690 in Crater Flat and the northern Amargosa Desert in 1.75 Myr), and the latest drilling results
3691 which reduce the number of suspected buried basalts of post-Miocene age. It is significant that
3692 no post-Miocene basalt was found in drilling magnetic anomalies in Jackass Flats. If buried
3693 Pliocene basalts had been found there, that would suggest that the Plio-Pleistocene volcanic
3694 zone of Crater Flat extends through Yucca Mountain significantly affecting the spatial models of
3695 volcanism and increasing the modeled probability of future repository intersection.

3696
3697 The rocks that comprise Yucca Mountain record an integrated tectonic-volcanic history
3698 since the ~ 13 Ma old surface rocks were deposited. No basaltic dikes have been found in the
3699 potential repository footprint at Yucca Mountain despite more than 20 years of intensive site
3700 characterization studies. It appears that the fault-bounded block that forms Yucca Mountain has
3701 been a zone of relative volcanic quiescence during the last 10 Myr. Since that time volcanism
3702 has instead mainly focused within the alluvial basins to the east, west, and south, with no
3703 evidence of post-Miocene activity (younger than ~ 5 Ma) east of Yucca Mountain in Jackass
3704 Flats.

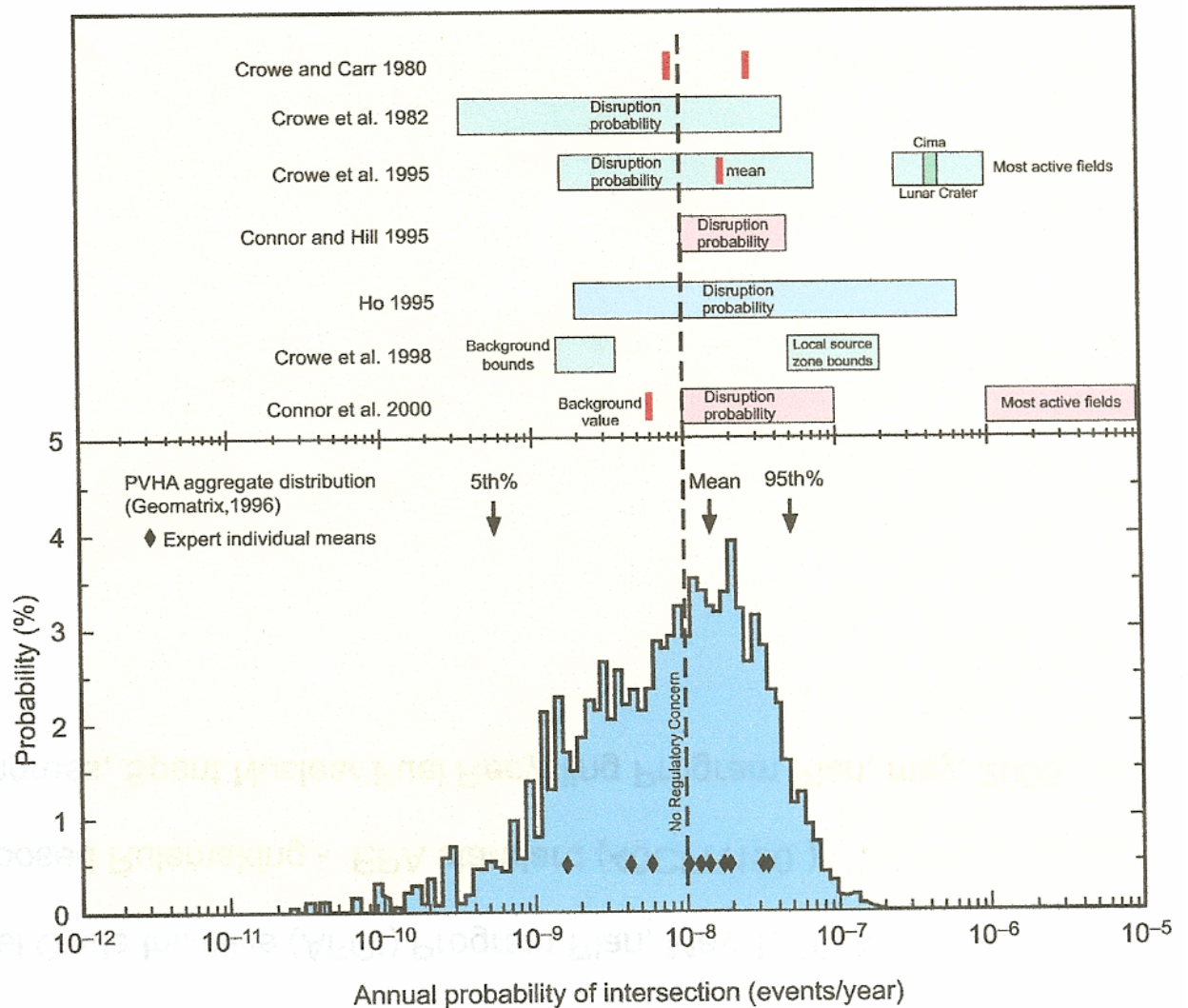


Figure 5.11. Comparison of selected estimates of the probability of future volcanic intersection of a repository at Yucca Mountain (from Perry et al., 2000).

6. Consequences of Igneous Activity Intersecting Repository

6.1. Introduction

The final question of the risk triplet, If the repository is intersected, what are the consequences of the igneous activity to the repository, to the stored HLW, and the impact of its potential release to the environment upon humans?, is the subject of this chapter. The consequences for future radiological exposures vary significantly among the hypothetical scenarios for volcanic interaction with the repository (described in Sections 3 and 6). They include an intrusive event, an extrusive (volcanic) event, and secondary breakouts of magma from a repository at some distance from the point of initial intersection ("dogleg" scenario). The logic flow charts, Figures 1.2c and d, show the components that enter into consideration of these scenarios. The dogleg scenario is a variation of the intrusion scenario. As noted, the potentially critical effects of quenching and solidification on waste packages and drift walls have

3726 yet to be evaluated by the DOE and NRC, but they do have the potential to limit the distance
3727 that magma can penetrate into drifts, making the “dogleg” scenario much less likely to occur
3728 than the other scenarios.

3730 **6.2. Effects from an Intrusive Event (Magma/Drift Interaction)**

3731
3732 Many quantitative studies have been published on the basaltic magma involved in igneous
3733 activity at Yucca Mountain. Some of the reports most pertinent to the present analysis of
3734 magma invading a repository drift are discussed here.

3736 **6.2.1 Critical Magmatic Aspects**

3737
3738 To evaluate the impact of a basaltic dike intersecting the proposed repository, the type,
3739 approximate composition, volatile content, and viscosity of the magma must be known or
3740 estimated.

3742 **6.2.1.1 Magma Composition**

3743
3744 The composition of the magma likely to erupt at Yucca Mountain is best estimated from
3745 nearby eruptive examples that have occurred in this region over the past 10 Myr. Each
3746 interested party has used this approach in specifying future magma, and assumed that the most
3747 likely magma will be alkali basalt. For example, decisions made with regard to the magma type
3748 and composition state:

3749
3750 “The base case chemical composition of basalt.....was derived.... through analysis
3751 of 45 samples taken from the Lathrop Wells Cone. The Lathrop Wells Cone is the
3752 youngest volcanic center in the Yucca Mountain region, and, therefore is considered an
3753 adequate analog for the composition of a possible igneous intrusion into Yucca Mountain.”
3754 (BSC, 2004, [p.4-6])

3755
3756 “Magmas in the Yucca Mountain region are typically alkali basalts.” (EPRI, 2003 [p. 2-9])

3757
3758 On the subject of magma volatile content, all parties have used petrologic indicators in
3759 the erupted nearest lavas (e.g., Lathrop Wells) to estimate indirectly the pre-eruptive volatile
3760 content of the magma. The presence of the mineral phase amphibole indicates a magma
3761 temperature at or below about 1050°C that, coupled with an overall low phenocryst content,
3762 suggests the magma was near its liquidus temperature. Magma water content had to have been
3763 in the range of 1-3 wt% for basaltic magma to have such a low liquidus temperature. Hence, the
3764 following assessments are made:

3765
3766 “No magmatic water has a zero probability of occurrence. This statement reflects our
3767 knowledge that very low volatile contents are rare. With 1 to 3 percent magmatic water, the
3768 probability should be uniform, reflecting that this is the most likely range of water contents.
3769 The probability should decrease linearly between 3 and 4 wt%, so that it is zero at 4 wt%,
3770 representing the expectation that at about 4 wt%, basaltic magmas will crystallize before
3771 reaching the surface to erupt.” (DOE, 2000 [p. 54])

3772
3773 “H₂O concentrations in the range 2.5 wt to 4 wt% with bulk mass H₂O/CO₂ ratios around 6-
3774 20 are representative.” (Detournay et al., 2003 [p.16])
3775

3776 “These basalts may have water contents of 0-4 weight% and a wide range of thermo-
3777 mechanical properties that reflect the water content and bubble (void) fraction.” (EPRI, 2003
3778 [p. 2-9]).
3779

3780 The context of the last quote from EPRI is that the magma involved may be taken for a
3781 range of processes to contain the stated amounts of water. That is, the original magma may
3782 contain 4 wt% water, but upon degassing it may as a lava, for example, contain far less water.
3783

3784 It is also important to note that, besides water, basaltic magmas typically contain
3785 significant amounts of CO₂ and SO₂ and lesser amounts of F and Cl. There are no reliable
3786 straightforward methods to estimate the pre-eruption concentrations of these volatile species,
3787 although enough is known about CO₂ in basalt to know that the ratio of H₂O to CO₂ is commonly
3788 in the range of about 6 to 20. Nicholis and Rutherford (2004) have corroborated the range of
3789 estimates of water content with additional experimental studies on samples of Lathrop Wells
3790 lava involving phase equilibria.
3791

3792 In summary, the type of magma likely to erupt in the future at Yucca Mountain, its
3793 chemical composition, and its volatile content are agreed upon. Of these three features, the
3794 exact basalt type and chemical composition is not of great importance, but the volatile content is
3795 important to know well for several reasons from characterizing the style of the eruption to
3796 gauging the rheology of the lava that may enter the repository drifts.
3797

3798 **6.2.1.2 Magma Viscosity**

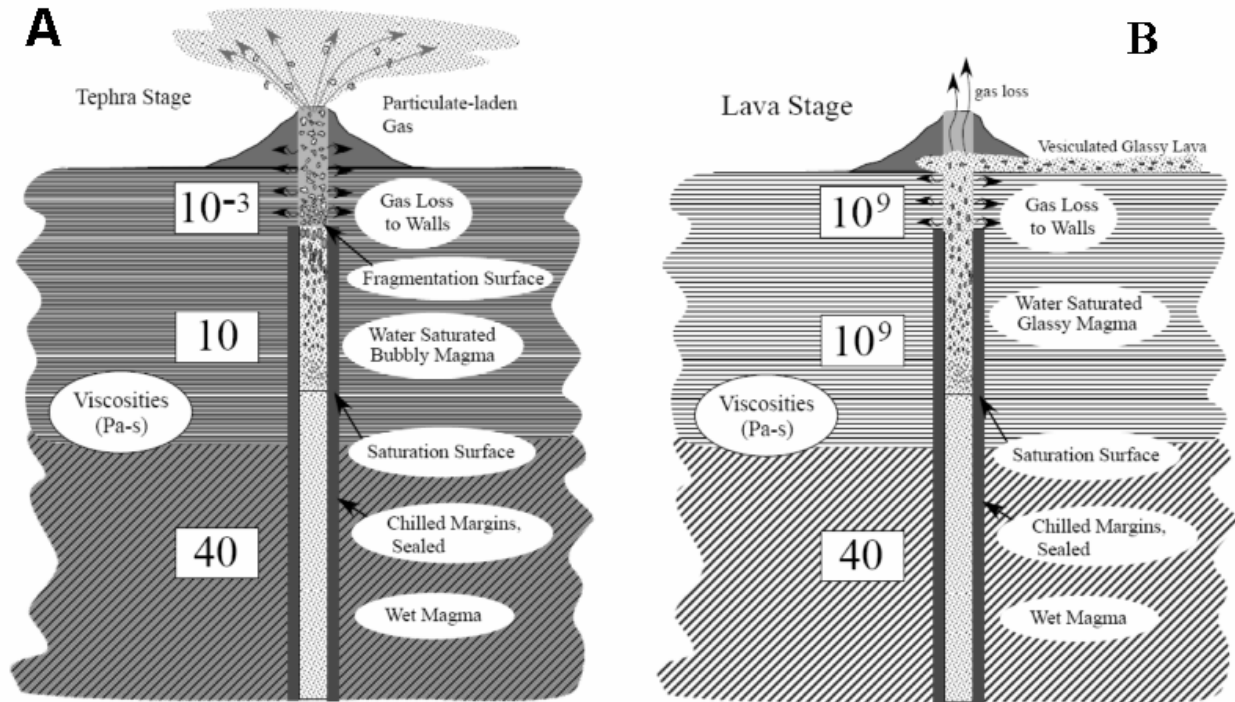
3799

3800 In the present context, there is no other magma property more important to know with
3801 certainty than viscosity. To be clear, this is the usual viscosity characterizing viscous shear
3802 flows and is sometimes denoted as the shear viscosity or Newtonian viscosity as opposed to the
3803 bulk viscosity, which is associated with volumetric expansion of fluids as in the work associated
3804 with adiabatic expansion.
3805

3806 There is no single value of viscosity that can be used to characterize the probable entire
3807 magmatic process at Yucca Mountain. There are at least four distinct phases of the magma,
3808 each of which will have a characteristic viscosity. At depths greater than about 6 km the
3809 anticipated magma will be a single fluid phase with a viscosity of about 50 poise (5 Pa s, see
3810 below). As the magma ascends bubbles will form and this magma will be described by a
3811 second viscosity. With continued ascent the bubble or gas phase becomes dominant with
3812 dispersed fragments of quenched magma, which is characterized by a third viscosity (see
3813 Figure 6.1A). If the magma degasses and extrudes as lava, this lava will be characterized by a
3814 fourth viscosity (see Figure 6.1B). In addition, within each of these phases temperature and
3815 crystallinity, particle content, or bubble content will have an effect.
3816

3817 The approach of all parties has been to estimate viscosity from the bulk chemical
3818 composition of the given basaltic magma at its liquidus temperature and the estimated amount
3819 of water. The most important factors governing magma viscosity are chemical composition
3820 (especially silica content), temperature, water content, and crystal content. Water and
3821 crystallinity have strong effects on viscosity. Water lowers viscosity and crystals increase
3822 viscosity. Bubbles can raise or lower viscosity depending mainly on their size. The effects of
3823 other volatile species are mixed and, at the concentrations expected, not likely to be major
3824 factors in deciding viscosity. The effect of crystals has generally been ignored in the Yucca
3825 Mountain studies primarily because the associated lavas at, for example, Lathrop Wells contain
3826 only ‘sparse’ amounts of phenocrysts, which are relatively large (~ 1 mm) conspicuous crystals

3827 that grew at depth long before eruption. Phenocrysts in contrast to groundmass crystals are
 3828 very small and grow in response to the sudden cooling or quenching attending various aspects
 3829 of eruption.
 3830

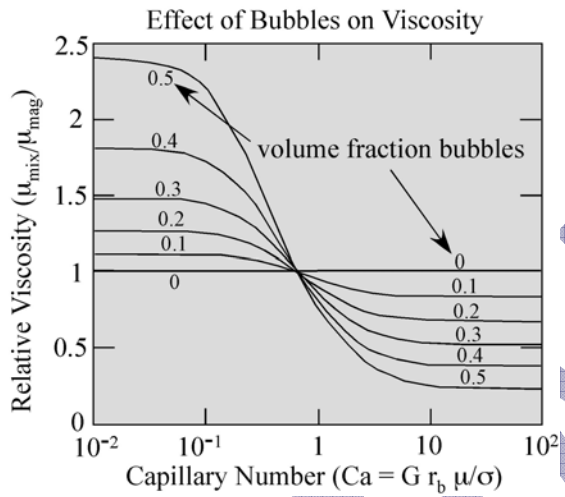


3831 **Figure 6.1** Schematic depiction of two stages of Cinder Cone volcanism and the underlying
 3832 magmatic eruptive column. Magma rich in dissolved volatiles saturates and vesiculates with
 3833 approach to Earth's surface and reduction in confining pressure. In essence the magma gets
 3834 the 'Bends.' Increased bubble formation eventually leads to fragmentation of the magma and
 3835 the explosive production of tephra and ash. Also shown for each stage are the governing
 3836 magma viscosities (left column) as estimated for each stage of the eruptive process. Notice the
 3837 large contrast in viscosity between the gas rich tephra and the late stage lava flows. (A) The
 3838 early stage of Cinder Cone formation and eruption, schematically depicting explosive tephra and
 3839 ash production leading to formation of the volcanic cone and an ash plume. (B) The later stage
 3840 of Cinder Cone eruption where the ascending magma has progressively degassed with
 3841 approach to the surface and the eruption is dominated by the extrusion of highly viscous,
 3842 sluggishly moving lava flows emanating from the basal area of the cone.
 3843

3844
 3845 The paucity of phenocrysts found in the lavas of the nearby basaltic magmas suggests
 3846 the pre-eruptive state of these magmas was at a temperature near the liquidus (~1000°C) and
 3847 the magma contained 2-4 wt% water. Given these conditions it is straightforward to estimate
 3848 viscosity using a number of reliable models. The viscosity of pre-eruptive magma is generally in
 3849 the neighborhood of 50 poise (5 Pa s), although there is significant disagreement. This issue
 3850 should be evaluated further.
 3851

3852 Detournay et al. (2003 [Appendix A2.6.1]) give a detailed discussion of magma rheology
 3853 at various stages in the eruption sequence, especially during the critical eruptive stages when
 3854 the magma is saturated with vapor and contains bubbles. In terms of rheology, the central issue
 3855 is the behavior of the bubbles and their size. Small bubbles act as rigid spheres and increase
 3856 viscosity, sometimes to the point of introducing non-Newtonian behavior. Large bubbles are

3857 deformable and act to, in effect, lubricate the magma, thus reducing viscosity. The quantitative
 3858 difference between small and large bubbles is measured by the *capillary number* (Ca), which is
 3859 a relative measure of the energy (i.e., work) of viscous shear relative to the interfacial surface
 3860 energy (σ) between vapor and magma. That is, viscous work is measured by the product of the
 3861 local shear or strain rate (G), a characteristic length scale, which is given by bubble radius (r_b),
 3862 and magma viscosity (μ). The capillary number is then given by $Ca = G r_b \mu / \sigma$. The effect of
 3863 bubble concentration as a function of Ca on the relative viscosity of the magma is given by
 3864 Figure 6.2 Relative viscosity (μ_r) is the ratio of the viscosity of the mixture of melt and bubbles
 3865 (often called the pseudofluid) relative to the viscosity of the melt itself (i.e., melt free of bubbles).
 3866
 3867



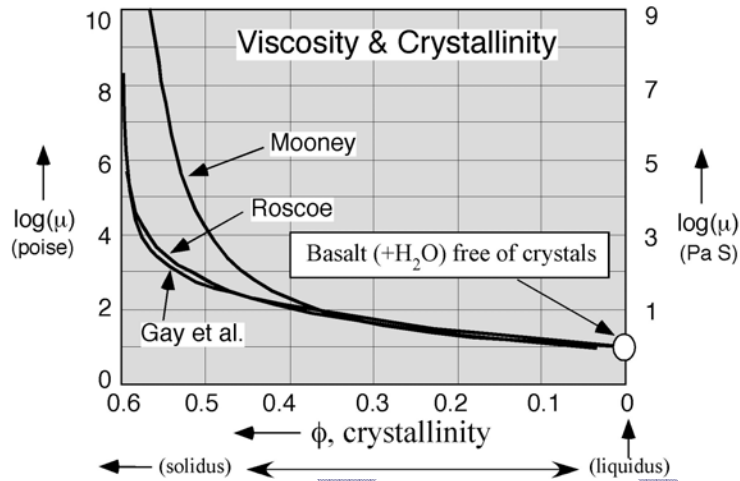
3868
 3869 Figure 6.2 Relative viscosity as a function of capillary number.
 3870

3871 The important result is that overall effect of capillary number on viscosity is relatively
 3872 small. For small Ca (i.e., $Ca < 1$) the bubbles are ‘hard’ spheres and viscosity is increased by at
 3873 most a factor of about 2.5 for a volume fraction of 0.5. At the other extreme for large Ca (i.e., Ca
 3874 $\gg 1$), where the bubbles are easily deformable by the shear flow, viscosity is reduced by a
 3875 factor of about four. This results because the high viscosity fluid (i.e., melt) still forms a
 3876 continuum, which essentially controls the rheology. This result, however, also depends on the
 3877 bubble size distribution, which controls packing and, ultimately, the bubble concentration at the
 3878 point of melt continuum breakdown and, eventually, the process of melt fragmentation.
 3879

3880 In light of these results, in the regime where the magma contains bubbles, but is still a
 3881 continuum of melt (i.e., the bubble concentration is below about 50 vol.%) containing isolated
 3882 bubbles, the dominant viscosity is determined by the composition of the magma. The effects of
 3883 the bubbles themselves are not large. There is another effect, however, that has caused some
 3884 confusion in defining the dominant viscosity.
 3885

3886 Magma viscosity is not only highly sensitive to chemical composition, including the
 3887 amount of dissolved water, but also to the concentration of solids or crystals in suspension.
 3888 Crystal content increases systematically with cooling from the liquidus (0 vol% crystals) to the
 3889 solidus (100 vol%). As the concentration of crystals reaches maximum packing at ~ 50 vol%,
 3890 the crystals interlock and the viscosity increases essentially without limit to that of an
 3891 assemblage of solids. This effect is shown in Figure 6.3 where viscosity is measured against
 3892 crystal fraction (Φ). There are many formulations available to calculate this effect and several
 3893 are used here to show the range of estimates. The most critical factor in each calculation is the

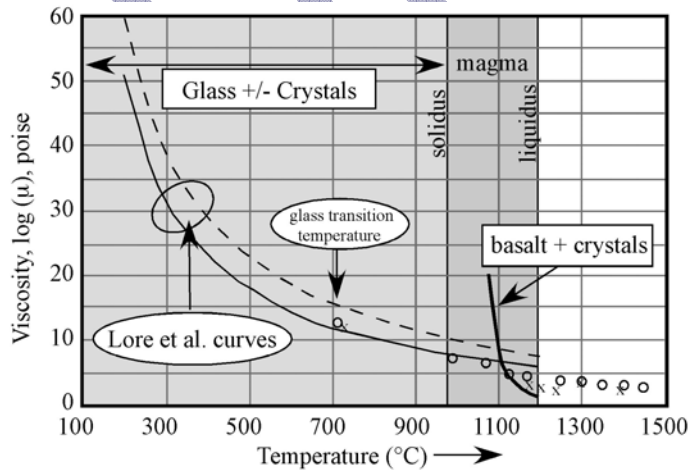
3894 point of maximum packing or critical crystallinity (Φ_c), which is well known for magmatic crystals
 3895 to be $\Phi_c \sim 0.55$ (i.e., 55 vol.%). When the magma contains water, bubbles will eventually appear
 3896 as crystallization proceeds and these will also affect the viscosity as noted above.
 3897



3898
 3899
 3900 Figure 6.3 Viscosity (μ) as a function of crystallinity (Φ). [After Mooney, 1951; Roscoe, 1952;
 3901 Gay et al., 1969]
 3902

3903 It is important to realize that this effect occurs relative to the liquidus and solidus, which
 3904 are, themselves, each highly sensitive to the water content of the magma. As water is added to
 3905 a magma, the liquidus and solidus are systematically (to a point) reduced in temperature. And,
 3906 because overall viscosity is a strong function of temperature (which includes the effect of crystal
 3907 buildup), it is essential when estimating magma viscosity to do so relative to the liquidus, at
 3908 whatever temperature it may be. Viscosity cannot be estimated from temperature alone.
 3909

3910 Lore et al. (2000) in studying the effect of cooling on fracturing of basalt lava from the
 3911 Snake River Plains presented a figure showing the viscosity of anhydrous basalt covering a
 3912 temperature range from 1500°C to 100°C. These results are shown in Figure 6.4 along with
 3913 other information that have been used by EPRI (2005) to estimate the viscosity of possible
 3914 Yucca Mountain magma.
 3915



3916
 3917
 3918 Figure 6.4 Magma phase diagram showing change in viscosity (μ) as a function of temperature.

3919 The approximate liquidus and solidus for a basalt of this type is indicated along with a
3920 curve, labeled basalt + crystals, showing the variation of viscosity for a magma of this
3921 composition undergoing crystallization as it solidifies. This variation is in accordance with the
3922 earlier results as presented above. Beginning at the liquidus, where the viscosity is about 100
3923 poise, the viscosity increases strongly midway through the crystallization interval as the crystal
3924 content approaches 50 vol.%. This is in contrast to the curves of Lore et al. that continue
3925 smoothly through the crystallization interval and only rise strongly below the glass transition
3926 temperature at about 700 °C, which is some 300°C below the solidus. The reason for this is that
3927 Lore et al. assume that the basalt does not crystallize but becomes a glass (solid curve)
3928 containing 20 vol.% crystals (dashed curve). Because they are interested in rapidly cooled lava
3929 this is an appropriate approximation at sub-solidus temperatures. Their curves are, however, not
3930 accurate near the liquidus nor within the melting range in general. And because this is an
3931 anhydrous (i.e., water –free) basalt, these results do not pertain to the possible Yucca Mountain
3932 magma at depth where it is expected to contain 2-4 wt% water.

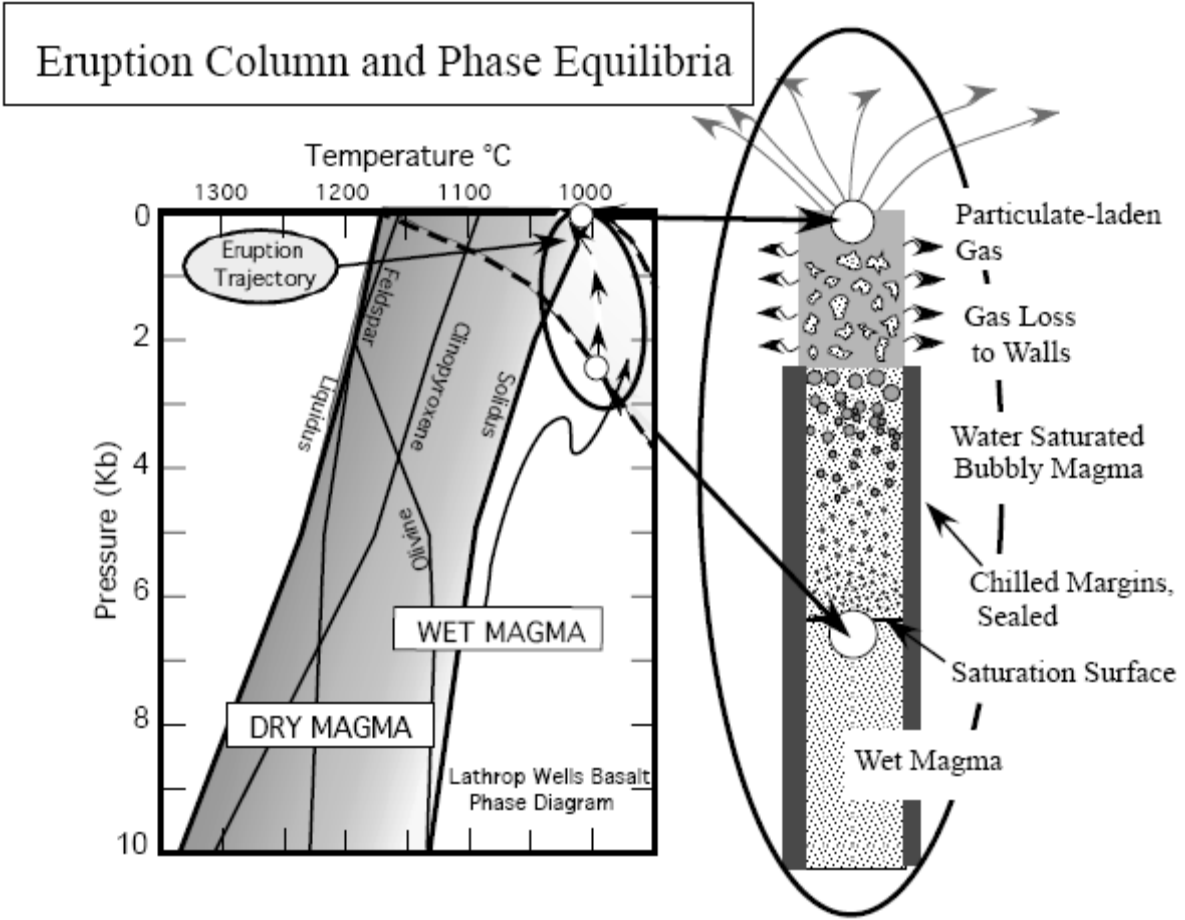
3933 **6.2.1.3 Perspectives on Magma Viscosity**

3934 **6.2.1.3.1 DOE Perspective**

3935 DOE (DOE, 2004 [p.6-29]) summarized the flow regimes for basaltic magma:
3936

- 3937 1. Homogeneous with small, low Reynolds number bubbles moving with the melt.
- 3938 2. Bubbly flow with bubbles rising faster than the melt.
- 3939 3. Slug flow with bubble sizes approaching the width of the dike (Vernioles and Jaupart,
3940 1986).

3941 DOE goes on to explain these regimes and the final choices for modeling as follows. The
3942 operative flow regime will be a function of many variables including, but not limited to moisture
3943 content, other gases present, pressure, melt viscosity and surface tension. Figure 6.5 shows the
3944 phase equilibria diagram for Lathrop Wells basalt, inverted from the normal presentation,
3945 together with the eruption column anticipated for these phases. As the magma first encounters
3946 a drift, it may do so under slug flow; as time progresses and the magma front continues up the
3947 dike, the flow entering the drift may become bubbly. The viscosity of the bubbly flow is very
3948 complicated and in certain cases will be non-Newtonian. This could include either shear thinning
3949 or shear thickening depending on the variables listed above (Detournay et al., 2003] [Appendix
3950 2, p. 1 Figure 2B]). Therefore, it is not possible to determine the effect of this uncertainty.
3951
3952
3953
3954
3955



3956
 3957
 3958
 3959
 3960
 3961
 3962
 3963
 3964
 3965
 3966
 3967
 3968
 3969
 3970
 3971
 3972
 3973
 3974
 3975
 3976
 3977
 3978
 3979

Figure 6.5 Phases in a volcanic eruption column showing the three regimes (wet magma, water saturated bubbly magma, and particulate-laden gas) and associated phase equilibria diagram for Lathrop Wells basalt.

6.2.1.3.2 EPRI Perspective

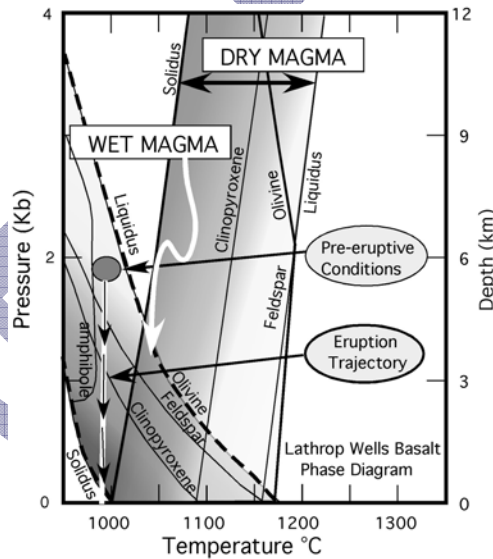
Using the experimental phase equilibria on basalts near Yucca Mountain, EPRI (2005 [p.3-1]) estimated magma viscosity as follows. Based on phase-equilibria stability diagrams (Nicholis and Rutherford, 2004), the magma ascended from depths >175 MPa (>7 km) with temperatures <975°C for the Little Cone samples and 1000-1010°C for the Lathrop Wells samples. The corresponding viscosities for this range of temperatures at repository depths are 10^5 - 10^7 Pa-s (10^6 - 10^8 poise) (Lore et al., 2000); Delaney and Pollard, 1982) and a magma rheology characteristic of an aa flow (Soule et al., 2004).

The problem with this approach to estimating viscosity is that these temperatures cannot be used directly with the above curves of Lore et al. because the liquidi of the hydrous Yucca Mountain magma and the dry Snake River basalt are greatly different. With each magma at the respective liquidus temperature, the Yucca Mountain magma will actually have a viscosity lower than that of the Snake River basalt because the Yucca Mountain magma contains water. That is, the Yucca Mountain magma at about 1000°C will have a viscosity about ten times smaller than the Snake River magma at 1200°C.

3980 In terms of estimating the viscosity of the degassed Yucca Mountain magma, which may
3981 form a glassy basalt through rapid cooling during ascent, the viscosity from the Lore et al.
3982 curves at a temperature of $\sim 1000^{\circ}\text{C}$ would be about 10^{10} poise. Under these conditions this
3983 value may be correct.

3984 6.2.1.3.3. Additional Comments on Magma Viscosity

3985 The various possible rheological regimes experienced by hydrous basaltic magma as it
3986 decompresses on approach to the surface are appreciated by all parties. But the application of
3987 this information is inconsistent and, in some areas, confused. The central point of confusion
3988 concerns the rheology of basalt as it degasses with ascent under isothermal conditions. That is,
3989 the most sophisticated calculations show that basalt degassing under adiabatic conditions will
3990 ascend essentially isothermally due to crystallization. For hydrous basalt beginning its ascent at
3991 a temperature of about 1000°C , as has been suggested from experimental phase equilibria, an
3992 isothermal ascent will produce either rapid crystallization or quenching to a glass (vitrification)
3993 containing some crystals. In either case the viscosity increases enormously. Rapid
3994 crystallization or vitrification occurs because the hydrous basalt begins its final ascent at
3995
3996
3997



3998 Figure 6.6 Phase diagram for Lathrop Wells basalt under dry and wet conditions. [After Marsh
3999 and Coleman, 2006]

4000 a temperature ($\sim 1000^{\circ}\text{C}$) that is at or below its low-pressure (i.e., near surface) solidus
4001 temperature. This is illustrated in the Figure 6.6 (Marsh and Coleman, 2006). As the
4002 concentration of solids (i.e., crystal) approaches that of maximum packing, which for basaltic
4003 magma is at $\sim 50\text{-}55\text{vol.}\%$, viscosity increases to $\sim 10^{18}$ Pa s with complete crystallization. If the
4004 basalt, instead, quenches to a glass, with a modest ($\sim 10\text{-}20\text{vol.}\%$) amount of crystals, the
4005 viscosity will become $\sim 10^{10}$ to 10^{12} Pa s, depending on the exact temperature. The attainment of
4006 this condition is reflected in the lack of mobility of lavas from Lathrop Wells.

4007
4008
4009
4010
4011 On the other hand, water-poor or anhydrous basaltic magma ascends along its high
4012 temperature liquidus and erupts at near liquidus temperatures. The viscosity is very low, about
4013 10 P s, and the magma is highly mobile. The bottom line is that hydrous magmas are explosive

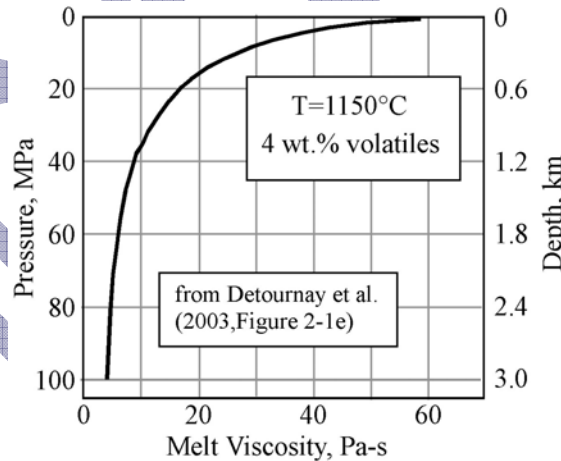
4014 as the gas exsolves and escapes, but the ensuing lavas are immobile. Dry magmas are not
4015 explosive, but the lavas are highly mobile.

4016
4017 There is confusion in all of the modeling over the viscosity of the basalt in the near surface
4018 regime. Either the magma is assumed to have its high-pressure, water-rich viscosity (DOE,
4019 2004, p. 6-30) or the magma is assumed to be unusually hot (~1200°C) and highly mobile.
4020 EPRI (2005) does assume a high viscosity magma, but for incorrect reasons. In particular, DOE
4021 states (BSC, 2004, p. 6-30-31):

4022
4023 “Many of the calculations used in this model are for magma less dense than 1300 kg/m³,
4024 which consists of more than 50 percent by volume gas. The viscosity of such a mixture
4025 is uncertain, so a viscosity of range of 10 Pa-s to 40 Pa-s, equivalent to the pure silicate
4026 liquid is used. The range of viscosities used in this analysis is derived from Detournay et
4027 al. (2003, Figure 2-1e). Most of the results in this report are for a viscosity of 10 Pa-s,
4028 representing a fluid magma that would quickly fill the drifts and, therefore, a more
4029 conservative condition from the perspective of dike/drift interaction.”

4030
4031 The Detournay et al. (2003 [Figure 2-1e]) results are shown in Figure 6.7 where the
4032 assumed conditions of the calculation are that the magma is at 1150°C, which is near the dry
4033 liquidus temperature, as opposed to about 1000°C for the potential Yucca Mountain wet
4034 magma.

4035



4036

4037
4038 Figure 6.7. Magma viscosity calculated at 1150° C during near-surface ascent and degassing
4039 [After Detournay et al., 2003].

4040

4041 Assuming this high temperature of 1150°C avoids having to consider the effects of
4042 crystallization and vitrification. This result is an illustrative assumption and should not be
4043 construed to represent the true rheology of the ascending basaltic magma. This can be seen by
4044 comparing this assumed temperature to the phase relations shown by Figure 6.6. A more
4045 meaningful calculation would put the magma starting temperature at 1000°C and, as it ascends,
4046 follow it through the course of crystallization and/or vitrification, which can be done using Figure
4047 6.3 from Lore et al. (2000). In this case, the magma viscosity reaches the much higher values
4048 mentioned earlier of 10¹⁰ to 10¹² Pa-s.

4049

4050 There is a field example of what happens to basaltic magma when it tries to flow through a
4051 narrow tube in rock that is relatively cold (251-256°C) compared to magma. In Iceland, on

4052 September 8, 1977, magma reached the depth range of boreholes in the Námafjail geothermal
4053 field. Three tons of volcanic ash erupted through an 1,138 m deep drill hole, forming a tephra
4054 sheet with a volume of 26 m³ (Larsen et al., 1979). The drill hole was part of the infrastructure
4055 for a hydrothermal field. The eruption lasted ~20 min. The borehole was cased to 625 m, had
4056 an uncased diameter of 0.16 m, and the main producing zones were reported at depths of 638
4057 m and 1038 m (Larsen et al., 1979). Tephra composition indicated temperatures at the time of
4058 chilling of 1153-1158°C. Compared to lava at Yucca Mountain, this Icelandic magma was dry
4059 and relatively mobile, but lava never flowed out of this borehole, which indicates limited vertical
4060 rise of magma due to quenching on borehole walls and increasing flow resistance and viscosity
4061 during ascent.
4062

4063 We use the short eruption time to estimate a lower limit for the magma viscosity. We
4064 assume that, after the initial pyroclastic phase, degassed magma entered the borehole via the
4065 deeper producing zone and began traveling up the uncased section. Using Poiseuille's Law for
4066 pressure-driven flow, and given an overburden pressure of $>2 \times 10^7$ N/m², viscosities for this
4067 mobile magma must nonetheless have exceeded 1000 poise (100 Pa-s), otherwise the velocity
4068 of the liquid magma front would have been great enough to reach and seal the cased part of the
4069 borehole in 20 min. This did not happen because steam production continued from this borehole
4070 *after* the magmatic event. For comparison, previous workers (Woods et al. 2002 and 2006)
4071 assumed low viscosities of 100-1000 poise for relatively immobile, wet magmas at Yucca
4072 Mountain.
4073

4074 In sum, researchers must be consistent in how they estimate the viscosity of Yucca
4075 Mountain basalt as it ascends and degasses near the surface. There has been a tendency to
4076 assume rheological properties pertaining to both wet, cool magmas and dry, hot magmas,
4077 leading incorrectly to the postulate of a highly explosive system with highly mobile lavas. The
4078 potential Yucca Mountain magma is likely a wet, cool magma. Wet basaltic magma is
4079 explosive, but relatively immobile as lava. Dry [e.g., Icelandic] magma is not explosive, but
4080 highly mobile as lava.
4081

4082 **6.2.2 DOE, EPRI, and NRC Perspectives on the Magma-Waste Package Interaction**

4083 **6.2.2.1 DOE Perspective**

4084
4085
4086
4087 DOE [e.g., BSC, 2004] and EPRI (2004, 2005) have considered many aspects of the
4088 dynamics of dike propagation, magma flow into drifts, magma-waste package interactions, and
4089 subsequent waste package-water interaction. For magma flow into a drift DOE uses various
4090 coupled models, analytical and numerical, of fluid flow from the dike to the drift. The magma is
4091 given a viscosity of 10-40 Pa-s, and the drift is filled in about 15 minutes. Effects of solidification
4092 on magma rheology is mentioned, but not explicitly used in flow modeling. This analysis
4093 suggests that waste packages may be softened, deformed, and corroded by the magma, but not
4094 be easily moved, and glassy waste forms are unlikely to be significantly altered by the magma.
4095 Yet because of the many uncertain facets of the process encountered in this investigation DOE
4096 concluded (BSC, 2004, p. 6-111): "On balance, it would be proper to adopt the conservative
4097 position that all waste packages and associated drip shields that come in contact with basalt
4098 magma immediately fail."
4099

4100
4101
4102

6.2.2.2 EPRI Perspective

EPRI (2004) analyzed an extrusive release scenario for Yucca Mountain and concluded that the waste package, if intact and still strong, can provide a significant barrier to inhibit the volcanic release of radionuclides. EPRI analyzed several failure mechanisms, including a direct hit on a waste package from below, and found reasonable expectation that no waste packages would fail. EPRI (2004) therefore concluded that the expected consequence of an igneous extrusive event would be no releases at all of radionuclides to the atmosphere. EPRI did note that waste packages located directly within a magmatic vent could conceivably contribute radionuclides during the Strombolian stage of an eruption.

Use of more reasonable (to them) assumptions in EPRI's (2005) work lead them to de-emphasize the importance of igneous scenarios in estimating probability-weighted peak doses. They suggest that DOE and NRC have used so many compounding conservatisms in their evaluations that igneous scenarios have taken on greater apparent risk importance than is justified. They conclude that present DOE and NRC assessments of repository performance are conservative, and reliance on more realistic scenarios and input data would demonstrate an even greater margin of compliance. Based on the results of two summary reports, EPRI (2004; 2005) reached the overall conclusion that there is reasonable expectation that an intrusive or extrusive igneous event at Yucca Mountain would not be expected to result in dose levels exceeding those levels anticipated for a base-case scenario with no igneous event, and that no further work need be pursued to address the igneous scenarios.

A key aspect of the EPRI [2005] analysis concerns the realization that magmatic eruptive temperatures are apt to be significantly lower than they (and DOE) have previously assumed. This stems from experimental phase equilibrium studies on basalt from nearby Crater Flat by (Nicholis and Rutherford, 2004). Their work suggests that, although the magma was at or near its liquidus temperature, because of the magma water content this temperature was much lower than previously assumed (i.e., ~1000°C vs 1150-1200°C). EPRI (2005) then used the viscosity-temperature relations of Lore et al. (2000) to find a much larger magma viscosity of 10^5 to 10^7 Pa·s. The difficulty with this approach is that the relation shown by Lore et al. (2000) is based on experiments for water-free melts and glasses and cannot be used for hydrous magmas. Even though the new temperature is much lower, the fact that it is at the liquidus of a water-rich magma, means that the viscosity will be as low (or possibly lower) than that initially assumed by EPRI and DOE. The correlation and regression given by Lore et al. [2000] is useful as an overall indication of rheology from melt to glass in lava, but it does not capture the detailed changes due to crystallinity, water content, and bulk composition within the liquidus-solidus range for magma in general. (More on rheology will be presented below.)

As mentioned already, Woods et al. [2002] also analyzed the case in which magma diverts along multiple emplacement drifts and into the main access drift from where it vents to the surface. They concluded that intersected drifts could quickly fill with magma, and that a large number of waste packages in the repository could be affected. They suggested that prolonged magma flow through the repository, enveloping and bathing the waste packages, over days to months leads to failure of waste packages and provides a mechanism to transport waste to the surface. They did not consider the effects of solidification on rheology or of quenching on waste packages.

6.2.2.3 NRC Perspective

As mentioned already, Woods et al. (2002) also analyzed the case in which magma diverts along multiple emplacement drifts and into the main access drift, from which it vents to the surface. Intersected drifts could thus quickly fill with magma, and a large number of waste packages in the repository could be affected. Woods, et al suggested that prolonged magma flow through the repository, enveloping and bathing the waste packages for days to months results in failure of waste packages and provides a mechanism to transport waste to the surface. They did not consider the effects of solidification on rheology or of quenching on waste packages.

Woods et al. (2002) also suggested the possibility of generation of a shock wave, which propagates through the drifts as the dike cuts the drift. The ideal experimental situation by which to produce a shock wave is to puncture a diaphragm separating a fluid under high pressure from a space at much lower pressure. Disruption of the diaphragm produces a pressure wave with a discontinuity in pressure at its leading edge.

Shock waves have indeed been recorded in volcanic eruptions at well-established volcanoes associated with island arcs such as at Nguaruhoe in New Zealand (Nairn, 1976) and Mount St. Helens (Reed, 1980). Shock waves have not been observed during venting of a dike in establishing a fissure-style eruption. The basic structure of island arc stratocone volcanoes, however, makes them ripe locations for shock wave production. Stratocone volcanoes almost always emit magma from a central summit vent. Korovin volcano on the island of Atka in the Aleutian Islands, for example, has such a cylindrical vent about 300 m wide and 1 km deep that has been periodically observed to be empty and later brimming with magma (Marsh, 1990). Should the summit area become plugged with congealed magma, which is commonplace, rising magma along with the inevitable exsolution of volatiles will overpressure the volcano until it suddenly ruptures. Moreover, many highly explosive island arc volcanoes erupt high crystallinity magma that is near the point of critical crystallinity (~55 vol. %: Marsh, 1981) where the magma becomes a shear resistant dilatant solid, forming an excellent plug at the summit. Merapi volcano in Indonesia is a clear example of this condition (e.g., del Marmol, 1989). Thus, large volcanoes repeatedly issuing magma from a central summit vent are, in essence, almost ideal shock wave generators. A dike entering a drift at Yucca Mountain would be distinctly different from this occurrence.

A propagating dike is a magma-filled elastic crack. The leading edge of the dike is knife-like and the width of the dike increases slowly away from the tip. Although this is sometimes difficult to calculate in highly fractured country rock with complex elastic properties, examples are available from field occurrences. For example, in the north wall of the east end of Wright Valley in the McMurdo Dry Valleys, Antarctica, the leading edge of the dike associated with the emplacement of the 300 m thick Basement sill is fully exposed (Marsh, 2004). Over a distance of about 5 km the dike thickness increases progressively from 1 cm at the leading tip to 300 m. A dike intersecting a subsurface cavity or drift will gradually open to its full thickness. Rapid quenching of (most probably) low crystallinity magma along all margins will further impede the rate of opening so that the pressure release will not be catastrophic, as with a punctured diaphragm, but will ramp-up over a finite time and not allow development of a discontinuity in the pressure field.

The scenario analyzed by Woods et al. (2002) creates a shock wave because of the way the problem and simulation is set up. The imposed initial conditions (both geometric and dynamic) essentially presuppose the solution. But it is the magma physics before the assumed

4205 initial conditions that actually determines the outcome. The proper portrayal of this part of the
4206 problem (e.g., the gradual opening of a leaky fracture into a cavity) precludes formation of a
4207 shock wave. BSC (2004) and EPRI (2004) also analyzed the possibility of a generation of a
4208 shock wave and the found magma-drift interactions to be far less severe than those
4209 hypothesized by Woods et al. (2002).

4210

4211 **6.2.2.4 Summary of Views**

4212

4213 A recent numerical analysis by Dartevelle and Valentine (2005) builds on the Woods et al.
4214 approach but includes full time dependence, 2-D geometry, and a multiphase flow of steam and
4215 pyroclastic particles. Although this work has attractive features in time dependence, spatial
4216 deposition of particles, and spatial dependence of flow speed and pressure, it also suffers in its
4217 fixed (i.e., non-time dependent) 2-D geometry. A shock wave forms at the outset in response to
4218 the fixed geometry and the initial conditions of the pressure contrast between the dike flow and
4219 the drift.

4220

4221 Detournay et al. (2003) present an extensive discussion of igneous consequences at Yucca
4222 Mountain, including the potential interactions between a basaltic dike and a repository. In their
4223 opinion, the probability that a violent erupting mixture could follow dog-leg conduits is small and
4224 more than offset by the degree of conservatism built into the existing estimates. They
4225 recommended that a number of new analyses be made, including development of a coupled 3D
4226 model for unsteady dike-drift flow for the scenario of a drift being intersected by a vertical dike,
4227 and that experimental studies be made on the chemical and mechanical effects of basaltic
4228 magma on waste packages in drift and conduit flows.

4229

4230 Overall, it appears that significant conservatisms exist in the DOE and NRC analyses of
4231 igneous scenarios. These conservatisms exist, in a large part, because of major uncertainties
4232 in the understanding of the interaction of magma with the repository, and much of the
4233 uncertainty centers on the problem of the thermo-viscous state of magma as it undergoes
4234 solidification. For example, Woods et al. (2002) assume that magma moving through a
4235 repository drift remains isothermal with “water-like” flow characteristics. This is based on the
4236 assumption that magma flow rates will be rapid (10s to 100s m/s) and the thermal inertia of the
4237 flow will be large as in flow in a lava tube. But repository drifts are small (~5.5 m diameter) and
4238 cool (100-300°C) and lava quenches and stagnates on all it touches. By not considering realistic
4239 scenarios for the thermal interaction of magma with tunnel openings, waste packages, and
4240 tunnel walls, there is a real possibility that important processes could be missed. This would not
4241 only have implications for understanding other processes (e.g., entrainment and eruption of
4242 waste) but also in correctly estimating the overall seriousness of the magma disruption process
4243 itself. A prime example in previous work is the serious omission of the exceedingly common
4244 phenomenon of magma solidification and quenching. An explanation for this view is given below
4245 after first describing the physical situation.

4246

4247 **6.2.3 Number of Waste Packages Potentially Affected by Dike Intrusion**

4248

4249 The extent to which a repository could be affected by a hypothetical dike intrusion depends
4250 on how far magma could penetrate drifts before it solidified. As discussed in the preceding
4251 section, this would be determined by the composition and rheology of the magma if it should
4252 encounter tunnels. Both DOE and EPRI have performed quantitative analyses of the number of
4253 waste packages that could be affected by hypothetical dike intrusion.

4254

4255

6.2.3.1 DOE Analysis

DOE (2004) states that the rate of magma flow into drifts will be limited by the rate of magma supply, except probably when the supply is very large (velocity on the order to 10 m/s) and the magma viscosity is on the order of 40 Pa·s. The time needed to fill 500 m of drift will be on the order of 15 minutes given a magma velocity of 1 m/s. The time needed depends on the supply rate, and the results can be linearly scaled to other drift lengths.

The presence of the drift will have an impact on the rise of the magma inside the dike. In fact, the magma front may stop rising, and a steady state flow into the drift (total magma flow inside the dike diverted into the drift) may be reached before it is completely filled. However, the magma will rise several tens of meters above the drift before it fully invades it. Pressures in the drift will be minimal (a few kilopascals) while the magma is invading it.

Uncertainty exists in the magmatic effects on waste package integrity. Flow of magma into drifts is likely to result in plastic deformation of waste packages, but it is unlikely to result in movement of waste packages over large distances. Exposure of packages to the high temperatures and corrosive gases of the magmatic environment are expected to enhance corrosion.

Commercial spent fuel is expected to eventually be reduced to relatively small particles due to oxidation. Glassy waste forms are not expected to be significantly altered by encounter with magma. On balance, it would be proper to adopt the conservative position that all waste packages and associated drip shields that come in contact with basalt magma immediately fail (BSC, 2004, [p. 6-111]).

DOE (2004) documents calculations of the number of waste packages that could be damaged in a potential future igneous event. The igneous intrusion scenario shows a range of consequences, extending from virtually no waste packages damaged to nearly all waste packages in the repository. The 50th percentile value indicates approximately 1600 waste packages could be impacted, out of over 11,000 waste packages in the repository. DOE made the following assumptions in these analyses:

1. For any drift intersected by a dike, all of the waste packages located in that drift will fail. In other words, they will provide no further protection for the waste.
2. For any drift not intersected by a dike, none of the waste packages located in that drift will fail.

The rationale for these assumptions is:

1. Since the emplacement drifts will not be backfilled, there are no credible mechanisms to block or mitigate the resulting effects from the dike intrusion upon the waste packages.

2. The presence of backfill in ventilation drifts, access drifts, and turnouts will serve as credible mechanisms, provided sufficient engineering is implemented, to protect waste packages in emplacement drifts which are not exposed directly to magma (i.e., drifts which are not intersected by a dike).

4307
4308
4309
4310
4311
4312
4313

6.2.3.2 EPRI Analysis

The results of EPRI's (2005) analysis of hypothetical magma intrusion are summarized in Table 6.1. Within the "red" zone they estimate that 0-6 waste packages could become engulfed by magma intrusion in a waste emplacement drift. They further estimate that in the "blue" zone 14-24 waste packages could be significantly affected by heat and corrosive gases.

Zone	Description of Zone	Extent of Zone	Total No. of Waste Packages (Both Directions)	Condition of Cladding	Condition of Alloy-22 WPOB and Drip Shield	Impact on Transport Properties
Red	waste packages engulfed by magma intrusion	0-20 m from magmatic dike	0-6	Failed	Additional considerations: <ul style="list-style-type: none"> • WPs are unlikely to fail by over-pressurization because of restraint by the external magmatic load. • Creep failure is considered unlikely as the magma will prevent sufficient strain of the WP. • Potential for DS displacement by magma intrusion. 	Fractured basalt <ul style="list-style-type: none"> • flow diversion • sorption • fractured matrix
Blue	waste packages experiencing significant thermal impacts	37-66 m from end of Red Zone (front of magma intrusion)	14-24	Failed	All of the WPs in the 'Blue Zone' are conservatively assumed to fail by creep. Additional considerations: <ul style="list-style-type: none"> • 1-2 WPs in the region immediately in front of an intruding magma plug, in addition a single WP that might be only partially engulfed by magma plug, are likely to fail by over-pressurization. • The hottest WPs may become sensitized and subject to enhanced general corrosion and greater localized corrosion susceptibility. • Corrosion due to volatile gases will range from 0.1-1 mm for the 10 hottest WPs. • Drip shield displacement unlikely. 	Open air

4314
4315
4316
4317
4318
4319

Table 6.1 Summary of the impacts on waste packages and specifically containment and controlled-release functions of barriers, for each of the three zones for the expected intrusive-release variant case. [After EPRI, 2005].

6.2.3.3 NRC/CNWRA Staff Considerations

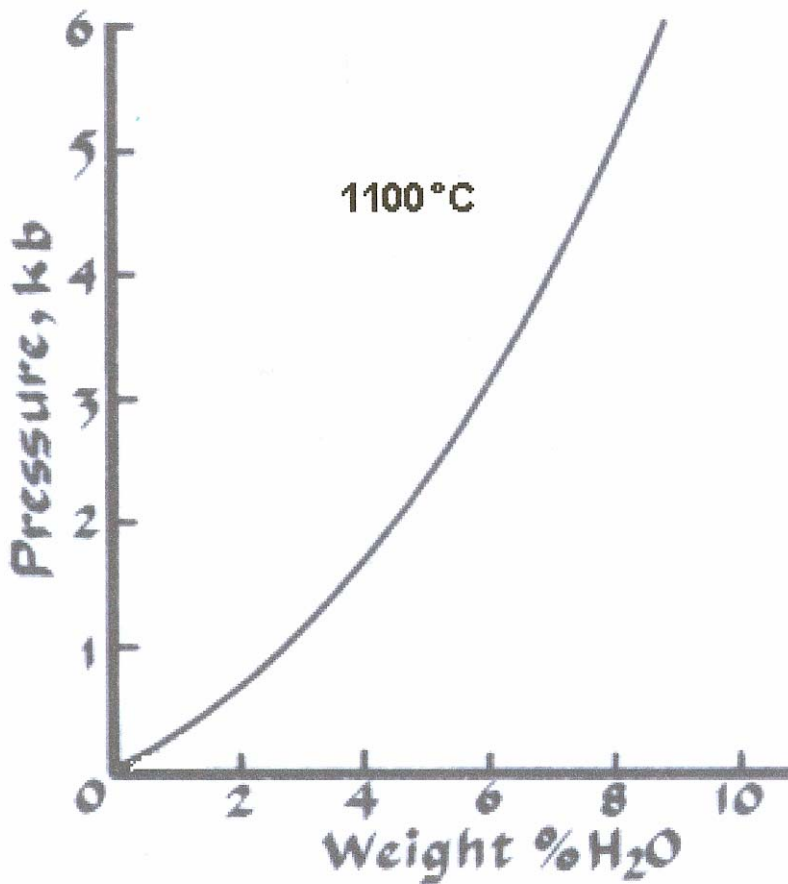
In TPA 4.1 (Mohanty et al., 2004) the NRC/CNWRA staff estimated a mean value of 37 magma-induced mechanical failures from an intrusion event, based on a log uniform distribution from 1 to 1402 waste package failures. Igneous activity causes the largest increase in dose conditionally from both groundwater and airborne pathways, but the risk is still small when the probability of the volcanic event is factored into the calculations. The probability-weighted dose from igneous activity is approximately 3.6 $\mu\text{Sv/yr}$ [0.36 mrem/yr], which is greater than the base case groundwater dose of 0.00021 mSv/yr [0.021 mrem/yr], but still small compared to the regulatory criterion of 0.15 mSv/yr [15 mrem/yr] (Mohanty et al., 2004).

4320
4321
4322
4323
4324
4325
4326
4327
4328
4329
4330
4331
4332
4333
4334
4335
4336

6.2.3.4 ACNW Comments on Magma Viscosity and Potential Dike Intrusion

The question of the number of waste packages involved in an eruptive event involves, in part, the length of drift exposed to magma. Magma viscosity is the key to evaluating this distance of magma penetration (Figure 6.9). If the eruptive material is pyroclastic debris, a local

4337 small subsurface cinder cone, in effect, would form and quickly plug the drift through
 4338 avalanching and welding. On the other hand, if the eruptive is low viscosity (e.g. $\sim 10^2$ Pa-s)
 4339 lava, a significant distance of drift may become involved. The flow of lava through a drift can be
 4340 estimated by assuming flow through a pipe whose radius shrinks in time due to magma
 4341 solidification around the margins of the drift. A prime difficulty in performing such calculations is
 4342 in the proper choice of the viscosity of the lava. Given the magma composition, temperature,
 4343 volatile content, and crystallinity, the estimation of viscosity is straightforward (e.g., Marsh,
 4344 1981). Each of these characteristics can be estimated for magma similar to alkali basalt
 4345 erupted nearby at Lathrop Wells, but there is a major problem in using this approach. As will be
 4346 explained in more detail in the subsequent section, because of the suspected high volatile
 4347 content, this magma will undergo volatile saturation at depth (~ 5 km) long before it reaches the
 4348 surface and will begin devolatilizing and solidifying rapidly in approaching the surface. When the
 4349 degassed magma reaches the surface it will already be near its 1-atm solidus temperature and
 4350 will be, in essence, a glassy paste-like material of enormous viscosity. This is strongly reflected
 4351 in the limited extent of the lava flows at Lathrop Wells (Figure 6.8).
 4352



4353
 4354
 4355 Figure 6.8. The solubility of volatiles in magmas is a function of temperature, pressure, and the
 4356 compositions of the liquids and gases. This diagram shows the solubility of water in basaltic
 4357 magma as a function of water pressure at 1100 deg. C. The pressure of another gas, such as
 4358 carbon dioxide, would decrease the solubility of water. At earth surface conditions (pressure =
 4359 1 bar) the solubility of water is virtually zero (vertical axis of diagram is marked in kilobars) [After
 4360 McBirney, 2007].
 4361

4362 The radial extent of the flow field at Lathrop Wells, shown in Figure 6.9 is about 1 km, and
4363 the volume of the lava field is about 0.03 km³ (e.g., Heizler et al., 1999). Although the duration of
4364 the flow is not known with any certainty, because of the nature of the flow the magnitude of the
4365 viscosity controlling the flow can be estimated. The flow can be approximated as a gravity
4366 current of viscous fluid spreading on a nearly flat surface (e.g., Huppert, 1982). This method
4367 has also been used to examine lava dome and lava growth associated with the 1979 eruptive
4368 event on Soufriere on St. Vincent (Huppert et al., 1982).
4369

4370 Approximating the radial spreading of lava as an isothermal viscous gravity flow is but one
4371 of several mechanisms suggested that govern lava spreading and lava dome growth (e.g., Fink
4372 and Griffiths, 1998; Griffiths, 2000; Lescinsky and Merle, 2005). The strength of the enveloping
4373 crust, the internal yield stress, and the role of damming at the toe of the flow may each also
4374 dominate the flow at certain stages of growth or stages of cooling. Although the rates of radial
4375 growth predicted by the various models are similar, lava dome height over time tends to favor
4376 growth controlled by the yield strength of the surficial crust. In terms of revealing an effective
4377 viscosity of the lava itself, however, the various models are mutually exclusive. That is, each
4378 model yields a set of physical properties not found in the other models, and additional, more
4379 detailed, physical features added to a model often yield a better fit to observation. The viscous
4380 model, for example, can be made to fit better if the effect of damming at the toe is larger or if the
4381 lava viscosity is significantly larger than that independently estimated from lava composition and
4382 temperature. In the latter respect, we show later that, due to the sudden loss of volatiles with
4383 approach to the surface, the Lathrop Wells alkali basalt underwent rapid quenching and may
4384 well have attained a viscosity much larger than otherwise anticipated. And this viscosity is
4385 remarkably consistent with that found from modeling the Lathrop Wells as a gravity flow. On
4386 these grounds and the fact that only through this model can an estimate of viscosity be found,
4387 we prefer to model the spread of lava as a viscous gravity flow.
4388

4389 The radial extent (R) of the viscous flow of a fixed volume of released magma is given by
4390 (Huppert et al., 1982)
4391

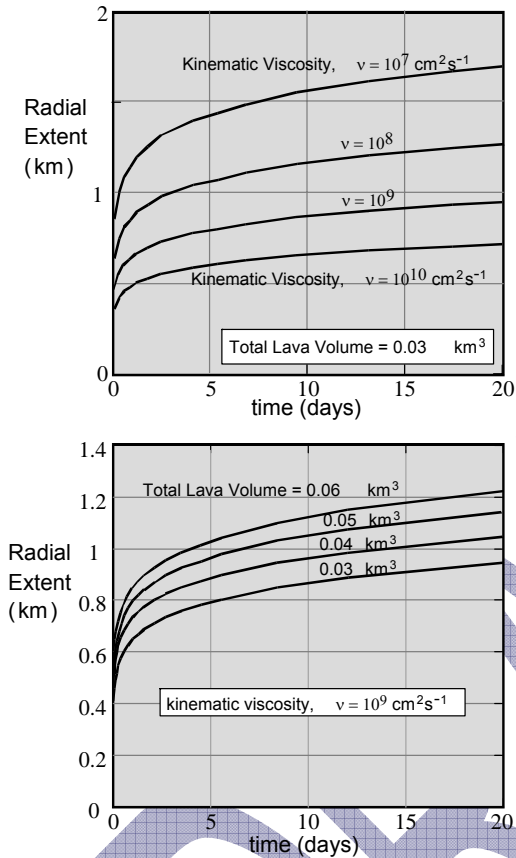
$$4392 \quad R = 0.894 \left[\frac{gV}{3v} \right]^{1/8} t^{1/8}$$

4393 where g is gravity, V is volume, v is kinematic viscosity (= μ/ρ where μ is shear viscosity and ρ is
4394 density), and t is time. Results from this equation are shown by Figure 6.8 for a variety of
4395 viscosities and total lava volume as a function of the duration of the event.
4396
4397

4398 From these results and with a maximum flow extent of ~1 km, the effective kinematic
4399 viscosity of the lava is unusually large, being in the vicinity of about 10⁹ to 10¹⁰ cm²/s. The exact
4400 duration of this ~80,000 year old flow is not known, but flow events of this nature generally last
4401 about a month to a year. The aa character of these flows suggests a flux rate of about 3 x 10⁴
4402 kg/s (Wood, 1980), which when used in concert with the observed volume suggests a duration
4403 of about 30 days.
4404

4405 A significantly larger viscosity (2 x 10¹² poise) was similarly deduced by Huppert et al. (1982)
4406 for Soufriere, which, apparently not believing the result, they ascribed to the influence of a high
4407 viscosity skin or quench rind enclosing the lava. Although this effect may be important, the fact
4408 that the Soufriere lava contains almost 50% (vol.) crystals is also a major factor in greatly
4409 increasing the viscosity (Marsh, 1981), making the derived result clearly realistic. At Lathrop
4410 Wells, although the crystallinity was not large, there is evidence in the steep flow fronts, the

4411 rafted well-formed vent blocks supported by the flow, and the degassing sequence of extrusion
 4412 (more below) that the viscosity was large. Together with the asymptotic character of these
 4413 curves the viscosity range noted above may well be reasonable and can be used in calculations
 4414 of magma travel distance.
 4415



4416
 4417

4418 Figure 6.9 Radial extent of the Lathrop Wells, Nevada lava field as a function of the duration of
 4419 the flow event. The observed flow extent is about 1 km.
 4420

4421 In modeling the flow of magma into a Yucca Mountain repository, insight into the nature of
 4422 the magma likely to be involved has been gathered from the nearby alkali basalt cinder cones.
 4423 The almost universal tendency has been to use a volatile-rich basaltic magma as the
 4424 characteristic magma involved in all interactions with the repository. This is the deep pre-
 4425 eruptive magma containing 2-4 wt.% water and with a viscosity of 50-500 p, making it both
 4426 explosive and highly mobile. Typical calculated flow velocities are 10-100 m/s (e.g., Woods et
 4427 al. [2002] estimated steady magma flow speeds of 10 m/s through a tunnel by assuming 2 wt%
 4428 water, isothermal flow without quenching, and a low viscosity of 100 p). This hypothetical lava
 4429 would flow a distance of 1 km in 10-100 seconds. A similar flow, assuming availability of enough
 4430 magma and a continuous downhill path, would reach the outskirts of Las Vegas (150 km) in as
 4431 short a time as 40 minutes. There is nothing in the character of the erupted lavas in the region
 4432 of Yucca Mountain that would suggest any behavior of this nature. On the contrary, the flows
 4433 from the cinder cones scattered throughout the region are exceedingly limited in spatial extent
 4434 (~1 km in radius). This limited extent is also not merely due to the limited volume of these
 4435 eruptions, although this is certainly partly the reason. For if the Lathrop Wells governing

4436 viscosity is reduced to 100 p (e.g., as in Woods et al., 2002), keeping the volume at 0.03 km³,
4437 the flow would have traveled 5 km in about 2 days.
4438

4439 Altogether this suggests that, should alkali basalt of the general nature of that erupted at
4440 nearby Lathrop Wells intersect and enter repository drifts at Yucca Mountain, the extent of flow
4441 would be exceedingly limited, perhaps no more than 10 meters. Even based simply on the
4442 nature of the flows at Crater Flat, the lava would be blocky and sluggish and advancement
4443 would be difficult in a cylindrical drift, especially one filled with waste packages. It certainly
4444 would not be a simple case of a viscous, non-solidifying fluid flowing along a pipe. And, contrary
4445 to the analysis of Woods et al. (2002), there is no chance that the lava would undergo any form
4446 of wholesale thermal convection whatsoever (Marsh, 1989; Brandeis and Marsh, 1989 and
4447 1990; Hort et al., 1999)
4448

4449 Prior to the arrival of lava, however, the leading region of the ascending dike would be
4450 laden with gas and tephra. That is, should an ascending dike of water-saturated basaltic magma
4451 encounter the repository, the already rapidly quenching magma will undergo even stronger
4452 exsolution-induced quenching. Instead of fluid magma entering the drift and flowing along to
4453 eventually fill it, as in filling a bathtub, a small cinder cone would begin developing at the point of
4454 intersection. Cinders would avalanche into the drift, rapidly piling up and plugging the drift; the
4455 fragmental material will not flow far, especially given the presence of waste packages and other
4456 components of the engineered barrier. The insulating effect of the close rock wall will minimize
4457 air-fall and radiant heat loss, allowing the pile of cinders and tephra to tack or partially anneal
4458 together to form a mass of considerable strength. Magma will continue to quench on this mass
4459 of cinders and tephra. This process would form a plug in the drift, sealing the point of
4460 intersection, which would either force the magma to continue upward to erupt on the surface or
4461 simply seal off the dike locally, redirecting the flow to other portions of the dike that have already
4462 reached the surface.
4463

4464 The initial 'hole' (at the point of tunnel intersection) in the wall of the ascending dike causes
4465 a local depressurization producing a perturbation in the pressure field driving the dike upward.
4466 This pressure perturbation will travel outward into the dike, informing, in effect, the broader flow
4467 of the presence of this vent. But because the vent into the repository is small relative to the
4468 surface area of the dike (for a typical dike length of 1 km, this ratio is $\sim 10^{-5}$), this perturbation is
4469 relatively small and will not travel far in the thin (~ 1 -10 m wide) dike before ($< \sim 1$ s) the rapidly
4470 ascending dike (\sim km/s) reaches the nearby surface, short-circuiting the flow from the repository
4471 drift to the surface.
4472

4473 The formation of a plug at the point of magma entry into the repository will also allow
4474 pressures on the dike side of the plug to return to the initial pressure. The initial magma
4475 pressure within a basaltic dike at Yucca Mountain would likely be in the range of 4.5 MPa to 8.0
4476 MPa (i.e., ~ 1 MPa larger than the horizontal far-field stress at repository depth) (BSC, 2004).
4477 The initial magma pressure can also be approximated by the lithostatic pressure at repository
4478 depth (i.e., < 7 MPa at 300 m, given a mean tuff density of < 2400 kg m⁻³). This can be
4479 compared to the expected strength of the tephra plug.
4480

4481 Schultz (1995) has measured the strength of the Cohasset basalt flow of the Columbia
4482 River Basalt Group. Intact basalt at 20°C and at < 9 MPa confining pressure has a compressive
4483 strength of 266 ± 98 MPa, a cohesive strength of 66 MPa, and a tensile strength of $\sim 14 \pm 3$
4484 MPa. Basalt has shear strength in the range of 20-60 MPa. A welded tephra plug need only
4485 achieve $\sim 3\%$ of the compressive strength or 1/3 to 1/8 of the shear strength of intact basalt to
4486 withstand the full pressure that could be exerted by magma in an adjacent dike. A compressive

4487 strength of 7 MPa, for example, is more typical of clay soils than of rocks. Increasing
4488 temperature into the melting range, however, significantly reduces the strength of basalt. The
4489 strength of partially molten basaltic magma under tension has been estimated from a summary
4490 of experimental and observational results by Marsh (2002). At ~50% crystals strength
4491 increases from about 0.03 MPa to about 30 MPa at ~ 100% crystals and about 1000°C. For
4492 compressive strength, these estimates increase by a factor of 10-20 (e.g., Jaeger and Cook,
4493 1979). Although these estimates hold only for massive, intact material, fragmental tephra will
4494 tend to tack together and form a continuum under these high temperature conditions.
4495

4496 The tephra plug also could not readily be pushed along the drift by either later higher density
4497 tephra or magma. Tephra will tend to tack to the tunnel walls and waste packages/drip shields
4498 and also be obstructed by waste packages aligned in series. More important, perhaps, is that
4499 tephra, being fragmental material at maximum packing will, like any particulate medium at near
4500 maximum packing, dilate upon shear and form a stiff plug (e.g., Marsh, 1981). The net effect is
4501 that, after a brief local perturbation, magma is most likely to continue flowing to the surface in
4502 the original dike. The area of the drift affected by the invading magma may be minimal, and the
4503 number of waste packages affected may therefore be very limited.
4504

4505 After the initial tephra phase, little magma would flow through the interstices of any welded
4506 tephra plug because of the high viscosity of the degassing magma, which would move as a high
4507 temperature glass.
4508

4509 **6.3. Effects from an Extrusive (Volcanic) Event**

4510

4511 The extrusive scenario involves the intersection of a tephra-cone-forming volcanic vent (i.e.,
4512 conduit) with the repository drift (see Figure 1.2e). The transition from flow in dikes to vent flow
4513 occurs early in an eruptive sequence, and vents form under various conditions. In low-viscosity
4514 basalts, the transition may occur when narrow parts of the dike freeze followed by mechanical
4515 and thermal erosion of wider sections as the flow is repartitioned (e.g., Bruce and Huppert,
4516 1990). A key difference between a volcanic vent and a dike is that the diameter of a vent is
4517 much smaller (generally <75 m) than the length of a dike (1-5 km or more). Given a repository
4518 drift spacing of >50 m, a vent could directly intersect only one drift and a relatively small number
4519 of waste packages in the cross-section area of the vent.
4520

4521 Due to the perceived complexity of the processes involved, both NRC (Mohanty et al., 2004)
4522 and DOE (2003) assume that the small number of waste packages (approximately 1-10)
4523 entrained within a conduit would be completely destroyed and the contents carried to the
4524 surface and ejected as tephra of varying sizes. The degree to which ceramic or glass waste
4525 forms could be reduced to fine particulate materials in a volcanic conduit is uncertain,
4526 particularly during the first 1000 years when the waste packages and waste forms should still be
4527 relatively intact. The manner and degree to which the fragments would be incorporated in
4528 volcanic tephra is uncertain, but would involve the well-known phenomenon of magma
4529 quenching.
4530

4531 **6.3.1 Number of Waste Packages Potentially Affected by an Eruption**

4532

4533 DOE has estimated that the median number of waste packages that would be disrupted in a
4534 volcanic eruption scenario (i.e., intercepted by a conduit) is fewer than 10 (DOE, 2004; Number
4535 of Waste Packages Hit by Igneous Intrusion). The NRC has determined that the number of
4536 waste packages affected by an extrusive volcanic event would have high significance to waste
4537 isolation because the consequences are directly proportional to how many waste packages

4538 would be intersected by an erupting volcanic conduit. Apparently due to the complexity of the
4539 processes involved, neither the NRC (Mohanty et al., 2004) nor DOE (2003) rely on evaluations
4540 of magma-drift-waste package interactions in any detail. They instead assume that a small
4541 number of waste packages are completely destroyed and the contents are carried to the surface
4542 via a volcanic conduit in a cone-forming event. Nevertheless, it is as yet unclear how or
4543 whether the Alloy-22 waste packages or the ceramic or glass waste forms themselves would be
4544 reduced to particles of respirable size, as is currently assumed by the DOE and NRC staff.
4545

4546 The number of affected packages is estimated based on observed conduit size at analog
4547 volcanoes. Alternative models of how a volcano may interact with repository drifts and develop
4548 a conduit could increase the number of entrained waste packages and thus increase the
4549 concentration of radionuclides in erupted ash. The following material is from NRC (2005a):
4550

4551 Normally, in the absence of subsurface drifts, volcanoes form roughly cylindrical
4552 conduits along the vertical plane of magma ascent. Based on analogy with deposits at
4553 active or deeply eroded volcanoes, the NRC staff determined that conduit diameters
4554 from 5 to 50 m represent the most likely range of diameters for a potential future eruption
4555 at the potential repository site (NRC, 1999; Doubik and Hill, 1999). In contrast, DOE
4556 considers potential conduit diameters up to 150 m, albeit with very low likelihoods of
4557 occurrence (e.g., CRWMS M&O, 2000b; BSC, 2003a). Actively erupting volcanic
4558 conduits have high temperatures and large physical stresses that most likely would
4559 completely disrupt any waste package directly intersected by the conduit (NRC, 1999;
4560 CRWMS M&O, 2000b). Thus, both NRC and DOE have concluded that any waste
4561 package entrained in an erupting volcanic conduit would reasonably fail to provide
4562 containment and release its contents into the rapidly flowing magma.
4563

4564 Open drifts at depths of 300 m could potentially cause magma ascent and flow
4565 processes to behave differently than in undisturbed geologic settings, because rising
4566 magma is a fluid with an overpressure sufficient to fracture and dilate surrounding wall
4567 rock. Intersection with a subsurface drift at essentially atmospheric pressure provides a
4568 horizontal pathway out of the original plane of vertical magma ascent, allowing flow
4569 localization and nonequilibrium expansion of volatiles (NRC, 1999; Woods, et al., 2002).
4570 Using the alternative conceptual model [dogleg scenario] from Woods, et al. (2002),
4571 magma could potentially flow down an intersected drift and break out at some point
4572 away from the point of original intersection. For randomly located points of intersection
4573 and breakout and a single drift containing 155 waste packages, an estimated average of
4574 51 waste packages would be located along the alternative flow path. In contrast, a
4575 normal, vertical conduit would intersect an estimated average of 4.5 waste packages
4576 using the TPA Version 4.1j code. There is a directly proportional relationship between
4577 the number of waste packages entrained and conditional dose (i.e., dose not weighted
4578 by the probability of scenario occurrence). This sensitivity appears reasonable, as the
4579 mass of high-level waste potentially entrained is relatively small compared to the mass
4580 of magma. It is assumed that high-level waste is uniformly distributed in the mass of a
4581 modeled eruption; thus, high-level waste behaves as a trace phase in the magma and
4582 does not appreciably affect the transport characteristics of a modeled eruption plume
4583 (NRC, 1999; CRWMS M&O, 2000b; BSC, 2003a).
4584

4585 In addition to alternative conceptual models for the magma-flow pathway, the number of
4586 volcanic conduits created during an igneous event also is uncertain. Using vent location
4587 information in Hill and Stamatakos (2002) and assuming medium-to-high confidence
4588 magnetic anomalies represent buried volcanoes, it is estimated that there are 17 paired

4589 and 13 nonpaired volcanoes in the Yucca Mountain region; most volcano pairs occur in
4590 alignments of three to five volcanoes. Volcano pairs have an average spacing of $2.0 \pm$
4591 1.3 km. Assuming that there is a uniform probability of one, two, or three volcanoes
4592 intersecting the repository during a potential extrusive event, and that the overall
4593 eruption character remains unaffected by the number of volcanic conduits, dose
4594 increases by approximately a factor of two from this process.
4595

4596 The expert panel of the ongoing PVHA-U has been asked provide expert opinions about
4597 volcanic conduit size in the Yucca Mountain region. However, the final report of the PVHA-U
4598 proceedings is not expected to be available until sometime in 2008.
4599

4600 **6.3.2 NRC Approach in Performance Assessment**

4601
4602 The NRC approach to evaluating an extrusive event is documented in Mohanty et al. (2004),
4603 which is NRC's "System-Level Performance Assessment of the Proposed Repository at Yucca
4604 Mountain Using the "System-level Performance Assessment of the Proposed Repository at
4605 Yucca Mountain Using the TPA Version 4.1 Code." This NRC document gives the following
4606 description of how the repository is described for the NRC calculations in TPA 4.1:
4607

4608 A final design for a repository at Yucca Mountain has not yet been identified by DOE, but
4609 would be contained in a license application (now expected in 2008). The waste
4610 emplaced at Yucca Mountain is assumed to total 70,040 MTU2 in an area of 5,400,000
4611 m^2 {approximately 5,000 m long and 1,000 m wide}. Assuming an average of 7.89 MTU
4612 per waste package and an equivalence between the spent nuclear fuel and other types
4613 of wastes, such as DOE spent nuclear fuel and glass high-level waste, approximately
4614 8,877 waste packages will be needed for waste disposal. The initial inventory activity is
4615 $\sim 6.65 \times 10^{20}$ Bq [1.8×10^{10} Ci]. Waste packages with a 5.3-m length and a 1.6-m
4616 diameter are emplaced in drifts 5.5 m in diameter, spaced 81.0 m apart. The average
4617 age of the spent nuclear fuel is 26 years.
4618

4619 The NRC staff currently assumes that volcanic vents will have an average diameter of ~ 50
4620 m (Mohanty et al., 2004). If the center of a vent were to coincide with the axis of a drift, then ~ 5
4621 waste packages would be entrained within the cross-section of the conduit and potentially
4622 transported to the surface (the worst case situation). The NRC/CNWRA staff has also
4623 performed calculations assuming that up to 100 waste packages could be impacted by an
4624 extrusive event (Mohanty et al., 2005). In considering eruptions from satellite vents in the TPA
4625 4.1 analyses (Mohanty et al., 2004), the staff assumed that a mean value of 51 waste packages
4626 could be entrained by an extrusive event and contained in volcanic ejecta.
4627

4628 Radiologic risks associated with volcanic eruptions are calculated in the TPA Version 4.1
4629 code by modeling airborne releases of radionuclides for simulated eruptions. The volcanism
4630 modules assume that a small number of waste packages become entrained in a developing
4631 volcanic conduit (vent). These waste packages are assumed to be destroyed within the conduit
4632 and their waste contents move upward with volcanic tephra to the land surface. At the surface
4633 the mixture of tephra and spent nuclear fuel is ejected into the atmosphere, from which it settles
4634 to form tephra deposits.
4635

4636 Igneous activity contributes to waste package failures for both extrusive and intrusive
4637 events. As modeled, extrusive events result in the direct release and deposition of radionuclides
4638 on the ground surface, whereas intrusive events contribute to releases to groundwater. In the
4639 NRC performance assessment, an igneous event occurs between 100- and 10,000-years

4640 postclosure, with a recurrence rate of 1×10^{-7} per year. After the hypothetical volcanic event
4641 penetrates the repository and exhumes spent nuclear fuel, the areal density of deposited ash
4642 and radionuclides is computed at the compliance point.
4643

4644 **6.3.3 EPRI Approach and Conclusions**

4645

4646 EPRI has summarized their views regarding the potential consequences of future volcanism
4647 at Yucca Mountain, if it should occur, are clearly stated in the executive summary of their report
4648 on the intrusive release scenario (EPRI, 2005). In brief, EPRI has reached an overall
4649 conclusion that there is reasonable expectation that neither an intrusive nor extrusive igneous
4650 event in the Yucca Mountain region would result in doses exceeding those anticipated for the
4651 case of no igneous event. EPRI has concluded that no further activities need be pursued to
4652 address the igneous scenarios. The summary from EPRI (2005) is quoted below:
4653

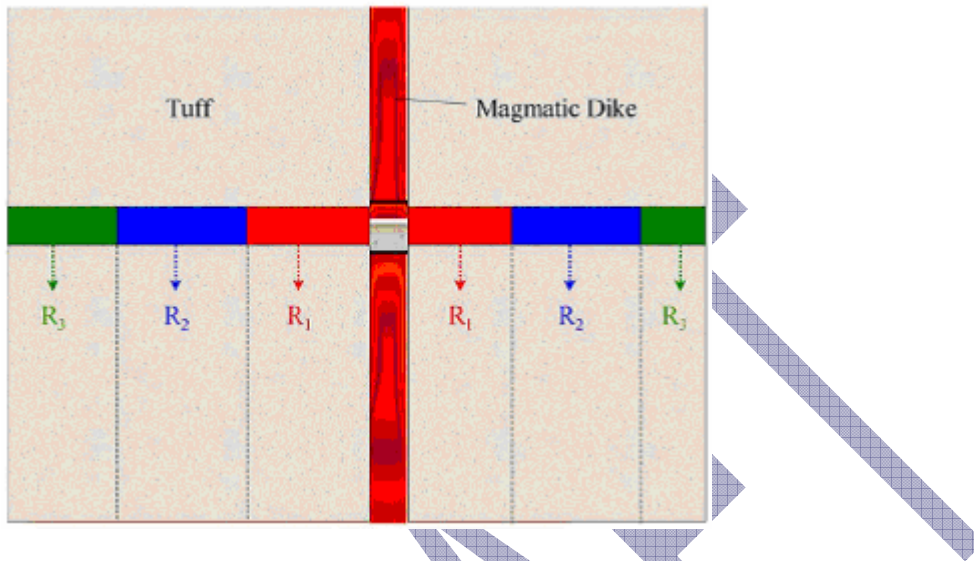
4654 There is evidence of volcanic centers near the proposed site at Yucca Mountain, Nevada
4655 for a geologic repository for the disposal of spent nuclear fuel (SNF) and high-level
4656 radioactive waste (HLW). This evidence indicates that potential future igneous activity
4657 (i.e., an “igneous event scenario”) may be a factor in the assessment of post-closure risk
4658 for the proposed repository. In 1996, a panel of independent technical experts for the
4659 Yucca Mountain Project’s Management and Operations (M&O) contractor [Geomatrix
4660 Consultants, 1996] conducted a study, the Probabilistic Volcanic Hazards Analysis
4661 (PVHA) study that estimated a mean annual probability of an igneous event occurring
4662 at/near the Yucca Mountain site at 1.6×10^{-8} /year [Geomatrix Consultants, 1996]. This
4663 probability, though extremely low, fell just above the 1.0×10^{-8} /year regulatory threshold
4664 that had been established for the dismissal of extremely low probability events.
4665

4666 Based on the findings of the 1996 PVHA Panel, a number of speculative analyses of the
4667 possible consequences of a future igneous event at Yucca Mountain have been
4668 conducted by the Yucca Mountain Project, (U.S. Department of Energy, DOE, and its
4669 contractor) (CRWMS M&O, 2000b; 2001), and the U.S. Nuclear Regulatory Commission
4670 (NRC), in conjunction with NRC’s contractor, the Center for Nuclear Waste Regulatory
4671 Analysis (CNWRA) (e.g., Woods et al., 2002). In brief, the igneous event itself is
4672 characterized as a rising dike of basaltic magma that intersects one or more emplacement
4673 drifts containing nuclear waste packages, shown schematically in Figure ES-1 [Fig. 6.10 in
4674 the present ACNW report]. Based on an in-depth, independent scientific review conducted
4675 by an Igneous Consequences Peer Review (ICPR) panel of experts (Detournay et al.,
4676 2003), the dike is postulated to most likely progress directly to the surface, intercepting a
4677 minimal number of waste packages within the conduit of the eruptive vent. Limited lateral
4678 magma flow through unbackfilled emplacement drifts is a credible possibility according to
4679 Detournay et al. (2003). Such lateral flow would lead to contact, and possible
4680 envelopment, of a limited number of “satellite” waste packages by magma away from the
4681 main locus of the dike-drift intersection.
4682

4683 Thus, two principal variant cases for a given igneous event can be specified:
4684

- 4685 • The extrusive-release case in which magma rising vertically in the conduit contacts
4686 waste packages in its path causing them to fail and possibly release radionuclides that
4687 would subsequently be erupted with the magma at the surface with subsequent
4688 radionuclide transport controlled by atmospheric and surficial processes, and
4689

4690 • The intrusive-release case in which waste packages, either directly contacted by the
4691 lateral flow of magma into the impacted drifts or indirectly affected by the elevated
4692 temperature and potential release of volatiles species from the intruding magma, would
4693 fail and release radionuclides via groundwater pathways at an earlier time than for waste
4694 packages unperturbed by these localized effects from an igneous event.
4695



4696 Figure 6.10. Schematic of zones of intruding magma effects in a repository drift on the
4697 engineered barrier system (EBS). Magma is assumed to completely the spaces in the “Red
4698 Zone,” with significant thermal/chemical effects on Alloy 22 in the adjacent “Blue Zones.” No
4699 effects on the EBS are assumed for the “Green Zones.” [After Figure ES-1 of EPRI, 2005]
4700
4701
4702

4703 EPRI, as part of its efforts to provide an independent technical/scientific assessment of
4704 issues that are anticipated to be important to the licensing of the proposed Yucca Mountain
4705 repository, has previously evaluated the extrusive-release case (EPRI, 2003; 2004a). This
4706 analysis refuted several of the more speculative consequences put forward by Woods et al.
4707 (2002) while indicating that the expected dose consequence for the extrusive-release variant
4708 case is at or near zero because of multiple factors including waste package durability, finite
4709 extent, duration and magnitude of likely future igneous events, and limitations imposed by
4710 realistic consideration of magma-waste package and magma-waste form interactions (EPRI,
4711 2004a).
4712

4713 The objectives of this report, which is a companion to EPRI (2004a), are to analyze the
4714 intrusive-release case and determine the potential impact on repository performance and
4715 safety, expressed as probability weighted mean annual dose rate, for the latter scenario.
4716

4717 EPRI’s analyses contained in this report adopt the igneous event probability of 1.6×10^{-8}
4718 /year previously derived by the Probabilistic Volcanic Hazards Analysis (PVHA) panel
4719 [Geomatrix Consultants, 1996]. The analyses also reflect recent data on basaltic eruptive
4720 centers in the Yucca Mountain region that support the conclusion that relatively low-
4721 temperature ($\sim 1010^{\circ}\text{C}$), high viscosity basaltic magmas, as opposed to the $\sim 1200^{\circ}\text{C}$
4722 magmas postulated by the DOE, are the most representative characteristics of future
4723 igneous events. Lower temperature implies lower and less prolonged thermal-perturbation
4724 of the host rock and contacted waste packages, and magma of much higher viscosity. The
4725 high viscosity supports the contention that such magma will only partially penetrate into

4726 emplacement drifts intersected by the magmatic dike, thereby only impacting a limited
4727 number of waste packages.

4728
4729 Partial intrusion of magma into emplacement drifts with controlled cooling and
4730 solidification of the magma implicitly leads to development of three “zones” within the
4731 emplacement drift (Figure 6.10):

- 4732
4733 • The ‘Red Zone,’ the area immediately adjacent to the rising magmatic dike and where
4734 drip shields and waste packages are assumed to be fully engulfed by magma. The ‘Red
4735 Zone’ is characterized by displaced/ disrupted drip shields, thermally sensitized Alloy-22,
4736 and spent fuel cladding that fails at the time of the igneous event,
4737
- 4738 • The ‘Blue Zone,’ the area just beyond the ‘Red Zone’ where drip shields and waste
4739 packages are not contacted directly by magma but experience significantly elevated, high
4740 temperatures. The ‘Blue Zone’ is characterized by intact drip shields, but failure of the
4741 Alloy-22 waste package outer barrier and spent fuel cladding within a relatively short time
4742 after the igneous intrusion event,
4743
- 4744 • The ‘Green Zone,’ the area beyond the ‘Blue Zone’ where waste packages experience
4745 modest (<350°C) and transitory high temperatures, with possible deposition of reactive
4746 magmatic volatiles onto the waste package surface. The ‘Green Zone’ is characterized by
4747 intact drip shields, Alloy-22 waste package outer barrier and spent fuel cladding that are
4748 unperturbed from their nominal corrosion behavior.

4749
4750 The range of the spatial extent and the number of waste packages in each zone are also
4751 derived in this report. These analyses show that the number of waste packages in the ‘Red
4752 Zone’ is extremely limited while those in the ‘Blue Zone,’ albeit more extensive, are still less
4753 than a majority of the waste packages in the impacted drifts.

4754
4755 Modification of the existing near-field source-term and radionuclide transport sub-model
4756 in EPRI’s Yucca Mountain total system performance assessment (TSPA) model, IMARC
4757 (EPRI, 2005), is made to specifically model radionuclide releases for each of the three zones.
4758 The release rate behavior for waste packages in the ‘Green Zone’ exactly conforms to the
4759 nominal case following failure of the Alloy-22 waste package outer barrier. The potential for
4760 favorable water diversion by solidification of massive basalt around waste packages in the ‘Red
4761 Zone’ is shown through sensitivity analyses, but this potential contribution is also conservatively
4762 ignored in the presented analyses. Near-field sub-model calculations show that there is a delay
4763 in the release of radionuclides from the ‘Red Zone’ attributable to sorption properties of the
4764 encompassing basalt, but that the long-term release rates for key dose-contributing
4765 radionuclides (Tc-99, I-129, Np-237, Th-229) from the ‘Red Zone’ and ‘Blue Zone’ eventually
4766 converge. The long-term release rates, on a per waste package basis, from both the ‘Red’ and
4767 ‘Blue’ zones are found to be higher (by a factor of ~40) than that for the nominal case (and
4768 ‘Green Zone’) because the time-dependent distribution of cladding failure would not be a factor
4769 in these instances.

4770
4771 A set of IMARC analyses was conducted to investigate the total system performance
4772 implications of the observations and analyses in each component of the system. First, IMARC
4773 was used to explore conditional dose analyses (“conditional” in the sense that the probability of
4774 occurrence of a magma intrusion event is set to one), to evaluate the dose consequences of the
4775 magma intrusion. There is reasonable expectation that the magma will only affect some of the
4776 waste packages in a drift intersected by a rising dike, with the remaining waste packages in the

4777 impacted drifts functioning in the same way as in drifts not intersected by the dike. In this
4778 situation, the peak conditional dose from the affected part of the repository is smaller than that
4779 produced from the unaffected part of the repository due to the small percentage of the total
4780 repository waste packages that are impacted. If the probability of a magma intrusion is also
4781 factored in, the contribution to overall probability-weighted peak dose becomes minuscule.
4782 Even when a series of conservative, "bounding" assumptions are made (e.g., full penetration of
4783 the magma into the drifts, and 100% of the drifts affected), the probability-weighted estimated
4784 bounding dose rates from such a bounding event only rise to be on par with the peak dose rates
4785 from the nominal case. It is, therefore, concluded there is reasonable expectation that magma
4786 intrusion is inconsequential with respect to peak dose.
4787

4788 Combining this conclusion with that of the earlier EPRI analysis of the extrusive igneous
4789 scenario (EPRI, 2004a) results in the overall conclusion that there is reasonable expectation
4790 that an igneous event in the Yucca Mountain region, either intrusive or extrusive, will not result
4791 in dose levels exceeding the levels anticipated for the nominal release (i.e., no igneous event)
4792 case. Given the above, robust conclusions regarding the relative lack of importance of the
4793 igneous scenarios to probability-weighted peak dose estimates, and the regulatory requirement
4794 that the DOE demonstrate that the probability-weighted peak doses for the repository will
4795 comply with applicable regulations, EPRI has concluded that no further activities need be
4796 pursued to address the igneous scenarios.
4797

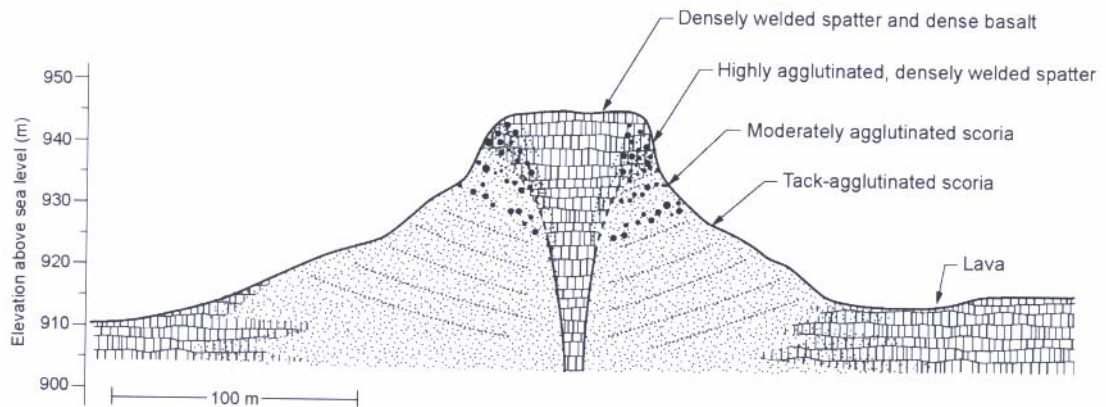
4798 **6.3.4 Comments on Potential Fate of High-Level Waste in a Volcanic Vent**

4799

4800 Available information provides practical insights about the plausible fate of high-level
4801 radioactive waste (HLW) if it should become entrained within a volcanic vent (conduit) and
4802 transported to the surface. Spent fuel contained in HLW packages would probably not be
4803 reduced to fine material within a volcanic conduit. The following points need to be considered in
4804 a realistic assessment of volcanic processes:
4805

4806 Most of the waste planned for disposal at Yucca Mountain consists of spent nuclear fuel
4807 rods from PWR, and BWR reactors. The physical form of the waste is ceramic pellets of UO_2 ,
4808 about a centimeter in diameter, with a melting point of $>2800^\circ C$. This is much higher than the
4809 magma temperatures of $1100-1200^\circ C$. A xenolith 30 cm in diameter has been found at the
4810 Lathrop Wells cone (Heizler et al., 1999) that may have been transported from considerable
4811 depth. The existence of this and other xenoliths is further evidence that UO_2 pellets could be
4812 expected to survive relatively intact over a much shorter conduit travel distance. The time of
4813 greatest hazard from a volcanic event is during the first 1000 years when waste packages and
4814 waste forms should still be relatively intact.
4815

4816 Volcanic conduits would be significantly smaller 300 m below the surface at repository depth
4817 than at ground surface (see Figure 6.11). This would minimize the number of waste packages
4818 that could be intersected by a conduit. Lithostatic pressure keeps the opening smaller at depth,
4819 whereas at the surface the vent periphery in the zone of fragmentation grows in diameter
4820 through active erosion by expelled tephra.
4821



4822
 4823 Figure 6.11 Schematic cross-section through Shirtcollar Butte, Crater Flat, Nevada, a Pliocene
 4824 (3.7 Ma) basalt volcano. The degree of fusing and welding of scoria increases up-section and
 4825 grades into dense basalt on the top of the butte. [Source: PVHA-U Field Trip Guidebook, May
 4826 1-4, 2006].

4827
 4828 A conduit is not born full size. Its diameter increases as the eruption proceeds. This
 4829 means that only one nuclear waste package could be initially entrained in the conduit, with
 4830 others becoming entrained within the final radius of the conduit at depth. Therefore additional
 4831 waste packages would be exposed to varying stages of the eruption sequence. It is also
 4832 possible that a conduit intersecting a repository could form in the separation distance between
 4833 drifts, and although an intrusive event would occur, no waste packages would be directly
 4834 intersected by the conduit.

4835
 4836 Present information shows that dikes are more likely to be injected into pre-existing faults.
 4837 Conduits form along dikes, therefore if DOE uses a “setback” strategy from faults (places waste
 4838 tunnels at a setback distance from faults), this would reduce the likelihood of a hypothetical
 4839 extrusive event impacting the repository.

4840
 4841 The expected time of travel in a conduit from repository depth to the surface would be less
 4842 than one minute. This allows little time for erosion of ceramic pellets, but does permit rapid
 4843 quenching of magma onto the relatively cold waste forms. The formation of a quench rind on
 4844 waste pellets would protect them during their rapid transit to the surface. This protective
 4845 quenching effect in volcanic conduits has not been considered by NRC or DOE in their
 4846 performance assessments (Mohanty et al., 2004; Codell, 2004; DOE, 2003).

4847
 4848 The relative volume of ash deposits vs. volume of scoria cone and lava flows can be used
 4849 to estimate practical limits on the fraction of ejected waste in the form of fallout that could be
 4850 available for fluvial and eolian transport. Waste incorporated in lava flows or tephra cones
 4851 would be protected from erosion and transport for many hundreds of thousands of years, as
 4852 demonstrated by the relatively pristine appearance of the million-year-old cones and flows in
 4853 Crater Flat near Yucca Mountain. Relatively little erosion has occurred even during the pluvial
 4854 climates of the Quaternary, when the climate of Yucca Mountain was significantly wetter than
 4855 today for most of the time. The 80,000 year old Lathrop Wells Cone is similar in dimensions to
 4856 the older Pleistocene cones. Bechtel/SAIC (2004) estimate the total volume of eruptive

4857 products at Lathrop Wells at $\sim 0.09 \text{ km}^3$ (cone, 0.02 km^3 ; lavas, 0.03 km^3 ; fallout, 0.04 km^3).
4858 Therefore, the fallout comprised less than half of the eruptive products.

4859 At Lathrop Wells, lithic fragments of conduit wall rock (tuff) are commonly found embedded
4860 within the scoria that make up the cinder cone. The tuff fragments were eroded from the walls
4861 of the volcanic conduit, vary in size from a fraction of a cm to 6 cm or larger, and have
4862 quenched rinds of basalt. The wall rock fragments are so abundant that they have been used to
4863 estimate the eroded volume of the Lathrop Wells conduit. The size of the lithic fragments
4864 indicates that HLW fuel pellets could be expelled in similar fashion during the cone-building
4865 phase of the eruption, intact and with protective quench rinds. The result is that entrained HLW
4866 would be likely to remain in relatively large fragments that would be deposited in or near a
4867 tephra cone, rather than as far-strewn, mobile ash.

4868
4869
4870
4871

6.4. Remobilization of Contaminated Volcanic Ash

6.4.1 Introduction

4872 Future basaltic volcanism intersecting the proposed repository at Yucca Mountain could
4873 lead to eruption of contaminated ash to the surrounding countryside during a violent
4874 Strombolian eruption phase. The contaminated ash would be derived from destruction of the
4875 waste packages within the volcanic conduit and entrainment of the fragmented waste into the
4876 erupting magma. It is unclear how much of the entrained radioactive waste could be ejected
4877 from the subsurface and to what degree the waste would be fractionated, thus there are
4878 differences in views about the resulting consequences of such an event. The discussion here
4879 pertains only to the fate of contaminated ash hypothetically ejected during a volcanic event and
4880 deposited in the drainage basin of Fortymile Wash where it would be subject to erosion and
4881 transport by both water (fluvial) and wind (eolian) processes into the immediate vicinity of the
4882 RMEI. Contaminated ash deposited elsewhere in the vicinity of Yucca Mountain would not reach
4883 the RMEI.

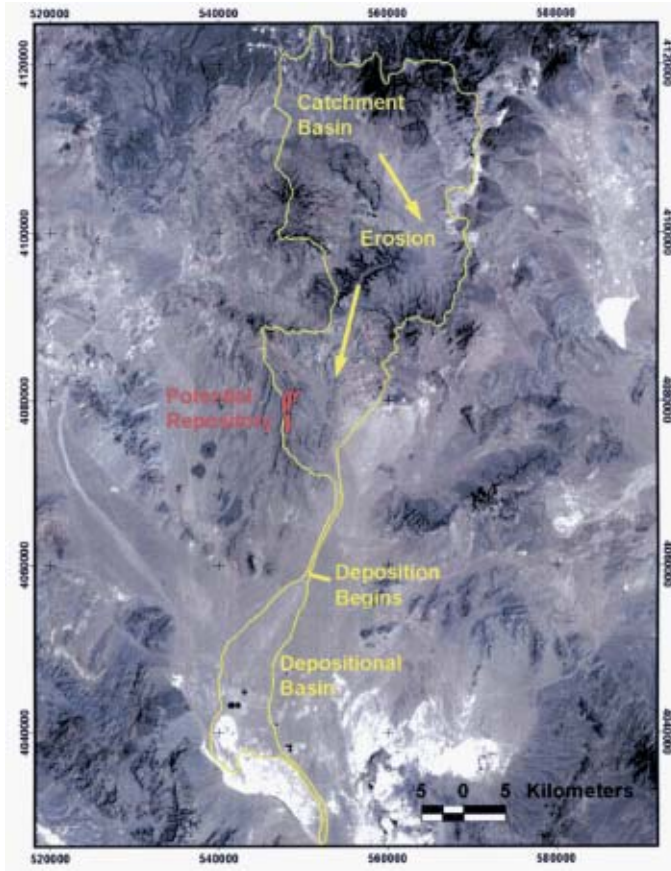
4884 Fluvial processes are limited in the Yucca Mountain region because the climate is arid to
4885 semi-arid with high rates of evapo-transpiration and low annual precipitation that averages
4886 about 165 mm/yr. Stream flow results from infrequent regional storms, mostly during the winter,
4887 and from localized but intense thunderstorms that occur primarily during summer months.
4888 There are no perennial streams in the Yucca Mountain area, and even the larger streams in the
4889 region are ephemeral. Throughout the Death Valley Basin, perennial flow only occurs
4890 downstream from springs and around the margins of low-lying playas where the water table
4891 intersects the land surface.

4892
4893
4894

6.4.2 Characteristics of the Fortymile Wash Drainage System

4895 Fortymile Wash is a fluvial system about 150 km long, that drains an area of 815 square
4896 km on the east and north of Yucca Mountain. It is an important fluvial system because it drains
4897 into the area near the RMEI where contaminated ash could be deposited from a volcanic vent
4898 intersecting the proposed repository. Surface water at Yucca Mountain drains mainly eastward
4899 toward Fortymile Wash, a tributary of the Amargosa River. The main tributaries to Fortymile
4900 Wash are Yucca Wash, located north of the proposed repository, Drill Hole Wash, which drains
4901 most of the potential repository area, and Busted Butte (Dune) Wash located south of the
4902 proposed repository.
4903

4904 Fortymile Wash crosses Highway 95 immediately east of Lathrop Wells (Amargosa
 4905 Desert) and continues southward, ultimately intersecting the Amargosa River. The Amargosa
 4906 River drains an area of about 8,000 square kilometers by the time it reaches Tecopa, California.
 4907 The mostly-dry river bed extends another 100 kilometers before ending in Death Valley.
 4908 Fortymile Wash has four distinct segments (Figure 6.12) with different morphologies: (1) a
 4909 broad northern area comprised of ephemeral streams (washes) that feed a central channel that
 4910 is incised in bedrock; (2) a central reach that deeply incises an alluvial fan of Plio-Pleistocene
 4911 age; (3) a segment near the intersection with Highway 95 that is referred to as the “active” fan
 4912 (northernmost part of the depositional basin); and (4) the remainder of the depositional basin
 4913 that consists of anastomosing channels that terminate at the juncture with the Amargosa River.
 4914



4915
 4916
 4917 Figure 6.12 LANDSAT Thematic Mapper image showing the Fortymile Wash drainage
 4918 system. The Pleistocene depositional basin has an Area of 136 km². Map Projection: Universal
 4919 Transverse Mercator, Zone 11 North, in Meters. [After Hooper (2005), Figure 3-1].
 4920

4921 The erosion, transport, and deposition of the sediments in Fortymile Wash are directly
 4922 related to the flow characteristics of the ephemeral stream and particularly to its flood
 4923 characteristics. Numerous continuous streamflow and peak-flow gauges have been operated
 4924 and monitored in the Yucca Mountain area. However, as of September 30, 1995 all but three
 4925 continuous and most of the peak-flow gauges were discontinued (DOE, 1997 [p. 3-14]). As of
 4926 September 30, 1997, the only continuous streamflow gauges operating near Yucca Mountain
 4927 were on Fortymile Wash near well UE-25 J-13 (“narrows” gauge) and near Amargosa Desert
 4928 (Bonner et al., 1998).
 4929

4930
4931
4932
4933
4934
4935
4936
4937
4938
4939
4940
4941
4942

The period of record for flooding in Fortymile Wash is less than 40 years. Waddell et al. (1984) reported that the U.S. Geological Survey (USGS) has collected monthly crest-stage data in the Yucca Mountain region since the early 1960s, using flood data from 12 crest-stage sites to estimate flood characteristics in the region. Data from 1969 to 1993, from six gauging stations are shown in Table 6.2.

The largest recorded flows occurred after a storm in February 1969, when the upper Amargosa River near Beatty, Nevada, carried a maximum flow of 450 m³/s. Squyres and Young (1984) estimated that in Fortymile Wash this flood had an estimated discharge of 93 m³/s and that the peak discharge may have reached 560 m³/s (Glancy and Beck, 1998). The 100-yr peak discharge for Fortymile Wash has been estimated at 340 m³/s (Squyres and Young, 1984).

Table 1-2. Peak Discharges at Stream Gauging Sites in the Fortymile Wash Area

Date	Peak Discharge (m ³ /s) [1 m ³ /s = 35.3 ft ³ /s]					
	10251250 Fortymile Wash at Narrows	10251252 Yucca Wash Near Mouth (Tributary)	10251254 Drillhole Wash at Mouth (Tributary)	10251255 Fortymile Wash Near Well J-13	10251256 Dune Wash Near Busted Butte (Tributary)	10251258 Fortymile Wash Near Amargosa Valley
January 25, 1969	— ^a	—	—	—	—	42.5
February 24–26, 1969	—	—	—	570	—	93.5
March 3, 1983	43.0	2.83	—	16.1	—	11.3
July 21–23, 1984	20.7	26.6	22.4	52.7	—	40.5
August 14–16, 1984	1.42	—	—	—	—	—
August 18–20, 1984	19.3	0.88	1.22	24.4	0.40	10.5
July 19–20, 1985	0.33	0.0003	0.48	0.17	2.66	0.09
February 23, 1987	—	—	—	—	—	0.02
May 7, 1987	—	< 0.003	—	—	—	—
November 6, 1987	—	—	—	—	—	0.02
September 23, 1990	—	—	—	—	—	0.02
August 12–13, 1991	—	—	—	—	—	—
September 7, 1991	—	—	—	—	0.12	—
February 12–15, 1992	0.68	0.42	—	—	0.04	—
March 30–31, 1992	—	< 0.03	—	—	0.03	—
January 17–19, 1993	1.50	2.26	—	—	—	—
February 9, 1993	—	—	—	—	—	—
February 23, 1993	—	—	—	—	—	—
January 25–27, 1995	0.20	5.24	—	—	0.08	—
March 11–13, 1995	85.0	—	0.003	85.0	0.08	34.0
February 23–24, 1998†	5.7	6.2	0.7	5.7	nd‡	9.6

4943
4944

4945
4946

Table 6.2. Peak discharges at stream gauges along Fortymile Wash [from Table 1-2 of Hooper, 2005, which was based on data from CRWMS M&O (2000a) and Tanko and Glancy, 2001].

4947
4948
4949
4950
4951
4952
4953
4954
4955
4956

The first documented case of a regional water-flow event during site characterization studies, in which Fortymile Wash and the Amargosa River flowed simultaneously throughout their reaches, took place on March 11, 1995 (Beck and Glancy, 1995). USGS and Nevada Test Site rain gauges showed that cumulative precipitation ranged from 5 to 15 cm during March 9 to 11, with the largest amounts falling at higher altitude sites. High-altitude snowmelt also probably contributed to the 10- to 12-hour runoff event in Fortymile Wash. The peak flow near the location where the existing Yucca Mountain access road crosses Fortymile Wash was

4957 reported at ~100 m³/s (Glancy and Beck, 1998 [p. 7]). This flow is much less than that
 4958 calculated as a 100-year flood event for Fortymile Wash (i.e., 340 m³/s).
 4959

4960 Squires and Young (1984) calculated discharge, area, width, mean velocity, and
 4961 maximum depth of flood flows for 100-year and 500-year exceedence recurrence frequencies
 4962 and maximum flood peak for various profiles across Fortymile Wash and its three major
 4963 tributaries in the Yucca Mountain area. Estimated peak discharges are shown in Table 6.3:
 4964

4965 Table 6.3. Estimated peak discharges along stream channels of Fortymile Wash at Yucca
 4966 Mountain.
 4967

4968 Wash	4969 Drainage Area (sq miles)	4970 100-year	4971 500-year	4972 Regional Maximum
4973 Fortymile	4974 810	4975 340	4976 1,600	4977 15,000
4978 Dune Wash (Busted Butte)	4979 17	4980 40	4981 180	4982 1,200
4983 Drill Hole	4984 40	4985 65	4986 280	4987 2,400
4988 Yucca	4989 43	4990 68	4991 310	4992 2,600

4978 Fortymile Wash apparently has not overflowed its banks near Yucca Mountain for
 4979 thousands of years. In the vicinity of wells J-12 and J-13 the channel is deeply incised in alluvial
 4980 fan deposits, and paleoindian artifacts are commonly seen on the surface adjacent to both
 4981 channel banks. They have not been carried away or buried by overbank flows.
 4982

4983 6.4.3 Approaches to Fluvial Sediment Transport and Erosion Evaluation

4984 6.4.3.1 NRC Approach to Fluvial Volcanic Ash Redistribution

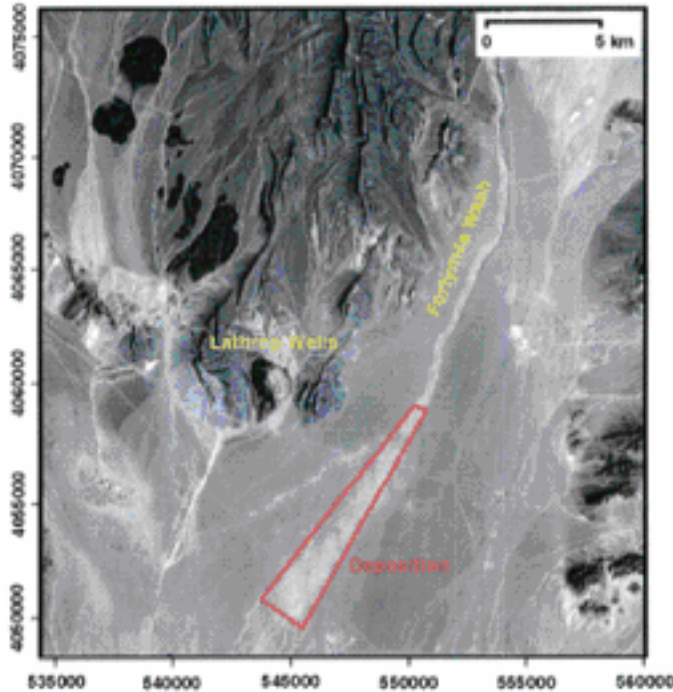
4987 Basaltic materials are common in the alluvial deposits along Fortymile Wash. Much of
 4988 this material probably originated from the extensive basalts in Jackass Flats, but some cobbles
 4989 and boulders have been rounded by abrasion during long-distance transport and may have
 4990 originated from the basalt units in the northern part of the drainage basin (i.e., Buckboard Mesa
 4991 and the basalts of Dome Mountain).
 4992

4993 NRC staff has developed a sediment budget approach to model the long-term fluvial
 4994 redistribution of basaltic tephra in Fortymile Wash (Hooper, 2005). In the event that extrusive
 4995 volcanism intersects the repository and transports waste in the volcanic tephra plume,
 4996 deposition of radionuclides may occur at the RMEI location from the remobilization of tephra by
 4997 water after initial deposition. A sediment budget was estimated to demonstrate the quantitative
 4998 relationship between components such as sediment yield, discharge to the depositional fan,
 4999 balance of remaining tephra, dilution by mixing of contaminated sediment with ambient
 5000 sediment, and associated changes in sediment storage over time. Using parameters specific to
 5001 Fortymile Wash and a hypothetical eruption at Yucca Mountain, Hooper (2005) concluded that
 5002 substantial tephra deposits can persist for more than 1,000 years in arid terrains, even with a
 5003 period of accelerated erosion after the eruption. Hooper (2005) estimated that ~98 percent of
 5004 the tephra deposit remains in the Fortymile Wash catchment basin after 100 years and 50
 5005 percent remains after 1,800 years. These results suggest that the amount of remobilized tephra
 5006 may be large—even when mixed with ambient sediment—and could significantly affect airborne
 5007 radioactive particle concentrations for the RMEI.

5008 The amount and distribution of hypothetical tephra deposits were calculated using the
5009 TEPHRA code (Connor et al., 2001). For each realization in performance assessment, the
5010 calculated tephra deposit is partitioned into (i) initial deposits (if any) at the receptor location, (ii)
5011 potential deposits in the Fortymile Wash drainage system that are subject to fluvial
5012 redistribution, and (iii) potential deposits in areas subject to wind erosion and transport (Benke
5013 et al., 2006). Areas of Fortymile Wash that lack tephra deposits are assumed to contribute
5014 uncontaminated sediment with the pre-eruption ambient sediment yield. A dilution factor is
5015 calculated as the ratio of contaminated sediment volume to the total (uncontaminated +
5016 contaminated) sediment volume assuming uniform mixing of sediments. The duration that
5017 Fortymile Wash yields contaminated sediment was estimated as the time for significant flow
5018 events to fully deplete the ash in the Fortymile Wash drainage system (Benke et al., 2006).
5019

5020 The NRC staff approach to fluvial ash redistribution assumes that all contaminated ash
5021 that is fluvially remobilized is deposited in the “active” fan, outlined in red in Figure 3-2 of
5022 Hooper (2005) [see Figure 6.13], but leaves the fan only by wind erosion. Wind then blows
5023 contaminated ash from the depositional fan toward the RMEI. However, wind is not permitted to
5024 remove contaminated ash from the drainage basin where ash was originally deposited. The
5025 entire tephra blanket in the drainage basin is assumed to ultimately be removed.
5026

5027 These assumptions appear to be conservative, leading to overestimates of hypothetical
5028 dose, because all contaminated ash removed by flooding is deposited and accumulated near
5029 the RMEI in a 24 km² area. The assumption that wind alone is permitted to move contaminated
5030 ash from the fan to the RMEI is inconsistent with the erosion model, in which the tephra blanket
5031 is eroded only by water - wind is not allowed to remove contaminated ash from the drainage
5032 basin. In reality, large floods would dominate the process of fluvial erosion and transport and
5033 would carry contaminated ash beyond the active fan and all the way to the Amargosa River and
5034 beyond. For example, in the short period of historical record, two large floods have reached
5035 Death Valley. The finer-grained materials that are potentially significant to the inhalation dose
5036 and could eventually be remobilized by wind would be the most likely components to stay in
5037 suspension during floods and to be deposited at and far beyond the active fan, the location of
5038 the RMEI. Moreover, major rain events can occur in parts of the system and not necessarily
5039 throughout the entire Fortymile Wash.



5040
5041

Figure 6.13 Landsat Thematic Mapper image showing the active part of the Fortymile Wash depositional (or alluvial) basin in red. Area of the active fan is $24 \pm 2 \text{ km}^2$ [$9.3 \pm 0.8 \text{ mi}^2$]. Map projection: Universal Transverse Mercator Zone 11 North, in meters.

5042

5043

5044

5045

5046

5047

5048

5049

5050

5051

5052

5053

5054

5055

5056

5057

5058

5059

5060

5061

Overall, the NRC approach appears to be a simplistic view of ephemeral stream dynamics. Fortymile Wash is not always dominated by erosion and the active fan is not always dominated by deposition. Small flow events would not even reach the fan and instead would produce deposits in the Wash that are flushed out by the biggest flow events. Precipitation in this basin is not homogeneous in space or time because most of the Fortymile Wash drainage basin occurs to the north at higher elevations. It is possible to have isolated rain events to the north that cause major flooding in the wash (and erosion of the depositional fan) but no local sheet wash erosion of the tephra blanket. Also, in arid regions such as Yucca Mountain, most of the erosion and long-distance sediment transport takes place during the largest discharge events, which are rare. The sediments most likely to be suspended and transported long distances are the smallest particles¹⁰. The sediments of Fortymile Wash fan are relatively coarse, consisting mainly of sand and gravel pavements that dropped out of suspension quickly following Stokes' Law, while the finer materials have been winnowed out and carried downstream. Particles of concern in health physics will not settle out of overland flows until the water infiltrates, evaporates, or ponds.

5062

6.4.3.2 EPRI Analysis of Fluvial Transport from Extrusive Volcanic Activity

5063

5064

5065

EPRI (2004) commented on various conservatisms used in the NRC and DOE analyses. EPRI's model of ash transport modeling showed that particles smaller than 130 microns in

¹⁰ The Wentworth scale classifies silt particles in the range from 4 - 62 microns. Clay particles are smaller than 4 microns. In a motionless water column, all of the sand drops out in 40 seconds and silts drop out of suspension in 2 hours (re: Stokes Law). After 2 hours only clays would remain in suspension.

5066 diameter would not be deposited at the compliance point (the RMEI). Both DOE and NRC use
5067 a conservative assumption that all deposited material is in the respirable size range, although
5068 neither NRC nor DOE discuss realistic mechanisms that would break down ash in this way.
5069

5070 **6.4.3.3 DOE Volcanic Ash Fluvial Redistribution Model**

5071
5072 DOE (2003) has developed a model for fluvial redistribution of volcanic ash that initiates
5073 with tephra being transported by hillside erosion. Sediment then moves into drainages and is
5074 transported via drainages that coalesce into larger and larger channels. Water and sediment
5075 from different channels begin a mixing process that ultimately leads to a homogeneous
5076 sediment containing materials from all drainages in the basin (Folk,1980). This mixing of
5077 sediments occurs everywhere that sediment is transported by water, including intermittent
5078 streams. Mixing occurs at higher rates and involves larger clasts in larger drainages than
5079 smaller ones and on steeper hillslopes than on low-gradient land surfaces. Sediment mixing
5080 also occurs from wind transport across the landscape. Drainage channels that develop across
5081 newly deposited tephra sheets exhibit the same processes as observed in streams, and,
5082 produce well-mixed sediment loads.
5083

5084 In the Yucca Mountain area, sediments in drainage channels are commonly clasts of
5085 welded tuff and wind-blown quartz sand, which are more durable than basaltic tephra. Mixing of
5086 sediments occurs very rapidly, and welded tuff clasts and quartz sand/silt deposits are more
5087 abundant in the larger channels, so that the ash component from Lathrop Wells has been
5088 progressively diluted during transport relative to the total sediment volume. Eolian processes
5089 also mix sand and silt with the fluvially transported materials. The ratio of basaltic ash to non-
5090 ash continues to decrease with the passage of time.
5091

5092 DOE has performed studies of ash redistribution near Lathrop Wells to evaluate the
5093 fraction of basaltic ash components as a function of distance from the tephra sheet. These data
5094 indicate that the concentration of basaltic ash in sediments decreases to about 50 percent within
5095 1 km of the head of the tephra sheet drainage on the eastern side of Lathrop Wells, whereas the
5096 channel on the west side has less than 40 percent basaltic ash after 1 km of transport. The
5097 indicated dilution factor is 50 to 60 percent per kilometer.
5098

5099 Fortymile Wash is a major 800-km² drainage basin that includes the entire eastern slope
5100 of Yucca Mountain and the Fortymile Wash alluvial fan. Understanding the redistribution
5101 processes along Fortymile Wash is important to volcanic-eruption consequence scenarios. The
5102 fan spreads out into the Amargosa Valley from the mouth of Fortymile Wash. In the upper or
5103 northern half of the fan, the channels are well defined and widely spaced, with sizable
5104 interstream area between all pairs of channels. These interstream divide tracts are more
5105 prominent on the upper fan. On the lower fan they are neither as topographically prominent nor
5106 as wide because the distributary channels become progressively closer on the lower fan.
5107 Previous worldwide aboveground nuclear tests introduced radioactive ¹³⁷Cs into the
5108 atmosphere. ¹³⁷Cs forms a time-stratigraphic marker in alluvial or eolian deposits and can be
5109 used to assess the extent of local erosion and deposition. The depth to which ¹³⁷Cs infiltrates
5110 into the soil can be used as a general proxy for the depth to which sorbing radionuclides may
5111 infiltrate after deposition with volcanic ash (DOE, 2003). To evaluate erosion rates on the upper
5112 Fortymile Wash fan, soil samples were taken for analysis of ¹³⁷Cs concentrations (BSC, 2003b).
5113 The analyses show that the upper-fan inter-stream divide areas have been eroding over the last
5114 50+ years and have lost 1 to 2 cm of the upper soil horizon, most likely as a result of wind
5115 erosion, rather than from removal by fluvial processes (BSC, 2003b). There is also evidence of
5116 some eolian deposition on these same surfaces.

5117
5118 The majority of the fan surface is interstream divide area, from which 1 to 2 cm of
5119 material, on average, has been removed during the last 50 years. When large floods occur, the
5120 flood waters can carry large quantities of sediment rapidly southward across the fan to the
5121 Amargosa River and may overflow channel banks forming small patches of overbank deposits.
5122 As flood levels subside, the suspended and bedload materials in the channel flow are deposited
5123 within the channels and are stored in the channel until the next flood occurs (BSC, 2003b). In
5124 contrast to the inter-stream divide areas, the amount of sediment deposited in channels varies
5125 greatly from location to location. In TSPA, DOE models distributary channel areas as having a
5126 layer of contaminated ash of uncertain thickness that appears immediately following the
5127 eruption. This layer will be of variable thickness, ranging from zero to several tens of
5128 centimeters (represented by a uniform distribution from 0 to 15 cm) (DOE, 2003). Although
5129 sediment thickness may exceed 15 cm, it is likely that contributions to dose from radionuclides
5130 at greater depths will be negligible. Observations of ¹³⁷Cs content also indicate that
5131 radionuclides are unlikely to migrate more than 9 cm into sediment below the ash layer due to
5132 the widespread presence of carbonate layers in soil (DOE, 2003). Within any portion of the fan
5133 contaminated ash will be removed and deposited continuously, and average values for layer
5134 thickness are used as input in TSPA. Dilution of contaminated tephra would occur during
5135 transport in distributary channels. However, field data are insufficient to quantify this reduction
5136 in concentrations for the Fortymile Wash drainage and fan (DOE, 2003). DOE's TSPA
5137 conservatively assumes that the concentration of radionuclides in the contaminated sediment in
5138 the channel areas is the same as that derived from ASHPLUME for the mid-line of a plume
5139 about 18 km from the vent. The extent to which this assumption overestimates concentrations is
5140 not well known but may be large, especially for eruptive events in which the wind is blowing
5141 from the west or southwest and the ash deposition occurs upstream from the location of the
5142 RMEI. DOE considers the use of a single concentration to represent a spatially variable
5143 parameter to be reasonable because exposures would be integrated over a region that is large
5144 compared to the scale of local variability (BSC, 2003b).

5145
5146 DOE reports, based on observations from the Lathrop Wells Cone, that volcanic ash
5147 would not remain indefinitely in the channel area. The time needed to remove most tephra from
5148 the basin is unknown but is substantially less than the age of the Lathrop Wells Cone (DOE,
5149 2003). Given the limited amount of residual ash observed near Lathrop Wells, the time required
5150 to remove most ash from the basin may be very short, perhaps on the scale of centuries.
5151 DOE's TSPA approach applies a uniform removal rate to channel deposits such that the initial
5152 layer is entirely removed within an uncertain period of time that is sampled uniformly between
5153 100 and 1,000 years. Some residual contamination will likely persist indefinitely after the tephra
5154 deposits are eroded (DOE, 2003).

5155
5156 DOE's current approach in modeling atmospheric dispersal and deposition of tephra
5157 from a potential volcanic eruption at Yucca Mountain is documented in the model report BSC
5158 (2005). The report documents the conceptual and mathematical model (Ashplume) for
5159 atmospheric dispersal and subsequent deposition of ash on the land surface from a potential
5160 volcanic eruption. The report also documents the conceptual model for ash (tephra)
5161 redistribution. The Ashplume conceptual model accounts for incorporation and entrainment of
5162 waste fuel particles associated with a hypothetical volcanic eruption through the repository and
5163 downwind transport of contaminated tephra. The Ashplume mathematical model describes the
5164 conceptual model in mathematical terms to allow for prediction of contaminated ash deposition
5165 on the ground. BSC (2005) also describes the conceptual model for tephra redistribution within
5166 Fortymile Wash and on its alluvial fan. Sensitivity analyses and model validation activities for the
5167 ash dispersal and redistribution models are presented. DOE considered models for

5168 atmospheric dispersal of contaminated tephra during and after violent Strombolian eruptions of
5169 the type that could occur in the Yucca Mountain region and for redistribution of contaminated
5170 tephra after the volcanic eruption. If such an eruption were to intersect the repository, the
5171 possibility exists for wastes to become entrained in the eruptive mixture and be transported via
5172 the same mechanisms as the ash plume. Although other eruption types that include nonviolent
5173 as well as violent phases exist, the violent Strombolian eruption has the greatest potential to
5174 erupt ash and waste particles high into the atmosphere, thus increasing the potential distance of
5175 dispersal. DOE's Ashplume conceptual model includes only the eruptive ash plume,
5176 convective/dispersive transport of contaminated ash particles downwind, and deposition on the
5177 ground surface. The Ashplume mathematical model can be used to evaluate ash and waste
5178 concentration at any point or multiple points on the surface relative to the volcanic vent. DOE's
5179 ash redistribution conceptual model describes the erosion and subsequent deposition of
5180 contaminated ash. A new set of wind data collected at Desert Rock (near Mercury, Nevada)
5181 was used to calculate wind speed and direction up to a height of 13 km. This data set replaces
5182 the Nevada Test Site data that were used for the TSPA-SR. Parameterization for the
5183 atmospheric dispersal model used in all ASHPLUME versions was documented in Igneous
5184 Consequence Modeling for the TSPA-SR (BSC, 2001). Tephra deposit thicknesses were
5185 simulated using ASHPLUME 1.4LV and compared with actual tephra deposit thicknesses from
5186 the 1995 eruptive event at the Cerro Negro volcano in Nicaragua. DOE's ash redistribution
5187 conceptual model is new and was not used in the TSPA-SR.
5188

5189 BSC (2005, Appx. I) also developed an alternative numerical model for ash and fuel
5190 redistribution that calculates near-surface and at-depth fuel (waste) concentrations through time
5191 in soil columns near the RMEI location. This alternative model was designed to provide a more
5192 complete representation of the redistribution mechanisms involved, and to eliminate the mass
5193 balance conservatism of the simplified ash redistribution conceptual model. This alternative
5194 model is still under development by DOE (BSC, 2005, Appx. I). It uses a spatially-distributed
5195 Geographic Information System (GIS) framework to calculate the ash and fuel transported to the
5196 RMEI location from the upper Fortymile Wash watershed by hillslope and fluvial processes. This
5197 redistributed ash and fuel is combined with any primary ash and fuel that was hypothetically
5198 deposited directly on the RMEI location. By explicitly modeling the primary ash fall and
5199 redistribution processes, the model directly computes how much volcanic ash and fuel would be
5200 transported to the RMEI location under any wind conditions.
5201

5202 DOE's alternative redistribution model (BSC, 2005, Appx. I) further considers the fate of
5203 ash and fuel delivered to the RMEI location, distinguishing between channels and recent (< 10
5204 kyr) depositional surfaces (i.e., "channels"), and older (> 10 kyr) interchannel divide surfaces on
5205 the RMEI location. In the model, ash and fuel delivered from the upper Fortymile Wash
5206 watershed are deposited only in channels. This treatment assumes that areas of the RMEI
5207 location that have not been subject to fluvial erosion or deposition over the last 10 kyr will not be
5208 subject to fluvial activity within the next 10 kyr. The model also distinguishes between channels
5209 and divides for the purposes of modeling fuel redistribution in the soil profile. Vertical
5210 redistribution within the soil profile is modeled as a diffusion process. The lower boundary of the
5211 soil layer represents the presence of impermeable soil horizons. The alternative redistribution
5212 model evaluates over time the surface and depth-averaged fuel concentration on channels and
5213 divides at the RMEI location after an eruption (BSC, 2005, Appendix I).
5214

5215 The alternative model does not incorporate eolian erosion or deposition or the long-term
5216 geologic dynamics of fan interchannel divide and channel interactions (BSC, 2005, Appx. I).
5217 Several key assumptions are made under the alternate model. First, it is assumed the climate
5218 through much of the regulatory period will be similar to today's climate and will have relatively

5219 little impact on the Fortymile Wash alluvial fan even with a projected increase in annual
5220 precipitation. The rationale for this is that the expected effects of increased precipitation would
5221 include more vegetation and this will result in less ash being derived from the hillslopes. Total
5222 precipitation during a pluvial climate would be greater, but increased storm intensities or peak
5223 channel discharges would not be expected. The precipitation increase would come primarily
5224 from more frequent rainfall events (BSC, 2005, Appendix I).
5225

5226 The second assumption is that the model assumes distributary channels in the RMEI
5227 location do not migrate (BSC, 2005, Appendix I). Therefore, the areal fraction of channels and
5228 interchannel divides would not change with time. The rationale for this is that fans are dynamic
5229 landforms that can evolve topographically over both long and short time scales. A distinction
5230 can be made, however, between the evolution of alluvial fans over millions of years and the
5231 evolution of “entrenched” alluvial fans over shorter time scales. In tectonically-active areas and
5232 over millions of years, alluvial fans *aggrade* by sedimentation in channels and by channel
5233 migration. Over these long time scales, alluvial fans are best considered to be subject to
5234 redeposition across the entire fan area. The Quaternary period has caused cycles of channel
5235 aggradation and incision on alluvial fans in the western US. As a result, fluvial activity on many
5236 fans is restricted to a small fraction of the piedmont area near the modern channels. Older
5237 terraces are commonly preserved from previous episodes of aggradation and incision, but are
5238 no longer subject to fluvial activity even during extreme events based on evidence of pavement
5239 development. Surface characteristics observed in the field, including well-developed *desert*
5240 *pavement* and *varnish*, provide evidence for the stability of channels and the lack of significant,
5241 soil-disruptive floods on interchannel divides. Well-developed desert pavements and varnish
5242 have been observed on divides near the RMEI location, indicating that most of these
5243 interchannel divides are Pleistocene in age and have not been flooded for at least 10,000 years.
5244 As a result, they may be considered stable for treatment in performance assessment (BSC,
5245 2005, Appendix I).
5246

5247 The third assumption is that the model assumes eolian transport to the RMEI location
5248 can be neglected compared with fluvial transport processes (BSC, 2005, Appendix I). The
5249 rationale for this is that fluvial transport is considered the dominant redistribution process for ash
5250 and fuel from the upper Fortymile Wash because (1) the prevailing wind is away from the RMEI
5251 location and towards the drainage basin (so eolian transport is most likely to redistribute ash
5252 into the drainage basin, away from the RMEI location), and (2) fluvial transport processes in a
5253 tributary drainage system focus transported material onto the RMEI location, while eolian
5254 processes disperse ash by repeated episodes of entrainment, turbulent dispersion in the
5255 atmosphere, and redeposition (BSC, 2005, Appendix I).
5256
5257

5258 **6.4.3.4 NWTRB Comments on Potential Consequences of Igneous Activity**

5259

5260 The Nuclear Waste Technical Review Board (NWTRB) has commented (NWTRB, 2002)
5261 that performance assessment calculations appear to show that “igneous activity is the largest
5262 contributor by far to radioactive dose during the first 10,000 years,” an observation that was
5263 repeated in a report the following year (NWTRB, 2003). However, the NWTRB observed in its
5264 2002 report that the igneous activity model proposed by NRC may be a “conservative end-
5265 member” model. It should be noted that this particular report of the NWTRB predates many of
5266 the observations and analyses discussed in previous sections of the present report.
5267

5268 At the September, 2002, meeting of the NWTRB, Dr. William Melson, a consultant on
5269 igneous activity issues to the NWTRB, commented that studies of the mama-waste package

5270 interaction should focus on identifying conditions that would lead to disruption of the waste
5271 package and release of radioactive material from the package, in particular the effects of
5272 temperatures in excess of 1200^o C. and the effects of corrosive gases on the package welds.
5273 Dr. Melson also commented on the “dog-leg” scenario, in which magma moves down the drift
5274 and then out through a secondary vent. This scenario would involve the largest number of waste
5275 packages with magma entering the drift. Dr. Melson noted that this was a worst-case scenario,
5276 and its probability of occurrence was small (Melson, 2002).
5277

5278 In 2003, the NWTRB made three recommendations regarding igneous activity:

5279 that the DOE conduct modeling studies of compressible fluids

5280 that the DOE study the waste package-magma interaction, including both
5281 chemical and mechanical interactions and

5282 that the DOE study aeromagnetic anomalies near the Yucca Mountain site.
5283
5284
5285

5286 These recommendations were repeated in the NWTRB’s 2004 report to Congress
5287 (NWTRB, 2004), and a further recommendation was made that the DOE study incompressible
5288 (as well as compressible) flow of magma into the repository.
5289
5290

5291 **6.4.4 NRC and DOE Analysis of Effects of Eolian Transport and Erosion**

5292
5293
5294 Eolian (wind) transport could result in an inhalation dose to the RMEI in the extrusive
5295 scenario. Eolian transport can move radioactively contaminated ash from fluvial deposits as well
5296 as from material deposited on the surface of the ground as a result of the eruption itself. The
5297 mechanism of eolian transport is the same in both cases: ash is remobilized by wind, and the
5298 remobilized ash is carried and dispersed predominantly downwind. The shape of the
5299 remobilized plume depends on particle mass and density and on meteorological conditions. A
5300 review of dispersion, including the dispersion of the initial plume, is presented in Section 3.4.
5301 The present section expands on that initial discussion and on the relationship between the
5302 dispersed ash plume and radiation dose to the RMEI.
5303

5304 **6.4.4.1 NRC Analysis**

5305
5306 The vent size, event power, and duration of each simulated eruption and atmospheric
5307 conditions determine the tephra dispersal and deposition pattern and thickness, and
5308 radionuclide soil concentrations. These parameters are treated statistical in performance
5309 assessment calculations. The calculated doses from an eruption are strongly influenced by the
5310 timing of the event. Events that occur more than 1000 years after repository closure would
5311 result in essentially no dose from even the longer-lived fission products like Cs-137 and Sr-90.
5312 Because any significant external dose would be a gamma dose from these fission products,
5313 such events would not result in an external dose. There could, however, be both inhalation and
5314 ingestion doses to the RMEI, though the former would be more significant than the latter.
5315

5316 The Suzuki model, which the NRC uses, models the initial plume as moving as much as
5317 60 km downwind, so that resuspended particles need move only short distances to be inhaled
5318 by the RMEI. Dose calculation then depends on the composition of the remobilized particles.
5319 Assuming that all remobilized particles are contaminated ash, as NRC does, is conservative to

5320 an unknown extent. Jarzempa et al. (1997) modified the Suzuki ash transport model and
5321 incorporated it in the TPA code (both Version 4.1 and Version 5.0) to calculate the distribution of
5322 the released radionuclides during a hypothetical eruption through a repository. The time-
5323 dependent density of deposited radionuclides takes into account the thickness of the tephra
5324 deposit, leaching and erosion rates, and radionuclide decay. Radionuclides can persist in the
5325 environment and can cause exposure hundreds to thousands of years after the event, although
5326 erosion and mixing with uncontaminated soil will decrease the concentration of radionuclides to
5327 which the RMEI is exposed.

5328
5329 NRC's TPA analysis indicates that the risk would be a maximum at about 225 years.
5330 The NRC treated the sensitivity analyses for volcanism parameters separately for the extrusive
5331 and intrusive scenarios. Radiation doses to the RMEI resulting from an extrusive scenario could
5332 be larger than doses from consumption of ground water so that these doses can be neglected
5333 (Mohanty et al., 2004). This suggests that ingestion doses are neglected also in the NRC
5334 analysis, because ingestion doses would arise from groundwater contamination. The NRC
5335 sensitivity analyses for igneous activity parameters calculate the sensitivity of a "conditional"
5336 dose to various parameters. This "conditional" dose does not include probability of a volcanic
5337 event. The relative sensitivity of the risk of this dose to various parameters might be different if
5338 the event probability were included in the calculation.

5339
5340 Mohanty et al. (2004 [Table 3-16]) list key parameters for igneous activity that were used
5341 in NRC's TPA analysis. Note that NRC treats the eruptive event as having a mean power of
5342 4.31×10^{10} watts and a mean duration of 4.85×10^5 seconds (5.6 days). The simulated volcanic
5343 conduit has a width ranging from 25 to 78 m (mean of 51 m). In TPA 4.1 all waste packages
5344 contacted by magma are assumed to fail (Mohanty et al., 2004). Waste packages within a drift
5345 penetrated by a dike, but outside the volcanic conduit, are assumed to fail and expose the spent
5346 nuclear fuel to subsequent water contact, while those within the conduit are assumed to become
5347 entrained in the magma and released directly to the surface and the biosphere. For a 50 m
5348 diameter conduit, 10 or fewer waste packages (each ~5 m long) could be entrained.

5349
5350 In the TPA analysis the wind direction during an eruption was assumed to always be
5351 toward the south, in the general direction of the RMEI; this is an assumption common to many
5352 dispersion calculations. A more realistic treatment of wind is now being incorporated in TPA.
5353 This is especially important given that the two most influential parameters in the sensitivity
5354 analysis relate to eolian dispersion (i.e., mass of soil in the air above a fresh volcanic ash
5355 blanket and wind speed) (see Table 4-5 of Mohanty et al., 2004).

5356
5357 The calculated risk from volcanism appears to be small within the 10,000-year simulation
5358 period (Mohanty et al., 2004). The igneous activity scenario increased the peak expected risk in
5359 10,000 years to 3.6 $\mu\text{Sv/yr}$ [0.36 mrem/yr]. Results from a range of alternative conceptual
5360 models for waste form dissolution, waste package lifetime, and radionuclide transport resulted in
5361 calculated doses that were well within the EPA standard. The ground water ingestion dose from
5362 igneous activity is similar to the dose in the basecase with faulting events (see Mohanty et al.,
5363 2004, Figure 3-14). The increase in groundwater dose from igneous activity is smaller than that
5364 for faulting events because only 53 waste packages are failed by the intrusive igneous activity
5365 as compared to 208 waste packages failed by the faulting event in the mean value, single-
5366 realization case. Without probability weighting, extrusive igneous events result in a peak ground
5367 surface dose of approximately 0.1 Sv/yr [10,000 mrem/yr] at 4,900 years, which is the time of
5368 the volcanic event, and the dose exponentially decreases thereafter (see Mohanty et al., 2004,
5369 Figure 3-14).

5370

5371 For the ground surface pathway, the areal densities calculated for each radionuclide,
5372 computed with the ASHPLUME (Jarzemba et al., 1997) ash transport model, are used in
5373 determining the total effective dose equivalents. Dose conversion factors are computed
5374 internally in the TPA Version 4.1 code by using GENTPA, a modification of the GENII computer
5375 code (Napier et al., 1988). Subsequent versions of the TPA code use Federal Guidance report
5376 13 (Eckerman et al, 1999).

5377
5378 The NRC has estimated particle size distribution of ash particles and has estimated the
5379 dimensions and density of spent fuel particles that could be incorporated into and dispersed with
5380 the ash. The code ASHPLUME (DOE, 2000) has been used to model this dispersion. The NRC
5381 has designed a new module, REMOB, for estimating resuspension and remobilization, but
5382 ACNW has not seen the equations or results for that model. Parameters like breathing rate and
5383 exposure time are generally estimated by engineering judgment, and should be the subject of
5384 sensitivity analyses. NRC has not considered an ingestion dose to the critical group or RMEI.

5385
5386 NRC does not appear to have accepted the Anspaugh formulation, but has postulated a
5387 larger fraction of resuspended material considering the longer times during which resuspension
5388 of contaminated ash can take place. NRC also assumes that all resuspended material,
5389 resuspended at any time after the eruption, is ash (i.e., none of it is the underlying original soil).

5390
5391 If there is an igneous event, the peak dose to the RMEI would occur earlier in the
5392 postclosure period than in the absence of an igneous event, and the dose to the RMEI would
5393 probably be larger. The difference between doses calculated using these scenarios gradually
5394 decreases with time, and is approximately an order of magnitude at 10,000 years.

5395
5396 The most recent NRC simulations of extrusive volcanism at Yucca Mountain are
5397 documented in Mohanty et al. (2005, p. iii), where the NRC staff summarized the following
5398 overall results:

5399
5400 Analyses to assist staff in understanding the significance of features, events, and
5401 processes associated with extrusive volcanism include estimates of the impact of (i)
5402 wind-field variability assumptions, (ii) ash deposition and remobilization, (iii) ash mass
5403 loading, (iv) assumptions regarding spent nuclear fuel incorporation and initial plume
5404 velocity, and (v) drift degradation on magma-waste package interactions. Results of
5405 these analyses for 10,000 years indicate (i) current assumptions for ash mass loading
5406 and wind-field speed and direction are reasonable; the assumptions have the potential to
5407 affect the dose estimate by approximately one order of magnitude, (ii) alternative mass
5408 loading reduces dose estimates by approximately a factor of two, (iii) current and
5409 alternative models for spent nuclear fuel incorporation and initial plume velocity cause
5410 only small differences in dose estimates, and (iv) no effects on the peak eruptive
5411 risk are estimated from coupling drift degradation with the number of entrained waste
5412 packages. Ash remobilization and wind variations are implemented in an alternative
5413 model.

5414
5415 Mohanty et al. (2005) present the following conclusions related to the volcanic extrusion
5416 scenario and ash deposition/remobilization:

5417
5418 Redistribution of contaminated ash appears unlikely to increase significantly the
5419 estimated peak dose arising from a volcanic eruption over the case in which the ash is
5420 directly deposited at the RMEI location. Although not a likely bounding approach, fixing

5421 the wind direction to the south appears reasonable to account for the effect of
5422 remobilization of the contaminated ash.

5423
5424 Overall, results suggest variability in the wind field does not significantly alter the
5425 estimated peak dose at the RMEI location. Fixing the wind direction to the south appears
5426 a reasonably conservative approach to account for the effect of a variable wind field.

5427
5428 Analysis estimates composite daily mass loading varies by approximately a factor of two
5429 for a wide range of duration for the peak values (i.e., 5 to 50 percent of the time). Using
5430 the medium value for the composite mass loading for fresh ash conditions {i.e., 1.12
5431 mg/m^3 [7.0×10^{-8} lbm/ft^3]} and soil conditions {i.e., 0.1 mg/m^3 [6.2×10^{-9} lbm/ft^3]} in the
5432 TPA code resulted in approximately a factor of two reduction in the overall dose
5433 estimate. The results from this analysis were considered in developing mass loading
5434 parameters in the latest version of the TPA code.

5435 5436 5437 **6.4.4.2 DOE Analysis**

5438
5439 The 50-year ^{137}Cs record suggests that eolian removal of material has been the major
5440 process causing erosion (DOE, 2003). In the interstream divides, erosion removes sediment at
5441 a relatively rapid rate of 1 to 2 cm per 50 years. DOE's TSPA model calculates doses using the
5442 initial ash-layer thicknesses and radionuclide concentrations from ASHPLUME, modified by a
5443 time dependent soil removal factor, estimated to range from 0.02 to 0.04 cm/yr (DOE, 2003).
5444 Given these erosion rates, ash layers will be removed within a few centuries, depending on
5445 initial thickness. Based on field observations, it is likely some fine-grained ash and
5446 radionuclides will persist in the soil below the initial ash layer, and some additional radionuclides
5447 may be brought into the interstream divide areas by infrequent flooding events that cover the
5448 entire fan. Based on ^{137}Cs data, it is estimated that residual contamination after erosion removal
5449 of the tephra deposits will be on the order of 0.01 of the initial ASHPLUME radionuclide
5450 concentration (BSC, 2003b).

5451
5452 Like the NRC, DOE uses ASHPLUME to model the initial eolian dispersion of
5453 contaminated ash, as well as the generally accepted convention that airborne resuspended
5454 material is dispersed in the same way as any airborne material. DOE has recently validated
5455 both its dispersion and inhalation models by using measurements of total suspended
5456 particulates raised both by eolian resuspension and by mechanical disturbance of the soil
5457 surface, as in farming (BSC, 2006). Validation of dispersion by wind and meteorological
5458 conditions has also used the dispersion of ash from other volcanic eruptions. DOE's literature
5459 reviews suggest that ash from basaltic volcanoes has a somewhat smaller concentration of very
5460 fine particles (10 microns or less) than ash from other volcanoes (like Mt. St. Helens), but that
5461 these are the particles that are carried furthest from the eruption site, to the vicinity of the RMEI
5462 if the RMEI is downwind from the eruption. In addition, BSC (2006) cites extensive literature
5463 reports of measurements of dispersed and remobilized particle sizes, and the sizes of particles
5464 that can contribute to inhalation dose, concentrating on particles of 10 microns diameter or less
5465 (particles designated as PM_{10} by EPA). The DOE biosphere model assumes that particles of 1
5466 micron aerodynamic diameter play the greatest role in inhalation dose (BSC 2006, p. 6-23) and,
5467 like Jarzempa and LaPlante (1997) assumes a triangular distribution.

5468
5469 DOE has validated its ASHPLUME modeling by examining the distribution of ash from the
5470 Lathrop Wells cone as well as from Cerro Negro (DOE, 2004). Hill et al. (1998) have also
5471 verified the use of the Suzuki (1983) formulation in modeling ash distribution from Cerro Negro.

5472 Apparently, DOE does not use the Anspaugh model for eolian redistribution, but depends on its
5473 own validation of redistribution as well as for the original atmospheric dispersion of ash. It is not
5474 clear that NRC has done a direct validation.
5475

5476 **6.4.5 Summary**

5477
5478 The radiation doses and risks to the RMEI associated with remobilization of contaminated
5479 ash from an igneous event depend on estimation of the following parameters:
5480

- 5481 • particle size and density of spent fuel and fission products released in the event
- 5482 • particle size and density of tephra and ash
- 5483 • diameter and density of particles that would be incorporated into ash dispersed from an
5484 igneous event
- 5485 • total mass of material from an igneous event
- 5486 • momentum vector of the emission
- 5487 • parameters used in applying the Suzuki and atmospheric dispersion models
- 5488 • areal extent of fluvial dispersion
- 5489 • areal extent of vegetation exposed to deposited material
- 5490 • elapsed time between the igneous even and exposure of the critical group.
- 5491 • DCF reference document used to calculate dose
- 5492 • breathing rate
- 5493 • external exposure time
5494

5495 Both NRC and DOE favor using Federal Guidance Report (FGR) 13 (Eckerman et al, 1999)
5496 rather than FGR 11 and 12 as a source of dose conversion factors. Since the uptake models of
5497 FGR 13 are a considerable refinement when compared to earlier clearance models, FGR 13
5498 dose conversion factors are widely accepted and agreed to.
5499

5500 Dose conversion factors like those specified in FGR 13, although presented as single
5501 values, rely on intake, retention, metabolism, and excretion models, and therefore include
5502 inherent uncertainties. Moeller and Ryan (2005) noted:
5503

5504 “The science of internal dosimetry has undergone significant progress and
5505 dramatic change during the years [since 1960].... It is
5506 essential, therefore, that the analysts and regulators acknowledge that these
5507 changes have occurred, that the dose estimates will differ depending on the
5508 basis on which they are made, and that caution must be exercised to ensure
5509 that these factors are taken into consideration in interpreting the outcomes
5510 Differences in dose coefficients can result in changes in dose estimates
5511 by an order of magnitude depending on the source from which [the dose
5512 coefficients] were obtained....
5513

5514 For example, the dose conversion factor for ^{129}I is strongly influenced by the intake of stable
5515 iodine in the diet (food and water) (Moeller and Ryan, 2004). Another example is from a recent
5516 paper on dose conversion factors for ^3H and ^{14}C (Richardson and Dunford, 2001) This paper
5517 notes:
5518

5519 “It is shown how the dose coefficients for intakes of tritium and ^{14}C
5520 compounds are affected by different interpretations of the methods
5521 recommended by the ICRP for two of the three classes of vapors and

5522 gases. Some aspects of the ICRP models, such as the percent
5523 oxidized, would benefit from reconsideration so as to produce tritium
5524 and 14C biokinetics that are less dependent on the radionuclide.”
5525

5526 The potential dose to the RMEI is the compliance criterion, and is also the culmination of
5527 all the assumptions that have gone into the analysis of an igneous event. Both NRC and DOE
5528 consider the inhalation dose (including inhalation of resuspended material) much more
5529 significant than an external dose. Neither agency has considered the possibility of an ingestion
5530 dose. NRC in its application of risk insights, calculates a quantity called a “probability-weighted
5531 dose” (Mohanty et al., 2005) that results from the inhalation of resuspended material. By the
5532 quantitative definition of how risk is calculated – the product of probability and consequence for
5533 the igneous activity scenario – this could be considered a risk. However, the significance of a
5534 “probability-weighted dose” is not clear. Since probabilities are always fractions, a probability-
5535 weighted dose will be a smaller number than the corresponding inhalation dose. From the
5536 receptor’s point of view, this can be confusing and perhaps misleading. NRC should be
5537 encouraged to clarify the meaning of this expression.
5538

5539 The NRC employed several alternative models, varied the degree to which SNF was
5540 incorporated in ash, varied the wind direction and other dispersion parameters, considered a
5541 range of remobilizations, and notes that these variations result in variations of the inhalation
5542 dose to the RMEI by factors between two and ten. This appears to be a useful approach to
5543 generating performance assessment inputs (inputs to the TPA) and results in a truly risk-
5544 informed analysis. The NRC considers that the maximum contribution to inhalation dose is from
5545 particles of approximately one micron AMAD (Compton, 2004) or less and that lesser effects are
5546 derived from larger particle sizes.
5547

5548 The DOE (2004) uses the same assumptions as NRC about the range of diameter and
5549 density of spent nuclear fuel particles that can be incorporated into ash particles, and also cites
5550 Jarzemba and La Plante (1997). DOE defines the particle density as a function of the fraction of
5551 magma incorporated into the ash particle. The resulting range of contaminated ash particle
5552 densities is similar to that postulated by NRC. DOE does make the point that the frequency of
5553 wind blowing toward the RMEI location is considerably smaller than wind blowing away from the
5554 RMEI, so that the probability of an inhalation dose from resuspended material is relatively small.
5555 DOE further postulates that the high winds in the vicinity of the RMEI make persistence of a
5556 thick remobilizable layer of undiluted contaminated tephra unlikely.
5557

5558 DOE considers two scenarios for RMEI exposure: (1) exposure to contaminated ash is
5559 primarily due to eolian dispersion, and (2) exposure is due to remobilized, resuspended fluvially
5560 dispersed ash. DOE postulated the first as less likely because of the relatively infrequent high
5561 winds in the direction of the RMEI.
5562

5563 **6.5 Summary (Igneous Consequences)**

5564 The consequences for future radiological exposures vary significantly among three
5565 hypothetical scenarios for volcanic interaction with the repository. These scenarios include an
5566 intrusive event, an extrusive (volcanic) event, and secondary breakouts of magma from a
5567 repository at some distance from the point of initial intersection (so-called “dogleg” scenario).
5568

5569 **The extrusive event** - DOE has estimated that the median number of waste packages that
5570 would be disrupted in a volcanic eruption scenario (i.e., intercepted by a conduit) is fewer than
5571
5572

5573 10. The NRC staff currently assumes that volcanic vents would have an average diameter of
5574 ~50 m. If the center of a vent were to coincide with the axis of a drift, then ~5 waste packages
5575 could be entrained within the cross-section of the conduit and potentially transported to the
5576 surface. Apparently due to the complexity of the processes involved, neither the NRC nor DOE
5577 evaluate magma-drift-waste package interactions in any detail. They instead assume that a
5578 small number of waste packages are completely destroyed and the contents are carried to the
5579 surface via a volcanic conduit in a cone-forming event. However, it is unclear how or whether
5580 the Alloy-22 waste packages or the ceramic or glass waste forms themselves would be reduced
5581 to particles of respirable size, as currently assumed by the DOE and NRC staff. EPRI has
5582 concluded, based on multiple lines of evidence, that it is unlikely that waste packages would be
5583 breached by magma during an active eruption period. EPRI found that the expected
5584 consequence of an igneous extrusive event would be zero releases of radioactive matter from
5585 the repository to the atmosphere.

5586
5587 **The intrusive event** - DOE has estimated the number of waste packages that could be
5588 damaged in a potential future igneous event. The igneous intrusion scenario shows a range of
5589 consequences, extending from virtually no waste packages damaged to nearly all waste
5590 packages in the repository. The 50th percentile value indicates approximately 1600 waste
5591 packages could be impacted, out of over 11,000 waste packages in the repository. In TPA 4.1
5592 the NRC staff estimated a mean value of 37 magma- induced mechanical failures from an
5593 intrusion event, based on a log uniform distribution from 1 to 1402 waste package failures.
5594 Igneous activity causes the largest increase in dose conditionally from both groundwater and
5595 airborne pathways, but the risk is still small when the probability of the volcanic event is factored
5596 into the calculations. EPRI concluded that magma viscosity would be larger than previously
5597 assumed. They estimate that only 0-6 waste packages could become engulfed by magma
5598 intrusion in a waste emplacement drift. They further estimate that 14-24 waste packages could
5599 be significantly affected by heat and corrosive gases (but not engulfed by magma).

5600
5601 Viscosity is the most important magma property to understand because it controls the
5602 flow behavior and the distance that magma could penetrate a repository in the unlikely event of
5603 volcanic intersection. ACNW observes that previous researchers have not been consistent in
5604 their approach to estimating the viscosity of the Yucca Mountain basalt as it ascends and
5605 degasses with approach to the surface. There has been a tendency to assume rheological
5606 properties pertaining to both wet, cool magmas and dry, hot magmas, leading incorrectly to the
5607 postulate of a highly explosive system with highly mobile lavas. Therefore, previous claims of
5608 severe consequences of igneous intersection appear to be poorly founded. The potential Yucca
5609 Mountain magma is likely a wet, cool explosive magma with relatively immobile lavas. The
5610 Pleistocene lava flows in Crater Flat and at Lathrop Wells demonstrate that the lavas had very
5611 high viscosities and were relatively immobile. Characteristics of these lava flows indicate
5612 viscosities orders of magnitude larger than had been assumed in analyses of igneous
5613 interaction with a repository. These high viscosities, along with magma solidification effects,
5614 would significantly reduce the distance that magma could penetrate into tunnels and thereby
5615 reduce the number of impacted waste packages.

5616
5617 The so-called “dogleg” scenario refers to a hypothetical scenario proposed by the NRC
5618 staff in which magma might rapidly fill a drift and create enough pressure to generate (at a
5619 distance from the entry point) a secondary dike to the surface. This “dog-leg” model was
5620 analyzed by the Igneous Consequences Peer Review (ICPR) Panel (Detournay et al., 2003), by
5621 EPRI, and by DOE. In TPA 4.1 analyses the NRC staff assumed that a mean value of 51 waste
5622 packages could be entrained by an extrusive event and contained in volcanic ejecta. ICPR
5623 considered the propagation of either a magmatic or pyroclastic “dog-leg” scenario to be quite

5624 improbable, found that the initial and boundary conditions in the model are unrealistic, but
5625 recommended further analyses to assess the impacts of a partially coupled pyroclastic flow
5626 scenario on repository performance. EPRI concluded that their independent modeling results
5627 show that pressure conditions in a repository intersected by magma would be significantly less
5628 forceful than postulated by the NRC staff. DOE concluded that the “dogleg” model
5629 overestimates the violence of magma-repository interaction. Use of realistic boundary
5630 conditions (including compressible walls and backfill, permeable country rock and backfill,
5631 phase separation in the magma-volatile mixture, partial blockage of the drift by waste canisters
5632 and other engineering features, and the axial spacing of the canisters) would greatly reduce the
5633 amplitude of any shock wave that might form. Use of realistic initial conditions such as a dike tip
5634 would preclude shock waves for all but the most rapid magma ascent rates.
5635

5636 **Remobilization** – Assuming a hypothetical volcanic eruption through a repository, DOE
5637 has performed studies of ash redistribution near Lathrop Wells to evaluate the fraction of
5638 basaltic ash components as a function of distance from the tephra sheet. These data indicate
5639 that the concentration of basaltic ash in sediments would decrease to about 50 percent within 1
5640 km of the head of the tephra sheet drainage on the eastern side of Lathrop Wells, whereas the
5641 channel on the west side has less than 40 percent basaltic ash after 1 km of transport. DOE’s
5642 TSPA model calculates doses using the initial ash-layer thicknesses and radionuclide
5643 concentrations from ASHPLUME, modified by a time dependent soil removal factor, estimated
5644 to range from 0.02 to 0.04 cm/yr. Given these erosion rates, ash layers would be removed
5645 within a few centuries, depending on initial thickness.
5646

5647 The NRC staff has developed a sediment budget approach to model the long-term fluvial
5648 redistribution of basaltic tephra in Fortymile Wash. Using parameters specific to Fortymile
5649 Wash and a hypothetical eruption at Yucca Mountain, they concluded that substantial tephra
5650 deposits can persist for more than 1,000 years in arid terrains, even with a period of accelerated
5651 erosion after the eruption. It is estimated that ~98 percent of the tephra deposit remains in the
5652 Fortymile Wash catchment basin after 100 years and 50 percent remains after 1,800 years.
5653 NRC suggests that the amount of remobilized tephra may be large—even when mixed with
5654 ambient sediment—and could significantly affect airborne radioactive particle concentrations for
5655 the RMEI. The NRC staff assumes that all contaminated ash that is fluvially remobilized would
5656 be deposited in an “active” fan located west of the RMEI, but once it gets there, no ash is
5657 permitted to leave this fan area *except* by wind erosion.
5658

5659 ACNW has observed that large floods would dominate the process of fluvial erosion and
5660 transport and would carry contaminated ash beyond the active fan and all the way to the
5661 Amargosa River and beyond. In the short period of historical record, two large floods in the
5662 Fortymile Wash/Amargosa River system have reached Death Valley. The sediments most likely
5663 to be suspended and transported long distances are the smallest particles – the same particles
5664 of concern for respiration or ingestion.
5665

5666 EPRI has commented on various conservatisms used in the NRC and DOE analyses.
5667 EPRI’s model of ash transport modeling showed that particles smaller than 130 microns in
5668 diameter would not be deposited at the compliance point. Both DOE and NRC use a
5669 conservative assumption that all deposited material is in the respirable size range, although
5670 neither NRC nor DOE discuss realistic mechanisms that would break down tephra in this way.
5671

5672 Eolian (wind) transport could result in an inhalation dose to the RMEI in the extrusive
5673 scenario. Eolian transport can move radioactively contaminated ash from fluvial deposits as
5674 well as from material deposited on the surface of the ground as a result of the eruption itself.

5675 The mechanism of eolian transport is the same in both cases: ash is remobilized by wind, and
5676 the remobilized ash is carried and dispersed predominantly downwind. The shape of the
5677 remobilized plume depends on particle mass and density and on meteorological conditions.
5678

5679 Both DOE and NRC have estimated triangular particle size distribution of ash particles,
5680 with the mean and mode at 1 micron aerodynamic diameter. Both agencies have estimated the
5681 dimensions and density of spent fuel particles that could be incorporated into and dispersed with
5682 the ash. The code ASHPULME has been used to model this dispersion. The NRC has
5683 designed a new module, REMOB, for estimating resuspension and remobilization, but ACNW
5684 has not seen the equations or results for that model. If there is an igneous event, the peak dose
5685 to the RMEI would occur earlier in the postclosure period than in the absence of an igneous
5686 event, and the dose to the RMEI would probably be larger. The difference between doses
5687 calculated using these scenarios gradually decreases with time, and is approximately an order
5688 of magnitude at 10,000 years.
5689

5690 Like the NRC, DOE uses ASHPULME to model the initial eolian dispersion of
5691 contaminated ash, as well as the generally accepted convention that airborne resuspended
5692 material is dispersed in the same way as any airborne material. DOE appears to have accepted
5693 the Anspaugh formulation of both long-term and short-term resuspension. DOE makes the
5694 point that the frequency of wind blowing toward the RMEI location is considerably smaller than
5695 wind blowing away from the RMEI, so that the probability of an inhalation dose from
5696 resuspended material is relatively small. DOE further postulates that the high winds in the
5697 vicinity of the RMEI make persistence of a thick remobilizable layer of undiluted contaminated
5698 tephra unlikely. NRC does not appear to have accepted the Anspaugh formulation, but has
5699 postulated a larger fraction of resuspended material considering the longer times during which
5700 resuspension of contaminated ash can take place. NRC also assumes that all resuspended
5701 material, resuspended at any time after the eruption, is ash (i.e., none of it is overburden). DOE
5702 has validated its ASHPULME modeling by examining the distribution of ash from the Lathrop
5703 Wells cone as well as from Cerro Negro. Both NRC and DOE favor using Federal Guidance
5704 Report (FGR 13) (Eckerman et al, 1999) rather than FGR 11 and 12 as a source of dose
5705 conversion factors. Since the uptake models of FGR 13 are a considerable refinement when
5706 compared to earlier clearance models, FGR 13 dose conversion factors are widely accepted
5707 and agreed to.
5708

5709 **7. Conclusions**

5710 [To be completed at the termination of the Igneous Activity Working Group meeting.]
5711

5712 **REFERENCES**

- 5713
5714
5715 ACNW, 2005. Letter to NRC Chairman N. Diaz from ACNW Chairman M. Ryan dated
5716 December 9, 2005. Review of the NRC Program on the Risk from Igneous Activity at the
5717 Proposed Yucca Mountain Repository. NRC Accession No. ML0534900650.
5718
5719 Anspaugh, L. R., Simon, S. L., Gordeev, K.I., Likhtarev, I. A., Maxwell, R.M., Shinkarev, S.M.
5720 2002. Movement of Radionuclides in Terrestrial Systems by Physical Processes, *Health*
5721 *Physics*, 82, 669-678.
5722
5723 Anspaugh, L. R., 2004, Perspectives on Resuspension Modeling, Presentation to the 153rd
5724 Meeting of the NRC Advisory Committee on Nuclear Waste, Las Vegas, NV, September, 2004.

5725
5726 BSC (Bechtel SAIC Company, LLC), 2003a. Characterize Framework for Igneous Activity at
5727 Yucca Mountain, Nevada. ANL-MGR-GS-000001 REV 01C. Las Vegas, Nevada: Bechtel SAIC
5728 Company. ACC: MOL.20030711.0103.
5729
5730 BSC 2003b. Atmospheric Dispersal and Deposition of Tephra from a Potential Volcanic
5731 Eruption at Yucca Mountain, Nevada. MDL-MGR-GS-000002 REV 00D. Las Vegas, Nevada:
5732 Bechtel SAIC Company. ACC: MOL.20030922.0197.
5733
5734 BSC (Bechtel SAIC Company, LLC), 2004, Dike/Drift Interactions. MDL-MGR-GS-000005 REV
5735 01, Las Vegas, Nevada: Bechtel SAIC Company.
5736
5737 BSC (Bechtel SAIC Company, LLC), 2005, Atmospheric Dispersal and Deposition of Tephra
5738 from a Potential Volcanic Eruption at Yucca Mountain, Nevada. MDL-MGR-GS-000002 REV 02.
5739 Las Vegas, Nevada: Bechtel SAIC Company.
5740
5741 BSC (Bechtel SAIC Company, LLC), 2006, Inhalation Exposure Input Parameters for the
5742 Biosphere Model. ANL-MGR-MD000001, REV 4 Las Vegas, Nevada: Bechtel SAIC Company.
5743
5744 Beck, D.A., and P.A. Glancy, 1995, Overview of runoff of march 11, 1995 in Fortymile Wash and
5745 Amargosa River, Southern Nevada, U.S. Geological Survey Fact Sheet FS-210-95.
5746
5747 Biasi, Glenn, 2005, Tomographic Imaging of the Crust and Upper Mantle in the Southern Great
5748 Basin – Interpretation, Narrative to accompany the DOE PVHA – II presentation, February 15,
5749 2005.
5750
5751 Blakely, R.J., V.E. Langenheim, D.A. Ponce, and G.L. Dixon, 2000, Aeromagnetic Survey of the
5752 Amargosa Desert, Nevada and California: A tool for Understanding Near-Surface Geology and
5753 Hydrology, U.S. Geol. Surv.. Open-File Report 00-188.
5754
5755 Bonner, L. J., P.E. Elliott, L.P. Etchemendy, and J.R. Swartwood, 1998, Water Resources Data,
5756 Nevada, Water Year 1997, US Geol. Surv. Water Data Rpt. NV-97-1, 636 p.
5757
5758 Brandeis, G., and B.D. Marsh, 1989, The convective liquidus in a solidifying magma chamber: A
5759 fluid dynamical investigation, *Nature*, 339, 613-616.
5760
5761 Brocher, T.M., W.C. Hunter, and V.E. Langenheim, 1998, Implications of seismic reflection and
5762 potential field geophysical data on the structural framework of the Yucca Mountain-Crater Flat
5763 Region, Nevada, *Geol. Soc. Of Am. Bull.*, 105, 947-971.
5764
5765 Bruce, P.M., and H.E. Huppert, 1990, Dolidification and melting along dykes by the laminar flow
5766 of basaltic magma. In M. P. Ryan (ed.) *Magma Transport and Storage*. J. Wiley and Sons, NY,
5767 87-101.
5768
5769 Byers, F.M., Jr., W.J. Carr, and P.P..Orkild, 1989, Volcanic centers of Southwestern Nevada:
5770 Evolution of Understanding, 1960-1988, *Jour. of Geophy. Res.*, 94, 5,908-5,924.
5771
5772 Carr, W. J., and L. D. Parrish, 1985, Geology of drill hole USW VH-2, and structure of Crater
5773 Flat, southwestern Nevada, U.S. Geol. Surv. Open File Rep. 85-475, 41 p.
5774
5775 Calabrese, E. J. and Kenyon, E. M. 1991. *Air Toxics and Risk Assessment*, Chelsea, MI.

5776
5777 CNWRA, 2004, System-Level Performance Assessment of the Proposed Repository at Yucca
5778 Mountain Using the TPA Version 4.1 Code, Revised March 2004.
5779
5780 Christiansen, R.L., P.W. Lipman, W.J. Carr, F.M. Byers, Jr., P.P. Orkild, and K.A. Sargent,
5781 1977, The Timber Mountain-Oasis Caldera complex of Southern Nevada, *Bull. Geol. Soc. Of*
5782 *Am.*, 88, 943-959.
5783
5784 Codell, R.B., 2004, Alternative igneous source term model for tephra dispersal at the Yucca
5785 Mountain repository, *Nuclear Tech.*, 48, 205-212.
5786
5787 Coleman, N. M., B. D. Marsh, and L. R. Abramson, 2004, Testing claims about volcanic
5788 disruption of a potential geologic repository at Yucca Mountain, NV, *Geophys. Res. Lett.*,
5789 doi:10.1029/2004GL021032.
5790
5791 Compton, K. C. 2004. NRC Staff Perspective on Modeling Doses Due to Igneous Events,
5792 Presentation to the ACNW, September 23rd 2004, Las Vegas, NV.
5793
5794 Connor, C. B., and B. H. Hill, 1995, Three nonhomogeneous Poisson models for the probability
5795 of basaltic volcanism: Application to the Yucca Mountain region, NV, *Jour. of Geophys. Res.*,
5796 100, 10,107– 10,125.
5797
5798 Connor, C. B., J. A. Stamatakos, D. A. Ferrill, and B. E. Hill, 1998, Detecting strain in the Yucca
5799 Mountain area (comment), *Science*, 282, 1007b.
5800
5801 Connor, C. B., J. Stamatakos, D. Ferrill, B. Hill, G. Ofoegbu, F. Conway, B. Sagar, and J. Trapp,
5802 2000, Geologic factors controlling patterns of small-volume basaltic volcanism: Application to a
5803 volcanic hazards assessment at Yucca Mountain, NV, *Jour. of Geophys. Res.*, 105, 417– 432.
5804
5805 Connor, L., C. Connor, and B. Hill, 2002, PVHA_YM Ver. 2.0 –Probabilistic volcanic hazards
5806 assessment methods for a proposed high-level radioactive waste repository at Yucca Mtn., NV,
5807 NRC Accession ML030240079, Center for Nuclear Waste Regulatory Analyses (CNWRA), San
5808 Antonio, Tex.
5809
5810 Crowe, B.M., 2005, Revisiting temporal models: Uncertainty perspectives, Proceedings of
5811 Workshop #2A of the DOE Probabilistic Volcanic Hazard Analysis Update, Las Vegas, NV,
5812 August 31, 2005.
5813
5814 Crowe, B. M., M. E. Johnson, and R. J. Beckman, 1982, Calculation of the probability of
5815 volcanic disruption of a high-level radioactive waste repository within southern Nevada, USA,
5816 *Radioactive Waste Management & Nuclear Fuel Cycle*, 3, 167– 190.
5817
5818 Crowe, B.M., S. Self, D. Vaniman, R. Amos, and F. Perry, 1983, Aspects of potential magmatic
5819 disruption of a high-level radioactive waste repository in southern Nevada, *Jour. Of Geol.*, 91,
5820 259-276.
5821
5822 Crowe, B. and nine others, 1995, Status of Volcanism Studies for the Yucca Mountain Site
5823 Characterization Project, Report of the Las Alamos National Laboratory LA-12908-MS.
5824

5825 Crowe, B. M., G. A. Valentine, F. V. Perry, and P. K. Black, 2006, *Volcanism: The Continuing*
5826 *Saga*, In A. Macfalane and R. Ewing (eds.) *Uncertainty Underground – Yucca Mountain and the*
5827 *Nation’s High-Level Nuclear Waste*, The MIT Press, Cambridge, MA, 131-148.
5828
5829 CRWMS M&O, 1998, *Synthesis of Volcanism Studies for the Yucca Mountain Site*
5830 *Characterization Project. Deliverable 3781MR1. Las Vegas, Nevada: ACC:*
5831 *MOL.19990511.0400.*
5832
5833 CRWMS M&O, 2000a, *Yucca Mountain Site Description Document, . Section 7—Surface Water*
5834 *Hydrology. TDR–CRW–GS–000001. Rev. 01 ICN 01. Las Vegas, Nevada:*
5835 *CRWMS M&O.*
5836
5837 CRWMS M&O, 2000b *“Total System Performance Assessment for the Site Recommendation.”*
5838 *TDR–WIS–PA–000001. Rev. 00 ICN 01. Las Vegas, Nevada: CRWMS M&O.*
5839
5840 CRWMS M&O, 2001, *Geochemical and Isotopic Constraints on Groundwater Flow Directions,*
5841 *Mixing, and Recharge at Yucca Mountain, Nevada. ANL-NBS-HS-000021. Las Vegas, Nevada.*
5842
5843 Dartevelle, S., and G.A Valentine, 2005, *Early-time multiphase interactions between basaltic*
5844 *magma and underground openings at the proposed Yucca Mountain radioactive waste*
5845 *repository, Geophys. Res. Lett., doi:1029/2005GL0241172.*
5846
5847 Decker, R., and B. Decker., 1997, *Volcanoes*, Freeman, San Francisco, CA, 321 p.
5848
5849 Delaney, P.T., and D.D. Pollard, 1981, *Deformation of host rocks and flow of magma during*
5850 *growth of minette dikes and breccia-bearing intrusions near Ship Rock, New Mexico, U.S. Gov.*
5851 *Print. Of., Washington, DC.*
5852
5853 Delaney, P.T., and D.D. Pollard, 1982, *Solidification of basaltic magma during flow in a dike,*
5854 *Am. Jour. Of Sc., 282, 856-885.*
5855
5856 Delaney, P.T., and A.E. Gartner, 1997, *Physical processes of shallow mafic dike emplacement*
5857 *near the San Rafael Swell, Utah, Bull. Geol. Soc. Of Am., 109, 1,172-1,192.*
5858
5859 Del Marmol, M., 1989, *The petrology and geochemistry of Merapi volcano, central Java,*
5860 *Indonesia. Ph.D., Dissertation, Johns Hopkins University, 384 p.*
5861
5862 Detournay, E., L. G. Mastin, J.R. Anthony Pearson, A. M. Rubin, and F. J. Spera, 2003, *Final*
5863 *Report [April 2003] of the [Yucca Mountain] Igneous Consequences Peer Review Panel, 86 pp.*
5864
5865 DOE (US Department of Energy), 1997, *Site Characterization Progress Report: Yucca*
5866 *Mountain, Nevada. Number 15, DOE/RW-0498, Washington, DC, Office of Civilian Radioactive*
5867 *Waste Management.*
5868
5869 DOE (US Department of Energy), 1999, *MGR External Events Hazards Analysis, ANL-MGR-*
5870 *SE-000004, Rev. 00, CRWMS M&O, Las Vegas, Nevada.*
5871
5872 DOE (U S Department of Energy), 2000. *ASHPLUME: Characterize Eruptive Processes at*
5873 *Yucca Mountain, Nevada ANL-MGR-GS-000002, Las Vegas, NV.*
5874

5875 DOE (U S Department of Energy), 2003, Volcanic Events, Tech. Basis Doc. 13, Bechtel SAIC
5876 Co., LLC, Las Vegas, Nev. (Available at [http://](http://www.ocrwm.doe.gov/documents/38453_tbd/index.htm)
5877 www.ocrwm.doe.gov/documents/38453_tbd/index.htm).
5878
5879 Doubik, P., and B. Hill, 1999, Magmatic and hydromagmatic conduit development during the
5880 1975 Tolbachik eruption, Kamchatka, with implications for hazards assessment at Yucca
5881 Mountain, NV, *Jour. Of Volcanology and Geothermal Res.*, 91, 43-64.
5882
5883 Eckerman, K. F. and J. C. Ryman, 1993, External Exposure to Radionuclides in Air, Water,
5884 and Soil US EPA, Washington, DC
5885
5886 Eckerman, K. F., R. W. Leggett, C. B. Nelson, J. S. Puskin, and A. C. B. Richardson, 1999,
5887 Cancer Risk Coefficients for Environmental Exposure to Radionuclides. US EPA, Washington,
5888 DC.
5889
5890 EPA (US Environmental Protection Agency), 1993, 40 CFR Part 191, Environmental Radiation
5891 Protection Standards for the Management and Disposal of Spent Nuclear Fuel, High-Level and
5892 Transuranic Radioactive Wastes", in the Federal Register 58 FR 66398, December 20, 1993.
5893
5894 EPA (US Environmental Protection Agency), 2001, 40 CFR 197: Public Health and
5895 Environmental Radiation Protection Standards for Yucca Mountain Nevada, Final Rule. Federal
5896 Register 66, 32074-32135, Washington, DC.
5897
5898 EPA (US Environmental Protection Agency), 2005, 40 CFR 197 Public Health and
5899 Environmental Radiation Protection Standards for Yucca Mountain Nevada, Proposed Rule,
5900 Federal Register 70, 49014-49065, Washington, DC.
5901
5902 EPRI (Electric Power Research Institute), 2003, Igneous Event Scenario, Technical Update
5903 Report No. 1007898, December 2003.
5904
5905 EPRI (Electric Power Research Institute), 2004, Potential igneous processes relevant to the
5906 Yucca Mountain repository: Extrusive-release scenario, Analysis and Implications, EPRI Tech.
5907 Rept. 1008169.
5908
5909 EPRI (Electric Power Research Institute), 2005, Program on Technology Innovation: Potential
5910 igneous processes relevant to the Yucca Mountain repository: Intrusive-release scenario, EPRI
5911 Tech. Rept. 1011165.
5912
5913 Evans, J.R., and M. Smith, III, 1992, Teleseismic tomography of the Yucca Mountain region:
5914 volcanism and tectonism, American Nuclear Society, *Proceedings of the Third Annual*
5915 *International Conference on High-Level Radioactive waste Management*, 2, 2,372-2,380.
5916
5917 Evans, J.R., and M. Smith, III, 1995, Teleseismic Investigations, Chapter 7, Major Results of
5918 Geophysical Investigations at Yucca Mountain and Vicinity, Southern Nevada (eds., Oliver,
5919 H.W., Ponce, D.A., and Hunter, W.C.), US Geol. Surv. Open-File Report 95-74, 135-156.
5920
5921 Ferrill, D.A., J.A. Stamatakos, S.M. Jones, B. Rahe, H.L. McKague, R.H. Martin, and A.P.
5922 Morris, 1996, Quaternary slip history of the Bare Mountain fault (Nevada) from the morphology
5923 and distribution of alluvial fan deposits, *Geology*, 24, 559-562.
5924

- 5925 Ferrill, D.A., J.A. Stamatakos, and D.Sims, 1999, Normal fault corrugation: Implications for
5926 growth and Seismicity of active normal faults, *Jour. Struct. Geol.*, 21, 1,027-1,038.
5927
- 5928 Fink, J.H., and R.W. Griffiths, 1998, Morphology, eruption rate and rheology of lava domes:
5929 Insights from laboratory models, *Jour. Of Geophys. Res.*, 103, p. 527-545.
5930
- 5931 Fisher, R.V., G. Heiken, and J.B. Hulen, 1997, *Volcanoes: Crucible of Change*, Princeton
5932 University Press, Princeton, NJ, 317 p.
5933
- 5934 Fleck, R. J., B. D. Turrin, D. A. Sawyer, R. G. Warren, D. E. Champion, M. R. Hudson, and S. A.
5935 Minor, 1996, Age and character of basaltic rocks of the Yucca Mountain region, southern
5936 Nevada, *Jour. of Geophys. Res.* 101, 8,205-8,227.
5937
- 5938 Fridrich, C., J. Whitney, M. Hudson, and B. Crowe, 1999, Space-time patterns of L. Cenozoic
5939 extension, vertical axis rotation, and volcanism in the Crater Flat Basin, SW Nevada, in
5940 Cenozoic Basins of the Death Valley Region, *Geol. Soc. Of Am. Spec. Pap.* 333, 197–212.
5941
- 5942 Garrick, B.J., and Kaplan, S., 1995, Radioactive and mixed waste: Risk as a basis for waste
5943 classification, National Council of Radiation Protection and Measurements Symposium
5944 Proceedings No. 2, Bethesda, MD, NCRP, 59-73.
5945
- 5946 Gay, E.C., P.A. Nelson, and W. P. Armstrong, 1969. Flow properties of suspensions with high solid
5947 concentrations. *Am.Inst. of Chem. Eng. Jour.*, 15, 815-822.
5948
- 5949 Geomatrix Consultants, 1996, Probabilistic volcanic hazard analysis for Yucca Mountain, NV,
5950 Rep. BA0000000-1717-2200-00082, Rev. 0, San Francisco, Calif.
- 5951 Glancy, P. A., and D. A. Beck, 1998, Modern flooding and runoff of the Amargosa River,
5952 Nevada-California, emphasizing contributions of Fortymile Wash, in Taylor, E.M., (ed.),
5953 Quaternary geology of the Yucca Mountain area, southern Nevada: Friends of the Pleistocene,
5954 Pacific Cell, October 1998, Field Trip Guide, 51-62.
- 5955 Grauch, V.J.S., D.A. Sawyer, and C.J. Fridrich, 1999, Southwestern Nevada Volcanic Field and
5956 Hydrogeologic Implications, U.S. Geol. Surv. Professional Paper 1608, 39 p.
- 5957 Griffiths, R.W., 2000, The dynamics of lava flow, *Annu. Rev. Fluid Mech.*, 32, 477-518.
- 5958 Hallett, R.B., 1992, Volcanic Geology of the Rio Puerco Necks." *San Juan Basin IV: NewMexico*
5959 *Geological Society, 43rd Annual Field Conference, September 30-October 3, 1992*, Lucas, S.G.;
5960 Kues, B.S.; Williamson, T.E.; and Hunt, A.P.; eds. 135-144. [Socorro, New Mexico]: New
5961 Mexico Geological Society.
- 5962 Hardy, M.P., and S.J. Bauer, 1991, Rock Mechanics Considerations in Designing a Nuclear
5963 Waste Repository in Hard Rock, US Symposium on Rock Mechanics, Sandia Rept. SAND-91-
5964 2853C, 19 p.
- 5965 Heizler, M. T., F. V. Perry, B. M. Crowe, L. Peters, and R. Appelt, 1999, The age of the Lathrop
5966 Wells volcanic center: An ⁴⁰Ar/³⁹Ar dating investigation, *Jour. Of Geophys. Res.* 104, 767-804.
5967

5968 Hill, B.E., C. B. Connor, M.S. Jarzempa, P.C. La Femina, M. Navarro, and W. Strauch, 1998,
5969 1995 eruptions on Cerro Negro volcano, Nicaragua, and risk assessment for future eruptions,
5970 *Bull. Geol. Soc. Of Am.* 110, 1,231-1,241.
5971
5972 Hill, B. E. and C. B. Connor, 2000, Technical basis for resolution of the igneous activity key
5973 technical issue, CNWRA report (NRC accession # ML011930254).
5974
5975 Hill, B. E., and J. A. Stamatakos, 2002, Evaluation of geophysical information used to detect
5976 and characterize buried volcanic features in the Yucca Mountain region, CNWRA report for U.
5977 S. Nuclear Regulatory Commission, Washington, D. C.
5978
5979 Ho, C.-H., 1992, Risk assessment for the Yucca Mountain high-level nuclear waste repository
5980 site: Estimation of volcanic disruption, *Math. Geol.*, 24, 347-364.
5981
5982 Ho, C.-H., E. I. Smith, D. L. Feuerbach, and T. R. Naumann, 1991, Eruptive probability
5983 calculation for the Yucca Mountain site, USA: statistical estimation of recurrence rates, *Bull. of*
5984 *Volcanology*, 54, 50-56.
5985
5986 Ho, C.-H., and E. I. Smith, 1997, Volcanic hazard assessment incorporating expert knowledge:
5987 Application to the Yucca Mountain region, NV, USA, *Math. Geol.*, 29, p. 615–627.
5988
5989 Ho, C.-H., and E. I. Smith, 1998, A spatial-temporal/3-D model for volcanic hazard assessment:
5990 Application to the Yucca Mountain region, NV, *Math. Geol.*, 30, 497–510.
5991
5992 Ho, C.-H., E.I. Smith, and D.L. Keenan, 2006, Hazard area and probability of volcanic disruption
5993 of the proposed high-level radioactive waste repository at Yucca Mountain, Nevada, USA, *Bull.*
5994 *Volcanol*, DOI 10.1007/s00445-006-0058-5.
5995
5996 Hooper, D.M., 2005, Modeling the long-term fluvial redistribution of tephra in Fortymile Wash,
5997 Yucca Mountain, Nevada, CWRA Report.
5998
5999 Hort, M., B.D. Marsh, R.G. Resmini, and M.K. Smith, 1999, Convection and crystallization in a
6000 liquid cooled from above: An experimental and theoretical study, *Jour. Petrology*, 40, 1,271-
6001 1,300.
6002
6003 Huppert, H.E., 1982, Flow and instability of a viscous current down a slope, *Nature*, 300, 427-
6004 429.
6005
6006 Jaeger, J.C., and N.G.W. Cook, 1979, *Fundamentals of rock mechanics*, Chapman and Hall,
6007 New York.
6008
6009 Jarzempa, M.S., and P. A. LaPlante, 1996, Preliminary Calculations Of Expected Dose From
6010 Extrusive Volcanic Events At Yucca Mountain, CNWRA Report.
6011
6012 Jarzempa, M.S., 1997, Stochastic Radionuclide Distributions after a Basaltic Eruption for
6013 Performance Assessments of Yucca Mountain. *Nuclear Technology*, 118, 132–141. La Grange
6014 Park, Illinois: American Nuclear Society.
6015
6016 Kaplan, S., and B.J. Garrick, 1981, On the quantitative definition of risk, *Risk Analysis*, 1, 11-27.
6017

6018 Keating, G.N., and G.A. Valentine, 1998, Proximal stratigraphy and syn-eruption faulting in
6019 rhyolitic Grants Ridge Tuff, New Mexico, USA, *Jour. Of Vol. and Geothermal Res.*,81, 37-49.
6020
6021 Kokajko, L.E., 2005, Staff Review of US Department of Energy Response to Igneous Activity
6022 Agreement Item IA.2.17, Letter with Enclosures (January 10) to J.D. Ziegler, DOE, Washington,
6023 DC, US NRC.
6024
6025 Krier, D., G.A. Valentine, F.V. Perry, and G. Heiken, 2006. Eruptive and geomorphic processes
6026 at Lathrop Wells scoria cone volcano, *Eos Trans.*, American Geophysical Union, 87, Fall Meet.
6027 Suppl., Abstract V51 A-1663.

6028 Larsen, G., K. Grönvold, and S. Thorarinsson, 1979, Volcanic eruption through a geothermal
6029 borehole at Námafjall, Iceland, *Nature* 278, 707 - 710 (19 April 1979), DOI:10.1038/278707a0.

6030 Lee, M.P., N.M. Coleman, and T.J. Nicholson, 2005, History of Water Development in the
6031 Amargosa Desert Area: A Literature Review, U.S. Nuclear Regulatory Commission, *NUREG-*
6032 *1710, Vol. 1*, February 2005.
6033
6034 Leggett, R.W., and K. F. Eckerman, 2003, Dosimetric Significance of the ICRP's Updated
6035 Guidance and Models, 1989-2003, and Implications for U.S. Federal Guidance. ORNL/TM-
6036 2003/207. Oak Ridge National Laboratory.
6037
6038 Lescinsky, D.T., and O. Merle, 2005, Extensional and compressional strain in lava flows and the
6039 formation of fractures in surface crust. In Manga, M. and G.Ventura (eds.), *Geol. Soc. Of Am.*,
6040 Special Paper 396, 163-179.
6041
6042 Lore, J., H. Gao, and A. Aydin, 2000, Viscoelastic thermal stress in cooling basalt flows, *Jour.*
6043 *Geophys. Res.*, 105, 23,695-23,709.
6044
6045 Marsh, B.D., 1981, On the crystallinity, probability of occurrence, and rheology of lava and
6046 magma, *Contr. Min. Pet.*, 78, 85-98.
6047
6048 Marsh, B.D., 1989, Convective style and vigour in magma chambers. *Jour. Petrology*, 30, 479-
6049 530.
6050
6051 Marsh, B.D., 1990, Atka, Central Aleutian Islands, In C.A. Wood and J. Kienle (eds.) *Volcanoes*
6052 *of North America, United States and Canada*, Cambridge University Press.
6053
6054 Marsh, B.D., 2002, On bimodal differentiation by solidification front instability in basaltic
6055 magmas, part I: basic mechanics, *Geochimica et Cosmochimica Acta*, 66, 2,211-2,229.
6056
6057 Marsh, B.D., 2004, A magmatic mush column rosetta stone: The McMurdo Dry Valleys of
6058 Antarctica, *EOS, Trans. Amer. Geophys. Union*, 85,.497-502.
6059
6060 Marsh, B. and N. Coleman, 2006, Near-surface eruptive state of wet versus dry magma. Paper
6061 No. 183-1, *Geological Society of America Abstracts with Programs*, 38, 445.
6062
6063 McBirney, A. R., 2007, *Igneous Petrology* (3rd Edition), Jones and Bartlett Publishers, Inc., 550
6064 p.
6065

6066 McKague, H. L., D. Ferrill, K. Smart, J. Stamatakos, D. Waiting, and B. Hill, 2006, Tectonic
6067 Model Synthesis Report for the Yucca Mountain Region, Center for Nuclear Waste Regulatory
6068 Analyses Report.
6069

6070 Melson, W., 2002. Memo to Leon Reiter "Report on Meeting of the Volcanic Consequences
6071 Peer Review: Presentation of Interim Report, September 8, 2002, Las Vegas, NV" September
6072 23, 2002.
6073

6074 Moeller, D.W., and M.T. Ryan, 2004, Limitations on upper bound dose to adults due to intake of
6075 ¹²⁹I in drinking water and a total diet – Implications relative to the proposed Yucca Mountain high
6076 level radioactive waste repository, *Health Physics*, 86, 586-589.
6077

6078 Moeller, D.W., and M.T. Ryan, 2005, Sensitivity analyses of the standards for the proposed
6079 Yucca Mountain repository – A review, evaluation, and commentary, *Health Physics*, 88, 459-
6080 468.
6081

6082 Mohanty, S., R. Codell, J.M. Menchaca, R. Janetzke, M. Smith, P. LaPlante, M. Rahimi, and A.
6083 Lozano, 2004, System-Level Performance Assessment of the Proposed Repository at Yucca
6084 Mountain Using the TPA Version 4.1 Code. CNWRA Report 2002–05. Rev. 2. San Antonio,
6085 Texas.
6086

6087 Mohanty, S., R. Benke, R. Codell, K. Compton, D. Esh, D. Gute, L. Howard, T. McCartin, O.
6088 Pensado, M. Smith, G. Adams, T. Ahn, P. Bertetti, L. Browning, G. Cragolino, D. Dunn, R.
6089 Fedors, B. Hill, D. Hooper, P. LaPlante, B. Leslie, R. Nes, G. Ofoegbu, R. Pabalan, R. Rice, J.
6090 Rubenstone, J. Trapp, B. Winfrey, L. Yang, 2005, Risk Analysis for Risk Insights Progress
6091 Report. CNWRA report.
6092

6093 Mooney, M., 1951. The viscosity of a concentrated suspension of spherical particles. *Jour. of*
6094 *Colloid and Interface Sc.*, 6, 162-170.
6095

6096 Napier, B.A., R.A. Peloquin, D.L. Strenge, and J.V. Ramsdell, 1988, GENII: The Hanford
6097 Environmental Radiation Dosimetry Software System. Vols. 1, 2, and 3: Conceptual
6098 Representation, User's Manual, and Code Maintenance Manual. PNL-6584, Richland, WA:
6099 Pacific Northwest National Laboratory.
6100

6101 Neuendorf, K.K.E., J.P. Mehl, Jr., and J.A. Jackson, 2005, Glossary of Geology (5th Ed.),
6102 American Geological Institute, Alexandria, VA, 779 p.
6103

6104 Nicholis, M. G. and M. J. Rutherford, 2004, Experimental constraints on magma ascent rate for
6105 the Crater Flat volcanic zone hawaiite, *Geology*, 32, 489-492.
6106

6107 NEI (Nuclear Energy Institute), 2006, Common objections to the Yucca Mountain Project, and
6108 What the Science Really Says (Available at <http://www.nei.org/doc.asp?catnum=2&catid=197>).
6109

6110 NRC (US Nuclear Regulatory Commission), 1999, Issue Resolution Status Report, Key
6111 Technical Issue: Igneous Activity, Rev. 2, Division of Waste Management, Washington, DC.
6112

6113 NRC (US Nuclear Regulatory Commission), 2004, Risk Insights Baseline Report, NRC
6114 Accession No. ML040560162, Division of Waste Management, Washington, DC (Available at:
6115 <http://www.nrc.gov/waste/hlw-disposal/reg-initiatives/ml040560162.pdf>).
6116

6117 NRC (US Nuclear Regulatory Commission), 2005a, Integrated Issue Resolution Status Report,
6118 NUREG-1762, Vol. 1 and 2, Rev. 1, US NRC, Office of Nuclear Material Safety and Safeguards,
6119 Available at: <http://www.nrc.gov/reading-rm/doc-collections/nuregs/staff/sr1762/>.
6120

6121 NRC (US Nuclear Regulatory Commission), 2005b, Rulemaking Issue SECY-05-0144,
6122 Proposed Rule; 10CFR63 "Implementation of a Dose Standard after 10,000 Years",
6123 Washington, DC.
6124

6125 NWTRB (Nuclear Waste Technical Review Board), 2001, Letter of Jared L. Cohon to the Hon.
6126 Dennis J. Hastert, April, 2001.
6127

6128 NWTRB (Nuclear Waste Technical Review Board), 2002, Report to the U. S. Congress and
6129 Secretary of Energy, January 1, 2001 to January 31, 2002.
6130

6131 NWTRB (Nuclear Waste Technical Review Board), 2003, Letter of Michael L. Corradini to Dr.
6132 Margaret S. Y. Chu, December 16, 2003.
6133

6134 NWTRB (Nuclear Waste Technical Review Board), 2004, Enclosure in letter of B. John Garrick
6135 to the Hon. Dennis J. Hastert, December 30, 2004.
6136

6137 OECD [Organisation for Economic Co-operation and Development] (2002). An International
6138 Peer Review of the Yucca Mountain Project TSPA-SR Total System Performance Assessment
6139 for the Site Recommendation (TSPA-SR) - A Joint Report by the OECD Nuclear Energy Agency
6140 and the International Atomic Energy Agency, Available at:
6141 <http://www.nea.fr/html/rwm/reports/2002/nea3682-yucca.pdf>.
6142

6143 O'Leary, D.W., 1996, Synthesis of Tectonic Models for the Yucca Mountain Area, Chapter 8 in
6144 Seismotectonic Framework and Characterization of Faulting at Yucca Mountain, Nevada (J.W.
6145 Whitney, Coordinator), U.S Geol. Surv. Report to the U.S. Department of Energy, WBS Number
6146 1.2.3.2.8.3.6, 153 p.
6147

6148 O'Leary, D.W., 2001, Tectonic controls on basaltic volcanism near Yucca Mountain, Nevada,
6149 GSA Annual Meeting, November 2001, Abstract No. 162-0 (Available at
6150 http://gsa.confex.com/gsa/2001AM/finalprogram/abstract_20245.htm)
6151

6152 O'Leary, D.W., E. A. Mankinen, R. J. Blakely, V. E. Langenheim, and D. A. Ponce, 2002,
6153 Aeromagnetic expression of buried basaltic volcanoes near Yucca Mountain, NV, U. S. Geol.
6154 Surv. Open File Report 02-020, 26 p. (Available at <http://geopubs.wr.usgs.gov/open-file/of02-020/of02-020nav.pdf>.)
6155

6156
6157
6158
6159

6160 Parsons, T., and G. A. Thompson, 1991, The role of magma overpressure in suppressing
6161 earthquakes and topography: Worldwide examples, *Science*, 253, 1,399-1,402.
6162

6163 Parsons, T., 1995, The Basin and Range Province, In K.H. Olsen (ed.), *Continental Rifts:
6164 Evolution, Structure, and Tectonics*, Elsevier, Amsterdam, 277-324.
6165

6166 Parsons, T., G.A. Thompson, A.H. Cogbill, 2006, Earthquake and volcano clustering via stress
6167 transfer at Yucca Mountain, Nevada, *Geology* 34, 785–788.

6166 Pearson, E. S., and H. O. Hartley (eds.), 1970, Table 40: Confidence limits for expectation of a
6167 Poisson variable, In *Biometrika Tables for Statisticians, Vol. 1*, Cambridge Univ. Press, New
6168 York.
6169
6170 Perry, F.V., B.M. Crowe, G.A. Valentine, and L.M. Bowker (eds.), 1998, *Volcanism Studies:*
6171 *Final Report for Yucca Mountain Project*, Los Alamos National Laboratories, LA-13478.
6172
6173 Perry, F. V., B. Crowe, and G. Valentine, 2000, Analyzing volcanic hazards at Yucca Mountain,
6174 Los Alamos Science, 492-493.
6175
6176 Perry, F.V., Cogbill, A.H., and Kelley, R.E., 2005, Uncovering buried volcanoes at Yucca
6177 Mountain, *EOS, Trans. Amer. Geophys. Union*, 86, 485-488.
6178
6179 Perry, F., A. Cogbill, R. Kelly, M. Cline, C. Lewis, and R. Fleck, 2006, Status and Interpretation
6180 of Aeromagnetic Survey and Drilling Program to Support Probabilistic Volcanic Hazard Analysis
6181 – Update, Presentation to Advisory Committee on Nuclear Waste, July 17, 2006, Rockville, MD.
6182
6183 Pollard, D.D., 1987, Elementary fracture mechanics applied to the structural interpretation of
6184 dykes, In H.C. Halls and W.F. Fahrig (eds.) *Mafic Dyke Swarms; A Collection of Papers Based*
6185 *on the Proceedings of an International Conference*, Geol. Assoc. of Canada, Toronto, p. 5-24.
6186
6187 Reed, J.W., 1980, Air pressure waves from Mount St. Helens eruptions, *EOS, Trans. Amer.*
6188 *Geophys. Union*, 61, 1,136.
6189
6190 Reyes, 2006, Letter to Michael T. Ryan (ACNW Chairman), dated February 7, 2006, titled
6191 “Review of the NRC Program on the Risk from Igneous Activity at the Proposed Yucca
6192 Mountain Repository,” NRC accession number ML060040264.
6193
6194 Richardson, R.B., and D.W. Dunford, 2001, Review of the ICRP tritium and ¹⁴C internal
6195 dosimetry models and their implementation in the Genmod-PC code, *Health Physics*, 81, 289-
6196 301.
6197
6198 Roscoe, R., 1952. The viscosity of suspensions of rigid spheres. *British Jour. Appl. Phys*, 3,
6199 267-269
6200
6201 Savage, J. C., 1998, Detecting strain in the Yucca Mountain area, NV (comment), *Science*, 282,
6202 1007b.
6203
6204 Savage, J. C., J. Svarc, and W. Prescott, 2001, Strain accumulation at Yucca Mountain, NV,
6205 1993–1998, *Jour. Of Geophys. Res.*, 106, 16,483– 16,488.
6206
6207 Savage, J.C., Svarc, J.L., and Prescott, W.H., 1999, Strain accumulation at Yucca Mountain,
6208 Nevada, *Jour. of Geophys. Res.*, 104. 17,627-17,631.
6209
6210 Sheridan, M.F., 1990, Volcano Occurrences, in *Demonstration of a Risk-Based Approach to High-Level*
6211 *Waste Repository Evaluation*, EPRI Report NP-7057, Palo Alto, CA.
6212
6213 Schmincke, H-U., 2004, *Volcanism*, Springer, Berlin, Germany, 324 p.
6214
6215 Schultz, R.A., 1995, Limits on strength and deformation properties of jointed basaltic rock
6216 masses, *Rock Mech. And Rock Eng.*, 28, 1-15.

6217
6218 Sheriff, R.E., 1991, Encyclopedic Dictionary of Exploration Geophysics (3rd Ed.), Society of
6219 Exploration Geophysicists, Tulsa, OK, 376 p.
6220
6221 Smith, E.I., Feuerbach, D.L., Naumann, T.R., and Faulds, J.E., 1990, The area of most recent
6222 volcanism near Yucca Mountain, Nevada: Implications for volcanic risk assessment: High-Level
6223 Radioactive Waste Management, In *Proceedings International Topical Meeting, Las Vegas,*
6224 *Nevada, April 8-12, 1990*, La Grange Park, Illinois, American Nuclear Society, 1, 81–90.
6225
6226 Smith, E. I., D. L. Keenan, and T. Plank, 2002, Episodic volcanism and hot mantle: Implications
6227 for volcanic hazard studies at the proposed nuclear waste repository at Yucca Mountain,
6228 Nevada, *GSA Today*, 4-10.
6229
6230 Smith, E. I., and D. L. Keenan, 2005, Yucca Mountain could face greater volcanic threat, *EOS*,
6231 *Trans. Amer. Geophys. Union*, 86, 317-321.
6232
6233 Soule, S.A., K.V. Cashman, and J.P. Kauahikaua, 2004, Examining flow emplacement through
6234 the surface morphology of three rapidly emplaced, solidified lava flows, Kilauea Volcano,
6235 Hawai'i, *Bull. Of Vol.*, 66, 1-14.
6236
6237 Squires, R.R., and R.L. Young, 1984, Flood Potential of Fortymile Wash and its Principal
6238 Southwestern Tributaries, Nevada Test Site, Southern Nevada, U.S. Geol. Surv. Water-
6239 Resources Investigations Report 83-4001, p. 33.
6240
6241 Stamatakos, J.A., C.B. Connor, and R.H. Martin, 1997, Quaternary basin evolution and basaltic
6242 volcanism of Crater Flat, Nevada from detailed ground Magnetic surveys of the Little Cones,
6243 *Jour. of Geol.*, 105, 319-330.
6244
6245 Stock, J.M, and J.H. Healy, S.H. Hickman, and M.D. Zoback, 1985, Hydraulic fracturing stress
6246 measurements at Yucca Mountain, Nevada and relationship to the regional stress field, *Jour. Of*
6247 *Geophys. Res.*, 90, 8,691-8,706
6248
6249 Stock, J.M., and J.H. Healy, 1988, Continuation of a deep borehole stress measurement profile
6250 near the San Andreas Fault 2. Hydraulic fracturing stress measurements at Black Butte, Mojave
6251 Desert, California, *Jour. Of Geophys. Res.*, 93, 15,196-15,206.,
6252
6253 Suzuki, T. 1983. A theoretical model for dispersion of tephra. *Arc Volcanism: Physics and*
6254 *Tectonics*. Tokyo: Terra Scientific Publishing, 95-113.
6255
6256 Tanko, D.J., and P.A. Glancy, 2001, Flooding in the Amargosa River Drainage Basin, February
6257 23–24, 1998, Southern Nevada and Eastern California, Including the Nevada Test Site, U.S.
6258 Geol. Surv. Fact Sheet 036–01. 4.
6259
6260 Tilling, R. I., L. Topinka, and D. A. Swanson, 1990. Eruptions of Mount St. Helens: Past,
6261 Present, and Future , U.S. Geol. Surv. Special Interest Publication, 56 p., Available online at:
6262 <http://pubs.usgs.gov/gip/msh//title.html>.
6263
6264 Valentine, G.A., and K.R. Groves, 1996, Entrainment of country rock during basaltic eruptions of
6265 the Lucero Volcanic Field, New Mexico, *Jour. Of Geology*, 104, 71-90.
6266

6267 Valentine, G. A., D. Krier, F. V. Perry, and G. Heiken, 2005, Scoria cone construction
6268 mechanisms, Lathrop Wells volcano, southern Nevada, USA, *Geology*, 33, 629-632.
6269

6270 Valentine, G. A., 2006, Igneous scenarios, Presented to DOE/NRC Technical Exchange on
6271 Total System Performance Assessment (TSPA) for Yucca Mountain, Las Vegas, NV.
6272

6273 Valentine, G. A., F. V. Perry, D. Krier, G. N. Keating, R. E. Kelley, and A. H. Cogbill, 2006a,
6274 Small-volume basaltic volcanoes: Eruptive products and processes, and post-eruptive
6275 geomorphic evolution in Crater Flat (Pleistocene), southern Nevada, *Bull. of Geol. Soc. of Am.*,
6276 doi:10.1130/B25956.1.
6277

6278 Valentine, G. A., and K. E. C. Krogh, 2006b, Emplacement of shallow dikes and sills beneath a
6279 small basaltic volcanic center – The role of pre-existing structure (Paiute Ridge, southern
6280 Nevada, USA), *Earth and Planetary Sc. Lett.* 246, 217-230.
6281

6282 Valentine, G. A., and F. V. Perry, 2006, Decreasing magmatic footprints of individual volcanoes
6283 in a waning basaltic field, *Geophys. Res. Lett.*, 33, L14305, doi:10.1029/2006GL026743.
6284

6285 Vergnolle, S., and C. Jaupart, 1986, Separated two-phase flow and basaltic eruptions, *Jour. Of*
6286 *Geophys. Res.*, 91, 12,842-12,860.
6287

6288 Waddell, R. K., J. H. Robison, and R. K. Blankennagel, 1984, Hydrology of Yucca mountain and
6289 Vicinity, Nevada-California – Investigative Results Through Mid-1983, USGeol. Surv. Water-
6290 Resources Investigations Report 84-4267, 72 p.
6291

6292 Wallace, R.F., 1987, Separated two-phase flow and basaltic eruptions, *Bull. of Seismol. Soc. Of*
6293 *Am.*, 77, 868-876.
6294

6295 Wark, K., C.F. Warner, and W.T. Davis, 1998, *Air Pollution: Its Origin and Control*, third edition.
6296 Harper & Row, New York, NY.
6297

6298 Wernicke, B., J. L. Davis, R. A. Bennett, P. Elosegui, M. J. Abolins, R. J. Brady, M. A. House, N.
6299 A. Niemi, and J. K. Snow, 1998, Anomalous strain accumulation in the Yucca Mtn. area, NV,
6300 *Science*, 279, 2,096–2,100.
6301

6302 Weigel, F., 1986, In Katz, J.J., G.T. Seaborg, and L.R. Morse (eds.), *The Chemistry of the*
6303 *Actinide Elements*, New York, NY
6304

6305 Wernicke, B., J.L. Davis, R.A. Bennett, J.E. Normandeau, , A.M. Friedrich, and N.A. Niemi,
6306 2004, Tectonic implications of dense continuous GPS velocity field at Yucca Mountain, Nevada,
6307 *Jour. of Geophys. Res.*, 109, B12404, doi:10.1029/2003JB002832.
6308

6309 WoldeGabriel, G., G.N. Keating, and G.A. Valentine, 1999, Effects of shallow basaltic intrusion
6310 into pyroclastic deposits, Grants Ridge, New Mexico, USA, *Jour. Of Volcanology and*
6311 *Geothermal Research*, 92, 389-411.
6312

6313 Wood, C. A., 1980, Morphometric evolution of cinder cones, *Jour. of Volcan. and Geotherm.*
6314 *Res.*, 7, 387-413.
6315

- 6316 Woods, A.W., S. Sparks, O. Bokhove, A.-M. LeJeune, C.B. Connor, and B.E. Hill, 2002,
6317 Modeling magma-drift interaction at the proposed high-level radioactive waste repository at
6318 Yucca Mountain, Nevada, USA, *Geophys. Res. Lett.*, 29, doi:10.1029/2002GL014665.
6319
- 6320 Woods A.W., O. Bokhove, A. de Boer, and B.E. Hill, 2006, Compressible magma flow in a two-
6321 dimensional elastic-walled dike, *Earth and Planetary Sc. Lett.*, 246, 241-250.
- 6322 Yogodzinski, G.M. and Smith, E.I., 1995, Isotopic domains and the area of interest for volcanic
6323 hazard assessment in the Yucca Mountain area, *EOS*, Transactions of the American
6324 Geophysical Union, 76, F669.
- 6325 Yogodzinski, G.M., T.R. Naumann, E.I. Smith, T.K. Bradshaw, and J.D. Walker, 1996, Evolution
6326 of a mafic volcanic field in the central Great Basin, south central Nevada, *Jour. Of Geophys.*
6327 *Res.*, 101, 17,425-17,445.
- 6328 Ziegler, J. D., 2003, Letter to NRC re: Igneous activity agreement 1.02, NRC Accession
6329 ML033110050, U. S. Nuclear Regulatory Commission, Washington, D. C.
- 6330
- 6331 Zoback, M.L., and M.D. Zoback, 1989, Tectonic stress field of the continental United States, In
6332 L.C. Pakiser and W.D. Mooney, *Geophysical Framework of the Continental United States*, *Geol.*
6333 *Soc. Of Am. Mem.* 172, 523-540.
- 6334
- 6335 Zreda, M. G., F. M. Phillips, P. W. Kubik, P. Sharma, and D. Elmore, 1993, Cosmogenic ³⁶Cl
6336 dating of a young basaltic eruption complex, Lathrop Wells, Nevada, *Geology*, 21, 57-60.
6337
6338
6339
6340
6341

6342 **Appendix A. Status of NRC Igneous Activity Key Technical Issue Responses (2006)**

6343

6344 The current status of differences between the DOE and the NRC is given by the status
 6345 of the Igneous Activity Key Technical Issues (KTI) as identified by the NRC. The following table
 6346 which is based on a 2006 compilation gives a brief description of each KTI the DOE response
 6347 date and the status of the agreement between the DOE and NRC. The significance of each KTI
 6348 to overall performance of the repository is also given. Of the 20 KTIs, fourteen have been
 6349 satisfactorily agreed to by both agencies, while six await further information from the DOE and
 6350 evaluation by the NRC. Four of the KTIs are ranked as of high importance to risk and three of
 6351 these remain open (IA. 1.02.2.07, 2.17, and 2.18).
 6352

NRC KTI Responses

KTI	Response Date	Description	Status	Risk
IA.1.01	4/30/2001	In addition to DOE's licensing case, include for Site Recommendation and License Application, for information purposes, the results of a single point sensitivity analysis for extrusive and intrusive igneous processes at 10E-7.	Complete	Medium
IA.1.02	11/5/2004	Examine new aeromagnetic data for potential buried igneous features (see U.S. Geological Survey, Open-File Report 00-188, Online Version 1.0), and evaluate the effect on the probability estimate.	NAI	High
IA.2.01	4/30/2001	Re-examine the ASHPLUME Code to confirm that particle density is appropriately changed when waste particles are incorporated into the ash.	Complete	Low
IA.2.02	4/14/2003	Document results of sensitivity studies for particle size, consistent with (1) above. (Eruptive AC-4) DOE agreed and will document the waste particle size sensitivity study in a calculation document.	Complete	Low
IA.2.03	3/31/2005	Document how the tephra volumes from analog volcanoes represent the likely range of tephra volumes from Yucca Mountain region (YMR) volcanoes.	Complete	Medium
IA.2.04	4/30/2001	Document that the ASHPLUME model, as used in the DOE performance assessment, has been compared with an analog igneous system.	Complete	Low
IA.2.05	6/6/2001	Document how the current approach to calculating the number of waste packages intersected by conduits addresses potential effects of conduit elongation along a drift.	Complete	Medium
IA.2.06	6/6/2001	Develop a linkage between soil removal rate used in TSPA and surface remobilization processes characteristics of the Yucca Mountain region (which includes additions and deletions to the system).	Complete	Medium
IA.2.07	6/6/2001	Document the basis for airborne particle concentrations used in TSPA in Rev. 1 to the Input Values for External and Inhalation Radiation Exposure AMR.	Complete	High
IA.2.08	4/30/2001	Provide additional justification on the reasonableness of the assumption that the inhalation of particles in the 10-100 micron range is treated as additional soil ingestion, or change the BDCFs to reflect ICRP-30.	Complete	Low
IA.2.09	3/31/2005	Use the appropriate wind speeds for the various heights of	Complete	Medium

		eruption columns being modeled. (Eruptive AC-5) DOE agreed and will evaluate the wind speed data appropriate for the height of the eruptive columns being modeled.		
IA.2.10	2/13/2003	Document the ICNs to the Igneous Consequences AMR and the Dike Propagation AMR regarding the calculation of the number of waste packages hit by the intrusion.	Complete	Medium
IA.2.11	6/14/2004	Provide an analysis that shows the relationship between any static measurements used in the TSPA and expected types and durations of surface disturbing activities associated with the habits and lifestyles of the critical group.	NAI	Medium
IA.2.12	8/2/2002	Provide clarifying information on how PM10 measurements have been extrapolated to TSP concentrations. This should include consideration of the difference in behavior between PM10 and TSP particulates under both static and disturbed conditions.	Complete	Low
IA.2.13	4/25/2002	Provide the justification that sampling of range of transition period BDCFs is necessarily conservative in evaluating long-term remobilization processes.	Complete	Low
IA.2.14	6/14/2004	Provide information clarifying the method used in TSPA to calculate how deposit thickness effects the average mass load over the transition period.	Complete	Low
IA.2.15	2/4/2004	Clarify that external exposure from HLW-contaminated ash, in addition to inhalation and ingestion, was considered in the TSPA.	Complete	Low
IA.2.16	8/20/2002	Document that neglecting the effects of climate change on disruptive event BDCFs is conservative. DOE will document that neglecting the effects of climate change on disruptive event BDCFs is conservative in a subsequent revision to AMRs.	Complete	Low
IA.2.17	1/10/2005	DOE will evaluate conclusions that the risk effects (i.e., effective annual dose) of eolian and fluvial remobilization are bounded by conservative modeling assumptions in the TSPA-SR, Rev 00, ICN1.	NAI	High
IA.2.18	1/10/2005	DOE will evaluate how the presence of repository structures may affect magma ascent, conduit localization, and evolution of the conduit and flow system.	NAI	High
IA.2.19	3/31/2005	DOE will evaluate waste package response to stresses from thermal and mechanical effects associated with exposure to basaltic magma, considering the results of evaluations attendant to IA Agreement 2.18.	NAI	Medium
IA.2.20	3/31/2005	DOE will evaluate how ascent and flow of basaltic magma through repository structures could result in processes that might incorporate HLW, considering the results of evaluations attendant to IA Agreements 2.18 and 2.19.	NAI	Medium

6353
6354
6355
6356
6357
6358

6359
6360
6361

Appendix B. List of Agencies, Organizations, and Individuals Receiving Preliminary Draft of this Report for Their Review and Comment

- | | |
|--|---------------------------------------|
| A. Kalt, Churchill County, NV | A. Elzeftawy, Las Vegas Paiute Tribe |
| R. Massey, Churchill/Lander County, NV | J. Treichel, Nuclear Waste Task Force |
| I. Navis, Clark County, NV | W. Briggs, Ross, Dixon & Bell |
| E. von Tiesenhausen, Clark County, NV | R. Murray, DOE/OCRWM |
| G. McCorkell, Esmeralda County, NV | G. Runkle, DOE/Washington, D.C. |
| R. Damele, Eureka County, NV | C. Einberg, DOE/Washington, D.C. |
| L. Marshall, Eureka County, NV | S. Gomberg, DOE/Washington, D.C. |
| A. Johnson, Eureka County, NV | W. J. Arthur, III, DOE/OCRWM |
| S. Schubert, Sen. Reid's Office | R. Dyer, DOE/OCRWM |
| M. Yarbrow, Lander County, NV | J. Espinoza, GAO |
| J. Donnell, DOE/OCRWM | A. Gil, DOE/OCRWM |
| M. Baughman, Lincoln County, NV | W. Boyle, DOE/OCRWM |
| L. Mathias, Mineral County, NV | M. Ulshafer, DOE/OCRWM |
| J. Saldarini, BSC | S.A. Wade, DOE/OCRWM |
| M. Henderson, Cong. J. Gibbon's Office | C. Hanlon, DOE/OCRWM |
| D. Swanson, Nye County, NV | T. Gunter, DOE/OCRWM |
| M. Simon, White Pine County, NV | A. Benson, DOE/OCRWM |
| E. Sproat, DOE/OCRWM | N. Hunemuller, DOE/OCRWM |
| D. Cornwall, NV Congressional Delegation | P. Harrington, OPM&E |
| T. Story, NV Congressional Delegation | M. Mason, BSC |
| R. Herbert, NV Sen. Reid's Office | S. Cereghino, BSC |
| M. Murphy, Nye County, NV | B. Gattoni, Burns & Roe |
| R. Lambe, NV Congressional Delegation | E. Mueller, BSC |
| K. Kirkeby, NV Congressional Delegation | J. Gervers, Clark County, NV |
| R. Loux, State of NV | D. Beckman, BSC/B&A |
| S. Frishman, State of NV | L. Rasura-Alfano, Lincoln County, NV |
| S. Lynch, State of NV | J. Kennedy, Timbisha Shoshone Tribe |
| P. Guinan, Legislative Counsel Bureau | B. Durham, Timbisha Shoshone Tribe |
| R. Clark, EPA | R. Arnold, Pahrump Paiute Tribe |

R. Anderson, NEI
 R. McCullum, NEI
 S. Kraft, NEI
 J. Kessler, EPRI
 D. Duncan, USGS
 K. Skipper, USGS
 W. Booth, Engineering Svcs, LTD
 C. Marden, BNFL Inc.
 J. Bacoeh, Big Pine Paiute Tribe of the Owens Valley
 P. Thompson, Duckwater Shoshone Tribe
 T. Kingham, GAO
 D. Feehan, GAO
 E. Hiruo, Platts Nuclear Publications
 G. Hernandez, Las Vegas Paiute Tribe
 K. Finfrock, NV Congressional Delegation
 P. Johnson, Citizen Alert
 M. Williams, DOE/OCRWM
 J. Williams, DOE/Washington, DC
 A. Robinson, Robinson-Seidler
 M. Plaster, City of Las Vegas
 S. Rayborn, Sen. Reid's Office
 L. Lehman, T-REG, Inc.
 B.J. Garrick, NWTRB
 T. Feigenbaum, BSC
 M. Urie, DOE
 J. Brandt, Lander County
 R. Holland, Inyo County
 B. Sagar, CNWRA
 V. Trebules, RW/DOE
 R. Warther, DOE/OCRWM
 J. Birchim, Yomba Shoshone Tribe
 R. Holden, NCAI
 C. Meyers, Moapa Paiute Indian Tribe
 C. Dahlberg, Fort Independence Indian Tribe
 D. Vega, Bishop Paiute Indian Tribe
 Egan, Fitzpatrick, Malsch, PLLC
 J. Leeds, Las Vegas Indian Center
 J. C. Saulque, Benton Paiute Indian Tribe
 C. Bradley, Kaibab Band of Southern Paiutes
 R. Joseph, Lone Pine Paiute-Shoshone Tribe
 L. Tom, Paiute Indian Tribes of Utah
 E. Smith, Chemehuevi Indian Tribe
 D. Buckner, Ely Shoshone Tribe
 V. Guzman, Walker River Paiute
 D. Eddy, Jr., Colorado River Indian Tribes
 M. Boyd, Public Citizen
 J. Wells, Western Shoshone National Council
 D. Crawford, Inter-Tribal Council of NV
 I. Zabarte, Western Shoshone National Council
 S. Devlin
 G. Hudlow
 D. Irwin, Hunton & Williams
 P. Golan, DOE
 M. Rice, Lincoln County, NV
 G. Hellstrom, DOE
 S. Joya, Sen. Ensign's Office
 M. Gaffney, Inyo County
 L. Desell, RW/DOE
 R. List, Esmeralda County
 D. Curran, Harmon, Curran, Spielberg &

B. Neuman, Carter Ledyard & Milburn L.L.P.

- 6363
- 6364
- 6365 Charles Connor, Florida Southern University
- 6366
- 6367 Bruce Crowe, Battelle Memorial Institute
- 6368
- 6369 George Hornberger, University of Virginia
- 6370
- 6371 Eric Smistad, DOE (Las Vegas)
- 6372
- 6373 William Melson, Smithsonian Institution
- 6374
- 6375 Art Montana, University of City of Los Angeles
- 6376
- 6377 Eugene Smith, University of Nevada, Las Vegas
- 6378
- 6379 Steve Sparks, University of Bristol
- 6380
- 6381

DRAFT